ESL-TR-82-17

ATMOSPHERIC REACTION MECHANISMS OF AMINE FUELS

ERNESTO C. TUAZON, WILLIAM P. L. CARTER, RICHARD V. BROWN,
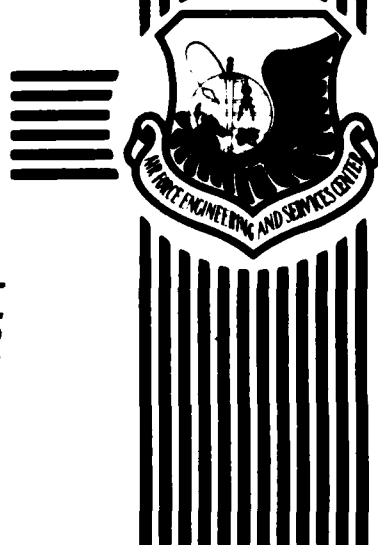ROGER ATKINSON, ARTHUR M. WINER, AND JAMES N. PITTS, JR.

STATEWIDE AIR POLLUTION RESEARCH CENTER
UNIVERSITY OF CALIFORNIA
RIVERSIDE, CALIFORNIA 92521

MARCH 1982

FINAL REPORT
1 JANUARY 1981 - 31 DECEMBER 1981

DTIC
ELECTE
AUG 1 6 1982

H

ENGINEERING AND SERVICES LABORATORY
AIR FORCE ENGINEERING AND SERVICES CENTER
TYNDALL AIR FORCE BASE, FLORIDA 32403

82 08 16 119

REPORT DOCUMENTATION PAGE		READ INSTRUCTIONS BEFORE COMPLETING FORM
1. REPORT NUMBER ESL-TR-82-17	2. GOVT ACCESSION NO. AD-A118267	3. RECIPIENT'S CATALOG NUMBER
4. TITLE (and Subtitle) Atmospheric Reaction Mechanisms of Amine Fuels		5. TYPE OF REPORT & PERIOD COVERED Final Report: January 1981–December 1981
		6. PERFORMING ORG. REPORT NUMBER
7. AUTHOR(s) Ernesto C. Tuazon, William P. L. Carter, Richard V. Brown, Roger Atkinson, Arthur M. Winer and James N. Pitts, Jr.		8. CONTRACT OR GRANT NUMBER(s) F08635-81-C-0041
9. PERFORMING ORGANIZATION NAME AND ADDRESS Statewide Air Pollution Research Center University of California Riverside, California 92521		10. PROGRAM ELEMENT, PROJECT, TASK AREA & WORK UNIT NUMBERS PE 61101F JON ILIR8101
11. CONTROLLING OFFICE NAME AND ADDRESS AIR FORCE ENGINEERING AND SERVICES CENTER Tyndall Air Force Base, Florida 32403		12. REPORT DATE March 1982
		13. NUMBER OF PAGES 204
14. MONITORING AGENCY NAME & ADDRESS(if different from Controlling Office)		15. SECURITY CLASS. (of this report) UNCLASSIFIED
		15a. DECLASSIFICATION/DOWNGRADING SCHEDULE

16. DISTRIBUTION STATEMENT (of this Report)

Approved for public release; distribution unlimited.

17. DISTRIBUTION STATEMENT (of the abstract entered in Block 20, if different from Report)

18. SUPPLEMENTARY NOTES

Availability of this report is specified on verso of front cover.

19. KEY WORDS (Continue on reverse side if necessary and identify by block number)

Hydrazine	Nitrogen Dioxide
Monomethylhydrazine	Atmospheric Reactivity
Unsymmetrical dimethylhydrazine	Amine Fuels
Ozone	Hydroxyl Radical

20. ABSTRACT (Continue on reverse side if necessary and identify by block number)

This report describes a detailed investigation of the atmospheric reactions of hydrazine (N_2H_4), monomethylhydrazine (MMH), and unsymmetrical dimethylhydrazine (UDMH) relevant to assessments of the impact of their releases to the atmosphere as a result of their wide use as fuels for military purposes. Experiments were conducted in 3800 ℓ and 6400 ℓ Teflon reaction chambers, with reactant and product concentrations measured by long pathlength (68.3–102.4 m) Fourier transform infrared (FT-IR) spectroscopy. The results of the present study greatly extend the data obtained in a previous exploratory investigation in these labor-

DD FORM 1473 EDITION OF 1 NOV 68 IS OBSOLETE
1 JAN 73

atories of the reactions of these hydrazines with the hydroxyl radicals, ozone and oxides of· nitrogen and includes new data on the reactions of the hydrazines with nitric acid and formaldehyde, two species which occur at significant concentrations in the polluted atmosphere.

The reactions of N_2H_4, MMH, and UDMH with O_3 were studied at varying reactant ratios, both in the presence and absence of a radical trap, and with added organic compounds which served as quantitative tracers for any hydroxyl radicals formed. The tracer and radical trap experiments unequivocably demonstrated the formation and participation of OH radicals in the reactions of O_3 with all three hydrazines. Hydrogen peroxide and diazene (HN=NH) were the major products observed by FT-IR spectroscopy in the $N_2H_4 + O_3$ reaction, along with small yields of N_2O and NH_3. In this study diazene was positively identified for the first time as a product of the $N_2H_4 + O_3$ reaction and of N_2H_4 decomposition in air. The major products of the MMH + O_3 reaction were CH_3OOH, CH_3NNH, HCHO, CH_2N_2, and H_2O_2, with lower yields of CH_3OH, HCOOH, CO, NH_3, and N_2O. The major product of the UDMH + O_3 reaction was N-nitrosodimethylamine, with significant yields of CH_3OOH, CH_3NNH, and H_2O_2 and minor amounts of CH_3OH, CH_2N_2, HCOOH, CO, HONO, NO_2, and NH_3 also being formed. Except for the formation of formaldehyde hydrazone, the reaction of Aerozine-50, an equimolar mixture of N_2H_4 and UDMH, with O_3 has been shown to be consistent with the reactions of O_3 with N_2H_4 and UDMH.

The verification of OH radical involvement and the direct observation of HN=NH support the essential features of the mechanism we proposed previously for the reactions of O_3 with N_2H_4 and MMH. However, certain aspects of the mechanism remain unclear; in particular, the question of whether the initial reaction pathway proceeds via H-atom abstraction or O-atom transfer to form an N-oxide formation is still unresolved. Moreover, the new set of data for the UDMH + O_3 reaction is inconsistent with the simple mechanism we postulated for this system.

Hydrazine, MMH, and UDMH all reacted at significant rates with NO_2 in the dark, but only negligibly with NO, unless NO_2 was also present. The UDMH + NO_2 reaction appears to be the simplest, yielding mainly nitrous acid and tetramethyltetrazene-2, with the reaction presumably proceeding through formation of the intermediate species $(CH_3)_2N-N$. An unknown product, suspected to be N-nitroso-N',N'-dimethylhydrazine, was additionally formed when NO was present in the UDMH + NO_2 reaction mixture. The products of the $N_2H_4 + NO_x$ reactions were HONO, N_2O, NH_3, HNNH, and $N_2H_4 \cdot HNO_3$; those from the MMH + NO_x reactions were HONO, CH_3NNH, CH_3OOH, CH_2OH, N_2O, NH_3, $HOONO_2$, and $CH_3NHNH_2 \cdot HNO_3$, together with two unidentified products that were probably formed in significant yields. Several uncertainties exist in the mechanisms for the $N_2H_4 + NO_x$ and MMH + NO_x reactions, including those which involve the source of HNO_3, the precursor to the nitrate salts observed.

All three hydrazines reacted with nitric acid in the vapor phase at rates that were too fast to measure by our techniques, and the 1:1 stoichiometry observed, even in the presence of excess HNO_3, indicated that the hydrazinium salts formed were primarily of the monobasic form in all cases.

Hydrazine and UDMH also react with HCHO with 1:1 stoichiometry to form the respective hydrazones with an unknown transient intermediate being observed during the initial stage of the N_2H_4 reaction. In both cases the kinetic data were inconsistent with simple second order processes, suggesting a heterogeneous or complex mechanism.

The possible atmospheric sink processes for dimethylnitramine and N-nitrosodimethylamine, both important oxidation products of UDMH, were investigated. Both compounds were shown to react at insignificant rates with O_3. The major atmospheric reaction pathway for dimethylnitramine is expected to be via reaction with OH radicals, with the OH radical rate constant measured in this study yielding an estimate of approximately 2 days for its tropospheric half-life. Daytime photolysis would be the primary degradation process for N-nitrosodimethylamine, as our measurements indicate that its photolysis rate is over three orders of magnitude faster than its rate of reaction with the OH radical.

PREFACE

This report has been reviewed by the Public Affairs Office (PA) and is releasable to the National Technical Information Service (NTIS). At NTIS it will be available to the general public, including foreign nationals.

DANIEL A. STONE, GS-13
Project Officer

RONALD E. CHANNELL, Maj USAF
Chief, Environmental Chemistry
Branch

MICHAEL J. RYAN, LtCol, USAF, BSC
Chief, Environics Division

FRANCIS B. CROWLEY III, Col, USAF
Dir, Engineering & Services
Laboratory

i

(The reverse of this page is blank)

TABLE OF CONTENTS

TABLE OF CONTENTS
(Continued)

TABLE OF CONTENTS
(Continued)

TABLE OF CONTENTS
(Concluded)

LIST OF FIGURES

LIST OF FIGURES
(continued)

LIST OF FIGURES
(concluded)

LIST OF TABLES

x

LIST OF TABLES
(continued)

xi

LIST OF TABLES
(continued)

LIST OF TABLES
(concluded)

SECTION I

INTRODUCTION

Hydrazine (N_2H_4) and its alkyl derivatives, monomethylhydrazine (MMH) and 1,1-dimethylhydrazine (unsymmetrical dimethylhydrazine or UDMH), constitute an important class of high-energy fuels which has found wide usage in military applications. Individually or in mixtures, these hydrazines are currently in use as rocket propellants and fuels for thrusters and small electrical power generating units. Specific examples are the use of Aerozine-50 (a 50-50 blend of N_2H_4 and UDMH) as fuel for the Titan II system and N_2H_4 as a source of emergency power for the F-16 fighter plane. In addition, the Space Shuttle System currently employs these fuels in large quantities. Hence, in addition to the health hazards of exposure to the hydrazines themselves (References 1, 2), a major concern is the possible adverse impact of their releases to the atmosphere stemming from storage, transfer, and venting operations.

In order to obtain the necessary information regarding the atmospheric transformations of these chemicals, the United States Air Force funded the Statewide Air Pollution Research Center (SAPRC) of the University of California at Riverside to carry out investigations concerning selected atmospheric reactions of these hydrazines. These studies were designed to obtain data needed to assess potential environmental impacts of these chemicals and the corresponding degree of control required on their releases to the atmosphere. Prior to the previous Air Force-sponsored study in this laboratory (Reference 3), only the studies by Stone (References 4-6) on the auto-oxidation of N_2H_4, MMH, UDMH, and Aerozine-50 had been carried out under experimental conditions approaching those in the actual atmosphere.

In our initial study (Reference 3), the following major results were obtained:

1) Absolute rate constants for the gas phase reactions of hydroxyl (OH) radicals with hydrazine and monomethylhydrazine (MMH) were determined over the temperature range 298-424 K using a flash photolysis-resonance fluorescence technique. The rate constants determined were, within the experimental errors (References 3, 7), independent of temperature, with

1

$k(OH + N_2H_4) = (6.1 \pm 1.0) \times 10^{-11}$ cm^3 molecule^{-1} sec^{-1} and $k(OH + CH_3NHNH_2) = (6.5 \pm 1.3) \times 10^{-11}$ cm^3 molecule^{-1} sec^{-1}. The magnitude of these rate constants and their lack of temperature dependences indicate that these reactions proceed via H-atom abstraction from the weak N-H bonds, i.e.,

$$OH + N_2H_4 \rightarrow H_2O + N_2H_3$$

Furthermore, from these data, a rate constant for the reaction of OH radicals with UDMH of $\sim(5 \pm 2) \times 10^{-11}$ cm^3 molecule^{-1} sec^{-1}, approximately temperature independent over the range 300-425 K, was estimated. With an average OH radical concentration of $\sim 1 \times 10^6$ cm^{-3} for the lower troposphere (Reference 8), the tropospheric 1/e lifetimes of these hydrazines due to reaction with the OH radical can then be calculated to be approximately 4 to 5 hours.

2) All three hydrazines were shown to react extremely rapidly with ozone, even for O_3 concentrations approaching those commonly found in the atmosphere. The dark reactions of the three hydrazines with O_3 were investigated in an $\sim 30,000$ ℓ Teflon® chamber using Fourier transform infrared (FT-IR) spectroscopy in conjunction with long-path optics. From the limited time-concentration data obtained, the rate constant for the reaction of ozone with N_2H_4 was estimated to be of the order of 1×10^{-16} cm^3 molecule^{-1} sec^{-1}, with MMH and UDMH reacting substantially more rapidly (i.e., on a time scale comparable to the spectrum acquisition time). Thus, in the presence of ~ 40 ppb of O_3 (the ambient concentration for the clean lower troposphere [Reference 9]), the lifetimes of the hydrazines due to reaction with O_3 would be ~ 3 hours for N_2H_4 and a factor of 10 or more shorter for MMH and UDMH.

3) A spectrum of products was identified in the reactions of the hydrazines with ozone, including certain highly toxic compounds such as diazomethane and N-nitrosodimethylamine. Briefly, specific products observed by FT-IR spectroscopy were:

- From hydrazine: hydrogen peroxide (H_2O_2) and nitrous oxide (N_2O).

- From MMH: methylhydroperoxide (CH_3OOH), methyldiazene ($CH_3N=NH$), diazomethane (CH_2N_2), formaldehyde (HCHO), methanol (CH_3OH),

2

and H_2O_2, with $CH_3N=NH$ and CH_2N_2 reacting further in the presence of excess O_3.

● From UDMH: N-nitrosodimethylamine [$(CH_3)_2NNO$] in large yield, together with lesser amounts of HCHO and H_2O_2.

4) From the product data obtained, the following mechanism was postulated for the reaction of O_3 with N_2H_4 (References 3, 10):

$$O_3 + N_2H_4 \rightarrow O_2 + OH + N_2H_3$$

$$OH + N_2H_4 \rightarrow H_2O + N_2H_3$$

$$N_2H_3 + O_2 \rightarrow HO_2 + HN=NH$$

$$O_3 + HN=NH \rightarrow HN=N^\cdot + OH + O_2$$

$$OH + HN=NH \rightarrow H_2O + HN=N^\cdot$$

$$HN=N^\cdot \rightarrow N_2 + H$$

$$H + O_2 + M \rightarrow HO_2 + M$$

$$HO_2 + HO_2 \rightarrow H_2O_2 + O_2$$
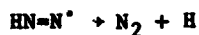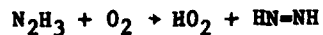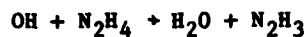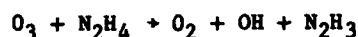
The reaction mechanism postulated for MMH was analogous, with CH_3OOH being formed from the combination reaction

$$CH_3O_2 + HO_2 \rightarrow CH_3OOH + O_2$$

and $CH_3N=NH$ formation being analogous to that of $HN=NH$ formation from hydrazine. The reaction of O_3 with $CH_3N=NH$ thus leads to the formation of CH_3 radicals, which rapidly react with O_2 to yield methylperoxy (CH_3O_2) radicals.

Reaction of OH radicals with $CH_3N=NH$ can lead to CH_2N_2 formation via the sequence:

$$OH + CH_3N{=}NH \rightarrow \overset{\bullet}{CH_2}N{=}NH + H_2O$$

$$\overset{\bullet}{CH_2}N{=}NH + O_2 \rightarrow CH_2N_2 + HO_2$$
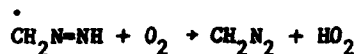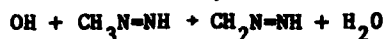
with CH_2N_2 possibly reacting with O_3 via

$$O_3 + CH_2N_2 \rightarrow HCHO + O_2 + N_2$$
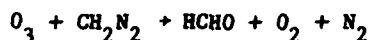
For UDMH, the reaction mechanism was postulated to be somewhat different due to the absence of H atoms on one of the nitrogen atoms. The proposed mechanism (References 3, 10) consisted of the reactions

$$(CH_3)_2NNH_2 + O_3 \rightarrow (CH_3)_2\overset{\bullet}{N}NH + OH + O_2$$

$$(CH_3)_2NNH_2 + OH \rightarrow (CH_3)_2\overset{\bullet}{N}NH + H_2O$$

followed by

$$(CH_3)_2\overset{\bullet}{N}NH + O_3 \rightarrow (CH_3)_2NN{\overset{\displaystyle H}{\underset{\displaystyle O\bullet}{<}}} + O_2$$

$$(CH_3)_2NN{\overset{\displaystyle H}{\underset{\displaystyle O\bullet}{<}}} + O_2 \rightarrow (CH_3)_2NNO + HO_2$$
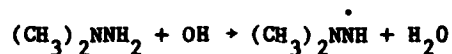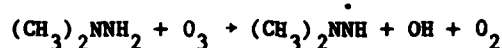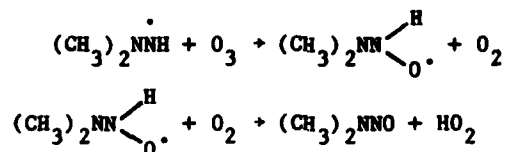
However, due to the limited data obtained, the possibility of other reaction mechanisms for all three hydrazines could not be eliminated.

5) A limited number of experiments were carried out on irradiated-NO_x-hydrazine-air mixtures in the ~30,000 ℓ Teflon® chamber. The products expected by analogy with the chemistry of irradiated NO_x-organic-air systems, which largely involve the reactions of O_3 and OH radicals, were observed. However, FT-IR observations indicated additional products and intermediates (mostly unidentified) arising from the dark reactions of NO_x with the hydrazines, particularly in the case of UDMH.

Although this initial study (Reference 3) of the reactions of hydrazines with O_3, OH radicals and NO_x provided much valuable information, further quantitative data concerning the rates, products, and reaction mechanisms were deemed necessary in order to assess more precisely the effects of hydrazine emissions on the atmosphere. Accordingly, in the

4

present program further studies of the atmospheric reactions of the hydrazines have been carried out to clarify some of the issues raised by our initial study, and to extend the scope of this first study. Specifically, in the program described below, we have carried out the following studies:

1) The reactions of N_2H_4, MMH and UDMH with O_3 were investigated at varying reactant ratios, both in the presence and absence of radical traps, and with added organic tracers to measure the levels of OH radicals formed. Estimates of the rates of reaction of O_3 with the individual hydrazines were made, and the identities and yields of the primary products and their dependence on initial reactant concentrations were determined.

2) The extent to which the products and their yields, as well as the hydrazine consumption rates, differ in the Aerozine-50 mixture from those observed for its individual components (N_2H_4 and UDMH) were investigated.

3) The dark reactions of N_2H_4, MMH, and UDMH with NO_x (NO and NO_2) were studied and yielded rate constants for the reactions of NO_2 with the individual hydrazines. The identification of tetramethyltetrazene-2 $[(CH_3)_2NN=NN(CH_3)_2]$ as the main organic product of the UDMH + NO_2 reaction resulted from these experiments. More definitive infrared spectra of unknown products in the MMH + NO_x and UDMH + NO_x reactions were obtained in the present study than was possible in the initial study, and may form the basis for their future identification.

4) The stoichiometry of the vapor-phase reactions of the hydrazines with HNO_3 was investigated. Preliminary studies of HCHO reactions with N_2H_4 and UDMH were carried out.

5) The reactions of N-nitrosodimethylamine and dimethylnitramine (both oxidation products of UDMH) with O_3 and with OH radicals were studied. The rate of photolysis of N-nitrosodimethylamine was measured under conditions which inhibited its reformation.

6) Embodied in the data from the above experiments are the behavior of some of the reaction products of the hydrazines with respect to reactive atmospheric species. Thus, for example, estimates of the rates of reaction of O_3 with diazomethane and formaldehyde hydrazone, and of NO_2 with methyldiazene, were also obtained from this study.

In the following sections, the experimental techniques used, the results obtained and our kinetic and mechanistic interpretations of these data are presented in detail.

SECTION II
EXPERIMENTAL

2.1 REACTION CHAMBER

The indoor reaction chamber used in this study was constructed from DuPont FEP Teflon® film. Teflon® is inert under the conditions of our experiments and the 50-μm (2-mil) thick film employed provided > 98% transmission of actinic radiation. The rectangular chamber was constructed by heat-sealing the Teflon® sheets together and reinforcing the seams externally with Mylar® tape. The bag was held semi-rigidly inside a rectangular (4 ft x 8 ft x 8 ft) aluminum frame which also supported two diametrically opposed banks of 40 Sylvania 40-W BL blacklamps. Figure 1 illustrates the chamber design and the arrangement of the interferometer and long-path optics.

The provisions for injection and sampling of gases consisted of glass tubes (9 mm i.d.) with sealed fittings extending to the middle of the chamber and a Teflon® disperser tube (13 mm i.d. and 8 ft in length) situated along the middle section of the chamber. For rapid mixing of reactants, a 10-in diameter Teflon®-coated, five-bladed fan (rated at 20,000 liter min^{-1}) was installed at the bottom of the chamber and was driven by an external motor via a sealed mechanical feedthrough.

The chamber was connected to the output of the air purification unit (Reference 11). To minimize possible health hazards, an exhaust system was devised to pass the contents of the bag through a charcoal filter bed after each experiment. The vacuum applied at the exhaust also served to balance the rate of air intake during the flushing operation. Teflon® gate valves isolated the chamber from the intake and exhaust lines after the final fill of matrix air.

The first reaction chamber constructed had a volume of ~6400 ℓ and was employed in several exploratory runs. Most of the final experiments were conducted later in a smaller ~3800 ℓ bag. The volumes, as determined by gas chromatographic (GC) and infrared (IR) methods, were reproducible to within ± 2% when the bags were fully inflated. The mixing time (as measured by monitoring O_3 after injection by Fourier transform-infrared [FT-IR] spectroscopy) was < 30 seconds for both chambers and was limited more by the rate of sample injection rather than by the efficiency of the mixing fan.
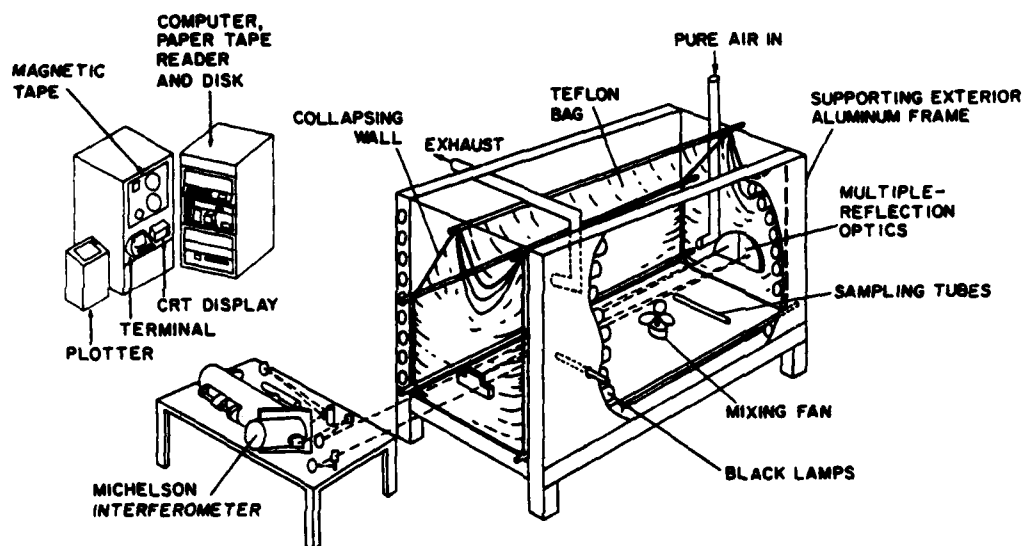
Figure 1. Schematic Diagram of Teflon® Reaction Chamber, Multiple-
Reflection Optics, and Fourier Transform Infrared
Spectrometer.

2.2 LONG-PATH OPTICS

The White-type multiple-reflection optics consisted of a small in-focus (nesting) mirror and two larger out-of-focus (collecting) mirrors with a common radius of curvature of 2.13 m. They were cut from a single, spherically figured 30-cm diameter Pyrex blank. The mirrors were gold-coated for maximum reflectivity (> 99.0%) in the infrared. Initially, silver with a thorium fluoride overcoat was used as the reflective surface, providing a performance slightly better than that of the gold overcoat. However, this particular coating showed a significant degradation upon continued exposure to reaction systems which generated gaseous nitrates, e.g., nitric acid (HNO_3).

The multiple of the basepath (2.13 m) attained, and thus the total pathlength, was determined by counting the number of spots from a He-Ne laser as seen on the nesting mirror. An optical alignment system was devised such that the beam of the He-Ne laser (external to the interferometer proper) could be brought into exact coincidence with the infrared source beam by interposing a removable mirror within the transfer optics.

Virtually all metal surfaces of the mirror mounting system within the reaction chamber were Teflon®-coated.

2.3 FT-IR SPECTROMETER

The White optics was interfaced to a rapid-scan Midac interferometer (Figure 1) with a maximum resolution capability of 0.06 cm^{-1}. Data collection and processing were performed with a Computer Automation LSI-2/20 minicomputer with 32 K word memory and a special fast Fourier transform (FFT) processor. System peripherals included a 2.5 M word dual-disk drive, raster plotter, line printer, oscilloscope display, CRT terminal, and magnetic tape unit.

The interferometer was equipped with a dual-element HgCdTe and InSb detector cooled with liquid nitrogen. The response of the HgCdTe element was adequate to cover the infrared region of interest (700-3000 cm^{-1}) and hence was the only detector element employed throughout this study.

2.4 MATERIALS

Anhydrous hydrazine (stated purity: 97+%) was procured from Matheson, Coleman and Bell. Methylhydrazine (98%), 1,1-dimethylhydrazine (99+%),

N-nitrosodimethylamine (99+%), n-octane (99+%), and 2,2,3,3-tetramethyl-butane (99%) were obtained from Aldrich. The above compounds were used without further purification. Small amounts (0-2%) of NH_3 were detected by infrared spectroscopy in the samples of all hydrazines injected into the chamber, but it was not clear whether these levels of the NH_3 impurities were present in the original samples or were generated in part or wholly by surface-catalyzed decomposition of the hydrazines.

Dimethylnitramine (m.p. 57°C) was prepared via oxidation of N-nitrosodimethylamine with peroxytrifluoroacetic acid (CF_3CO_3H), as described by Emmons (Reference 12).

Formaldehyde vapor was generated by heating a degassed sample of paraformaldehyde (95% HCHO; Matheson, Coleman and Bell) in a vacuum line and collected in Pyrex bulbs.

Peroxyacetyl nitrate ($CH_3\overset{O}{C}OONO_2$) was prepared at SAPRC by oxidation of an ethyl nitrite-oxygen mixture in a photochemical reactor as described by Stephens (Reference 13). The impure sample, collected and mixed with N_2 gas in a low-pressure tank, was passed through a tube packed with nylon fibers prior to injection into the reaction chamber to remove nitric and acetic acid impurities. Traces of methyl nitrate and ethyl nitrate were detected by infrared spectroscopy in the final sample.

Samples of nitric oxide (commercial purity 99.0%; Matheson Gas Company) from a lecture bottle were drawn directly into gas-tight, all-glass syringes which had been pre-flushed with N_2 gas to exclude O_2 that could cause immediate conversion of NO to NO_2 prior to injection into the chamber. Nitrogen dioxide was prepared by transferring a measured volume of nitric oxide in a syringe to another syringe containing twice the volume of O_2.

Ozone was produced in a Welsbach T-408 ozone generator and collected in 2 ℓ and 5 ℓ Pyrex bulbs. The input flow of O_2 to the ozonizer was maintained constant (1.5 liter min^{-1} at 8 psig) and the voltage applied to the electrodes was adjusted (60-100 V) to yield the desired O_3 concentration. The O_3/O_2 mixture being flushed into the Pyrex bulb flowed through a 10 cm cell equipped with KBr windows. The O_3 concentration was determined by its infrared absorption at 1055 cm^{-1}.

Methyl nitrite was prepared by dropwise addition of 50% H_2SO_4 to a saturated solution of sodium nitrite ($NaNO_2$) in methanol. The product

vapors were carried by an N_2 stream first through a concentrated NaOH solution and then over anhydrous $CaCl_2$ into a trap cooled to 196 K (Reference 14). The product, as purified by vacuum distillation, showed only traces of methanol impurity in the infrared spectrum.

2.5 METHODS OF PROCEDURE

2.5.1 Sample Handling and Injection

Prior to the final fill of purified air for each experiment, the reaction chamber was flushed with > 7 volumes of air derived from the air purification system (Reference 11).

Vapors of the hydrazine to be studied were measured into calibrated 2 ℓ and 5 ℓ Pyrex bulbs on a vacuum line equipped with an MKS Baratron capacitance manometer (0-100 and 0-1000 torr heads). The contents of the Pyrex bulbs were flushed with N_2 gas into the fully inflated Teflon® chamber via the glass injection tubes at measured flow rates of 20 liter min^{-1} for the 2 ℓ bulb and 50 liter min^{-1} for the 5 ℓ bulb, with the stirring fan operating for 1 minute. This procedure ensured that $> 99\%$ of the sample was introduced into the chamber within 30 seconds.

Ozone, nitric oxide, and nitrogen dioxide were flushed through the Teflon® disperser tube. The latter was not used for injections of the hydrazines in order to avoid possible surface-initiated decompositions (e.g., to NH_3), as observed in the previous study (Reference 3).

In the majority of the experiments, the hydrazine (N_2H_4, MMH, or UDMH) sample was the first reactant injected into the chamber and the predetermined amount of the second reactant (O_3, NO, or NO_2) was then injected, with the stirring fan in operation, from a Pyrex bulb or syringe with an N_2 stream. However, in some of the experiments (such as those with excess O_3), the hydrazine was the last reactant introduced. In these cases, the hydrazine sample in the Pyrex bulb was pressurized to 760 torr total pressure prior to injection so as to avoid back filling by the chamber's contents, thus minimizing the possibility of reactions occurring within the sample bulb prior to injection into the chamber.

The large quantities of n-octane ($\sim$7-10 ml) required as a radical trap in several hydrazine-ozone experiments were introduced into the chamber by bubbling a stream of heated N_2 gas through the warm liquid. Dimethylnitramine was introduced by passing a stream of N_2 gas over a

gently heated solid sample. Peroxyacetyl nitrate was metered from the low-pressure storage tank into the chamber (after passing through a tube packed with nylon fibers) and its final concentration verified by infrared spectroscopy using its known absorption coefficient (Reference 13).

2.5.2 Data Collection and Spectral Processing

The time-concentration profiles of products and reactants were monitored by FT-IR spectroscopy (see, however, the following section on support instrumentation and supplementary experiments). Pathlengths of 68.3 and 102.4 m were normally employed with 1 cm^{-1} spectral resolution. The infrared region of interest (700-3000 cm^{-1}) was adequately recorded with a HgCdTe photoconductive detector. Under the above conditions, typical noise levels in the ratio of two background spectra of 32 co-added interferograms were < 0.003 and < 0.005 absorbance units (base e), for regions around 1000 cm^{-1} and 2800 cm^{-1}, respectively.

To monitor the relatively fast reactions encountered in this study, the interferometer scan was initiated at the start of injection of the last reactant. By pre-storing successive sets of co-added interferograms (subsequently transformed into spectra after the experiment), the progress of the reaction could be followed with a time resolution as short as 15 seconds. Thus, certain experiments involving the reactions of O_3 with MMH and UDMH were carried out with data collection every 15 seconds using 6 co-added interferograms per spectrum. In general, however, 32 scans were averaged per spectrum during the early stages of a reaction which allowed for a convenient 1 min time resolution. Slower events were recorded by co-adding 64 interferograms for an improved signal-to-noise ratio, followed by immediate computation of each spectrum. Concentration data derived from each spectrum are reported as those corresponding to the midpoint of the scan averaging period. Midpoints for the sets of scans were 0.10, 0.38, and 0.78 minute for 6, 32, and 64 scans, respectively.

Reactant and product concentrations were obtained from the intensities of the infrared absorption bands by spectral desynthesis, i.e., successive subtraction of absorptions by known species. Low-noise reference spectra for the hydrazines and several reaction products were generated specifically for this purpose. The most desirable reference spectra were those recorded at the highest concentrations possible that still allowed linear subtraction to be made. Since the subtraction

process is purely arithmetic, the low factors permitted thus reduced to a minimum the noise added to the residual spectrum.

2.5.3 Support Instrumentation

The concentrations of small amounts (< 0.2 ppm) of 2,2-dimethylpropane, cyclohexane, n-octane and 2,2,3,3-tetramethylbutane, which served as OH radical tracers in the reaction of O_3 with the individual hydrazines, were quantitatively monitored by gas chromatography with flame ionization detection. The instrument used was a Varian Series 1400 gas chromatograph equipped with a 20-ft x 1/8-in stainless steel column packed with 5% DC703/C20M on 100/120 mesh AW, DMCS Chromosorb G and operated at 333 K. Analyses were carried out with no sample preconcentration.

Temperature and relative humidity inside the reaction chamber were monitored with a Thunder Scientific Corporation Model HS-2CHDT-2A digital humidity and temperature measurement system. Relative humidity readings from this instrument were periodically checked by dry bulb-wet bulb thermometry.

A Dasibi Model 1003AH ozone monitor was used as the standard to measure absorption coefficients directly applicable to the particular instrumental resolution employed. The instrument's calibration had been verified previously at the laboratory of the California Air Resources Board (El Monte, California).

Likewise, NO and NO_2 infrared absorption coefficients were based on readings from a Thermo Electron Corporation (TECO) chemiluminescence instrument which had been calibrated by flow methods. As revealed by our preliminary experiments, the latter instrument was ill-suited for direct measurements of NO and NO_2 in the present reaction systems due to severe and non-linear interferences from the individual hydrazines (and possibly from other nitrogen-containing products) at the concentration levels of the reactants employed.

2.5.4 Supplementary Experiments in ~175 ℓ Teflon® Reaction Bags

In support of the FT-IR measurements of the reaction rates of the hydrazines with O_3 in the 3800 ℓ and 6400 ℓ environmental chambers, several such reactions were conducted in ~175 ℓ Teflon® reaction bags. The latter were constructed out of 2-mil-thick, 180-cm x 140-cm FEP

Teflon® sheets, heat-sealed around the edges, and fitted with Teflon® injection and sampling ports at each end of the bag.

The experimental technique, described in detail elsewhere (Reference 15) is based on observing the increased rate of ozone decay in the presence of a known excess of a reactive compound.

The Teflon® bag was initially divided into two subchambers of approximately equal volume by means of metal rods (Reference 15). One of these two subchambers was filled with a known volume of ultra-high purity air; ~20 cm³ of ~1% O_3 in O_2 (produced by a Welsbach T-408 ozone generator) were then injected using an all-glass gas-tight syringe. This amount of ozone was sufficient to yield an O_3 concentration of ~1 part-per-million (ppm) in the entire reaction bag. The hydrazine reactant and the OH radical trap (when required) were introduced into the other subchamber, again using ultra-high purity air as the diluent gas.

The reaction was then initiated by removing the metal rods and mixing the contents of the two subchambers by pushing down on alternate sides of the entire reaction bag for ~1 min. O_3 concentrations were monitored as a function of time after the mixing by a Monitor Labs Model 8410 chemiluminescence ozone analyzer. The reactant concentrations in the entire bag were calculated from the amount of reactant introduced and the total volume of air used to fill the two subchambers.

Background ozone decay rates, in the absence of added reactants, were ~10^{-5} sec^{-1} and were totally negligible. Known pressures of hydrazine and monomethylhydrazine were introduced from ~5 ℓ Pyrex bulbs, and all reactions were carried out at ~296 K.

SECTION III

RESULTS AND DISCUSSION

3.1 INFRARED ABSORPTION COEFFICIENTS

The absorption coefficients (at appropriate frequencies) for deter-
mining the concentrations of the hydrazines, associated products and other
reactant species were determined in the reaction chamber at pathlengths of
~20-120 m at known ppm concentrations. The same instrumental functions as
used in all of the ensuing reaction studies were employed. In particular,
the stated resolution of 1 cm^{-1} is that of an unapodized spectrum which
was transformed from data recorded at an optical path difference (OPD) = 1
cm with sampling every 2λ of the He-Ne laser line to yield a minimum-size
(8192 points) interferogram. These absorbance measurements used spectra,
as displayed on the oscilloscope or on hard-copy plots, with no additional
interpolation of points. Results of these measurements are summarized in
Table 1.

The precise values of the frequencies given in Table 1 are the posi-
tions of discrete points as generated by our computational method and may
differ slightly with those derived from other systems. The frequencies
reported for each compound are accurate to within ± 0.10 cm^{-1}. For
several compounds the absorption coefficient is reported only for the
distinct Q branch of a band envelope. Two frequency positions in paren-
theses [e.g., (974.36-973.39) for N_2H_4] signify that the absorption
coefficient is derived from peak-to-valley measurement of a narrow Q
branch or resolved rotational fine structure. All other determinations
were peak-to-baseline measurements.

The present values of the absorption coefficients for the hydrazines
are slightly higher than those measured in our previous study (Reference
3), possibly due to a slower loss of the hydrazines to the walls of the
much larger chamber used in the present measurements.

For O_3, NO and NO_2, measurements were made using chemiluminescence
instruments as standards (see Secton 2.5.3). In our previous study
(Reference 3), absorption coefficients published by McAfee, et al. (Refer-
ences 21, 22) for O_3 were employed. Since these absorption coefficients
correspond to the lower resolutions obtained with a dispersive instrument,
our previous procedure (Reference 3) was to reduce the 1 cm^{-1} resolution

14

TABLE 1. INFRARED MEASUREMENT FREQUENCIES AND ABSORPTION COEFFICIENTS.

Compound	Frequency $(cm^{-1})^a$	Absorption Coefficient [cm^{-1} atm^{-1} (base e), 1 cm^{-1} resolution RTP^b]	Reference	Detection Limit (ppm) at 68.3 m
N_2H_4	957.48	6.6	c	0.20
	(974.36–973.39)	3.3	c	0.22
MMH	889.02	9.8	c	0.10
	889.02(Q)	7.2	c	0.10
UDMH	909.75	7.5	c	0.20
	1144.55(Q)	3.2	c	0.23
HCHO	2778.92(Q)	7.8(ave)	c	0.15
	2781.33(Q)			
HCOOH	1105.49(Q)	67.8	c	0.01
CH_3OH	1033.66(Q)	22.6	c	0.03
CH_3OOH	1321.00(Q)	1.5	d	0.50
CH_2N_2	2102.03(Q)	16.4	e	0.04
$(CH_3)_2NNO$	1015.82	20	c	0.05
$(CH_3)_2NNO_2$	1307.02	34	c	0.04
$(CH_3)_2NN=NN(CH_3)_2$	1008.59	37	Reference 16	0.03
CH_3ONO_2	(855.76–857.20)	22.1	c	0.03
	(1291.59–1293.52)	22.0	c	0.03
CO	(2169.53–2170.01)	12.8	c	0.05
	(2172.90–2172.42)	13.0	c	0.05

15

TABLE 1. INFRARED MEASUREMENT FREQUENCIES AND ABSORPTION COEFFICIENTS (CONCLUDED).

Compound	Frequency $(cm^{-1})^a$	Absorption Coefficient [cm^{-1} atm^{-1} (base e), 1 cm^{-1} resolution RTP^b]	Reference	Detection Limit (ppm) at 68.3 m
O_3	1055.35	15.1	c	0.10
	(1055.35-1054.87)	6.4	c	0.11
H_2O_2	1251.09	8.8	f	0.17
	(1251.58-1252.06)	4.2	f	0.17
NO	1875.92	2.7	c	0.27
NO_2	(1605.93-1605.45)	10.8	c	0.07
	(1631.00-1631.48)	15.9	c	0.05
N_2O	2213.40	21	c	0.04
	2237.02	27	c	0.04
HONO	852.86(Q)	13.3 total HONO	g	0.06
	1264.11(Q)	18.6(cis + trans)		0.04
HNO_3	879.38(Q)	27	c	0.03
HO_2NO_2	803.21(Q)	27	Reference 17	0.03
N_2O_5	1246.27	40	Reference 18	0.03
NH_3	967.61	24.6	c	0.03
	931.45	20.6	c	0.04

[a](Q) indicates absorption coefficient value for the Q-branch height only; two frequencey positions in parentheses denotes peak-to-valley measurement of Q-branch or resolved fine structure.
[b]Room temperature (296 K) and pressure (~740 torr). [c]This work.
[d]Derived from data of H. Niki (see text). [e]Derived from data of Urry, et al. (Reference 19).
[f]From L. Molina and M. Molina (private communication).
[g]Derived from data of Calvert, et al. (Reference 20).

FT-IR spectrum to that of a lower resolution (by means of a [sinx]/x smoothing function) which approximates the above authors' published spectra. It was recognized at that time that care was necessary in translating data from a dispersive instrument to those derived with an FT-IR system, particularly for absorption bands with resolvable fine structures. The discrepancy arises from the difference in instrumental functions between the two types of instruments, as well as from the difference in definitions of spectral resolution (Reference 23). For example, McAfee, et al. (References 21, 22) reported an absorption coefficient of 9.7 cm^{-1} atm^{-1} (base e) for the 1055 cm^{-1} O_3 peak at ~1 cm^{-1} resolution; however, their spectra are more comparable to our FT-IR spectra smoothed to a resolution of 2-4 cm^{-1}. In the present work, a value of 15.1 cm^{-1} atm^{-1} at our defined 1 cm^{-1} resolution was measured for the absorption coefficient of the 1055.4 cm^{-1} O_3 peak (Table 1).

The absorption coefficient for the Q branch of methylhydroperoxide at 1321.0 cm^{-1} was derived by comparing intensities of the broad features (i.e., P and R branches) of our 1 cm^{-1} resolution spectrum with those of a calibrated high-resolution (1/16 cm^{-1}) spectrum which was provided by Dr. Hiromi Niki of the Ford Motor Research Laboratories (see also Reference 24). The value for the 2102.0 cm^{-1} Q branch of diazomethane (CH_2N_2) was similarly derived from the data of Urry, et al. (Reference 19), while those for nitrous acid (HONO) were derived from the work of Calvert, et al. (Reference 20). Drs. L. Molina and M. Molina (University of California, Irvine) provided the absorption coefficient for H_2O_2, which was measured by employing a constant flow of H_2O_2 vapor through a 1 m pathlength absorption cell. The absorption coefficients given in Table 1 for pernitric acid ($HOONO_2$), tetramethyltetrazene-2[$(CH_3)_2NN=NN(CH_3)_2$], and nitrogen pentoxide (N_2O_5) are literature values (References 16-18).

For product spectra involving heavily overlapped absorptions by two or more species, the use of peak-to-valley measurement of a resolved fine structure is more convenient and often more accurate than peak-to-baseline measurement. This is true, for example, when the heavily structured band system of N_2H_4 centered at ~940 cm^{-1} is strongly interfered by the well-resolved vibration-rotation lines of the NH_3 inversion doublet at ~950 cm^{-1}. In this case, neither N_2H_4 nor NH_3 can be subtracted based on peak-to-baseline absorbances in order to measure the other component. A

detailed comparison of the spectra of the pure compounds showed that the peak-to-valley measurement of the 974.4 cm^{-1} fine structure of N_2H_4 (i.e. the intensity difference between points at 974.36 and 973.39 cm^{-1}, Table 1) is not interfered with by NH_3 absorptions. Despite the lower absorption coefficient associated with this procedure, it was favored over the 957.48 cm^{-1} peak-to-baseline measurement for N_2H_4. Where appropriate, similar procedures were followed in the measurement of other compounds (e.g., O_3, H_2O_2, NO_2).

The approximate detection limits listed in Table 1 are for a pathlength of 68.3 m (as noted above, total pathlengths of 68.3 m and 102.4 m were employed throughout this study). For the narrow Q-branch features and the peak-to-valley measurements, the calculated instrument sensitivity is based on detection of an absorption of 0.005 absorbance units. Detection limits for peak-to-baseline measurements are based on ~0.01 absorbance units, since inclusion of the broader band envelopes introduces an additional uncertainty in the baseline position.

3.2 DARK DECAY OF THE HYDRAZINES

Two sets of experiments were carried out in two separate chambers (constructed of Teflon® film from the same roll of material) to study the disappearance from the gas phase of the hydrazines in the dark. The first set of experiments was conducted in the ~6400 ℓ chamber to investigate the dark decay of N_2H_4, MMH, and UDMH in dry air (RH < 17%, T ~24°C). Approximately 0.02 ppm each of cyclohexane and 2,2-dimethylpropane were introduced into each hydrazine-air mixture to serve as "tracers" for OH radicals that might be formed during the dark decay. The second set was carried out in the ~3800 ℓ chamber for the individual hydrazines and for Aerozine-50 under both dry and humidified (RH > 50%, T ~21°C) conditions. No organic tracers were employed in this second set of experiments.

The dark decay half-lives measured are summarized in Table 2, along with the conditions for each experiment. Gas chromatographic analyses showed no significant changes in the concentration ratio of the organic tracers for each of the first set of experiments. This indicates that no measurable levels of OH radicals (i.e., $< 4 \times 10^5$ cm^{-3}) were generated

TABLE 2. DARK DECAY OF HYDRAZINES IN TEFLON® CHAMBERS.

Date	Compound	% Relative Humidity "Dry"	"Wet"	T(°C)	Length of Experiment (hrs)	Initial Conc. (ppm)	Half-Life (hrs)[b]
27 May 1981	N_2H_4	13[a]		24	6	11.4	16.4 ± 0.5
12 Nov 1981	"	12		23	4	11.4	6.8 ± 0.2
13 Nov 1981	"	12		22	6	12.8	10.8 ± 0.2
13 Nov 1981	"		55	22	3.5	11.5	4.9 ± 0.1
29 May 1981	MMH	10[a]		24	8	11.5	49.8 ± 2.8
17 Nov 1981	"	17		22	6	10.3	30.1 ± 0.7
17 Nov 1981	"		60	21	4.5	9.3	19.8 ± 2.3
28 May 1981	UDMH	11[a]		24	10	12.3	841 ± 384
16 Nov 1981	"	17		22	6	13.1	341 ± 64
16 Nov 1981	"		50	22	4.5	13.7	70.9 ± 9.6
18 Nov 1981	Aerozine-50:	17		21	6		
	N_2H_4					12.4	11.3 ± 0.3
	UDMH					13.5	204 ± 44
24 Nov 1981	Aerozine-50:		51	20	4		
	N_2H_4					12.3	7.6 ± 0.3
	UDMH					14.1	113 ± 24

[a]Carried out in the 6400 ℓ chamber; experiments in November 1981 were conducted in the 3800 ℓ chamber.
[b]Errors given correspond to one standard deviation.

during the decomposition of N_2H_4, MMH and UDMH. (The use of a pair of organic compounds, one with low reactivity [in this case, 2,2-dimethylpropane] and the other with relatively high reactivity [cyclohexane] towards OH radicals in measuring levels of OH radicals and their rates of reaction with other species is explained in more detail in Section 3.3).

The decay experiments in each chamber were carried out with no intervening experiments involving other types of reactions (e.g., hydrazines + O_3). Prior to the first dark decay experiment with N_2H_4 (27 May 1981, Table 2), a preliminary $N_2H_4 + O_3$ reaction under condition of excess N_2H_4 was the only experiment conducted in the 6400 ℓ bag. An experiment to determine the mixing time by injecting ozone into the chamber was the only run performed in the 3800 ℓ bag prior to the first (12 Nov 1981) dark decay experiment with N_2H_4 in this chamber.

3.2.1 Hydrazine

As seen in Table 2, the decay rate of N_2H_4 in dry air was faster in the 3800 ℓ chamber (12 Nov and 13 Nov 1982 runs) than in the 6400 ℓ chamber (27 May 1981 run). Of the two experiments carried out in dry air in the smaller chamber, the second (13 Nov 1981) showed a significantly slower N_2H_4 decay rate than the first (12 Nov 1981). The decomposition rate of N_2H_4 has been reported by several workers (References 4, 25) to be highly affected by the surface characteristics of the reaction vessel. Thus, the difference in the decay rates observed in the above two runs in dry air may be largely a result of "conditioning" of the chamber's Teflon® walls.

The experiment in humidified air resulted in a half-life of 4.9 hours in the 3800 ℓ bag compared to 10.8 hours found in the previous run in dry air on the same day (13 Nov 1981). The accelerated decay of the hydrazines in wet air has also been reported by previous workers (References 6, 26).

The decomposition products observed were ammonia (NH_3) and diazene (HN=NH). For the dark decay experiments on 13 November 1981, the increases in NH_3 concentration observed at the end of the reactions corresponded to ~6% and ~9% of the N_2H_4 lost for dry and humidified air, respectively. No quantitative measure of the diazene formed can be given since the infrared absorption coefficients for this species have yet to be determined. Based on relative absorbances, however, the proportionate

20

yield of diazene at the end of the first three hours was 2.7 times higher in humidified air than in dry air. (The positive identification of diazene through its infrared spectrum is discussed in Section 3.3.2).

The main end-products of N_2H_4 decomposition were presumably N_2 and H_2O, as was found in auto-oxidation studies by Bowen and Birley (Reference 25) in the temperature range $100-160°C$ and by Stone (Reference 4) in more recent experiments at room temperature. Of course, the amounts of N_2 and H_2O that were possibly generated by N_2H_4 decomposition represent only minute fractions of these species' initial concentrations in the chemical systems we employed, and thus could not be measured.

3.2.2 Monomethylhydrazine

The decay of MMH in dry air was significantly slower in the 6400 ℓ chamber (29 May 1981 run) than in the 3800 ℓ chamber (17 Nov 1981 run). The dark decay in the 3800 ℓ bag with humidified matrix air proceeded ~1.5 faster than in dry air (17 Nov 1981 experiments).

The only products observed by infrared spectroscopy were NH_3 and methyldiazene $(CH_3N=NH)$. At the end of the experiments, NH_3 formation constituted only 2% and 4% of MMH loss in dry and humidified air, respectively (17 Nov 1981 runs). Within the errors of the absorbance measurements, approximately the same proportionate amounts of methyldiazene were formed during the first 4 hours of the above two experiments conducted in the 3800 ℓ chamber. Reliable absorption coefficients from direct measurements are not available for methyldiazene; however, an approximate estimate of methyldiazene concentration at the end of 4 hours in both experiments (17 Nov 1981 runs) is ~0.3 ppm. [This estimate of methyldiazene yield was based on an absorption coefficient derived from the material balance in MMH + O_3 systems (see Section 3.3.3).]

Methane and nitrogen were observed by Vernot, et al. (Reference 27) to be the major products in the auto-oxidation of MMH at room temperature. In the decay of MMH at ppm concentrations, Stone (References 4, 28) detected methane, methanol, methyldiazene, and other products with unknown absorptions in the infrared. However, the material, size, and surface characteristics of the reaction vessels used by the above authors differed considerably from those of the reaction chambers used in the present study.

3.2.3 Unsymmetrical Dimethylhydrazine

UDMH displayed the highest stability among the three individual hydrazines, with half-lives in dry air of 841 ± 384 hours in the 6400 ℓ chamber and 341 ± 64 hours in the 3800 ℓ chamber. The large errors in the decay half-lives reported in Table 2 are inherent to the measurement of minute concentration changes with time. A comparison of t,e two runs on 16 Nov 1981 shows that, analogous to N_2H_4 and MMH, UDMH decayed significantly faster in humidified air. At the end of each experiment on 16 Nov 1981, less than 5% of the small total losses in UDMH could be accounted for by NH_3 formation. No other product was detected by infrared spectroscopy.

Results of earlier studies which are relevant to the above experiments are those of Loper (Reference 29), Stone (References 6, 28), and Urry, et al. (Reference 19). All found that the dark reaction of UDMH in oxygen atmospheres produces nitrogen, water and formaldehyde dimethylhydrazone [$(CH_3)_2NN=CH_2$]. Detectable amounts of the latter product were not generated in our reaction systems during the durations of these experiments (~5-10 hours).

3.2.4 Aerozine-50

In addition to the dark decay studies of the individual hydrazines, the decomposition of an approximately equimolar mixture of N_2H_4 and UDMH (Aerozine-50) was monitored in the 3800 ℓ chamber. The samples of N_2H_4 and UDMH were introduced separately into the chamber as vapors.

In dry air, the observed decay rate of the N_2H_4 component was approximately the same as that of N_2H_4 alone (Table 2). A shorter half-life for the UDMH component than for UDMH alone was found, but the large errors involved makes this comparison less certain. Note that when the errors are taken as two standard deviations, the half-life for UDMH in the Aerozine-50 experiment (18 Nov 1981) overlaps with that of the 16 Nov 1981 UDMH run.

Relative to the decay rate in dry air (18 Nov 1981), the Aerozine-50 components decayed faster in humidified air (24 Nov 1981). However, in this humidified system both N_2H_4 and UDMH displayed longer half-lives compared to the individual hydrazines in experiments of similar conditions (13 Nov and 16 Nov 1981 runs).

Ammonia and diazene were the only observed products in the Aerozine-50 decay experiments, suggesting that no detectable amounts of products were formed from UDMH. The amount of NH_3 formed accounts for only ~3% and ~4% of N_2H_4 lost in dry and humidified air, respectively. As in the N_2H_4 experiments, more diazene was formed in humidified air (by approximately a factor of two at the end of 4 hours) than in dry air.

The only previous data on Aerozine-50 decay in oxygen atmospheres are those from the work of Stone (Reference 6). Using FT-IR spectroscopy, the same major products as those formed in the decomposition of the individual hydrazines were observed: NH_3 and H_2O from N_2H_4, and formaldehyde dimethylhydrazone from UDMH. However, Stone observed a dramatic increase in the decay rate of the UDMH component in a 20% O_2 - 80% He mixture over that of UDMH alone in the same atmosphere and observed that the N_2H_4 component had a half-life a factor of two longer than did N_2H_4 alone. Our decay experiment with Aerozine-50 in humidified air showed a relative decrease in the decay rate of the N_2H_4 component (13 Nov and 24 Nov 1981 runs, Table 2). However, the experiments in dry air, which are more comparable to Stone's experiments, did not show a significant difference between the decay of the N_2H_4 component (18 Nov 1981) and that of N_2H_4 alone (13 Nov 1981); because of the large uncertainties, the apparent increase in the decay rate of UDMH in Aerozine-50 may not be real. The disparity between our findings and those of Stone (Reference 6) strongly suggests that the contribution of heterogeneous processes in our respective systems were significantly different.

3.2.5 Summary

Although references have been made to previous relevant auto-oxidation studies, particularly with respect to the identities of the products observed, the present data on the dark decomposition rates of the fuel hydrazines are generally not comparable to those of the earlier investigations. The obvious differences stem not only in the use of different concentration regimes (i.e., ppm vs. torr concentrations), but more importantly in our use of reaction chambers which are orders of magnitude larger than those previously employed and are constructed of a material (Teflon®) which has significantly different surface characteristics.

23

Even within our consistent set of experiments in the large-volume Teflon® chambers, the influence of surface-to-volume ratio and altered surface characteristic were evident. Thus, significant differences in the decay rates for all hydrazines were observed between the 6400 ℓ and 3800 ℓ chambers, with faster decompositions occurring in the smaller chamber. Likewise, the effect of surface "conditioning" was apparent in the two N_2H_4 decay experiments conducted in dry air. The dark decay rates observed in these experiments are significantly lower than those observed in our initial study (Reference 3) which employed an ~30,000 ℓ outdoor Teflon® chamber. In the latter study, however, the chamber was susceptible to particulate contamination (e.g., dusts and aerosols from air pollution) since it was routinely flushed with ambient air before the final flush and fill of purified air.

No simple explanation can be given for the accelerated decay rates with increased humidity. The common alkyl hydrazines are known to be hygroscopic and fume in moist air; hydrazine itself forms an extremely stable hydrate, b.p. 119–120°C, from which it is released only by solid alkali (Reference 30). The baseline slope of the infrared spectrum in the region above 2000 cm^{-1} noticeably increased with time in the experiments with MMH in humidifed air, normally an indication of particulate formation, but no similar pattern occurred in the case of UDMH or N_2H_4. Our infrared spectroscopic observations are thus inconclusive with respect to the possible formation of the hydrazine hydrates in the vapor phase.

The mechanistic aspect of the decomposition process (autooxidation) for the hydrazines remain largely unexplained (Reference 31) and our experiments were not intended to deal with this topic. However, the use of organic tracers in one set of experiments did not reveal measurable levels of OH radicals formed during the dark decay of the hydrazines. The dark decomposition rates determined for the individual hydrazines allowed approximate corrections for such losses to be made in measurements of their reactions with atmospheric species such as O_3 and NO_x, the subjects of this investigation.

3.3 THE REACTIONS OF HYDRAZINES WITH OZONE

The reactions of ozone with N_2H_4, MMH, and UDMH were studied in the indoor Teflon® chambers under at least three different reaction conditions

and employing three different sets of initial reactant concentrations. The reactant concentrations employed were: (1) excess hydrazine, in which ~5 ppm of O_3 was flushed into the chamber already containing 10-20 ppm of the hydrazine; (2) equimolar, in which ~10 ppm of O_3 was flushed into the chamber containing ~10 ppm of the hydrazine; and (3) excess O_3, in which ~5 ppm of the hydrazine was flushed into the chamber containing 10-20 ppm of O_3. The experiments were carried out in air (1) without any other added reactants present, (2) with ~0.2 ppm each of n-octane and 2,2,3,3-tetramethylbutane [or hexamethylethane (HME)] present as "tracers" to monitor hydroxyl radical levels (see below), or (3) with ~270 ppm of added n-octane present as an OH radical trap. In addition, one equimolar N_2H_4 + O_3 run was conducted in an N_2 atmosphere instead of air, and several kinetic experiments were performed in which the rates of O_3 decay in the presence of excess N_2H_4 and MMH in a ~175 ℓ Teflon® bag were measured. One experiment on the reaction of Aerozine-50 with O_3 at initial equimolar amounts in air was also carried out. All runs were conducted at 20-25°C and at generally low (< 25%) relative humidities.

The "tracer" experiments were carried out to determine whether, and at what levels, hydroxyl radicals were generated in the reaction of the hydrazines with ozone. n-Octane and 2,2,3,3-tetramethylbutane were chosen since they react with hydroxyl radicals with significantly different rates [with rate constants of 9.0×10^{-12} and 1.1×10^{-12} cm^3 molecule^{-1} sec^{-1}, respectively (References 32, 33)], they do not react with O_3, and they can be readily analyzed together on the same gas chromatographic column (see Section 2.5.3). Since under the conditions of the experiments, reaction of these species with O_3, the hydrazines, and HO_2 are negligible, and since it is improbable that they react significantly with N_2H_3 radicals, diazenes, or any other intermediates or products expected to be involved in the hydrazine + O_3 system (other than the OH radical), the only mode of consumption of these two organics in these systems should be via reaction with OH radicals. Thus,

$$d[\text{n-octane}]/dt = -(k_1[\text{OH}] + D)[\text{n-octane}] \qquad (I)$$

$$d[\text{HME}]/dt = -(k_2[\text{OH}] + D)[\text{HME}] \qquad (II)$$

25

where k_1 and k_2 are the OH radical rate constants for n-octane and HME, respectively, and D reflects the slight dilution in the tracers which occurs when the second reactant (O_3 or hydrazine) is injected into the chamber. The effect of dilution is removed by combining equations (I) and (II) and rearranging,

$$\frac{d \ln ([HME]/[n\text{-}octane])}{dt} = (k_1 - k_2) [OH] \qquad (III)$$

Integrating equation (III) over the entire O_3 + hydrazine reaction time (t_1 to t_2) and rearranging then yields

$$\int_{t_1}^{t_2} [OH]dt = \frac{\Delta \ln ([HME]/[n\text{-}octane])}{(k_1 - k_2)} \qquad (IV)$$

Thus the change in the ratio of the tracers can be used to measure the integrated OH radical levels formed in the hydrazine + O_3 reactions. Since n-octane, the more reactive of the tracers, reacts with OH radicals approximately seven times slower than does hydrazine, the presence of 0.2 ppm each of the tracers in reaction mixtures with initial hydrazine concentrations of > 4 ppm should have an essentially negligible perturbation on the overall hydrazine + O_3 reactions. This prediction was proven valid, since it was found that addition of the tracers had no noticeable effect on the observed reaction rates, reactant stoichiometries, or product yields (Sections 3.3.2-3.3.4).

Since OH radicals were observed to be present in these O_3 + hydrazine systems, the radical trap experiments were carried out in order to determine the effect of significantly reducing hydroxyl radical levels on the overall reaction rates, product yields, and reactant stoichiometries. n-Octane was chosen as the radical trap because it has the highest OH radical rate constant among the hydrocarbons which have minimal interferences in the infrared analyses and also do not react with O_3. With 270 ppm of n-octane present, the OH radical levels should be reduced by at least a factor of 3 in the excess hydrazine experiments (based on the known OH + n-octane [Reference 32] and OH + hydrazine [Reference 7] rate constants), and by at least a factor of 8 in the excess O_3 runs.

The detailed concentration-time data from the environmental chamber experiments in which O_3 was reacted with N_2H_4, MMH, UDMH, and Aerozine-50

26

are given in Appendices A to D. For the purpose of the discussion of the results given below, the experiments are identified by the table number in the Appendix, e.g., run B-2 refers to the MMH + O_3 experiment whose detailed results are given in Table B-2 of Appendix B. In the following sections, the results of the N_2H_4 + O_3 and MMH + O_3 kinetic experiments performed in the small (~175 ℓ) bags, and of the reactions of O_3 with N_2H_4, MMH, UDMH and Aerozine-50 in the large-volume environmental chambers, are discussed and a mechanistic interpretation of the results is given.

3.3.1 Rates of Reaction of O_3 with N_2H_4 and MMH in ~175 ℓ Reaction Bags

Ozone decay rates were measured in the presence and absence of excess N_2H_4 and MMH in the ~175 ℓ Teflon® reaction bags employing the experimental techniques described in Section 2.5.4. For three of the experiments involving hydrazine and for that with monomethylhydrazine, as well as for one of the background decay determinations, large excess amounts of an OH radical trap (either cyclohexane or n-octane) were added. In the absence of added hydrazine, the O_3 decay rates ranged from 0.0005 - 0.0016 min^{-1}, which is within the range typically observed for these bags. In the presence of excess N_2H_4, the O_3 decays were very much more rapid, with O_3 lifetimes being of the order of ~1 min, though the decays exhibited a significant amount of scatter around the fitted exponential decays. This scatter may have been due to instrumental noise, since the ozone monitor necessarily had to be set on a relatively fast time constant (1 sec), or it may have been due to the reaction occurring on the order of the mixing time. The O_3 decay was even more rapid in the single experiment carried out with MMH, with the observed decay rate of ~0.7 sec^{-1} (42 min^{-1}) possibly being limited by the chart recorder pen response time. The initial conditions and the observed decay rates for these experiments are summarized in Table 3.

If it is assumed that consumption of O_3 by reactions with the products and intermediates formed is negligible, then the processes removing O_3 are:

$$O_3 + wall \rightarrow loss\ of\ O_3 \qquad\qquad (1)$$

$$O_3 + hydrazine \rightarrow products \qquad\qquad (2)$$

TABLE 3. INITIAL CONCENTRATIONS AND O_3 DECAY RATES FOR THE
REACTION OF O_3 WITH HYDRAZINE AND MONOMETHYLHYDRAZINE IN THE
~175 ℓ TEFLON® REACTOR.

| Run No. | Initial Concentrations (ppm) | | | | O_3 Decay Rate (min^{-1}) |
	O_3	N_2H_4	MMH	Radical Trap[a]	
1	1.07	-	-	-	0.0005
2	0.79	-	-	~103	0.0016
3[b]	1.19	-	-	-	0.0015
4	0.40	9.7	-	-	0.652 ± 0.05
5	0.15	10.7	-	-	1.47
6	0.24	10.7	-	-	1.58
7	0.21	10.8	-	~100	1.38
8	1.03	-	-	-	0.0014
9	0.32	5.7	-	-	0.67
10	0.26	5.4	-	-	0.67
11	0.16	5.6	-	~100	0.76
12	0.26	15.6	-	~200	1.44
13	~0.4[c]	-	5.2	~350[d]	> 42

[a]Radical trap = cyclohexane, except as noted.
[b]100 ppm NH_3 added.
[c]Estimated concentration; decay rate too rapid to determine initial value.
[d]Radical trap = n-octane.

and hence

$$-d[O_3]/dt = (k_1 + k_2[hydrazine])[O_3] \qquad (V)$$

where k_1 and k_2 are the rate constants for reactions (1) and (2). With
the hydrazine concentration in large excess over the initial O_3 concentra-
tion ($[hydrazine]/[O_3]_{initial} > 10$), the hydrazine concentration remains
essentially constant throughout the reaction, and equation (V) may be
rearranged to yield:

$$-dln[O_3]/dt = k_1 + k_2[hydrazine] \qquad (VI)$$

Thus, from the dependence of the ozone decay rate, $-dln[O_3]/dt$, on the
reactant concentration, and with a knowledge of the background ozone decay
rate, k_1, the apparent rate constant k_2 may be readily obtained.

The ozone decay rates observed in the N_2H_4 experiments are plotted against the hydrazine concentration in Figure 2. The data, although appreciably scattered, yield an apparent rate constant of 0.106 ± 0.022 ppm^{-1} min^{-1} [$(7 \pm 2) \times 10^{-17}$ cm^3 molecule^{-1} sec^{-1}], with the radical trap having no obvious effect. The O_3 rate observed in the O_3 + MMH experiment, which probably reflects primarily mixing time and/or instrument response time, yields a lower limit apparent rate constant of ~ 8 ppm^{-1} min^{-1} ($\sim 5 \times 10^{-15}$ cm^3 molecule^{-1} sec^{-1}).

It should be noted that the apparent rate consants, k_2, derived in this way would reflect the true, elementary O_3 + hydrazine rate constant only if no product is formed which reacts much more rapidly with O_3 than does the parent hydrazine. (If a product reacted equally rapidly, it would not influence the measurement significantly because the hydrazine, being in excess, would be present at much higher concentrations.) Unfortunately, the results of the environmental chamber experiments, described in the following sections, indicate that, at least for hydrazine, this is probably not the case. Thus the O_3 + N_2H_4 rate constant derived using this technique must be considered an upper limit value.

3.3.2 Reactions of Hydrazine with Ozone in Environmental Chambers

A total of nine experiments in which N_2H_4 was reacted with O_3 in air and one in which it was reacted in N_2 were performed. The detailed concentration-time data for the reactants and products monitored by FT-IR for all ten of these experiments are given in Appendix A and a summary of the conditions and results are given in Table 4. In two of the excess hydrazine runs (with and without the n-octane radical trap: A-1 and A-7), a second injection of O_3 was carried out following the consumption of the initially-added O_3, and the results of these second injections are also summarized in Table 4.

In all cases but one, the reaction went to completion within the time frame of the experiments, with either hydrazine or ozone being completely consumed within 2-20 minutes, depending on the conditions. The only exception was run A-4, the equimolar run with added tracers, where neither reactant was in excess throughout the reaction (Table A-4), and small levels of both reactants (< 0.2 ppm) were present when monitoring stopped after ~ 21 minutes. For the other runs, the times required for the reactions to go to completion are evident from the detailed data in Appendix

29
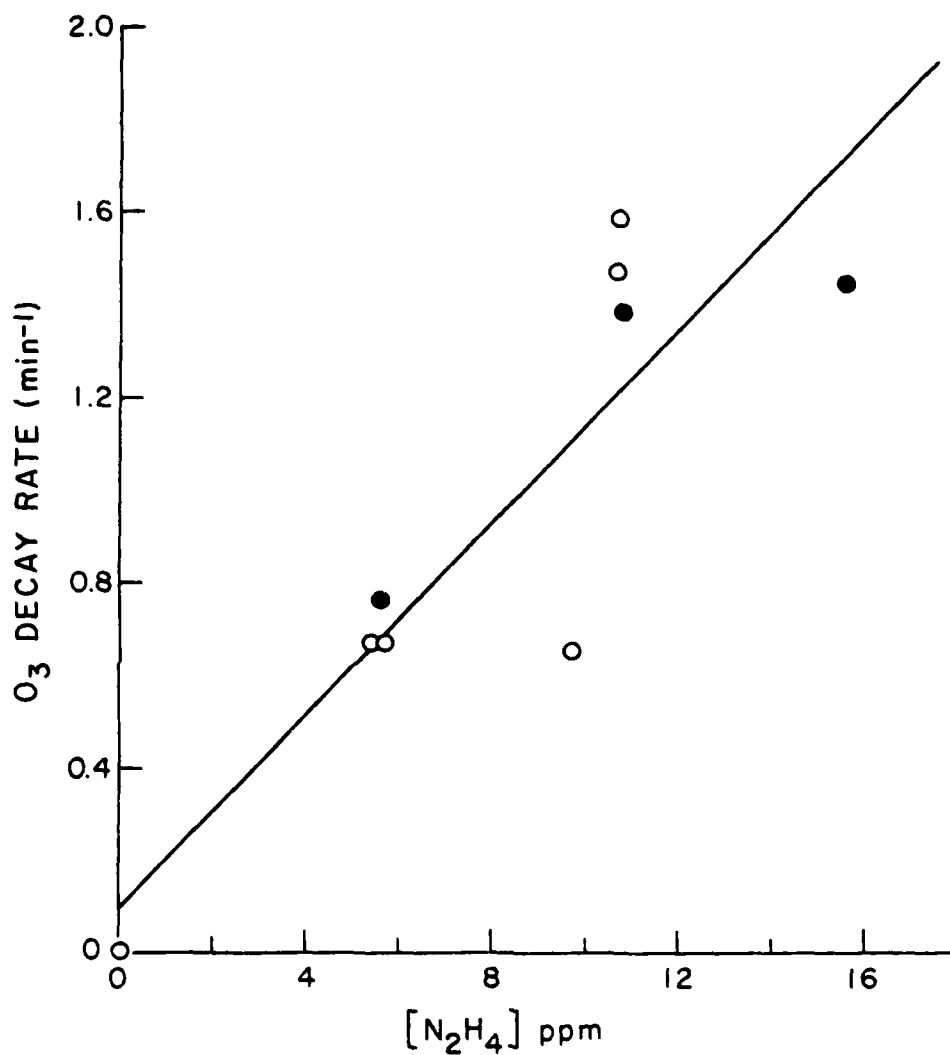
Figure 2. Plot of O_3 Decay Rates Against Hydrazine Concentration for Experiments Carried Out in ~175 ℓ Teflon® Reaction Bag. O - No Radical Trap Present; ● - Radical Trap Present.

TABLE 4. SUMMARY OF CONDITIONS AND RESULTS FOR THE $N_2H_4 + O_3$ EXPERIMENTS.

Expt. ID[a]	Conditions			Initial Conc.		Reaction Time (min)	$\Delta[N_2H_4]$[d] (ppm)	$\dfrac{\Delta[O_3]}{\Delta[N_2H_4]}$	$\dfrac{\int[OH]dt}{\Delta[N_2H_4]}$ $(10^{-6}\,\text{min})$[e]	$\dfrac{(\text{Product})}{\Delta[N_2H_4]} \times 100$[f]				
	Radical Trap[b]	Tracer[c]	Matrix Gas	N_2H_4 (ppm)	O_3 (ppm)					N_2H_2 (Δ/ppm)[g]	H_2O_2	N_2O	HONO	NH_3
A-1	No	No	Air	18.0	5.0	4.4	6.9	0.7		0.65	51	< 0.6	< 0.6	1.6
A-2	No	Yes	Air	12.3	3.5	5.4	4.5	0.8	0.7	0.65	60	< 0.9	< 0.9	1.1
A-3	No	No	Air	9.2	10.2	7.4	9.2	1.0		~0	49	< 0.4	< 0.4	2.5
A-4	No	Yes	Air	9.8	10.2	20.8	9.6	1.0	2.5	~0	54	< 0.5	< 0.4	1.5
A-5	No	No	Air	4.3	16.6	1.4	4.3	1.3		~0	40	< 1.4	< 0.9	< 4.7
A-6	No	No	Air	4.8	15.9	3.4	4.8	1.5	4.9	~0	42	1.5	< 0.8	< 2.1
A-7	Yes	No	Air	17.0	4.4	6.4	4.5	1.0		0.42	24	< 0.9	< 0.9	1.1
A-8	Yes	No	Air	10.3	10.0	21.8	7.3	1.4		~0	7.5	< 0.9	< 0.5	1.6
A-9	Yes	No	Air	4.2	16.6	7.4	4.2	1.9		~0	< 4	< 0.9	< 0.9	< 1.4
A-10	No	No	N_2	11.7	11.7	2.4	8.2	1.4		0.61	18	2.0	2.4	< 4.8
A-1[h]	No	No	Air	10.8	25.3	1.4	10.8	1.2		<	32	2.7	< 0.4	2.7
A-7[h]	Yes	No	Air	11.9	26.1	8.8	11.9	1.5		<	0.7	< 0.3	< 0.3	1.0

a. Run identification (ID) refers to table number in Appendix A where data are given in detail.

b. "No" means ~270 ppm of n-octane was present as radical trap.

c. "Yes" means ~0.2 ppm each of n-octane and hexamethylethane (HME) were added as organic tracers for OH radicals (see footnote e).

d. Amount of N_2H_4 consumed within the reaction time indicated.

e. $\int[OH]dt$ was calculated from change of $\ln([HME]/[n\text{-octane}])$ using $k(OH + HME) = 1.1 \times 10^{-12}$ cm^3 molecule^{-1} sec^{-1} (Reference 33) and $k(OH + n\text{-octane}) = 9.0 \times 10^{-12}$ cm^3 molecule^{-1} sec^{-1} (Reference 32).

f. Values preceded by "<" sign were based on detection limit; others were measured values.

g. Absorbance of the 1276.7 cm^{-1} Q branch (at 1 cm^{-1} resolution, 68.3-meter path) divided by $\Delta[N_2H_4]$.

h. Second O_3 injection to a reacted mixture: product yields reflect changes in concentrations.

i. N_2H_2 was initially present in the reacted mixture and was consumed by the additional O_3 injected.

31

A, and are indicated in Table 4 as the "reaction time" — the time of the first or second spectrum acquisition performed after one of the reactants was consumed.

Estimates of the apparent overall rate constants for the reaction of ozone with hydrazine were obtained from the rates of decay of hydrazine in the presence of excess ozone and from the rates of decay of O_3 in excess N_2H_4. These rates depended on whether or not the n-octane radical trap was present. As shown in the plots of $\ln[O_3]$ against time in Figure 3, the O_3 decays in the excess N_2H_4 runs in the absence of the radical trap were exponential and corresponded to apparent overall $O_3 + N_2H_4$ rate constants of $(8.7 \pm 1.4) \times 10^{-2}$ and $(8.3 \pm 1.2) \times 10^{-2}$ ppm^{-1} min^{-1} ($[6.0 \pm 1.0] \times 10^{-17}$ and $[5.7 \pm 0.8] \times 10^{-17}$ cm^3 $molecule^{-1}$ sec^{-1}) for runs A-1 and A-2, respectively, in good agreement with the apparent rate constant of $(7 \pm 2) \times 10^{-17}$ cm^3 $molecule^{-1}$ sec^{-1} derived from the experiments employing the ~175 ℓ Teflon® bags (Section 3.3.1). (The uncertainties in the rate constants derived for runs A-1 and A-2 reflect primarily those of the changes in the hydrazine concentration used to calculate the rate constant; the uncertainties introduced by the scatter of the O_3 decay data were much smaller.)

The good agreement between the results of runs A-1 and A-2 indicates that the presence of the radical tracers did not affect the overall rate of reaction. The O_3 decay in the excess N_2H_4 run (A-7) conducted in the presence of the radical trap, included in Figure 3, was also exponential, but corresponded to an overall rate constant of $(5.9 \pm 0.6) \times 10^{-2}$ ppm^{-1} min^{-1} ($[4.1 \pm 0.4] \times 10^{-17}$ cm^3 $molecule^{-1}$ sec^{-1}), which is a factor of 1.4 lower than those obtained in the absence of the radical trap. This result is in apparent conflict with the results of the ~175 ℓ Teflon® bag runs, where the presence of the radical trap was observed to have no measurable effect.

The apparent rate constant obtained from the rate of decay of hydrazine in excess O_3 depended even more strongly on the presence of the radical trap. Without the trap, the overall reaction in the excess O_3 runs was much more rapid than observed in the excess N_2H_4 or the equimolar runs, with N_2H_4 being completely consumed in less than ~1.4 minutes (runs A-1 [second injection], A-5, and A-6). This corresponds to an upper limit apparent rate constant of ~0.4 ppm^{-1} min^{-1} (~3 × 10^{-16} cm^3 $molecule^{-1}$
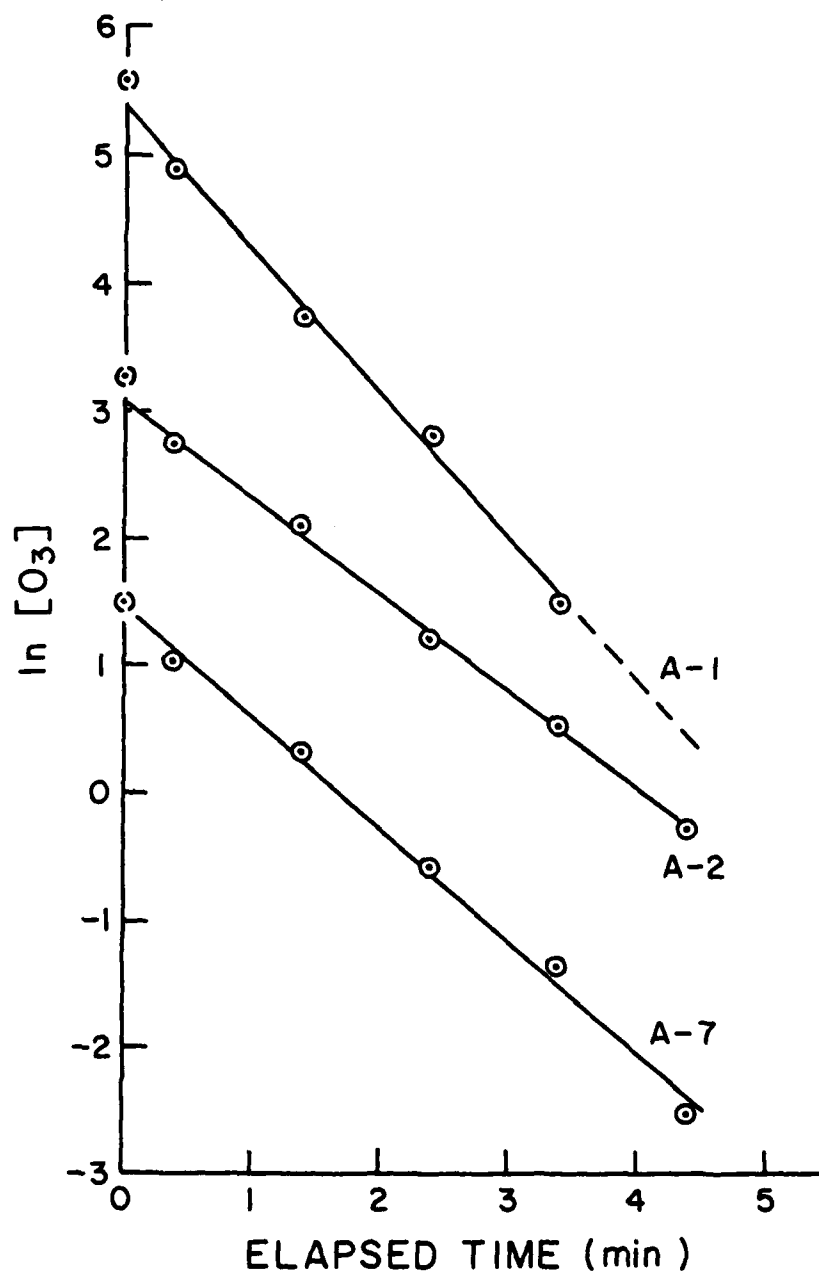
Figure 3. Plots of ln[O_3] Against Elapsed Time for the N_2H_4 + O_3 Chamber Experiments in which N_2H_4 Was in Excess. ([O_3] in ppm; Plots Offset by +4 Log Units for Run A-1, and by +2 Units for A-2.) ⊖ – Experimental Points Used to Calculate Least Squares Lines Shown; (·) – Calculated O_3 Injected (Not Used to Calculate Lines).

sec^{-1}), which is over a factor of 3 higher than the rate constant derived from the excess hydrazine runs. In the presence of the radical trap, the N_2H_4 decay in excess O_3 was considerably slower (run A-9), and is shown in Figure 4, where a plot of $\ln[N_2H_4]$ against time is given. The N_2H_4 decay was reasonably exponential and corresponds to an overall rate constant of $(4.3 \pm 0.5) \times 10^{-2}$ ppm^{-1} min^{-1} ($[3.0 \pm 0.3] \times 10^{-17}$ cm^3 molecule^{-1} sec^{-1}). This is about 30% lower than the rate constant derived from O_3 decay in excess N_2H_4 when the radical trap was present.

In the three runs with the added n-octane and HME tracers, both HME and n-octane were observed to decline when O_3 and N_2H_4 reacted, with the
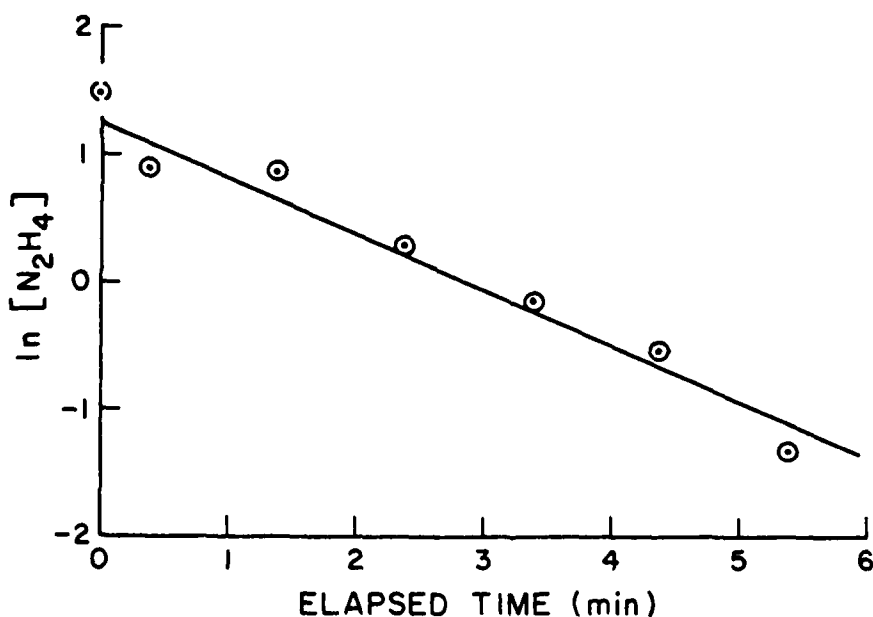
Figure 4. Plot of $\ln[N_2H_4]$ Against Elapsed Time for the $N_2H_4 + O_3$ Chamber Run A-9 Performed in Excess O_3 in the Presence of the Radical Trap. $\ominus$ - Experimental Points Used to Calculate the Least Squares Line Shown; ($\cdot$) - Calculated N_2H_4 Injected (Not Used to Calculate Line).

amount of tracers consumed and the [HME]/[octane] ratio increasing as the initial $[O_3]/[N_2H_4]$ ratio increased. As discussed above, this indicates the formation of OH radicals in this system, with their overall levels being higher when O_3 is in excess. This is consistent with the results of the radical trap experiments, where the suppression of the overall rates by the radical traps also indicated the intermediacy of hydroxyl radicals, and where the greatest effect was observed in the excess O_3 system, indicating greater radical levels in that system. Mechanistic implications of this are given in Section 3.3.6.

The hydrazine-O_3 stoichiometry was also observed to vary with the initial $[O_3]/[N_2H_4]$ ratio and to be affected by the addition of the radical trap. In the absence of the radical trap, the ratio of the reactants consumed ($\Delta[O_3]/\Delta[N_2H_4]$) ranged from ~0.7 when N_2H_4 was in excess, to ~1.0 in equimolar mixtures, to ~1.4 when O_3 was in excess (Table 4). The presence of the radical trap appeared to increase the amount of O_3 consumed for a given amount of N_2H_4 reacted, with the $\Delta[O_3]/\Delta[N_2H_4]$ ratio ranging from ~1.0 in excess N_2H_4 to almost 2 in excess O_3.

The major products observed by FT-IR spectroscopy in the $N_2H_4 + O_3$ experiments were hydrogen peroxide (H_2O_2) and diazene (N_2H_2). Much smaller increases in ammonia (NH_3), over its initial levels as an impurity, were observed during the reactions. Nitrous oxide (N_2O) was observed as a minor product and was generally above the detection limit only in runs with excess O_3 in the absence of radical trap; however, significantly higher yields were measured in the reaction conducted in an N_2 atmosphere.

The concentration-time profiles observed in the $N_2H_4 + O_3$ experiment with approximately equimolar reactants (run A-4) are shown in Figure 5, and Figure 6 illustrates the reactant and product spectra at selected times in that experiment. The strongest absorptions of N_2H_2 could be clearly seen only upon subtraction of the H_2O_2 absorption band centered at 1266.0 cm^{-1}. H_2O_2, NH_3, and N_2O were observed in our previous study (Reference 3), but this is the first time that we report the detection of N_2H_2 as a product of the $N_2H_4 + O_3$ reaction. Our previous study employed much longer pathlengths (~500 m) such that the relatively larger H_2O interferences at > 1250 cm^{-1} made it difficult to confirm the presence of N_2H_2.

Figure 5. Concentration-Time Plots for Reactants and Selected Products
Observed in the N_2H_4 + O_3 Run A-3 with Equimolar Reactants.

Figure 6. Infrared Spectra from N_2H_4 + O_3 Experiment with Equimolar Reactants (Run A-4); Res = 1 cm^{-1}, Pathlength = 68.3 m. (a) Initial N_2H_4, (b) Reaction Mixture at t = 1.4 min, (c) Reaction Mixture at t = 20.8 min.

37

The spectrum of N_2H_2 in the ~1300-cm^{-1} region is presented in Figure 7 and was derived from an $N_2H_4 + O_3$ experiment (A-1) carried out under conditions of excess N_2H_4. The general location of the absorptions corresponds to those expected for the anti-symmetric NNH bending and the torsional modes of N_2H_2 (References 34, 35). Individual line positions, indicated in Figure 7, agree closely with those tabulated by Blau and Hochheimer (Reference 36) for gaseous N_2H_2 as produced by streaming anhydrous N_2H_4 through a low-power microwave discharge. Additional weak lines were observed in the 3000-3200 cm^{-1} region which generally agreed with those reported by the above authors (Reference 36), but this region was relatively noisier due to the lower response of the HgCdTe detector in this spectral range. Neudorfl, et al. (Reference 37) found no evidence for isomers other than trans-N_2H_2 in samples prepared by the microwave discharge method or by thermal decomposition of alkali metal tosylhydra-zides (Reference 38). Thus, the spectrum of N_2H_2 presented in Figure 7 is most likely that of the trans form.

The detailed concentration-time data for the major and minor products observed in these runs are given in Appendix A, and the relative yields are summarized in Table 4. (For N_2H_2, the IR absorption coefficients are unknown, and thus the yields are expressed in absorbance units. Although the absolute yields of N_2H_2 could not be determined, the absorbance norm-alized by the amount of reacted N_2H_4 [Table 4] can give an indication of how the relative yields are affected by reaction conditions.) The N_2H_2 yields were strongly affected by the O_3/N_2H_4 ratio. In air, N_2H_2 remained at the end of the reaction only in the excess hydrazine runs and was observed as a transient intermediate in the equimolar runs and the excess O_3 runs, with only very low levels observed in the latter case. In addition, when O_3 was added to a reacted mixture already containing N_2H_2 (runs A-1 and A-7), the latter species rapidly disappeared, indicating a fast reaction between O_3 and N_2H_2. The presence of the radical trap did not significantly affect the diazene yields in the excess hydrazine runs or the rate of diazene decay when O_3 was added to mixtures already containing N_2H_2. However, the transient N_2H_2 levels in the equimolar run with the radical trap were somewhat lower than those in the equimolar runs without the trap (with a maximum N_2H_2 absorbance of only 0.008 units
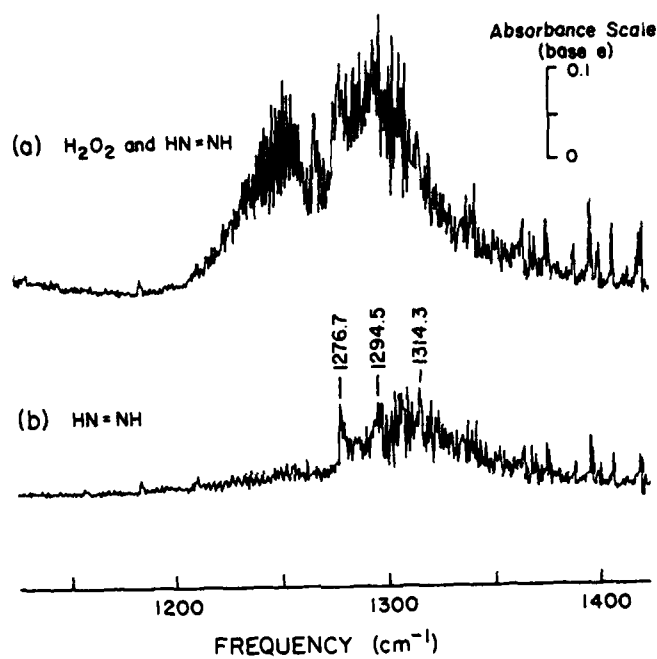
Figure 7. Spectra Illustrating Detection of Diazene in $N_2H_4 + O_3$
Reaction (Run A-1, t = 1.4 min.); Res = 1 cm^{-1}, Path-
length = 68.3 m. (a) Superimposed Absorptions of H_2O_2
and HN=NH, (b) HN=NH Spectrum after Subtraction of
H_2O_2 Absorptions.

observed in run A-8, compared with maxima of 0.038 and 0.042 in runs A-3 and A-4, respectively).

The H_2O_2 yields were far less sensitive to the initial O_3/N_2H_4 ratio in the runs without the radical trap than in experiments with the radical trap present. In the absence of the trap, the relative H_2O_2 yields ranged from 50-60% of the N_2H_4 reacted in excess N_2H_4 down to ~40% in excess O_3. When the trap was present, the H_2O_2 yields were suppressed by just over a factor of 2 in excess hydrazine to over a factor of 10 in excess O_3 relative to the H_2O_2 yields for the runs without the trap.

One run was performed in which hydrazine was reacted with an equal amount of O_3 in an atmosphere of N_2 rather than air. (The system was not completely free of O_2 since ~1300 ppm O_2 was added with the O_3 sample.) No radical trap or tracers were present. The results of this run differed from the corresponding equimolar runs in air in the following respects: (1) The reaction occurred significantly faster in N_2, with the initial rate of O_3 decay being approximately a factor of 2-3 higher. (2) About 40% more O_3 was consumed per hydrazine consumed in the run carried out in N_2 compared to the run in air, i.e., $\Delta[O_3]/\Delta[N_2H_4] \simeq 1.4$ instead of 1. (3) The N_2H_2 yield was higher in the N_2 run than in the corresponding equimolar runs done in air; this could be due to the fact that in the former case the O_3 was consumed more rapidly. (4) The H_2O_2 yield was almost a factor of 3 lower in the run carried out in the N_2 atmosphere than in the run carried out in air. (5) Small amounts of HONO and N_2O were observed in the N_2 run. Although these were still minor products (being < 3% and < 2% of the N_2H_4 consumed, respectively), they were not detected in most of the runs performed in air. In the few cases where N_2O was detected, the yields were lower. The results of this experiment clearly indicate that O_2 must play a role in the $N_2H_4 + O_3$ mechanism.

3.3.3 Reactions of Monomethylhydrazine with Ozone in Environmental Chambers

The detailed concentration-time data for the reactants and products monitored by FT-IR spectroscopy in the nine experiments in which O_3 was reacted with MMH are given in Appendix B, and a summary of the conditions and results are given in Table 5. In two of the excess MMH runs (B-1 and B-7) and two of the equimolar runs (B-3 and B-8), a second injection of O_3 was made in order to observe further reaction of the

TABLE 5. SUMMARY OF CONDITIONS AND RESULTS FOR THE MMH + O_3 EXPERIMENTS.[a]

Expt. ID[b]	Conditions Radical Trap[c]	Conditions Tracer[d]	Initial Conc. MMH (ppm)	Initial Conc. O_3 (ppm)	Δ[MMH] (ppm)	$\frac{\Delta[u.]}{\Delta[MMH]}$	$\frac{\int[OH]dt}{\Delta[MMH]}$ $(10^{-6}\,s\,min)$[e]	([Product]/Δ[MMH]) × 100[f] CH_3NNH	CH_3OOH	CH_2N_2	HCHO	CH_3OH	CO	HCOOH	H_2O_2	N_2O	NH_3
B-1	No	No	15.8	4.2	4.8	0.9		41	40	13	<3	2	<1	<0.2	21	<0.8	0.2
B-2	No	Yes	17.8	5.1	6.0	0.9	0.2	35	32	13	<3	3	<1	<0.2	16	<0.7	~0
B-3	No	No	8.9	9.5	8.9	1.1		14	52	11	14	6	2	0.7	15	<0.5	0.3
B-4	No	Yes	10.0	10.3	10.0	1.0	1.0	15	49	11	13	6	2	0.7	15	<0.4	0.4
B-5	No	No	4.0	15.1	4.0	1.3		~0	65	~0	33	10	8	0.8	14	<1.0	0.8
B-6	No	Yes	4.9	15.4	4.9	1.3	7.1	~0	51	2	31	8	7	1.0	11	<0.8	<2.7
B-7	Yes	No	18.9	4.3	5.8	0.7		27	28	13	9	3	<1	<0.2	8	<0.7	~0
B-8	Yes	No	9.6	9.5	8.2	1.2		23	33	27	18	9	<1	<0.1	4	<0.5	0.6
B-9	Yes	No	4.5	17.5	4.5	1.9		~0	32	16	53	19	2	0.7	7	<0.9	<1.1
B-1[h]	No	No	10.7	25.8	13.3[i]	1.1		1	50	k	26	9	5	2	9	<0.6	1.3
B-2[h]	No	No	0	9.5	2.0[j]	1.0		1	30	k	35	6	7	1	~0	~0	~0
B-7[h]	Yes	No	12.8	24.2	14.4[m]	1.2		1	28	2[n]	39	17	0.5	1.0	3	~0	~0
B-8[h]	Yes	No	0.9	9.5	4.0[o]	0.9		1	15	k	58	14	2	0.5	0.8	~0	~0

[a] All reactions were carried out in air; reaction time = 2 min. for all experiments.

[b] Run identification (ID) corresponds to the table number in Appendix B.

[c] "Yes" means ~270 ppm of n-octane was present as radical trap.

[d] "Yes" means ~0.2 ppm each of n-octane and hexamethylethane (HME) were present as tracers for OH radicals (see footnote e).

[e] $\int$[OH]dt was calculated from the change of ln([HME]/[n-octane]) with the use of known rate constants for the reaction of OH radicals with HME (Reference 33) and n-octane (Reference 32).

[f] Values preceded by "<" sign were based on detection limit; others were measured values.

[g] Estimated uncertainty is ± 35%; absorption coefficient was derived from carbon balance in these experiments (see text).

[h] Second O_3 injection to a reacted mixture: product yields reflect changes in concentrations.

[i] Includes 2.0 ppm CH_3NNH and 0.6 ppm CH_2N_2 also consumed in the reaction with O_3.

[j] Initially present and was consumed following the addition of O_3.

[k] Initially present and decreased following the addition of O_3.

[l] Includes 1.1 ppm CH_3NNH and 0.9 ppm CH_2N_2 that were consumed; no MMH present.

[m] Includes 1.6 ppm CH_3NNH which was consumed.

[n] Increased in concentration and then decreased.

[o] Includes 1.7 ppm CH_3NNH and 1.3 ppm CH_2N_2 that were consumed.

41

remaining MMH and the reactive products formed after the initially-injected O_3 was consumed. The results of these second injections are also summarized in Table 5.

With the exception of run B-4 (equimolar reactants with added tracers), the consumption of the initial reactants (MMH or O_3) was complete within 1 minute, although in some cases reactions of the products continued. This reaction time held even for the experiments carried out with radical traps, where a time resolution for FT-IR analysis as short as 0.25 min was attempted. The observed anomalous reaction time for run B-4 might have resulted from unmonitored variations in our injection procedures (see Section 2.5.1) which caused non-uniform mixing within the time scale of the reaction.

Although the use of FT-IR spectroscopy allowed the reactant concentrations to be measured every 0.25 min in the runs with radical traps, the data points recorded were within (or just a few seconds beyond) the mixing time (~30 sec) in the chamber (see Section 2.1). Thus, these data are probably not suitable for rate calculations. On the basis of reaction times of less than ~2 min in the above experiments, all we can conclude is that the overall apparent MMH + O_3 reaction rate is $>$ 1 ppm^{-1} min^{-1} or $>$ 10^{-15} cm^3 $molecule^{-1}$ sec^{-1}, which is consistent with the probable lower limit of ~5 x 10^{-15} cm^3 $molecule^{-1}$ sec^{-1} obtained using a ~175 ℓ reaction bag.

As in the N_2H_4 + O_3 system, the stoichiometry of the reactants consumed in the MMH + O_3 system depended on the ratio of initial reactants and on the presence of radical traps. Indeed, within the experimental uncertainties the results were in most cases essentially the same as those in N_2H_4 + O_3 systems. Thus $\Delta[O_3]/\Delta[MMH]$ ranged from ~0.9 in excess MMH to 1.3 in excess O_3 in the absence of the radical trap (compared to ~0.8-1.4 for N_2H_4 + O_3), and ranged from 0.7 in excess MMH to 1.9 in excess O_3 when the radical trap was present (compared to 1.0-1.9 for N_2H_4 + O_3). It is not clear whether the difference between the MMH + O_3 and N_2H_4 + O_3 stoichiometries in the excess hydrazine with radical trap runs (0.7 for MMH vs. 1.0 for N_2H_4) are significant or merely reflect the experimental uncertainties.

The MMH + O_3 system was also similar to the N_2H_4 + O_3 system in that the n-octane and HME tracers were observed to decrease as the hydrazine

42

and O_3 reacted, with the amount consumed increasing as the initial O_3/hydrazine ratio increased. However, in the MMH case, the dependence on the O_3/hydrazine ratio was more extreme, with the change in the ratio of the tracers (i.e. the integrated hydroxyl radical levels) in the MMH + O_3 system being less than that in the corresponding N_2H_4 run with excess hydrazine or with equimolar reactants, but being greater than for N_2H_4 in excess O_3.

The major products observed in the O_3 + MMH system were CH_3OOH, CH_3NNH, HCHO, CH_2N_2, and H_2O_2, with lower yields of CH_3OH, CO, and HCOOH; traces of NH_3 and N_2O were also formed. The majority of the above products were observed in our previous study (Reference 3). There is no evidence for the formation of nitrous acid or aerosol in this system, and it is believed that all significant products have been identified.

Figure 8 illustrates the concentration-time profiles for the reactants and products observed in the MMH + O_3 reaction with initial equimolar amounts of reactants (run B-3), and Figure 9 shows IR spectra of the major products observed in that experiment. The spectral region at ~2800 cm^{-1} where HCHO was measured is not included in Figure 9, due to space limitations. Also, the NH_3 absorptions have been subtracted for the sake of clarity. The product spectrum recorded at 1.4 min from the start of the first O_3 injection (Figure 9b) clearly shows the formation of CH_3NNH, CH_3OOH, CH_3OH, H_2O_2, and CH_2N_2. A second injection of O_3 was made 12 min after the first. Figure 9c was recorded 1.4 min after the start of this second O_3 injection. It shows the disappearance of CH_3NNH and a marked decrease in the amount of CH_2N_2 (which eventually was consumed), with a corresponding growth of CH_3OOH and CH_3OH.

The infrared absorption coefficients for CH_3NNH are not available, thus only the absorbance values for its Q branch at 845.2 cm^{-1} are given in the tables in Appendix B. However, an estimated absorption coefficient of 7 ± 2.5 cm^{-1} atm^{-1} can be derived based on the carbon balance in the MMH + O_3 runs in which methyldiazene was formed. This absorption coefficient was used to obtain the CH_3NNH yields shown in Table 5, with an estimated uncertainty of $\pm$ 35%. The relative changes of these yields with reaction conditions are much less uncertain, however.

The above estimate of an absorption coefficient for CH_3NNH was made possible by the good carbon balance generally observed in the MMH + O_3
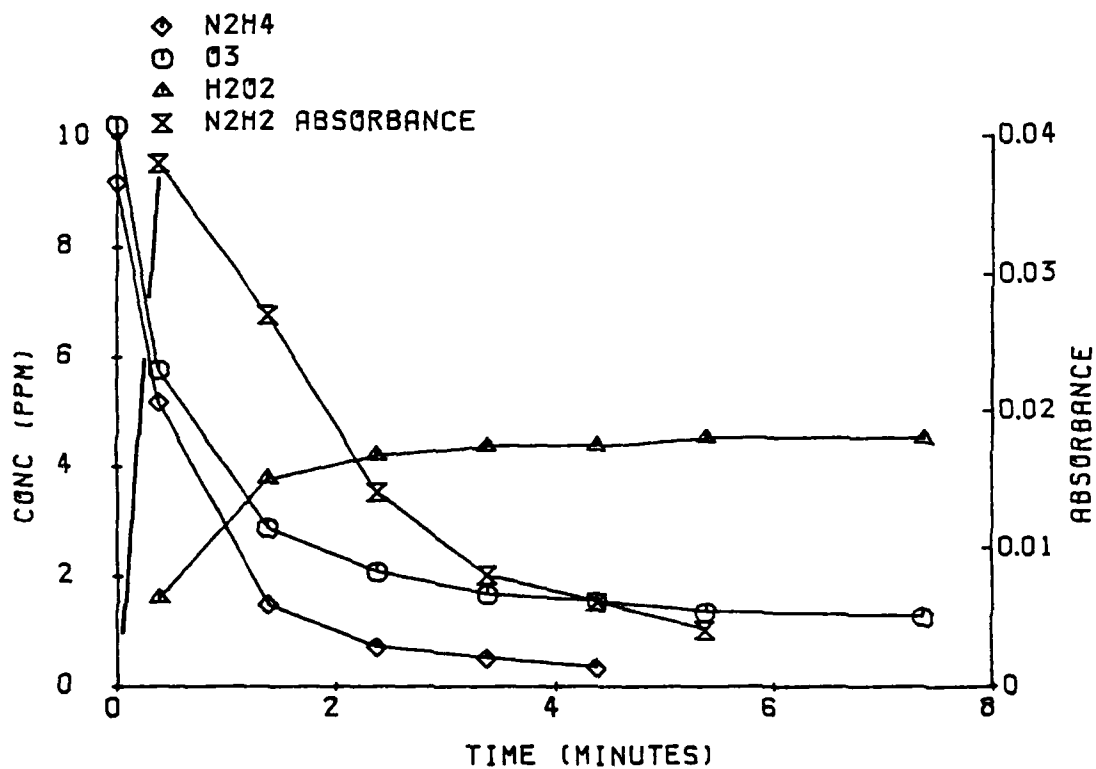
43
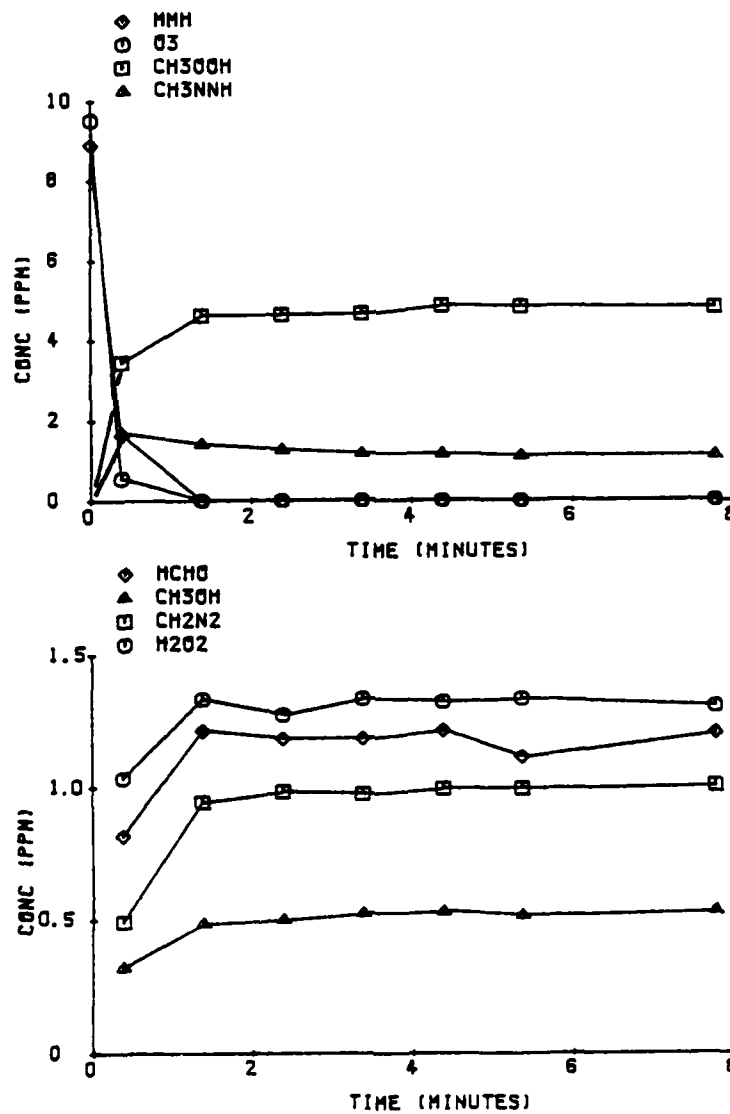
Figure 8. Concentration-Time Plots for Reactants and Selected Products Observed in the MMH + O_3 Run B-3 with Equimolar Reactants.
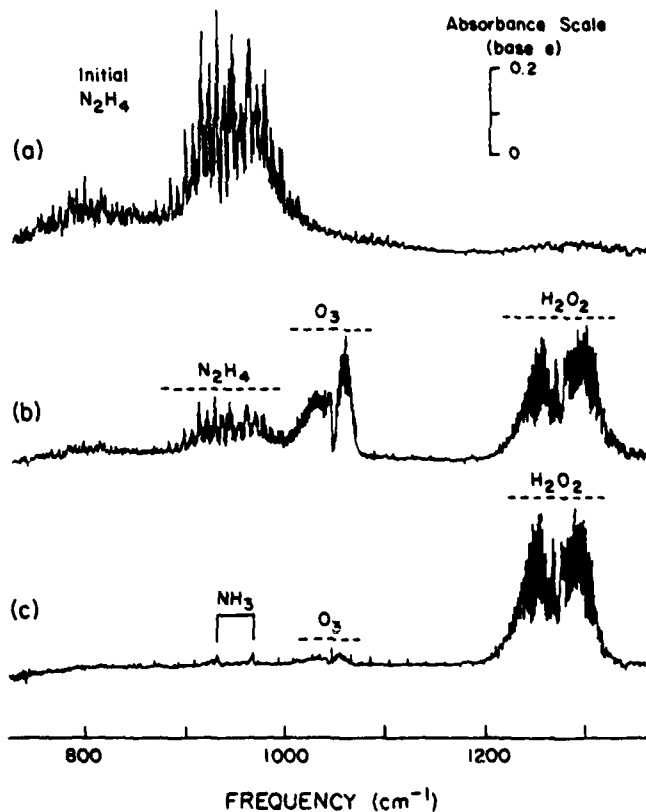
44

Figure 9. Infrared Spectra from MMH + O₃ Experiment with Equimolar
Reactants (Run B-3); Res = 1 cm⁻¹, Pathlength = 68.3 m.
(a) Initial MMH, (b) Reaction Mixture at t = 1.4 min
after First O₃ Injection, (c) Reaction Mixture at t =
1.4 min after second O₃ Injection. *The Absorptions of*
NH₃ have been Subtracted from (a), (b), and (c).

45

systems. That all major carbon-containing products were accounted for was verified from the results of the second O_3 injection in runs with excess MMH or equimolar reactants, with or without radical traps. Following the second O_3 injection and consumption of CH_3NNH in runs B-1, B-3, and B-8 (see Appendix B for detailed data), the products observed accounted for 92-98% of the initial carbon; however, only ~85% of the initial carbon was accounted for by products in run B-7 (excess MMH, radical trap). For runs with initial excess ozone, the carbon balances observed were ~118% for B-5, ~104% for B-6, and ~111% for B-9. It is possible that for the latter runs the initial MMH concentrations were not as well determined, since in these runs MMH was injected into the reaction chamber already containing O_3; for runs with excess MMH and equimolar reactants, MMH was injected first and its concentration verified by its infrared spectrum before reaction with O_3.

As seen in Table 5, the relative yields of the organic products varied considerably depending on the initial O_3/MMH ratio and, to a lesser extent, on the presence of radical trap. The yields of methyldiazene (like its analogue, diazene, formed in the $N_2H_4 + O_3$ system) decreased markedly as the O_3/MMH ratio increased, and methyldiazene was not observed when O_3 was in excess. The observation that CH_3NNH already present in a reacted mixture disappeared in less than ~1 min after excess O_3 was added (see Tables B-1, B-3, B-7, and B-8) can be attributed to a rapid reaction between CH_3NNH and O_3. The diazomethane yields were also observed to decrease as the O_3/MMH ratio increased, indicating that diazomethane also reacts with O_3. The reduced CH_3NNH and CH_2N_2 yields in the higher O_3 runs were offset primarily by increased yields of HCHO and CH_3OOH, with HCHO not being observed in the excess MMH runs, but becoming a major product in excess O_3.

The relative yields of the organic products, and their dependences on the initial O_3/MMH ratio, changed somewhat when the radical trap was present. The presence of the radical trap caused HCHO to increase under all conditions, though it was still highly dependent on the O_3/MMH ratio. On the other hand, CH_2N_2 yields were much less dependent on the O_3/MMH ratio in the presence of the trap than in the runs without the trap. In the presence of the trap, the increased yields of HCHO and of CH_2N_2 at higher O_3/MMH ratio, were offset primarily by reduced yields of

46

CH_3OOH. The CH_3OOH yields and their dependence on the O_3/MMH ratio did not appear to be as strongly influenced by the presence of the traps as the yields of the other major products.

The H_2O_2 yields in the MMH + O_3 system were a factor of ~3 lower than those in the corresponding N_2H_4 + O_3 runs, but exhibited the same dependence on the $O_3/hydrazine$ ratio and on the presence of the radical trap. Thus, the H_2O_2 yields in the MMH + O_3 system in the absence of the radical trap ranged from 15-20% of the MMH consumed in the excess MMH run to 10-15% in the excess O_3 run, with the yields in the presence of the trap being much lower and more dependent on the O_3/MMH ratio.

In the runs in which O_3 was added to mixtures already containing the MMH + O_3 products, both methyldiazene and diazomethane were observed to be consumed (runs B-1, B-3, B-7, and B-8). The apparent reaction between O_3 and diazomethane was considerably slower than that between O_3 and methyldiazene, since the former reaction occurred at measurable rates, while the latter was essentially "instantaneous" relative to the time resolution of the FT-IR monitoring technique. In all cases, the diazomethane decay was exponential.

Figure 10 shows plots of $\ln[CH_2N_2]$ against time for the four runs (B-1, B-3, B-7, and B-8) where O_3 was added to the reacted mixture, and for the excess O_3-radical trap run (B-9) where O_3 and CH_2N_2 co-existed. The slight curvature observed around the end of runs B-7 and B-8 are attributed to a decrease in the O_3 concentration due to reaction. For the runs carried out in the presence of the radical trap (runs B-7, B-8 and B-9), the apparent rate constants were (in units of 10^{-17} cm^3 molecule^{-1} sec^{-1}) 3.3 ± 0.3, 3.2 ± 0.2 and 3.5 ± 0.1, respectively; these values give an average apparent rate constant of $(3.3 ± 0.1) \times 10^{-17}$ cm^3 molecule^{-1} sec^{-1}. In the absence of the radical trap, the agreement was not as good; the apparent rate constants (in units of 10^{-17} cm^3 molecule^{-1} sec^{-1}) were 8.1 ± 0.2 and 9.3 ± 1.3 for runs B-1 and B-3, respectively, which were factors of 1.5-3 higher than observed when the trap was present. These data suggest that secondary reactions of CH_2N_2 (other than with O_3) were occurring in the absence of the radical trap.

When O_3 reacted with CH_2N_2, increased levels of CO and HCHO were observed in those runs where a sufficient amount of diazomethane reacted (Tables B-7 and B-8). N_2O was also observed to increase when CH_2N_2

47
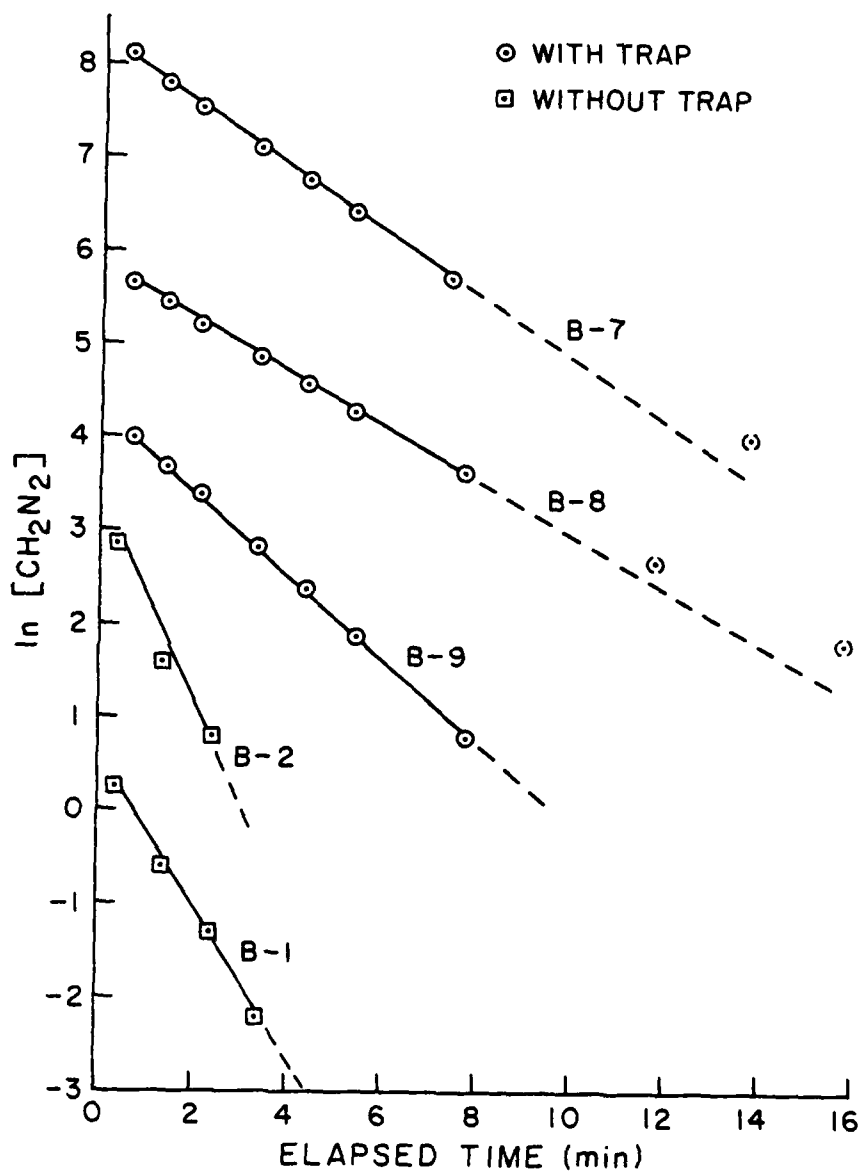
Figure 10. Plots of ln[CH$_2$N$_2$] Against Elapsed Time for MMH + O$_3$ Runs in which
Diazomethane Reacted in the Presence of Excess O$_3$. ([CH$_2$N$_2$] in
ppm; Plots Offset by +7, +5, +4, and +3 Log Units for Runs B-7,
B-8, B-9 and B-2, Respectively.) ⊙, ☐ - Experimental Points Used
to Calculate the Least Squares Lines Shown; (·) - Points Not Used
to Calculate the Least Squares Line.

reacted with O_3 in run B-1, but not in the other runs. The amount of O_3 consumed was ~65-80% of the diazomethane reacted. The increase in CO and HCHO was only ~50% of the amount of diazomethane reacted, suggesting the formation of other products. However, no significant changes in the levels of CH_3OOH, CH_3OH, HCOOH, H_2O_2, NH_3, N_2O or HONO were observed to result from the $CH_2N_2 + O_3$ reaction, although the possibility of CO_2 being formed cannot be ruled out.

3.3.4 Reactions of Unsymmetrical Dimethylhydrazine with Ozone in Environmental Chambers

The detailed concentration-time data for the reactants and products in the seven UDMH + O_3 experiments are given in Appendix C, and a summary of the conditions and results are given in Table 6. In the excess UDMH and equimolar runs without the radical trap and tracers (runs C-1 and C-3), and in the excess UDMH and equimolar runs with the radical trap (runs C-6 and C-7), a second O_3 injection was carried out to react with the remaining UDMH; the results of these second injections are also summarized in Table 6.

The rate of reaction of UDMH with O_3 was observed to be at least as fast as that of MMH with O_3. The detailed concentration-time data in Appendix C show that either UDMH or O_3 was completely consumed within the mixing time (~30 sec) in the reaction chamber. In fact, for the equimolar run in the presence of radical trap (run C-7), where FT-IR monitoring included analyses at 15 sec intervals, no O_3 was detected in the second spectrum recorded at t = 0.35 min from the start of O_3 injection. Since an upper limit of ~2 min can be safely assumed for the reaction times in these experiments, the overall apparent rate constant for the UDMH + O_3 reaction must be greater than ~10^{-15} cm^3 molecule^{-1} sec^{-1}. The reaction stoichiometry ($\Delta[O_3]/\Delta[UDMH]$) was 1.3 - 1.4 for the excess hydrazine and equimolar runs without the radical trap (runs C-1, C-2, C-3, and C-4), and 1.5 - 1.8 for all other runs. It could not be ascertained from these data whether the stoichiometry depends significantly on the O_3/UDMH ratio and the presence of radical trap, or whether the variations observed resulted from experimental uncertainties. This contrasts with the other hydrazines (N_2H_4 and MMH), where there was a clear dependence on both the reactant ratio and the presence of the radical trap.

Expt. ID[b]	Conditions		Initial Conc.		Δ[UDMH]	$\frac{\Delta[O_3]}{\Delta[UDMH]}$	$\frac{\int[OH]dt}{\Delta[UDMH]}$	([Product]/Δ[UDMH]) x 100[f]										
	Radical Trap[c]	Tracer[d]	UDMH (ppm)	O_3 (ppm)	(ppm)		(10^{-6} min)[e]	$(CH_3)_2NNO$	HCHO	CH_3NNH[g]	CH_3OOH	CH_3OH	CO	HCOOH	H_2O_2	HONO	NO_2	NH_3
c-1	No	No	8.1	3.5	2.4	1.4		57	14	9	< 14	1	< 1	< 0.4	5	4	< 2	< 0.8
c-2	No	Yes	16.4	4.3	3.2	1.3	0.4	53	12	7	< 16	1	3	0.3	5	3	< 2	0.6
c-3	No	No	10.1	9.9	6.9	1.4		59	16	5	13	1	0.3	0.4	8	4	1	< 1.3
c-4	No	Yes	9.6	9.9	6.9	1.4	1.0	61	16	6	10	1	0.7	0.3	7	3	< 1	0.7
c-5	No	Yes	4.5	16.7	4.5	1.8	2.4	67	24	~0	21	2	< 1	0.4	9	1	< 2	< 0.7
c-6	Yes	No	8.0	3.3	2.0	1.7		71	< 5	< 3	< 17	1	< 2	< 0.3	< 6	1	< 2	< 1.0
c-7	Yes	No	10.9	10.3	6.7	1.5		72	9	~3	< 6	2	< 0.7	0.1	3	1	< 1	< 0.4
c-1[h]	No	No	5.6	10.6	5.8[i]	1.6		61	13	j	26	2	1	0.5	8	2	2	< 0.3
c-2[h]	No	No	3.1	15.9	3.5[k]	1.7		62	29	j	35	4	4	1	9	0.3	6	~0
c-6[h]	Yes	No	6.0	10.3	6.0	1.		75	9	4	17	2	0.7	0.3	4	1	~0.8	~0
c-7[h]	Yes	No	4.2	16.3	4.5[l]	1.4		73	18	j	20	3	< 1	0.4	4	~0	< 2	~0

[a] All reactions were carried out in air; reaction time = 2 min. for all experiments.

[b] Run identification (ID) corresponds to the table number in Appendix C.

[c] "Yes" means either ~230 ppm or ~270 ppm of n-octane was present as radical trap.

[d] "Yes" means ~0.2 ppm each of n-octane and hexamethylethane (HME) were present as tracers for OH radicals (see footnote).

[e] $\int[OH]dt$ was calculated from the change of $\ln([HME]/[n\text{-}octane])$ with the use of known rate constants for the reaction of OH radicals with HME (Reference 33) and n-octane (Reference 32).

[f] Values preceded by "<" sign were based on detection limit; others were measured values.

[g] Estimated uncertainty is ± 35%; absorption coefficient was derived from carbon balance in MMH + O_3 experiments (see text).

[h] Second O_3 injection to a reacted mixture: product yields reflect changes in concentrations.

[i] Includes 0.13 ppm of CH_3NNH which was consumed.

[j] Initially present and was consumed following the injection of O_3.

[k] Includes 0.38 ppm of CH_3NNH which was consumed.

[l] Includes 0.23 ppm of CH_3NNH which was consumed.

50

As with the other hydrazines, the n-octane and HME tracer concentrations decreased when O_3 and UDMH reacted, with increased amounts of the organic tracers consumed as the O_3/UDMH ratio increased. The integrated OH radical levels calculated from the changes in the ratio of the tracers are approximately 50% of those observed in the N_2H_4 system, and the effect of changing the O_3/hydrazine ratio appears to be the same for both N_2H_4 and UDMH. This contrasts with MMH, where changing the O_3/hydrazine ratio had a much greater effect. This is somewhat surprising, in view of the fact that other data indicates the $N_2H_4 + O_3$ mechanism is more similar to that of the $MMH + O_3$ system than the $UDMH + O_3$ mechanism (Reference 3); but this may be due to the larger variety of reactive products in the MMH system, relative to those from N_2H_4 and UDMH.

The major product observed in the $UDMH + O_3$ system was N-nitrosodimethylamine (NDMA), with significant yields of CH_3OOH, CH_3NNH, and H_2O_2, minor yields of CH_3OH, CO, HCOOH, HONO, NO_2 and NH_3, and traces of CH_2N_2 also being observed. There was no evidence for aerosol formation in this system. A representative IR spectra obtained from the $UDMH + O_3$ experiment with equimolar initial reactants (run C-3) are shown in Figure 11. The absorption bands of NDMA are seen to be the dominant features of the product spectrum (Figure 11b). An unidentified product, with its strongest absorption at ~976 cm^{-1}, was detected upon subtraction of the NDMA absorptions (Figure 11c). This unknown product was observed to form in all experiments conducted in the absence of the radical trap.

As seen in Table 6, the NDMA yields were generally ~55-65% of the UDMH consumed in the absence of the radical trap and ~70-75% when the radical trap was present. The yields of the other products were suppressed significantly by the presence of the radical trap. Within each class of runs, i.e., with and without the radical trap, the NDMA yields increased slightly with the initial O_3/UDMH ratio. In general, the HCHO and CH_3OOH yields increased with the O_3/UDMH ratio, while the CH_3NNH yield decreased. The $UDMH + O_3$ system differed from those of the other hydrazines in that HONO, and to a lesser extent NO_2, were produced. The highest yields of HONO were observed in the runs without the radical trap and when the O_3/UDMH ratio was low. The $UDMH + O_3$ system also differed from the others in that H_2O_2 concentrations were not only lower than observed from the other hydrazines + O_3 systems, but that they increased when the

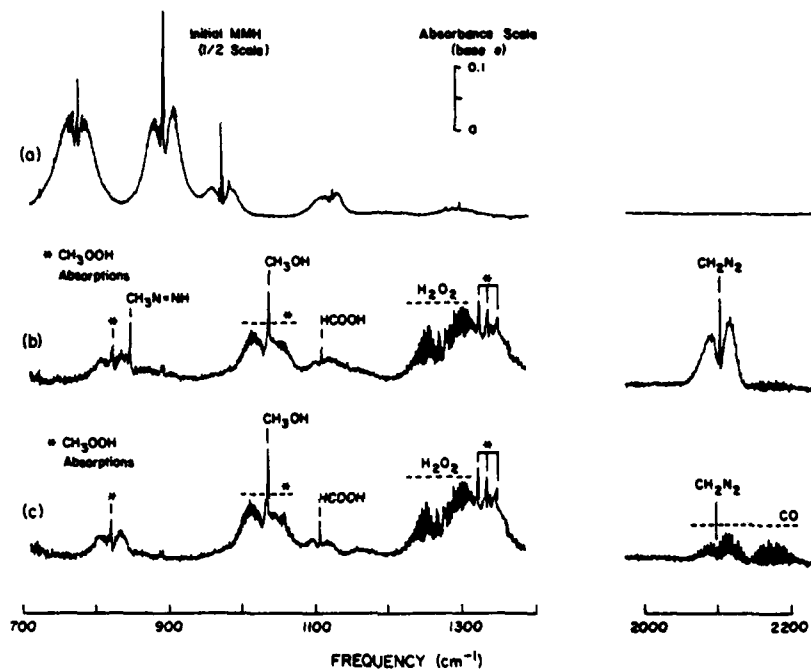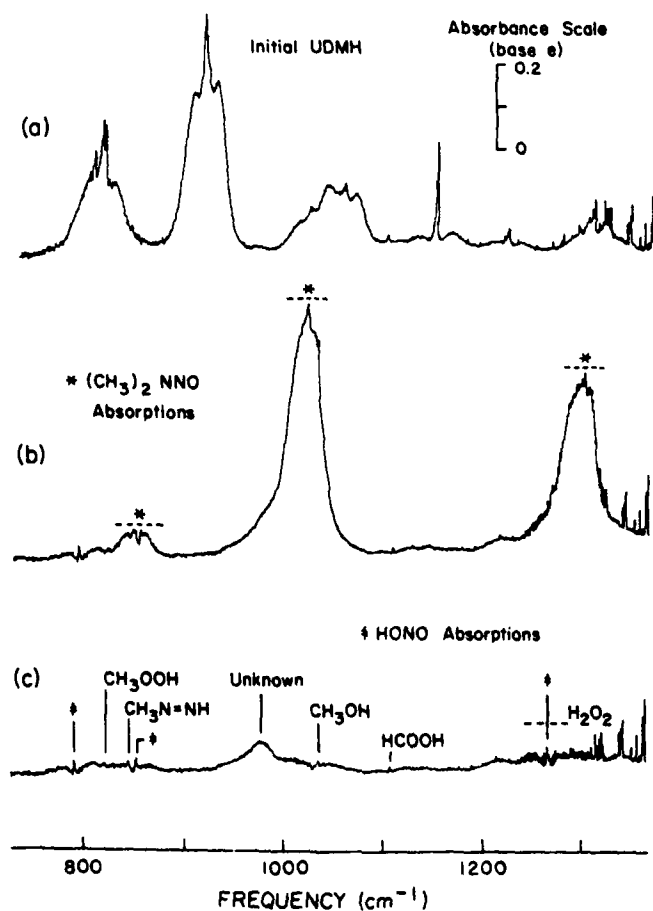Figure 11. Infrared Spectra from UDMH + O_3 Experiment with Equimolar Reactants (Run C-3); Res = 1 cm^{-1}, Pathlength = 68.3 m. (a) Initial UDMH, (b) Reaction Mixture, Minus Unreacted UDMH, at t = 1.4 min, (c) from (b) with $(CH_3)_2NNO$ Bands Subtracted.

O_3/hydrazine ratio increased, the opposite of what was observed in the N_2H_4 and the MMH systems.

The products enumerated above account for most of the initial carbon. For reactions carried out with excess UDMH (runs C-1, C-2, and C-6) 91-93% of the initial carbon could be accounted for by the products detected (see detailed tables in Appendix C); for the equimolar runs (C-3, C-4, and C-7) the range was 84-87%. Under excess O_3 conditions, such as those for the second O_3 injections in runs C-1, C-3, C-6, and C-7, the product analyses yielded a carbon balance of 81-87%; an exception was the higher value of 91% for run C-5 (carried out with tracers), where the intial UDMH concentration was not as well-determined as those for the others.

3.3.5 Reactions of Aerozine-50 with O_3 in Environmental Chambers and Measurements of the Rate of Reaction of Formaldehyde Hydrazone with Ozone

One experiment was carried out in which Aerozine-50 (consisting of ~8 ppm each of N_2H_4 and UDMH) was reacted with ~17 ppm of O_3, followed by a second addition of ~17 ppm ozone after the initial reaction had gone to completion. No radical trap or tracers were present in this experiment. The detailed concentration-time data of the reactants and products are given in Table D-1, and are illustrated in Figure 12.

As observed in the reaction of O_3 with UDMH alone, the reaction of O_3 with the UDMH component of Aerozine-50 went to completion in less than 2 min; during that period, approximately 60% of the N_2H_4 component and almost 95% of the O_3 were consumed. The rate of N_2H_4 decay during this period was similar to that observed in the N_2H_4 + O_3 run A-3, where similar levels of N_2H_4 reacted in the presence of a slight excess of O_3 and where more than half the N_2H_4 was consumed in the first few minutes. The subsequent decay rate of the remaining O_3 in the presence of the excess remaining N_2H_4 component was also reasonably consistent with the results of runs A-1 and A-2, where N_2H_4 alone was reacted with O_3 under condition of excess N_2H_4. The overall Aerozine-50 + O_3 stoichiometry $[\Delta[O_3]/\Delta([N_2H_4] + [UDMH])]$ during the initial period was ~1.3, which is also consistent with results obtained in the individual N_2H_4 + O_3 and UDMH + O_3 systems. Thus, there is no evidence of any synergistic effects on
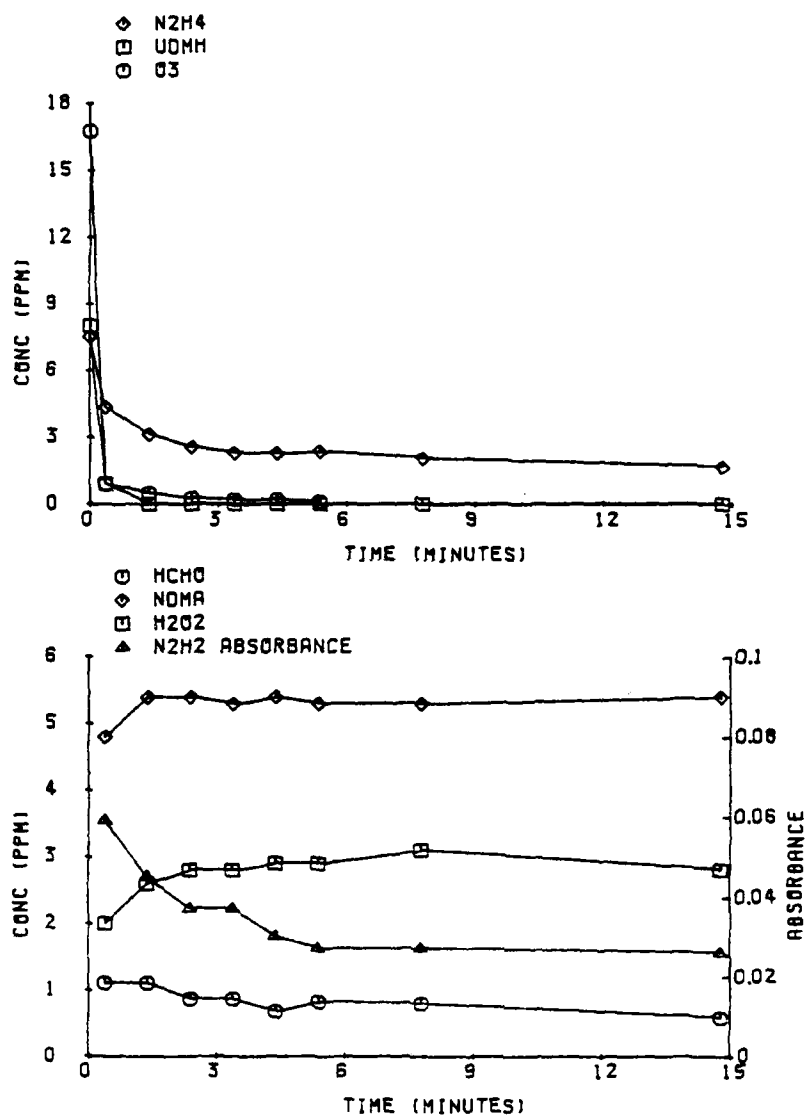
Figure 12. Concentration-Time Plots for Reactants and Selected
Products Observed in the Aerozine-50 + O_3 Run D-1.

the rates of reaction or reactant stoichiometry when a mixture of N_2H_4 and UDMH are reacted with O_3.

The expected products from the UDMH + O_3 reaction (i.e., NDMA, HCHO, CH_3OOH, HCHO, and HONO) were observed to be formed immediately when UDMH was consumed, and with approximately the same relative yields as those observed when O_3 was reacted with UDMH alone. Diazene, formed from the N_2H_4 + O_3 reaction, was also observed. The H_2O_2 yield corresponded very closely to that expected, based on the amount of each hydrazine consumed and the relative H_2O_2 yields from each of the hydrazines, when reacted separately under similar conditions. The only additional product observed was formaldehyde hydrazone ($H_2NN=CH_2$), which was produced from the reaction of the remaining N_2H_4 with the HCHO generated by the UDMH + O_3 reaction. Further studies of the reactions of the hydrazines with formaldehyde are discussed in Section 3.5.

When the second injection of ozone was made into the reacted mixture, both the remaining N_2H_4 and the formaldehyde hydrazone were consumed. The N_2H_4 + O_3 reaction went to completion in less than ~1 min, this rapid rate being in general agreement with the results of the N_2H_4 + excess O_3 experiments performed in the absence of other reactants or with the organic tracers (runs A-5 and A-6, respectively). The hydrazone decay followed a good exponential curve, as is shown in Figure 13, which gives a plot of $\ln[H_2NN=CH_2]$ against time following the second O_3 injection. The slight curvature observed can be attributed to some consumption of O_3 during the experiment. The $H_2NN=CH_2$ concentrations, though not necessary for this first order plot, were calculated using an absorption coefficient of 5.8 cm^{-1} atm^{-1} for the 921.3 cm^{-1} Q branch, derived from a material balance of the N_2H_4 + HCHO experiment described in Section 3.5.1. The decay rate corresponds to an apparent $H_2NN=CH_2$ + O_3 rate constant of $(3.6 \pm 0.2) \times 10^{-2}$ ppm^{-1} min^{-1} ($[2.5 \pm 0.1] \times 10^{-17}$ cm^3 $molecule^{-1}$ sec^{-1}). Formaldehyde and, to a much lesser extent, formic acid appear to be the major organic products formed in the reaction of formaldehyde hydrazone with O_3, since these products increased in concentration during the duration of that reaction.

3.3.6 Mechanism for the Reactions of Hydrazines and Their Reaction Products with Ozone

The results of the hydrazines plus ozone experiments discussed
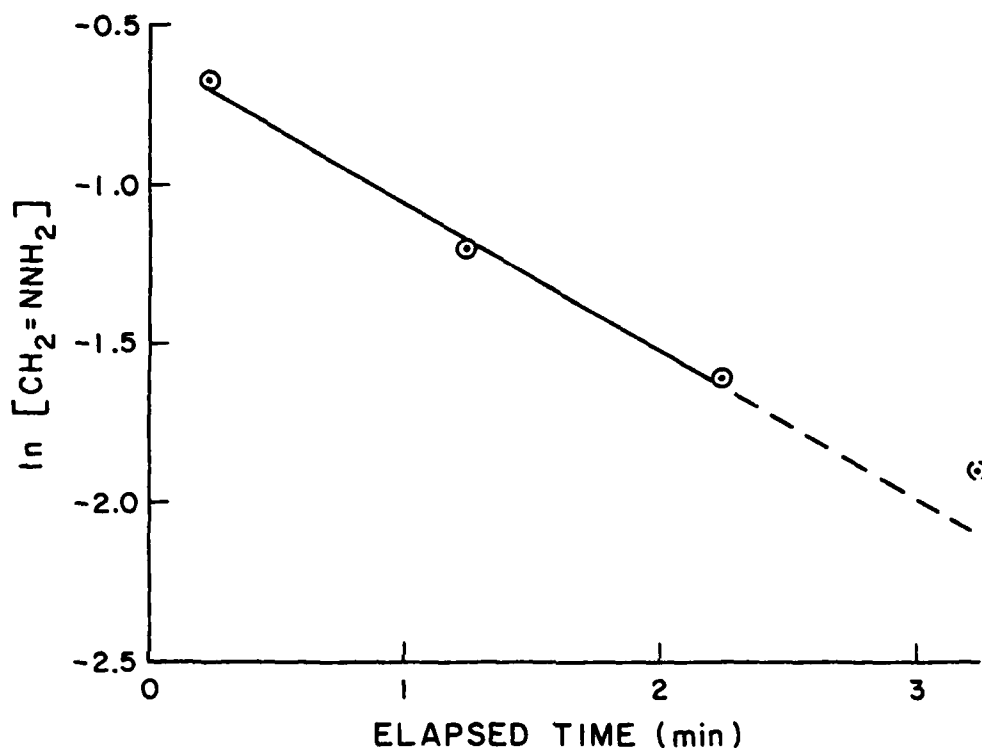
Figure 13. Plot of $\ln[CH_2=NNH_2]$ Against Elapsed Time for the Aerozine-50
Run Following the Second Ozone Injection ($[CH_2=NNH_2]$ in ppm).
⊖ - Experimental Points Used to Calculate Least Squares Line;
(·) - Experimental Point Not Used to Derive Line.

in the previous sections are for the most part consistent with the mechan-
istic interpretation we gave in our previous publications (References 3,
10, 39), based on the data obtained in our initial study of the hydrazines
+ O_3 systems.   In particular, based on mechanistic considerations, we
predicted that diazene (N_2H_2) should be an intermediate formed in the N_2H_4
+ O_3 system which can react readily with O_3, and that hydroxyl radicals
are involved in the reactions of all three hydrazines with ozone. These
predictions have been experimentally confirmed as a result of our present
experiments. We have also observed in this work that the addition of an
OH radical trap significantly affects the overall reaction rates, product
yields, and reactant stoichiometries in all three systems. On the other

hand, the reactant stoichiometries in the $N_2H_4 + O_3$ and MMH $+ O_3$ systems were more variable than expected, and our failure to suppress diazomethane yields in the O_3 + MMH system by the addition of the radical trap means that our original explanation for diazomethane formation in that system, which involved the reaction of OH radicals with methyldiazene, was incorrect. In addition, the data which show that OH radicals are involved in the UDMH $+ O_3$ reaction and that the presence of a radical trap does not change the reactant stoichiometry are difficult to reconcile with reasonable reaction mechanisms for that system.

In the following sections, our previously proposed mechanisms for the reactions of the hydrazines with ozone are reviewed and discussed in light of the new data, and the possibility of alternative or additional reactions occurring are discussed, based on a reevaluation of the mechanism.

3.3.6.1 <u>Reaction Mechanism for $N_2H_4 + O_3$</u>. In our previous reports of our initial study (References 3, 10), we proposed that the overall $N_2H_4 + O_3$ mechanism was a chain reaction with OH, N_2H_3 and N_2H_2 acting as the chain carriers. Under atmospheric conditions, the process is initiated by the attack of O_3 on N_2H_4, which was assumed to occur as follows:

$$H_2NNH_2 + O_3 \rightarrow H_2N\dot{N}H + OH + O_2 \qquad (3)$$
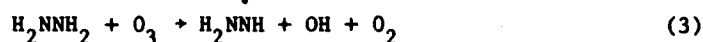
with propagation by the following reactions:

$$H_2NNH_2 + OH \rightarrow H_2N\dot{N}H + H_2O \qquad (4)$$

$$H_2N\dot{N}H + O_2 \rightarrow HN=NH + HO_2 \qquad (5)$$

$$HN=NH + O_3 \rightarrow OH + O_2 + \dot{H}N_2 \qquad (6)$$

and termination by

$$\qquad \qquad \qquad \qquad \overset{O_2}{\longrightarrow} HO_2 + N_2$$

$$HN=NH + OH \rightarrow H_2O + \dot{H}N_2 \qquad (7)$$

$$\qquad \qquad \qquad \qquad \overset{O_2}{\longrightarrow} HO_2 + N_2$$
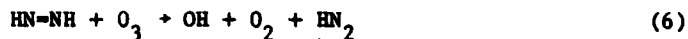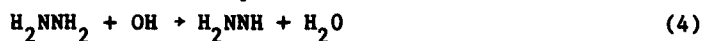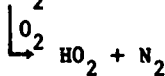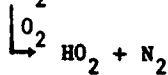
(Under conditions of sufficiently low O_3, relative to N_2H_4, termination also occurs due to the net buildup of N_2H_2.) The major fate of HO_2 is self-reaction to form H_2O_2:

$$HO_2 + HO_2 \rightarrow H_2O_2 + O_2 \tag{8}$$

The results obtained in this study are generally consistent with the above scheme since: (a) N_2H_2, which previously was just a postulated intermediate, has now been directly observed, (b) the results of the hydrocarbon tracer and the radical trap experiments indicate that the hydroxyl radical is indeed involved in the mechanism, and (c) the results of the exploratory $N_2H_4 + O_3$ "equimolar" experiment performed in an N_2 atmosphere (run A-10), in which a higher overall reaction rate and ~40% more O_3 consumption was observed than the corresponding equimolar runs performed in air (runs A-3 and A-4; see Table 4), clearly indicate that O_2 is involved in the mechanism. The higher overall rate and the increased O_3 consumption in the N_2 atmosphere can be attributed to the chain branching resulting from the reaction of O_3 with N_2H_3

$$H_2N\overset{\bullet}{N}H + O_3 \rightarrow HN=NH + OH + O_2 \tag{9}$$
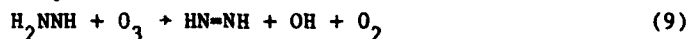
becoming competitive with the reaction of O_2 with N_2H_3 under low O_2 conditions.

The observed dependences of stoichiometry, product yields, and integrated hydroxyl levels on initial reactant ratios shown in Table 4 are reasonably consistent with the above scheme. The variable stoichiometry, with $\Delta[O_3]/\Delta[N_2H_4]$ increasing with the initial O_3/N_2H_4 ratio in both the presence and the absence of the radical trap, can be attributed to the competition between the reactions of O_3 with N_2H_2 (reaction 6) and with N_2H_4 (reaction 3). Thus, under conditions of high N_2H_4/O_3 ratios, the N_2H_4/N_2H_2 ratio is also high so that less O_3 is consumed by reaction with N_2H_2. This in turn means less O_3 is consumed per N_2H_4 reacted than would be the case in excess O_3, where most of the N_2H_2 formed consumes an additional molecule of O_3. The decrease in N_2H_2 yields with increased O_3/N_2H_4 ratios is also consistent with this. In addition, the fact that the integrated hydroxyl radical levels increase with the O_3/N_2H_4 ratio is

consistent with the reaction of N_2H_4 with O_3 being a source of OH radicals and the reaction of OH radicals with N_2H_4 being an OH radical sink, since the former process increases in importance and the average N_2H_2 level decreases as the O_3/N_2H_4 ratio is increased.

The results of the radical trap runs are also consistent with the above scheme. The addition of n-octane causes the following reaction to dominate over reactions (4) and (7)

$$n\text{-octane} + OH \xrightarrow{O_2} RO_2 + H_2O \qquad (10)$$
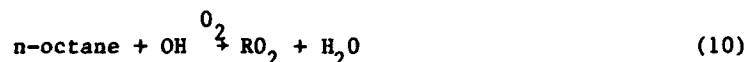
where RO_2 represents the four possible octylperoxy radical isomers formed by the rapid reaction of the initially formed 1-, 2-, 3-, or 4-octyl radicals with O_2. The major fate of RO_2 under these conditions is probably reaction with HO_2

$$RO_2 + HO_2 \rightarrow RO_2H + O_2 \qquad (11)$$

since consumption of RO_2 by self-reaction

$$RO_2 + RO_2 \rightarrow ROH + R'\overset{O}{\overset{\|}{C}}R'' + O_2 \qquad (12a)$$

or

$$RO_2 + RO_2 \rightarrow 2\ RO + O_2 \qquad (12b)$$
$$\overset{O_2}{\underset{}{\longrightarrow}} R'\overset{O}{\overset{\|}{C}}R'' + HO_2$$
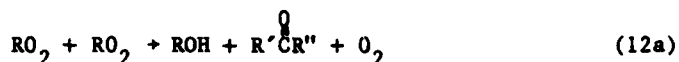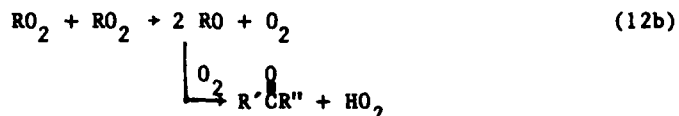
is less important, because the rate constant for the self-reaction of secondary peroxy radicals, the dominant type of RO_2 formed by reaction (10) (Reference 32), is ~1000 to 5000 times lower than that for reaction with HO_2 (Reference 40). Reactions (10) and (11) account for the observation that the addition of the radical trap greatly suppresses the H_2O_2 yield, especially under high O_3/N_2H_4 conditions. The fact that some H_2O_2 is observed to be formed in the excess hydrazine-radical trap run (A-7) could be due to the fact that not all of the OH radicals formed react with the trap (based on the OH + n-octane [Reference 32] and OH + N_2H_4

[Reference 7] rate constants), such that the rate of formation of HO_2 is greater than that of RO_2, resulting in the HO_2 formed not all being consumed by reaction (11).

In the presence of excess radical trap, the reaction mechanism, primarily reactions (3), (5), (6), (10), and (11) is no longer a chain process, and the overall reaction can be represented by

$$N_2H_4 + O_3 + \text{n-octane} \xrightarrow{O_2} N_2H_2 + RO_2H + H_2O$$
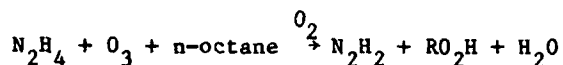
in the limit of sufficiently high N_2H_4 such that the competing reaction of O_3 with N_2H_2 is negligible, and by

$$N_2H_4 + 2 O_3 + 2 \text{ n-octane} \xrightarrow{O_2} N_2 + 2 RO_2H + 2 H_2O$$
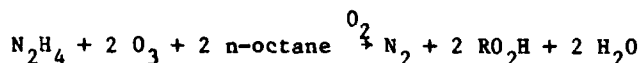
if O_3 is in excess. This is entirely consistent with the reactant stoichiometries observed in the $O_3 + N_2H_4$ runs with the radical trap (see Table 4).

In order to determine whether the above scheme is quantitatively, as well as qualitatively, consistent with our data, exploratory computer kinetic model calculations were performed. Although the results of these model calculations could be made to fit the experimental results semi-quantitatively over the range of conditions studied, the large number of uncertain rate constants rendered the results inconclusive; thus, their detailed results are not presented here. In particular, these preliminary calculations and rate constant estimates indicated that the following reactions of the hydrazyl radical (N_2H_3)

$$H_2N\overset{\bullet}{N}H + H_2N\overset{\bullet}{N}H \rightarrow N_2H_4 + HN=NH \tag{13}$$

$$H_2N\overset{\bullet}{N}H + HO_2 \rightarrow H_2NNH_2 + O_2 \tag{14a}$$

$$H_2N\overset{\bullet}{N}H + HO_2 \rightarrow HN=NH + H_2O_2 \tag{14b}$$

$$H_2N\overset{\bullet}{N}H + HO_2 \rightarrow H_2N-NH-OOH \rightarrow H_2O + [H_2NNO] \tag{14c}$$
$$\phantom{H_2N\overset{\bullet}{N}H + HO_2 \rightarrow H_2N-NH-OOH} \rightarrow H_2O + N_2$$

$$H_2\dot{N}NH + RO_2 \rightarrow HN=NH + RO_2H \qquad (15a)$$

$$H_2\dot{N}NH + RO_2 \rightarrow H_2N-NH-OOR \rightarrow ROH + [H_2NNO] \qquad (15b)$$
$$\phantom{H_2\dot{N}NH + RO_2 \rightarrow H_2N-NH-OOR \rightarrow ROH + [H_2N}\downarrow H_2O + N_2$$
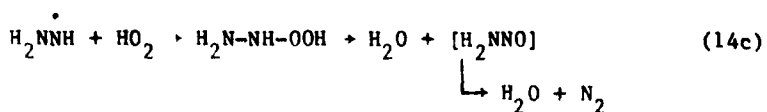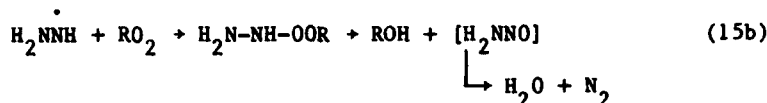
may be non-negligible and may compete significantly with reactions of N_2H_3 with O_2 (reaction 5) or O_3 (reaction 9) under certain conditions.

More information concerning N_2H_2 and N_2H_3 reaction rate constants is required before such calculations can have any predictive value. It is interesting to note, however, that the model with the set of rate constants which best fit our data predicted that, in the absence of the radical trap, most of the hydrazine is consumed by reaction with OH radicals and not by the initiating $O_3 + N_2H_4$ reaction, with the reaction with O_3 accounting for ~20% of the hydrazine consumed in the excess N_2H_4 runs, and only ~8% of the N_2H_4 consumed in excess O_3. This is consistent with our characterization of the overall $N_2H_4 + O_3$ mechanism as a chain reaction and with the fact that the apparent $N_2H_4 + O_3$ rate constants derived from our data (Section 3.3.2) are significantly lower when the radical trap is present, particularly under conditions of excess O_3. The rates of O_3 and/or N_2H_4 decay were reasonably well fit by the model calculations using an elementary rate constant of ~3 x 10^{-2} ppm^{-1} min^{-1} (2 x 10^{-17} cm^3 molecule^{-1} sec^{-1}) for the initial $O_3 + N_2H_4$ reaction, which is ~33% lower than the apparent rate constant derived from N_2H_4 decay in excess O_3 in the presence of the radical trap.

Although the scheme presented above is consistent with our $N_2H_4 + O_3$ data, it is not necessarily the only mechanism for which this is true. In particular, we found, using the computer kinetic model calculations discussed above, that the data could be equally well fit if the initial $N_2H_4 + O_3$ reaction is assumed to be

$$N_2H_4 + O_3 \rightarrow N_2H_2 + H_2O + O_2 \qquad (16)$$
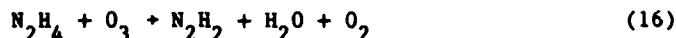
instead of reaction (3). The major difference is that if reaction (16) dominates, OH radicals are not formed in the initial reaction, as would be the case if reaction (3) occurred; thus, the only OH radical source in

this case would be the O_3 + N_2H_2 reaction (reaction 6). This would make no difference when the radical trap is present, since most of the OH radicals formed are removed from the system by reaction with the trap. In addition, as indicated by our model calculations, a relatively small fraction of the N_2H_4 is consumed by the initiating reaction with O_3 in the absence of the radical trap; thus, the OH radicals provided by the initial N_2H_4 + O_3 reaction are apparently not required to drive the chain reaction. In our previous report (Reference 3), reaction (16) was eliminated from consideration, based on the claim that it was inconsistent with the observed reactant stoichiometry, but subsequent consideration reveals that this analysis was erroneous, since we did not properly take into account the chain nature of the overall mechanism. Thus, the currently available data are still inadequate to unambiguously determine the exact nature of the initial N_2H_4 + O_3 reaction.

It is also difficult to determine which is the most reasonable initial N_2H_4 + O_3 reaction pathway from thermochemical and mechanistic considerations. Reaction (3) can be thought of as an H-atom abstraction process which is somewhat analogous to the known reaction of O_3 with HO_2,

$$O_3 + HO_2 \rightarrow OH + 2\ O_2 \qquad (17)$$
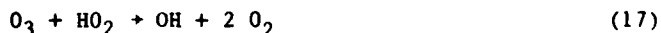
though reaction (17) is much more energetically favorable than reaction (3) ($\Delta H_R \cong -27$ kcal mole^{-1} for reaction [17] [Reference 41] vs. $\Delta H_R \cong + 2$ kcal mole^{-1} for reaction [3] [References 41-43]). However, since reaction (17) is also approximately two orders of magnitude faster than reaction (3) would have to be in order to be consistent with our data ($k_{17} \cong 1.6 \times 10^{-15}$ cm^3 molecule^{-1} sec^{-1} [Reference 40] vs. $k_3 \cong 2 \times 10^{-17}$ cm^3 molecule^{-1} sec^{-1}), this may reflect the differences in thermochemistry between the two reactions. If reaction (3) is assumed to have an Arrhenius factor 4 times that of reaction (17) (because of the fourfold reaction path degeneracy for reaction [3]), then an activation energy of > 4 kcal mole^{-1} for reaction (3) is calculated, which is > 2 kcal mole^{-1} greater than its endothermicity. This is comparable to the overall activation energy of 1.2 kcal mole^{-1} (Reference 40) for the O_3 + HO_2 reaction, and thus the rate parameters for reaction (3), if it is the major initial N_2H_4 + O_3

reaction, are not inconsistent with those for the analogous $HO_2 + O_3$ reaction, provided that the effect of exothermicity on activation energy is assumed to be small. It should be noted, however, that HO_2, unlike N_2H_4, is an odd-electron species, so their reactions may not be strictly analogous; also, ~2 kcal mole^{-1} is an unusually low activation energy for an H-atom abstraction reaction from a stable molecule (Reference 44).

Reaction (16), the alternate pathway for the initial $N_2H_4 + O_3$ reaction, can be rationalized as an O-atom transfer analogous to the known rapid reaction of O_3 with NO forming NO_2, followed by rapid rearrangement and H_2O elimination.

$$N_2H_4 + O_3 \rightarrow \begin{bmatrix} \overset{O}{\underset{(I)}{H_2N\text{-}NH_2}} \end{bmatrix} + O_2 \qquad (16)$$

$$\longrightarrow \begin{bmatrix} H_2N\text{-}N \underset{(II)}{\overset{OH}{\diagdown}} H \end{bmatrix} \rightarrow HN\text{=}NH + H_2O$$
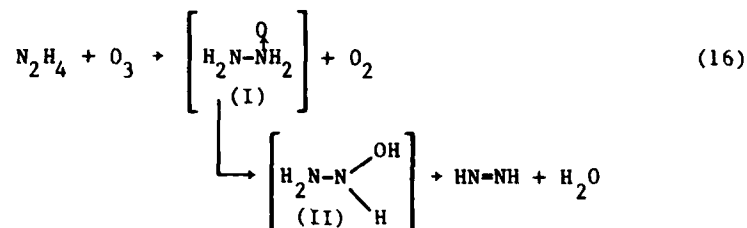
Evidence for this reaction pathway comes from studies of the reactions of oxygen $O(^3P)$ atoms with amines (Reference 45) and hydrazines (Reference 46), where the data indicate that the reactions proceed via the initial formation of an energy-rich N-oxide (analogous to compound [I], above] followed (when possible) by transfer of an α-hydrogen to form a hydroxyl-amine (e.g., compound [II], above), which subsequently decomposes. In the $O + N_2H_4$ and $O + MMH$ systems, direct formation of N_2H_2 or CH_3NNH, respectively, is observed (Reference 46), indicating a mechanism entirely analogous to that of reaction (16). The main difference in the $O_3 +$ hydrazine system is that the N-oxide (I), if formed, would result from an O-atom transfer rather than from direct O-atom addition, and that there is much less energy available in the $O_3 + N_2H_4$ system than in the case of $O + N_2H_4$. Thus, it is possible that the heat of formation of the N-oxide may be too high for it to be formed in the O_3 system; to our knowledge, there is no information available concerning the thermochemistry of species such as (I).

3.3.6.2 **Reaction Mechanism for Monomethylhydrazine + Ozone,** **and Reactions of Products Formed.** The MMH + O_3 system is similar to that for $N_2H_4 + O_3$ in that variable reactant stoichiometry and product yields

and evidence for hydroxyl radical involvement was observed. As indicated in our previous reports (References 3, 10), the MMH + O_3 and the N_2H_4 + O_3 reaction mechanisms are probably similar in their overall features, so much of the above discussion concerning the N_2H_4 + O_3 reaction applies to this system as well. The major differences in the MMH case are the fact that the MMH + O_3 reaction occurs at least an order of magnitude faster than the N_2H_4 + O_3 reaction under all reaction conditions, and that a variety of carbon-containing products are formed from MMH. In this section, mechanistic considerations appropriate to the MMH + O_3 system are discussed.

The high rate of the overall MMH + O_3 reaction, relative to N_2H_4 + O_3, could be due to a higher rate constant for the elementary O_3 + hydrazine reaction, but could also conceivably be due to increased radical chain lengths or to the occurrence of significant chain branching processes. However, the fact that the addition of radical traps does not slow the MMH + O_3 reaction to measureable rates indicates that it is unlikely that the high reaction rate reflects exclusively radical chain processes. Thus, the more rapid rate of the overall reaction is attributed to a higher initial rate constant.

The most probable initial pathways following the initial attack of O_3 on MMH all involve the formation of methyldiazene, analogous to diazene formation from N_2H_4 + O_3:

$$CH_3NH-NH_2 + O_3 \rightarrow \begin{bmatrix} CH_3\overset{\bullet}{N}H-NH \\ or \\ CH_3\overset{\bullet}{N}-NH_2 \end{bmatrix} + OH + O_2 \qquad (18a)$$

$$\overset{O_2}{\longrightarrow} CH_3N=NH + HO_2$$

or

$$CH_3NH-NH_2 + O_3 \rightarrow \begin{bmatrix} CH_3NH-\overset{O}{\overset{\|}{N}}H_2 \\ or \\ CH_3\overset{O}{\overset{\|}{N}}HNH_2 \end{bmatrix} + O_2 \qquad (18b)$$

$$\downarrow$$

$$\left[\begin{array}{l} CH_3NH-N \diagup^{OH}_{\diagdown H} \\ \quad \text{or} \\ CH_3\overset{OH}{\underset{|}{N}}-NH_2 \end{array} \right] \rightarrow CH_3N{=}NH + H_2O$$
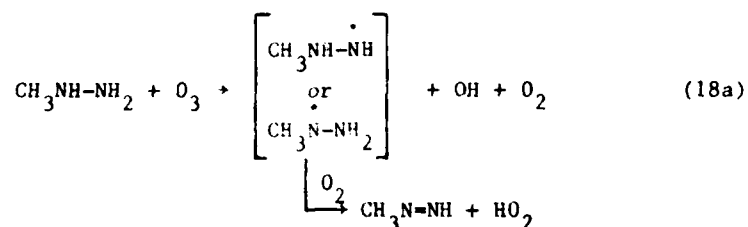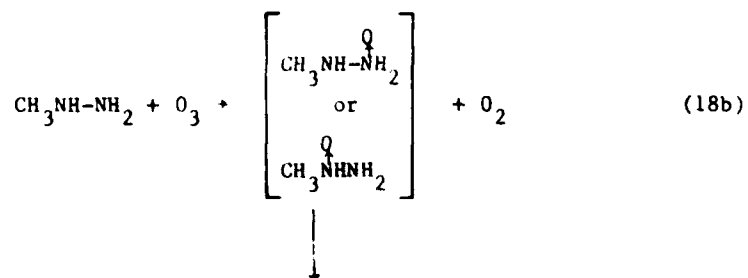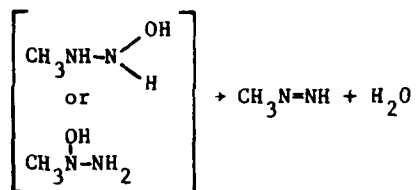
Methyldiazene formation also occurs in the radical-propagating attack of OH radicals on MMH, which, based on our analysis of the analogous N_2H_4 system, is probably the major process consuming MMH in the absence of the radical trap.

$$CH_3NH-NH_2 + OH \rightarrow \left[\begin{array}{l} CH_3\overset{\bullet}{N}H-NH \\ \quad \text{or} \\ CH_3\overset{\bullet}{N}-NH_2 \end{array} \right] + H_2O \qquad (19a)$$

$$\overset{O_2}{\underset{\longrightarrow}{|}} CH_3N{=}NH + HO_2$$
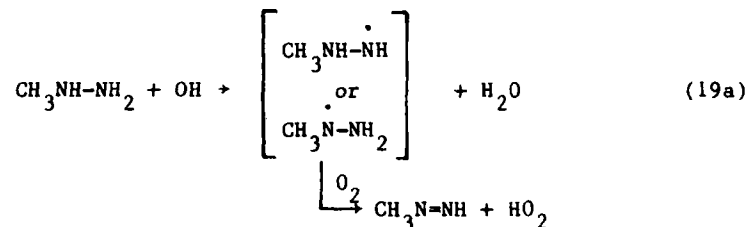
However, in the MMH system, there is an alternate pathway for the MMH + OH reaction:

$$CH_3NH-NH_2 + OH \rightarrow \overset{\bullet}{C}H_2NH-NH_2 + H_2O \qquad (19b)$$
$$(III)$$
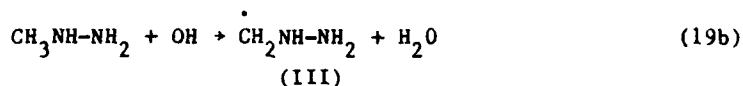
Species (III) is expected to undergo rapid O_2 addition, with the peroxy radical probably reacting primarily via an exothermic H-shift isomerization with a relatively unstrained 6-member ring transition state, and the latter subsequently undergoing fragmentation or reaction with O_2:

$$\overset{\bullet}{C}H_2NH-NH_2 + O_2 \rightarrow \overset{OO\bullet}{\underset{|}{C}H_2NHNH_2} \rightarrow \quad \underset{\substack{H_2C \diagdown \\ NH}}{\overset{O}{\diagup}}\overset{O\cdots H}{\underset{NH}{\diagdown}} \rightarrow HOOCH_2\overset{\bullet}{N}HNH \rightarrow OH + CH_2O + N_2H_2$$

$$\overset{O_2}{\underset{\longrightarrow}{|}} HOOCH_2N{=}NH + HO_2$$
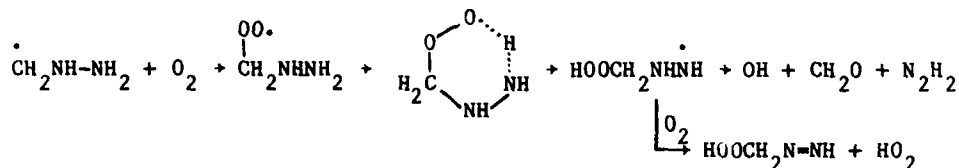
However, since there is no evidence for formation of significant yields of diazene or unknown products in the MMH + O_3 system, reaction (19b) is

65

probably a relatively minor pathway, and initial formation of methyldi-
azene must predominate. In this regard, it should be noted that the rela-
tive methyldiazene yields, and their dependence on initial $[O_3]/[MMH]$
ratios and the presence of the radical trap, are similar to the relative
N_2H_4 yields calculated for the $N_2H_2 + O_3$ system when 100% initial diazene
formation is assumed in the model simulations.

The methyldiazene formed in the initial $MMH + O_3$ or $MMH + OH$ reaction
will undergo significant secondary reactions with O_3 and OH radicals, with
essentially all of it being consumed under conditions of excess O_3,
regardless of whether the radical trap is present or not. Formation of
methyl radicals and N_2 is probably an important reaction pathway in both
cases,

$$CH_3NNH + O_3 \rightarrow [CH_3\overset{\bullet}{N}N] + OH + O_2 \tag{20a}$$

$$\downarrow$$

$$CH_3 + N_2$$

$$\uparrow$$

$$CH_3NNH + OH \rightarrow [CH_3\overset{\bullet}{N}N] + H_2O \tag{21a}$$
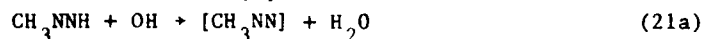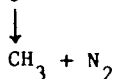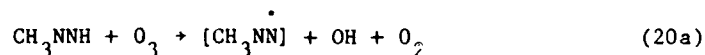
with the subsequent reactions of the methyl radicals formed accounting for
the high yields of methylhydroperoxide observed

$$CH_3 + O_2 \overset{M}{\rightarrow} CH_3OO \tag{22}$$

$$CH_3OO + HO_2 \rightarrow CH_3OOH + O_2 \tag{23}$$
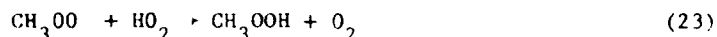
Reaction (23) also accounts for the lower yields of H_2O_2 in the $MMH + O_3$
system, relative to the $N_2H_4 + O_3$ reaction, and the fact that the H_2O_2
yields decrease as the CH_3OOH yields increase (Table 5), since reaction
(23) also removes HO_2, the precursor to H_2O_2.

The observation of diazomethane and/or formaldehyde in relatively
high yields in the $MMH + O_3$ system indicates that the above reactions are
not the only processes important in this system. In our previous report
(Reference 3), diazomethane formation was attributed to an alternate mode
of the reaction of OH radicals with methyldiazene,

$$CH_3NNH + \overset{\bullet}{O}H \rightarrow \overset{\bullet}{C}H_2NNH + H_2O \qquad (21b)$$

followed by

$$\overset{\bullet}{C}H_2NNH + O_2 \rightarrow CH_2N_2 + HO_2$$
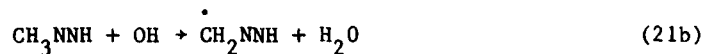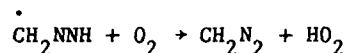
with formaldehyde being formed from reactions of CH_2N_2 with O_3 or OH:

$$CH_2N_2 + O_3 \rightarrow CH_2O + N_2 + O_2$$

$$CH_2N_2 + OH \rightarrow [HO\overset{\bullet}{C}H_2-NN] \rightarrow HO\overset{\bullet}{C}H_2 + N_2$$
$$\downarrow O_2$$
$$\rightarrow CH_2O + HO_2$$
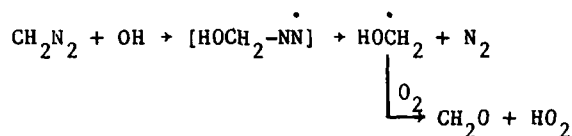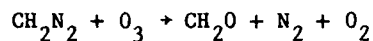
However, if reaction (21b) is the only significant mode of diazomethane formation, the addition of the radical trap should suppress CH_2N_2 yields, yet this was not observed; indeed, under conditions where MMH was not in excess, the addition of the radical trap actually resulted in increased yields of CH_2N_2. Thus, the major process forming CH_2N_2 cannot involve OH radical reactions.

Since reactions of OH radicals cannot account for the observed formation of diazomethane, its formation most likely results from a reaction involving O_3. We are unable to derive a reasonable scheme for CH_2N_2 to be formed in the initial reaction of MMH with O_3, but it may be formed in one of two possible alternate routes in the O_3 + methyldiazene system:

$$CH_3NNH + O_3 \rightarrow \overset{\bullet}{C}H_2NNH + OH + O_2 \qquad (20b)$$
$$\downarrow O_2$$
$$CH_2N_2 + HO_2$$

or

$$CH_3NNH + O_3 \rightarrow \left[CH_3-N\overset{O}{=}NH \right] + O_2 \qquad (20c)$$
$$\downarrow$$
$$\left[CH_3N=N\diagdown^{OH} \right] \rightarrow CH_2N_2 + H_2O$$
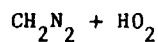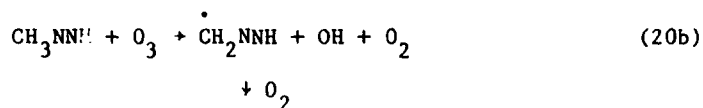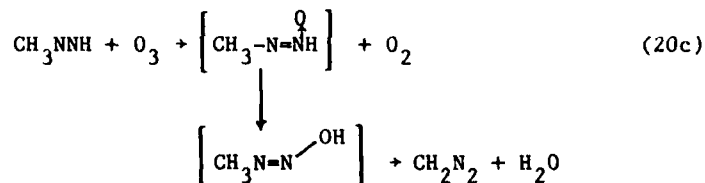
The present data are inadequate to determine the relative importance of reactions (20b) and (20c). This mode of CH_2N_2 formation is consistent with the observation that CH_2N_2 apparently increases with the $[O_3]/[MMH]$ ratio in the presence of the radical trap (Table 5) since the amount of CH_3NNH reacting with O_3 also increases with the O_3/MMH ratio. The fact that the CH_2N_2 yield decreases with the O_3/MMH ratio in the absence of the trap can be explained by CH_2N_2 being consumed mainly by reaction with OH radicals under those conditions, since OH radical levels (as indicated by the tracer data [Table 5] and as discussed previously for the $N_2H_4 + O_3$ system [Section 3.3.6.1]) increase as the O_3/MMH ratio increases.

The yields of formaldehyde observed in the absence of the radical trap are consistent with its dominant mode of formation being via the reaction of diazomethane with OH radicals and/or O_3 as indicated above. The HCHO yield increased with the O_3/MMH ratio while the CH_2N_2 yield decreased, and the sum of the yields of these two products also increased with the O_3/MMH ratio, as did the CH_2N_2 yields in the radical trap system (where secondary consumption of CH_2N_2 is apparently less important). However, in the presence of the radical trap, somewhat higher HCHO yields are observed, despite the fact that less CH_2N_2 is apparently consumed. This can be attributed to an alternate mode of formaldehyde formation which can occur if the radical trap is present:

$$n\text{-octane} + OH \xrightarrow{O_2} RO_2 + H_2O$$

$$CH_3NNH \xrightarrow[O_2]{O_3/OH} CH_3O_2 + \text{other species}$$

$$CH_3O_2 + RO_2 \rightarrow HCHO + ROH + O_2 \qquad (24a)$$
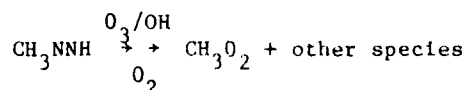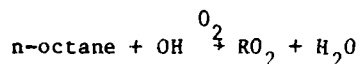
This explanation is also consistent with the reduced yields of CH_3OOH in the presence of the radical trap, because reaction (24a), which is important only when the trap is present, competes with methylhydroperoxide formation via reaction (23).

The other carbon-containing products observed are methanol, formic acid, and CO, with the yields being relatively minor compared to the other

products discussed above. Formic acid is known to be formed in the reaction of HO_2 with formaldehyde (Reference 47), and indeed its yield increased as formaldehyde increased. CO can be formed by the reaction of OH with formaldehyde

$$OH + HCHO \rightarrow \overset{\bullet}{H}CO + H_2O$$
$$\downarrow O_2$$
$$\longrightarrow CO + HO_2$$
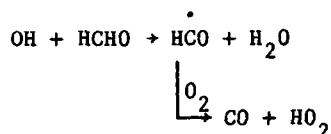
and possibly also from fragmentations of highly energetic species formed when CH_2N_2 reacts with O_3 or OH, both pathways being consistent with the observed yields of CO increasing with the initial O_3/MMH reactant ratio and being suppressed by the radical trap (Table 5). Methanol can be formed from the self-reaction of the CH_3O_2 radicals formed in the reactions of CH_3NNH with OH or O_3,

$$CH_3O_2 + CH_3O_2 \rightarrow CH_3OH + HCHO + O_2$$
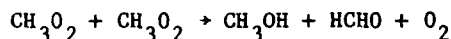
though this is expected to be a fairly minor process compared with reaction of CH_3O_2 with HO_2 forming CH_3OOH. The methanol yield increased in the presence of the radical trap, which can be attributed to an alternate pathway for the reaction of CH_3O_2 with RO_2,

$$CH_3O_2 + RO_2 \rightarrow CH_3OH + R'\overset{O}{\overset{\|}{C}}R'' + O_2 \tag{24b}$$
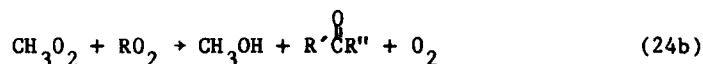
Thus, the identities and yields of the minor products are reasonably consistent with our assumed mechanism.

3.3.6.3 Reaction Mechanism for Unsymmetrical Dimethylhydrazine + Ozone.

The UDMH + O_3 system differs from those of N_2H_4 and MMH in that the initial formation of a diazene, via removal of a hydrogen from each of the nitrogens, cannot occur. Instead, high yields of a nitrosamine, namely N-nitrosodimethylamine (NDMA), are observed, with smaller yields of fragmentation products also being formed. In addition, the reactant stoichiometry in the UDMH + O_3 system is far less dependent on reaction conditions, with $\Delta[O_3]/\Delta[UDMH]$ being ~1.5 ± 0.2 under most conditions. On the other hand, UDMH is similar to the other hydrazines in

that the hydroxyl radical is clearly involved in the mechanism for its reaction with O_3, since the organic tracers are observed to be partially consumed when included in the reaction mixture, and inclusion of the radical trap affects the product yields (though not the reactant stoichiometry). The facts that the reactant stoichiometry is relatively insensitive to reaction conditions and that formation of a single product predominates suggest that the reaction mechanism in the O_3 + UDMH system may not be as complex as those for the other hydrazines. However, as discussed below, no single and straightforward mechanism appears to be totally consistent with all of the UDMH + O_3 data obtained in this study.

Based on mechanistic considerations and the results of our initial UDMH + O_3 experiments performed in our previous program (References 3, 10), the following simple 4-step mechanism for the UDMH + O_3 system was proposed.

$$(CH_3)_2N-NH_2 + O_3 \rightarrow (CH_3)_2N-\overset{\bullet}{N}H + OH + O_2 \qquad (25)$$

$$(CH_3)_2N-NH_2 + OH \rightarrow (CH_3)_2N-\overset{\bullet}{N}H + H_2O \qquad (26a)$$

$$(CH_3)_2N-\overset{\bullet}{N}H + O_3 \rightarrow (CH_3)_2N-N\overset{O^{\bullet}}{\underset{H}{\diagup}} + O_2 \qquad (27)$$

$$(CH_3)_2N-N\overset{O^{\bullet}}{\underset{H}{\diagup}} + O_2 \rightarrow (CH_3)_2N-NO + HO_2 \qquad (28)$$
$$(NDMA)$$
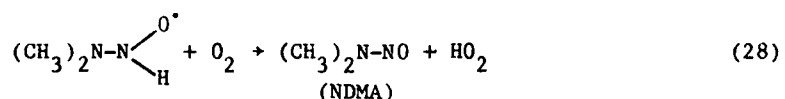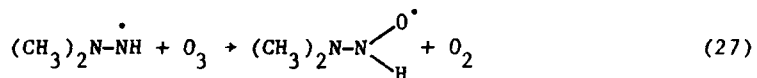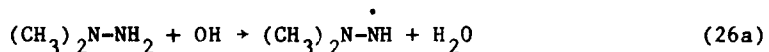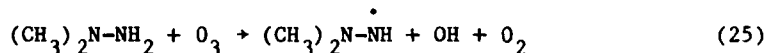
Overall these reactions can be represented by

$$2\ (CH_3)_2N-NH_2 + 3\ O_3 \overset{O_2}{\rightarrow} 2\ (CH_3)_2N-NO + 2\ HO_2$$
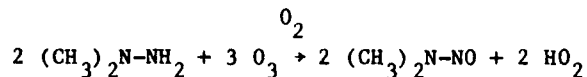
The above mechanism correctly predicts the observed 1.5:1, O_3:UDMH stoichiometry and the formation of NDMA, and was thus considered to be reasonably consistent with the earlier data. An alternative mechanism, which gives rise to the same overall reaction, is to assume that the dimethylhydrazyl radical reacts primarily with O_2 to form the diazo

compound (IV)

$$(CH_3)_2N\overset{\bullet}{N}H + O_2 \rightarrow (CH_3)_2\overset{+}{N}=\overset{-}{N} + HO_2 \qquad (29)$$

followed by   (IV)

$$(CH_3)_2\overset{+}{N}=\overset{-}{N} + O_3 \rightarrow (CH_3)_2NNO + O_2 \qquad (30)$$
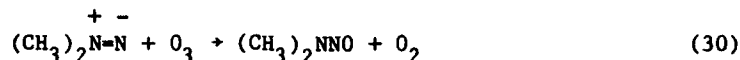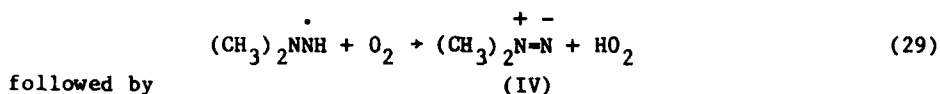
This scheme is suggested by the evidence for the intermediacy of (IV) in the UDMH + NO_x system, though the reactant stoichiometries observed in those runs are not consistent with their formation via reaction (29) (see Section 3.4.4.1).

Unfortunately, neither of these simple mechanisms is consistent with all of the data which has now been obtained. In particular, it is observed that the addition of the radical trap does not significantly change the reactant stoichiometry. When the radical trap is included, these mechanisms predict that reaction (26a) would be suppressed and would cause the overall process to become

$$(CH_3)_2N-NH_2 + 2 O_3 \overset{O_2}{\rightarrow} (CH_3)_2NNO + HO_2$$
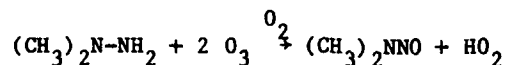
which implies a $\Delta[O_3]/\Delta[UDMH]$ of 2 instead of the observed 1.5. In addition, the above simple mechanisms are similar to the $N_2H_4 + O_3$ mechanisms in that one molecule of HO_2 is formed per UDMH reacted, with the only major sink for HO_2 being H_2O_2 formation via

$$HO_2 + HO_2 \rightarrow H_2O_2 + O_2, \qquad (8)$$

yet much smaller H_2O_2 yields were observed in the UDMH + O_3 experiments than were observed from the $N_2H_4 + O_3$ experiments. Thus, the above mechanisms are either incorrect in some or all of their parts, or additional reactions must be occurring in this system.

The observed formation of non-negligible yields of CH_3NNH (not detected in our previous study [Reference 3] of the UDMH system), HCHO, and CH_3OOH also indicate that the reactions listed above cannot be the only processes occurring. The formation of these products can be attributed to the occurrence of an alternate reaction route for OH + UDMH:

71

$$(CH_3)_2N\text{-}NH_2 + OH \rightarrow \overset{\bullet}{CH_2}\!\!\diagdown N\text{-}NH_2 \diagup CH_3 + H_2O \qquad (26b)$$

followed by

$$\overset{\bullet}{CH_2}\!\!\diagdown N\text{-}NH_2 \diagup CH_3 + O_2 \overset{M}{\rightarrow} \overset{OOCH_2}{\diagdown} N\text{-}NH_2 \diagup CH_3 \rightarrow \left[\begin{array}{c} H_2C \overset{O\text{---}O\cdots H}{\diagdown} N\text{---}N\overset{\cdots}{\diagup}_H \diagup CH_3 \end{array} \right]$$

$$\overset{HOOCH_2}{\diagdown}\overset{\bullet}{N}\text{-}NH \diagup CH_3 \rightarrow OH + CH_2O + CH_3\text{-}N\text{=}NH$$
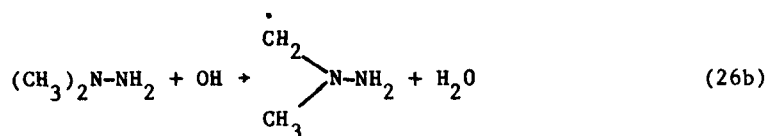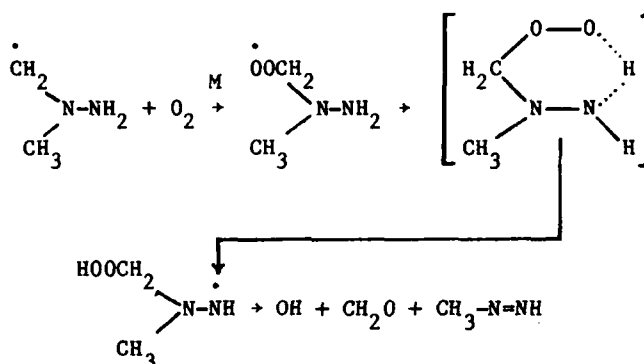
This accounts for the observed formation of HCHO and CH_3NNH in the runs performed without the radical trap.

As discussed in Section 3.3.6.2, CH_3NNH undergoes secondary reaction with O_3 to form methylhydroperoxide and, to a lesser extent, diazomethane; this accounts for the observed formation of CH_3OOH and traces of CH_2N_2, and for the fact that the CH_3OOH yield increases while that of CH_3NNH decreases, as the initial O_3/UDMH ratio is increased in the absence of the radical trap. The fact that the total yields of these fragmentation products increase as the initial O_3/UDMH ratio increases can also be attributed to the $O_3 + CH_3NNH$ reaction, since that process also forms OH radicals, which will increase the relative importance of reaction (26b). This scheme is also consistent with the fact that these products are suppressed when the radical trap is present (and thus the NDMA yield is higher), as implied by reactions (26a) and (26b).

The relatively low yields of H_2O_2 in the absence of the radical trap and the fact that the reactant stoichiometry does not change when the radical trap is added, despite the evidence for OH radical formation in this system and the expected rapid reaction of OH radicals with UDMH, is more difficult to explain. The lower H_2O_2 yields could be due in part to

the consumption of HO_2 in the reaction

$$CH_3OO + HO_2 \rightarrow CH_3OOH + O_2$$
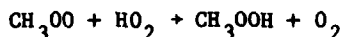
causing CH_3OOH formation following the $O_3 + CH_3NNH$ reaction. However, this explanation is not consistent with the observed slight increase of H_2O_2 yields with the initial O_3/UDMH ratio, which is also accompanied by a relatively larger increase in CH_3OOH. An alternate explanation, which is more consistent with the product yields observed, is that HO_2 may be consumed by reaction with the dimethylhydrazyl radical,

$$(CH_3)_2\overset{\bullet}{N}NH + HO_2 \rightarrow \left[(CH_3)_2N\text{-}N\underset{H}{\overset{OOH}{\diagup}} \right] \rightarrow (CH_3)_2NNO + H_2O \quad (31)$$
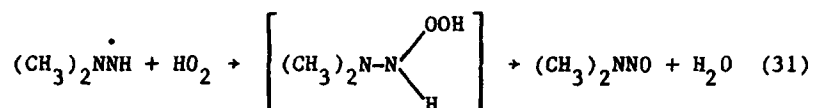
which also gives rise to the observed main product, NDMA. (If $[CH_3]_2NNH$ does not react with O_2, its atmospheric concentration would be higher than those of CH_3NHNH or N_2H_3 under similar circumstances, since the latter radicals are expected to react rapidly with O_2, and thus their reactions with HO_2 would be correspondingly less important.) However, if reaction (31) is the major fate of HO_2 formed in this system, and thus a mechanism based on reactions (25)-(28) followed by (8) is assumed, then the predicted $\Delta[O_3]/\Delta[UDMH]$ would be 1.0, in significant disagreement with the observed value of 1.5.

An alternate method of converting the dimethylhydrazyl radicals to NDMA without forming HO_2 (and thus H_2O_2) would be their self reaction (a reaction which is invoked to explain our UDMH + NO_x data [Section 3.4.4.1]). This reaction would be expected to dominate if the reactions of the hydrazyl radicals with O_3 are slow:

$$2 \ (CH_3)_2\overset{\bullet}{N}\text{-}NH \rightarrow (CH_3)_2\overset{+}{N}\text{=}\overset{-}{N} + (CH_3)_2N\text{-}NH_2 \quad (32)$$
$$\underset{\overset{\displaystyle\downarrow O_3}{}}{} (CH_3)_2NNO + O_2$$
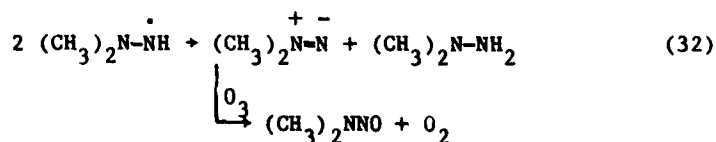
However, a mechanism based on reactions (25), (26) and (32) predicts that

$\Delta[O_3]/\Delta[UDMH] = 2$ in the absence of the radical trap and 3 when it is present, which is clearly contrary to our data.

It should be noted that the above discussion is based on the assumption that the initial reaction consuming UDMH is reaction (25), i.e., that formation of dimethylhydrazyl and OH radicals occurs. As discussed in Section 3.3.6.1, an alternate initial reaction pathway for O_3 + hydrazines is O-atom transfer, which may also occur in the UDMH system:

$$(CH_3)_2N-NH_2 + O_3 \rightarrow \left[(CH_3)_2N-\overset{O}{\overset{|}{N}}H_2 \right] \rightarrow (CH_3)_2N-\overset{\overset{OH}{|}}{N}-H$$

$$(CH_3)_2N\overset{\overset{OH}{|}}{N}H \rightarrow (CH_3)_2\overset{+}{N}=\overset{-}{N} + H_2O$$
$$\downarrow O_3$$
$$(CH_3)_2NNO + O_2$$

or
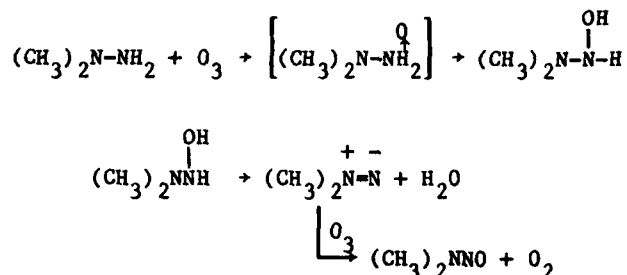
$$(CH_3)_2N-\overset{\overset{OH}{|}}{N}H + O_3 \rightarrow \left[(CH_3)_2N-\overset{O}{\overset{|}{N}}\overset{}{OH}_H \right] \rightarrow \left[(CH_3)_2N-N\overset{OH}{\underset{OH}{\diagdown}} \right] \rightarrow (CH_3)_2NNO + H_2O$$

and

$$(CH_3)_2NNH_2 + O_3 \rightarrow \left[(CH_3)_2\overset{O}{\overset{|}{N}}NH_2 \right] \rightarrow \left[(CH_3)_2\overset{\overset{OH}{|}}{\underset{+}{N}}-\overset{-}{NH} \right] \rightarrow (CH_3)_2\overset{+}{N}=\overset{-}{N} + H_2O$$
$$\downarrow O_3$$
$$(CH_3)_2NNO + O_2$$

However, these schemes not only predict an incorrect $\Delta[O_3]/\Delta[UDMH]$ value of 2, but they also provide no mechanism for the formation of hydroxyl radicals in this system. Since our experiments positively indicate that OH radicals are formed in the UDMH + O_3 system, then regardless of the details of the reactions of the intermediates formed, the initial reaction most likely occurs via reaction (25).

74

3.4 THE REACTIONS OF HYDRAZINES WITH NITROGEN OXIDES

The reactions of NO and NO_2 with N_2H_4, MMH, and UDMH in the dark were studied in the large-volume Teflon® chambers under the following conditions: (1) ~10 ppm of the hydrazine was injected into the chamber (~3800 ℓ configuration) containing ~6 ppm of NO in N_2, with ~6 ppm of NO_2 subsequently added; (2) ~20 ppm of NO was injected into the chamber (6400 ℓ configuration) containing 4-5 ppm of the hydrazine in dry air (~12% RH at room temperature); (3) ~6 ppm of NO_2 was injected into the 3800 ℓ chamber containing 9-10 ppm of the hydrazine in dry air; and (4) ~20 ppm of NO_2 was injected into the 6400 ℓ chamber containing ~4-5 ppm of the hydrazine in dry air. The detailed concentration-time data for environmental chamber experiments in which NO_x was reacted with N_2H_4, MMH and UDMH are given in Appendices E, F, and G, respectively. As in Section 3.3, a particular experiment is identified by the table number in the Appendix for purposes of discussion.

3.4.1 Chamber Experiment Results for Hydrazine + NO_x

The concentration-time data for the reactants and products monitored by FT-IR spectroscopy in the four N_2H_4 + NO_x experiments are detailed in Appendix E and a summary of the conditions and results is given in Table 7. For the purpose of summarizing the results in Table 7, the starting and ending times represent the time of the first measurement after the reactants were adequately mixed and the time of the last measurement respectively, with the product yields and amounts of reactants consumed given in the table reflecting the concentration changes due to reaction over this time interval. In Table 7 and in the following discussion, the observed N_2H_4 loss has been corrected for the N_2H_4 dark decay, thus yielding the amount of N_2H_4 consumed by reaction ($\Delta[N_2H_4]$). Similarly, the observed changes in the NO and NO_2 concentrations have been corrected for the NO dark oxidation (Reference 48) to yield changes due to reaction, i.e., $\Delta[NO]$ and $\Delta[NO_2]$.

When N_2H_4 was mixed with NO in N_2, there was no significant consumption of NO or N_2H_4 (other than what can be attributed to the dark decay of the latter) and no appearance of products other than small amounts of NH_3 was observed (run E-1). In contrast, significant reactions occurred in both N_2 and air when NO_2 was present, with the consumption of N_2H_4 and NO_x being accompanied by the formation of large yields of HONO, the formation

75

TABLE 7. SUMMARY OF CONDITIONS AND RESULTS
FOR THE N_2H_4 + NO_x EXPERIMENTS.

Run ID[a]		E-1	E-2	E-3	E-4
Matrix Gas		N_2	Air	Air	Air
Time Range (min)[b]		82.8–177.8	2.8–182.8	5.8–120.8	9.8–172.8
Initial N_2H_4	(ppm)	8.0	3.5	8.1	4.3
NO	(ppm)	5.9	19.0	-	-
NO_2	(ppm)	5.3	2.4	4.4	20.0
Average NO_2	(ppm)	~4	~6	~3	~18
N_2H_4 dark decay[c]	(ppm)	0.9	0.3	0.8	0.3
$\Delta[N_2H_4]$[d]	(ppm)	1.0	1.9	2.6	2.7
NO oxidized[e]	(ppm)	~0	9.2	-	-
$\Delta[NO]$[f]	(ppm)	0.3	0.4	-	-
$\Delta[NO_2]$[g]	(ppm)	2.4	2.5	2.9	4.7
$\Delta[NO]/\Delta[N_2H_4]$		0.3	0.2	-	-
$\Delta[NO_2]/\Delta[N_2H_4]$		2.5	1.3	1.1	1.8
Yields/($\Delta[NO_x]$):					
HONO		0.46	0.58	0.52	0.71
Yields/($\Delta[N_2H_4]$):					
N_2O		0.13	0.15	0.04	0.23
NH_3		0.23	0.22	0.08	0.29
$(N_2H_4 HNO_3)$[h]		0.21	0.22	0.13	0.37
N_2H_2 (units[i]/ppm)		< 7	< 3	10	< 2

[a]Refers to table number in Appendix E where detailed data are given.
[b]Times given in corresponding data table in Appendix E used for initial
and final reactant and product concentrations.
[c]Calculated amount of hydrazine lost due to decay in the absence of NO_x using
N_2H_4 dark decay = $k_d \int [N_2H_4]dt$, where k_d is the unimolecular decay rate
appropriate for the conditions of the run, and the $[N_2H_4]$ is integrated over
the indicated time range. For run E-1, k_d=1.4 x 10^{-3} min^{-1}, based on N_2H_4
decay rate in N_2 in the presence of NO observed in this run prior to the NO_2
injection; for runs E-2 and E-4, k_d=7.0 x 10^{-4} min^{-1}, appropriate for the
6400-liter chamber (see Section 3.2); and for run E-3, k_d=1.1 x 10^{-3} min,
appropriate for the 3800 ℓ chamber.
[d]The "Δ" sign indicates the amount consumed by reaction over the indicated
time range and has been corrected for the N_2H_4 dark decay.
[e]Calculated amount of NO oxidized due to the reaction NO + NO + O_2 + $2NO_2$ =
$2k[O_2]\int[NO]^2dt$, where k = 1.9 x 10^{-38} cm^6 $molecule^{-2}$ sec^{-1} (Reference 48)
and $[NO]^2$ is integrated over the indicated time range.
[f]$\Delta[NO]$ = $\Delta[NO]^{obs}$ - (NO oxidized).
[g]$\Delta[NO_2]$ = $\Delta[NO_2]^{obs}$ + (NO oxidized).
[h]See text for method used to estimate concentration.
[i]Units = [(1277 cm^{-1} absorbance)/(IR pathlength)] x 10^5.

of hydrazinium nitrate ($N_2H_4 \cdot HNO_3$; see below), N_2H_2 (in excess N_2H_4 only), and the formation of smaller amounts of N_2O and NH_3. This is illustrated in Figures 14 and 15, which give concentration-time plots of the reactants and observed products for the $N_2H_4 + NO_2$ runs performed in air with excess N_2H_4 (run E-3) and excess NO_2 (run E-4), respectively. Although reaction occurred when N_2H_4 was mixed with NO in air, this can be attributed to N_2H_4 reacting with the NO_2 formed from the reaction of NO with O_2. Therefore, the results of the four experiments discussed here clearly indicate that N_2H_4 reacts with NO_2, but that the reaction of N_2H_4 with NO, if it occurs, is too slow to be measured with our experimental techniques.

The reactant stoichiometry and the relative product yields observed in the $N_2H_4 + NO_2$ reaction were found to be quite variable, depending on the reaction conditions. When the reaction was conducted in air, the $\Delta[NO_2]/\Delta[N_2H_4]$ ratio (Table 7) was found to increase with the initial NO_2/N_2H_4 reactant ratio, with values of ~1.1 in excess N_2H_4 (run E-3) and ~1.8 in excess NO_2 (run E-4); the $\Delta[NO_2]/\Delta[N_2H_4]$ ratio in run E-2, where NO_x was injected initially as pure NO in excess amount, is intermediate between the above values. The amount of NO_2 consumed was much higher in the N_2H_4 plus NO and NO_2 run performed in N_2 (run E-1), with the $\Delta[NO_2]/\Delta[N_2H_4]$ ratio being ~2.5.

When NO was present along with NO_2 in the reaction mixture, some consumption of NO also occurred. The $\Delta[NO]/\Delta[N_2H_4]$ ratios are similar for the two experiments (runs E-1 and E-2), with values of 0.3 in N_2 and 0.2 in air. This indicates that although N_2H_4 and NO do not react in the absence of NO_2, NO is apparently oxidized by some of the intermediates formed when N_2H_4 reacts with NO_2.

The HONO yields generally were ~50-70% of the NO_x consumed, but were more variable relative to the amount of N_2H_4 reacted. N_2O and NH_3 were observed to be formed in all runs, with yields which generally increased with the initial NO_2/N_2H_4 reactant ratio. Diazene was detected only in the runs with excess N_2H_4, with a trace amount observed at the end of the run in N_2 (run E-1) and with relatively higher amounts seen for most of the reaction period in the run in air where N_2H_4 was in excess (Table E-3). Based on the behavior of methyldiazene formed in the MMH + NO_2 system (Section 3.4.2, below), these observations probably indicate that N_2H_2 reacts with NO_2.

77
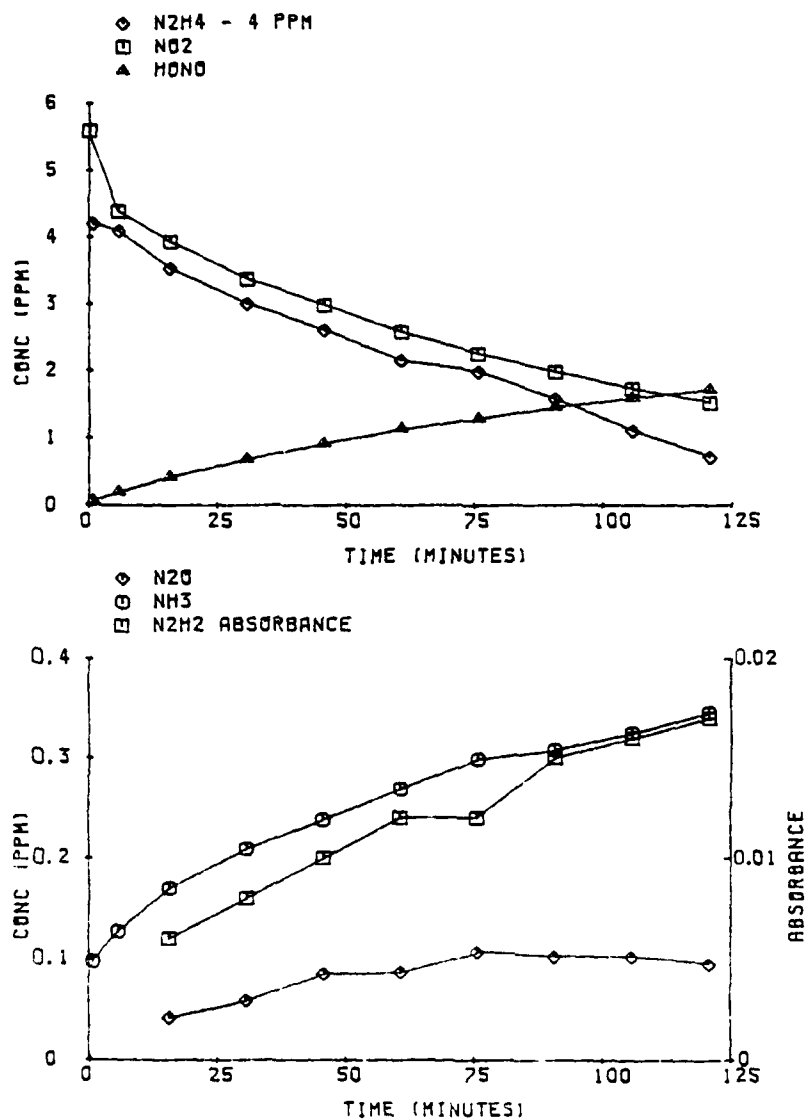
Figure 14. Concentration-Time Plots for Reactants and Selected Products Observed in the N_2H_4 + NO_2 Run E-3 with Excess N_2H_4.
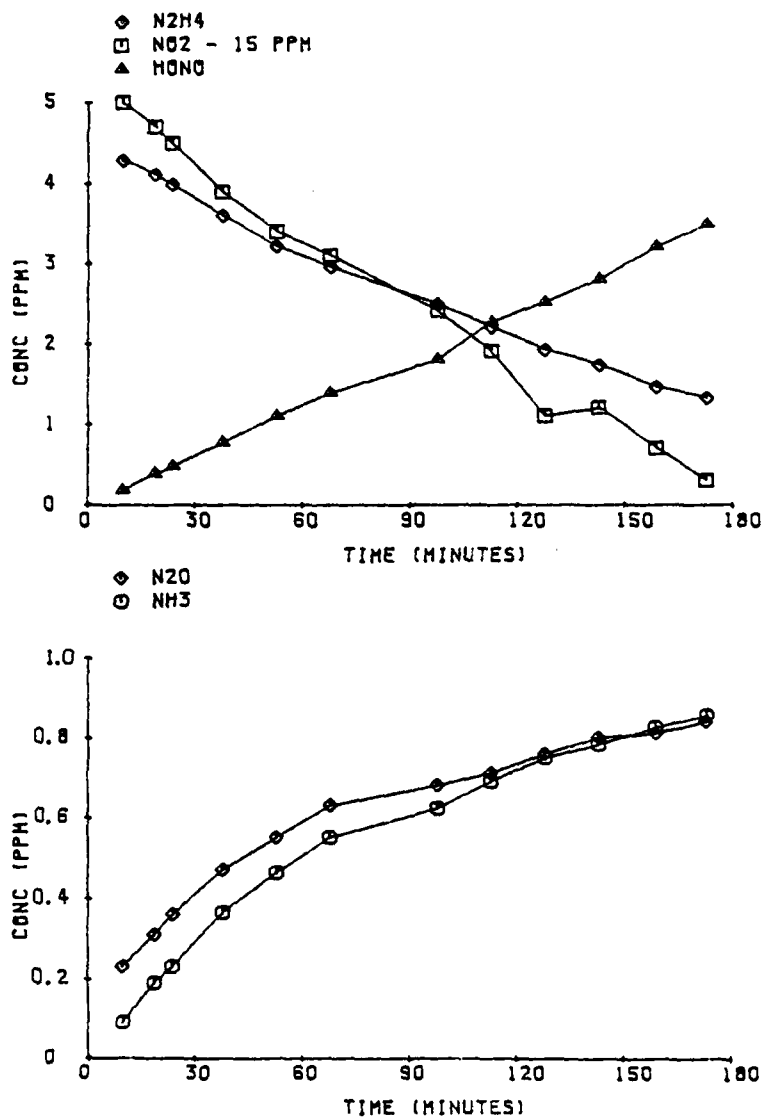
Figure 15. Concentration-Time Plots for Reactants and Selected Products Observed in the N_2H_4 + NO_2 Run E-4 with Excess NO_2.

When HONO, N_2O, and NH_3 are the only products considered in the N_2H_4 + NO_x runs, the nitrogen balances over the reaction time intervals given in Table 7 were found to be as follows: 83% for run E-1, 84% for run E-2, 63% for run E-3, and 82% for run E-4. The nitrogen balances for runs E-1 and E-3 increase to 90% and 71%, respectively, when the N_2H_4 decay calculated in Table 3.4.1 is assumed to yield mainly N_2 and this is included in the estimate. The value for run E-3 does not include the nitrogen in diazene, since the lack of an absorption coefficient value prevented the calculation of its absolute concentrations. Run E-3, the only one in which diazene was detected at significant levels, yielded the poorest nitrogen balance; however, it is considered unlikely that diazene could account for a large fraction of the missing nitrogen.

To varying extents, part of the missing nitrogen can be accounted for by the hydrazinium nitrate ($N_2H_4 \cdot HNO_3$) formed in the above experiments. The highest yield of this compound was observed in the run in air with excess NO_2 added to N_2H_4 (run E-4). The spectrum recorded at the end of this experiment is presented in Figure 16a, with the absorptions of unreacted N_2H_4 subtracted, and shows the easily identified absorption bands of HONO and NH_3. The relatively strong, broad absorption feature seen at ~1390 cm^{-1} is brought out more clearly in Figure 16 by masking the superimposed H_2O lines beyond ~1300 cm^{-1}. Upon subtraction of HONO, NH_3, and N_2O absorptions (N_2O has a weak absorption at 1285.3 cm^{-1}), the contour of the broad band at ~1390 cm^{-1} and the weak absorption at ~826 cm^{-1} (both characteristics of nitrate salts) are clearly seen in Figure 16b. This residual spectrum is similar to that of the product obtained from the direct reaction of N_2H_4 and HNO_3 in the vapor phase (discussed later in Section 3.6.1), thus confirming the formation of hydrazinium nitrate in the reaction of N_2H_4 with NO_2.

It is difficult to obtain an exact measure of hydrazinium nitrate, since it was presumably formed in both gaseous and aerosol phase in our experiments and was probably susceptible to losses on the chamber walls. However, an estimate of its concentration is attempted here by comparing the intensity of the ~1390 cm^{-1} band with that of a spectrum from the N_2H_4 + HNO_3 reaction (see Section 3.6.1) associated with a known amount (2.0 ppm) of completely reacted N_2H_4. The yields of the hydrazinium nitrate
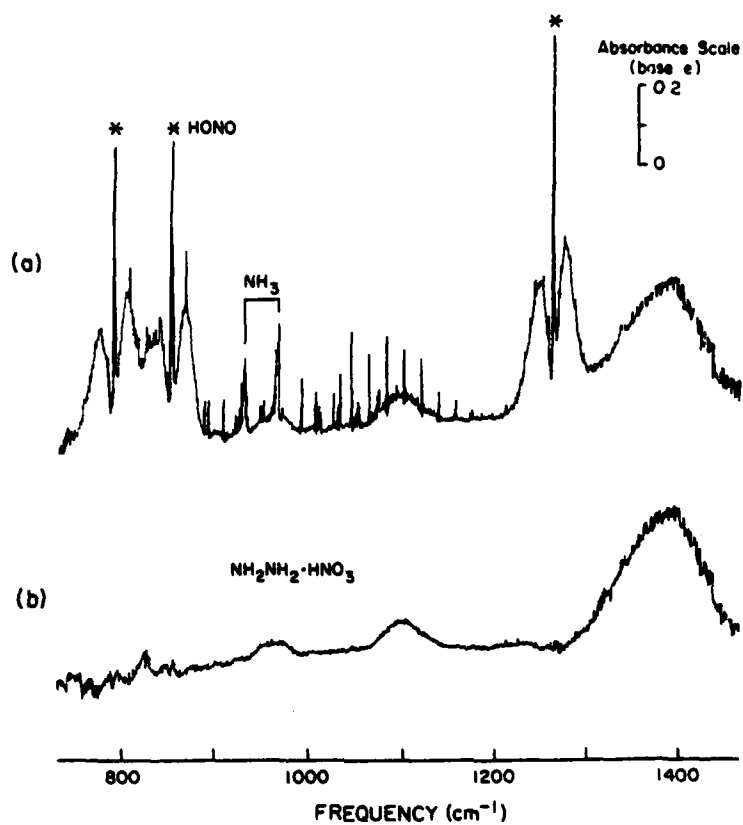
Figure 16. Product Spectra from N_2H_4 + Excess NO_2 Reaction (Run E-4); Res = 1 cm^{-1}, Pathlength = 102.4 m. (a) At t = 187.8 min, (b) Residual Spectrum from (a).

thus obtained are presented in Table 7 as fractions of the N_2H_4 which reacted. They correlate roughly with the initial NO_2/N_2H_4 ratio. The results suggest that formation of the hydrazine salt was significant in all of the experiments, but particularly under excess NO_2 conditions. When the nitrogen in hydrazinium nitrate is taken into account, the final nitrogen relative to the initial nitrogen yields are calculated as follows: 92% for run E-1, 90% for run E-2, 75% for run E-3, and 94% for run E-4. It is not certain why run E-3 (N_2H_4 + NO_2 with excess N_2H_4) shows a significantly poorer nitrogen balance. However, the presence of significant concentrations of diazene throughout this experiment may suggest a higher degree of ultimate conversion of N_2H_4 to N_2.

Hydrazinium nitrate is the only product which appeared in the residual spectra in the N_2H_4 + NO_2 experiments (runs E-3 and E-4). For the reaction of N_2H_4 with NO_2 in the presence of initially added NO, weak absorption bands at ~1020 cm^{-1} for the run in air and at ~1032 cm^{-1} for the run in N_2 were also observed; however, no other clear absorption bands in the infrared spectrum could be associated with these features to provide positive identification. Despite the large yields of HONO generated in the N_2H_4 + NO_x systems, hydrazinium nitrite ($N_2H_4 \cdot HONO$) was not formed, as evidenced by the absence of a strong broad absorption at ~1270 cm^{-1} expected from a stretching fundamental of the -ONO group. HONO is apparently not a strong enough acid to form its salt with N_2H_4 in the vapor phase reaction.

The reaction of N_2H_4 with NO_2 is significantly slower than the reaction of N_2H_4 with O_3 (Section 3.3); the N_2H_4 + NO_2 reaction was still incomplete after the 2-3 hour duration of these experiments. The decay curves of NO_2 in excess N_2H_4 (runs E-1 and E-3) and of N_2H_4 in excess NO_2 (run E-4) are reasonably exponential, as shown in Figure 17, where plots of $\ln[N_2H_4]$ (run E-4) and $\ln[NO_2]$ (runs E-1 and E-3) against reaction time are shown. This suggests that the reaction is first order in each reactant. However, the apparent bimolecular rate constants derived from the decay rates shown in Figure 17 depended significantly on the reaction conditions, even when the observed stoichiometry factor ($\Delta[NO_2]/\Delta[N_2H_4]$) was used to relate rate constants derived from rates of NO_2 decay to those derived from N_2H_4 decay, and when the N_2H_4 decay rate in run E-4 was corrected by subtracting the N_2H_4 dark decay rate of ~10^{-3} min^{-1} before
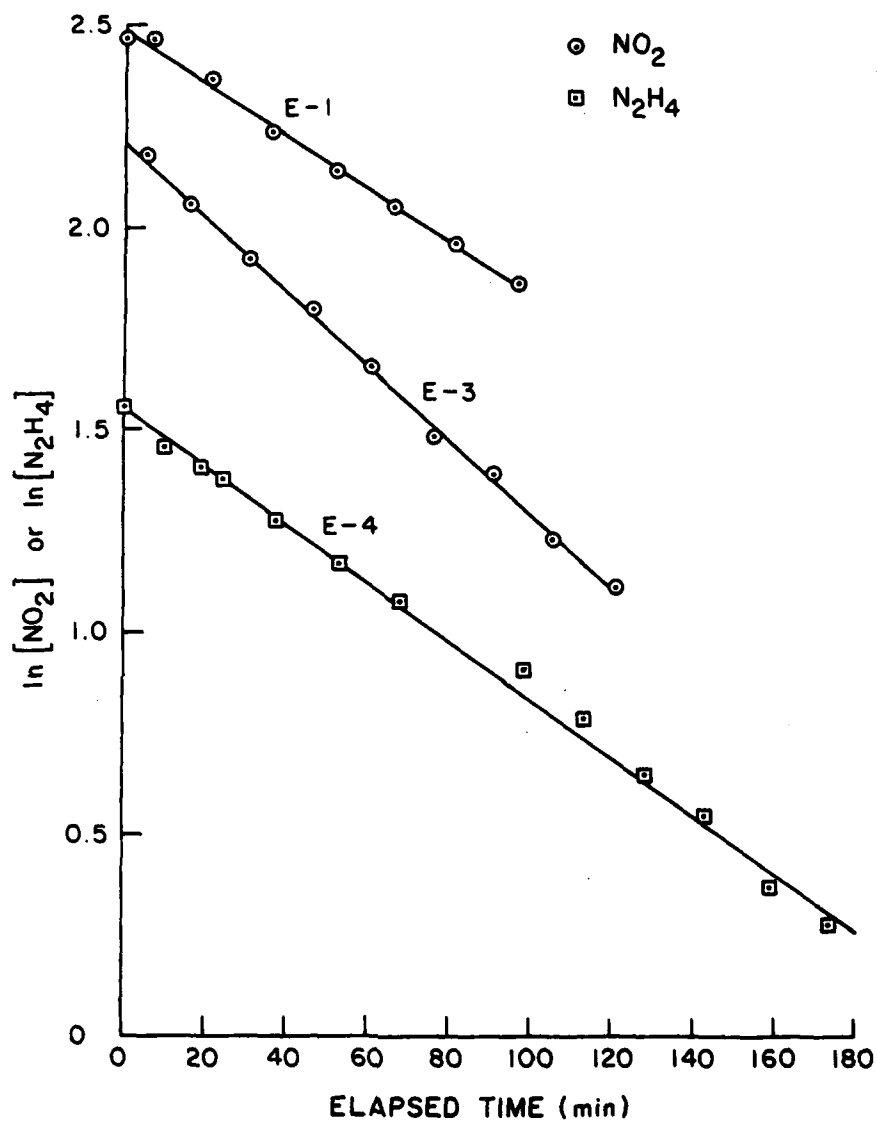
Figure 17. Plots of ln[N₂H₄] or ln[NO₂] Against Elapsed Time for Selected N₂H₄ + NOₓ Experiments (Concentrations are in ppm, and Data for Runs E-1 and E-3 are Offset by +0.8 and +0.7 Log Units, Respectively).

83

calculating the apparent rate constant. In particular, although the apparent rate constants derived from NO_2 decay in excess N_2H_4 in N_2 (run E-1) and that derived from N_2H_4 decay in excess NO_2 (run E-4) and in excess $NO + NO_2$ (run E-2) were in good agreement, being $(3.7 \pm 0.4) \times 10^{-4}$ ppm^{-1} min^{-1} for run E-1 and $(3.5 \pm 0.4) \times 10^{-4}$ ppm^{-1} min^{-1} for run E-4 (or $\sim 2.5 \times 10^{-19}$ cm^3 $molecule^{-1}$ sec^{-1} for both), the rate constant derived from NO_2 decay in excess N_2H_4 (run E-3) was a factor of ~ 4 higher, being $(1.5 \pm 0.3) \times 10^{-3}$ ppm^{-1} min^{-1}. Based on the lower rate constants observed, we derive an upper limit rate constant of $\sim 2.5 \times 10^{-19}$ cm^3 $molecule^{-1}$ sec^{-1} for the elementary reaction.

3.4.2 Chamber Experiment Results for Monomethylhydrazine + NO_x

The detailed concentration-time data for the reactants and products in the four MMH + NO_x experiments are given in Appendix F and a summary of the conditions and results are given in Table 8. As in the case of the N_2H_4 + NO_x data above, corrections for the amount of the MMH lost due to dark decay and for NO conversion to NO_2 via reaction with O_2 (in run F-2) have been taken into account in establishing the amounts of the reactants actually consumed by the MMH + NO_x reactions during the time intervals of interest. These corrected values were used to derive the reactant stoichiometries and product yields referred to in the following discussion.

The results of the MMH + NO_x runs in N_2 (Table F-1) indicate that MMH, like N_2H_4, reacts with NO_2 but does not react at a measurable rate with NO. The MMH + NO_2 reaction occurred at a rate approximately six times faster than N_2H_4 + NO_2 (see below). As with the N_2H_4 + NO_x system, the reaction stoichiometry and relative product yields (Table 8) varied with experimental conditions, though in all cases more NO_x than MMH was consumed in the reactions. As in the N_2H_4 case, the $\Delta[NO_2]/\Delta[MMH]$ ratio increased with the initial NO_2/MMH reactant ratio for the runs conducted in air (runs F-2, F-3 and F-4). The $\Delta[NO_2]/\Delta[MMH]$ ratio in the N_2 run (run F-1) also followed the trend observed in the runs in air; it differs, however, from that of the N_2H_4 + NO_x run in N_2 in that the $\Delta[NO_2]/\Delta[N_2H_4]$ ratio was found to be significantly higher than in air. When NO was present in the reaction mixture, some NO consumption occurred, with the relative amount consumed being higher in the MMH + NO_x system than in the N_2H_4 + NO_x system (see Tables 7 and 8).

84

Run ID[a]		F-1	F-2	F-3	F-4
Matrix Gas		N_2	Air	Air	Air
Time Range (min)[b]		101.8-185.8	1.8-131.8	1.4-94.8	3.8-55.8
Initial MMH	(ppm)	9.1	4.2	9.4	3.2
NO	(ppm)	5.7	19.4	-	-
NO_2	(ppm)	5.1	1.7	5.0	18.8
Average NO_2	(ppm)	~3	~3	~3	~14
MMH dark decay[c]	(ppm)	0.3	0.1	0.3	~0
Δ[MMH]	(ppm)	2.7	3.7	3.4	3.2
NO oxidized[d]	(ppm)	~0	6.3	-	-
Δ[NO][e]	(ppm)	1.5	5.1	-	-
Δ[NO_2][f]	(ppm)	4.5	3.1	4.6	9.2
Δ[NO]/Δ[MMH]		0.6	1.4	-	-
Δ[NO_2]/Δ[MMH]		1.7	0.8	1.3	2.9
Yields/(Δ[NO_x]):					
HONO		0.69	0.64	0.72	0.50
Yields/(Δ[MMH]):					
CH_3NHN[g]		0.5	0.2	0.2	0.03[h]
CH_3OOH		< 0.2	< 0.1	0.4	< 0.1
CH_3OH		0.04	0.02	0.03	0.03
N_2O		0.04	0.05	< 0.01	0.01
NH_3		0.01	0.02	0.03	0.02
Unknown 1(units[h]/ppm)		~2	~1	~1	~13
Unknown 2(units[i]/ppm)		~4	~4	-	~2
Maximum $HOONO_2$	(ppm)	< 0.03	< 0.02	0.10[j]	0.13[j]

[a]Refers to table number in Appendix F where detailed data are given.
[b]Times given in corresponding data table in Appendix F used for initial
 and final reactant and product concentrations.
[c]Calculated amount of hydrazine lost due to decay in the absence of NO_x using
 MMH dark decay = $k_d \int$[MMH]dt, where k_d is the unimolecular decay rate appro-
 priate for the conditions of the run, and the [MMH] is integrated over the
 indicated time range. For runs F-2 and F-4, k_d=2.3 x 10^{-4} min^{-1}, appropriate
 for the 6400-liter chamber (see Section 3.2); and for runs F-1 and F-3,
 k_d=3.8 x 10^{-4} min, appropriate for the 3800-liter chamber.
[d]Calculated amount of NO oxidized due to the reaction NO + NO + O_2 → $2NO_2$ =
 $2k[O_2]\int$[NO]^{2}dt, where k = 1.9 x 10^{-38} cm^6 $molecule^{-2}$ sec^{-1} (Reference 48)
 and [NO]^2 is integrated over the indicated time range.
[e]Δ[NO] = Δ[NO]^{obs} - (NO oxidized).
[f]Δ[NO_2] = Δ[NO_2]^{obs} + (NO oxidized).
[g]IR absorption coefficient based on carbon balance in MMH + O_3 runs (Section
 3.3.3).
[h]Units = [(1300 cm^{-1} absorbance)/IR pathlength)] x 10^4.
[i]Units = [(1032 cm^{-1} absorbance)/IR pathlength)] x 10^4.
[j]Built to a maximum and subsequently declined.
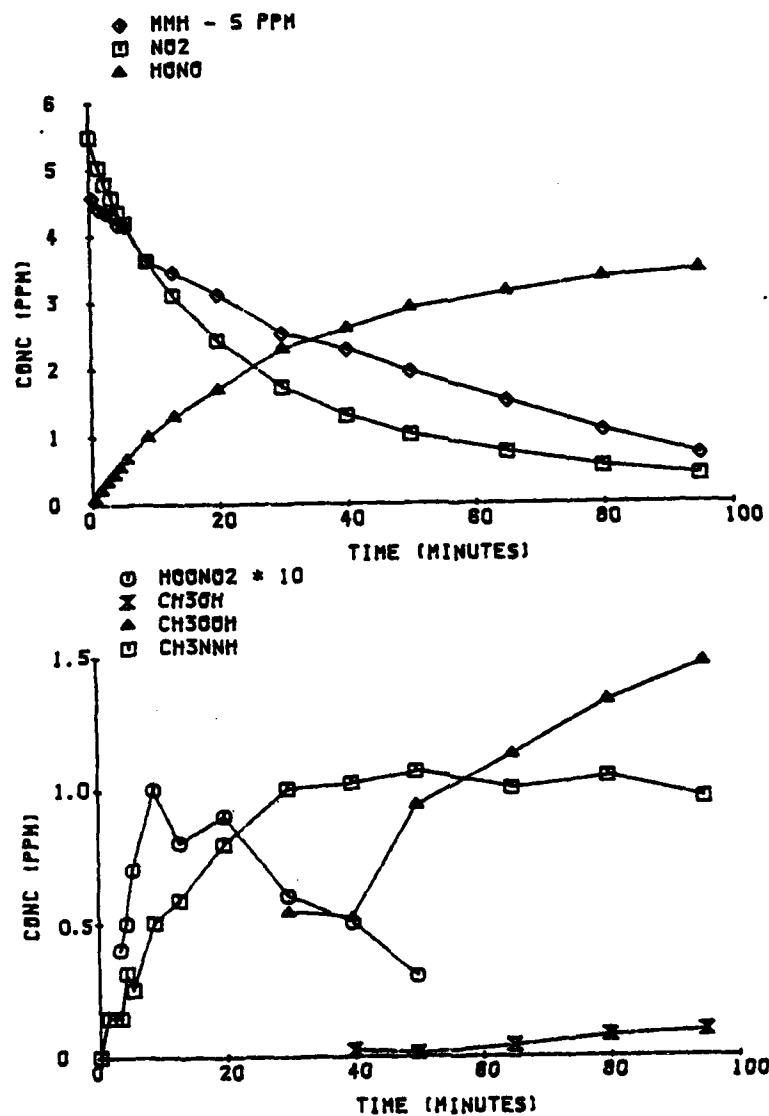
Figure 18. Concentration-Time Plots for Reactants and
Selected Products Observed in the MMH + NO_2
Run F-3 in Excess MMH.
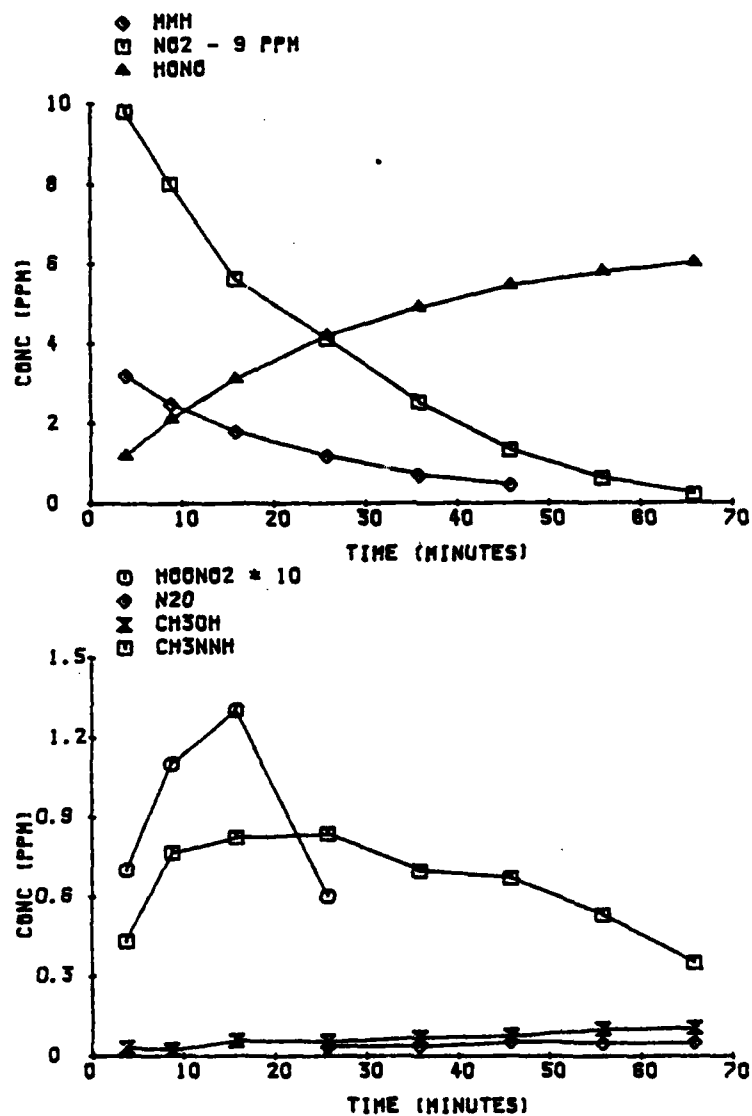
Figure 19. Concentration-Time Plots for Reactants and Selected Products Observed in the MMH + NO_2 Run F-4 in Excess NO_2.

The infrared spectra obtained in these experiments were characterized by several unidentified absorption bands, indicating that the mixture of products generated in the MMH + NO$_x$ reaction was considerably more complex than that observed in the N$_2$H$_4$ + NO$_x$ system. The concentration-time plots for the reactants and the product species which were identified and quantitatively measured by FT-IR spectroscopy for the runs performed in air with excess MMH (run F-3) and with excess NO$_2$ (run F-4) are shown in Figures 18 and 19, respectively. HONO and CH$_3$NNH were the identified and quantitatively measured major products, with N$_2$O, NH$_3$ and CH$_3$OH being formed in minor yields. A significant amount of CH$_3$OOH, equivalent to approximately 40% of the MMH consumed, was formed when NO$_2$ was reacted with excess MMH in air (run F-3; Table 8). Other than the formation of low levels of HOONO$_2$ as a transient intermediate in the runs without NO (runs F-3 and F-4; see Figure 18 and 19), the inorganic products were the same as those observed in the N$_2$H$_4$ system. HONO yields were 50-70% of the NO$_x$ consumed, or 100-180% of the hydrazine consumed. The methyldiazene yield did not depend strongly on whether the reaction was conducted in air or in N$_2$, but was suppressed in the presence of excess NO$_2$ (run F-4).

Taking into account only the product species identified above, the carbon and nitrogen balances were calculated from the data of Appendix F for the reaction periods given in Table 8. Although only the absorbance values of CH$_3$NNH are presented in Tables F-1 through F-4, estimates of its concentration were made using the absorption coefficient of 7 cm^{-1} atm^{-1} derived from the MMH + O$_3$ experiments (Section 3.3.3). The final carbon balances relative to the initial carbon are 80% for run F-1, 32% for run F-2, 86% for run F-3, and 17% for run F-4. The corresponding values for the nitrogen balance are 82%, 72%, 72%, and 61%, respectively, for runs F-1, F-2, F-3, and F-4. The poorest carbon balances are found in runs F-2 and F-4 which are characterized by high initial NO$_x$/MMH ratios, while the significantly lower nitrogen content found in the products of run F-4 could be related to the much higher initial NO$_2$ in this experiment. These findings qualitatively agree with the analyses of the infrared spectra, where the stronger absorptions of methylhydrazinium nitrate (CH$_3$NHNH$_2$·HNO$_3$) and other other unknown products were observed for runs F-2 and F-4.
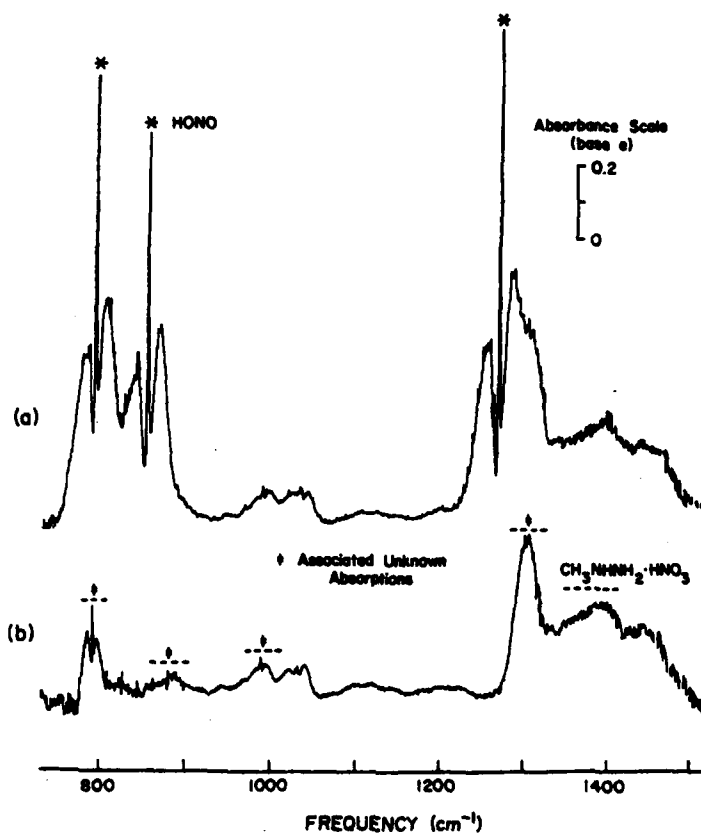
Figure 20. Product Spectra from MMH + Excess NO_2 Reaction (Run F-4); Res = 1 cm^{-1}, Pathlength = 102.4 m. (a) At t = 65.8 min, (b) Residual Spectrum from (a).

89

The product spectra from the reaction of MMH with excess NO_2 in air (run F-4) are presented in Figure 20. Figure 20a shows the infrared spectrum of the products in the ~750-1500 cm^{-1} region recorded at the end of the experiment (t = 65.8 min in Table F-4) and shows that MMH was completely consumed. Figure 20b resulted from subtracting the absorptions of the known components, i.e., HONO, NH_3, N_2O, and CH_3OH. (Strong interferences from the unmatched H_2O absorptions were masked to bring out more clearly the contour of broad absorptions beyond ~1300 cm^{-1}. The intense absorptions of HONO observed in Figure 20a necessitated obtaining a similar reference spectrum for subtraction. However, HONO could not be prepared without accompanying large amounts of NO and NO_2 whose absorptions dominate the ~1550-2000 cm^{-1} region. The use of such a HONO reference spectrum for subtraction severely distorted the ~1550-2000 cm^{-1} region of the product spectrum which was already characterized by unmatched H_2O absorptions. Thus, the region above ~1500 cm^{-1} cannot be clearly presented here. Strong NO_2 lines from the HONO reference spectrum also cause some degree of distortion among the absorptions around 800 cm^{-1}.

By analogy with the N_2H_4 + NO_x system, formation of methylhydrazinium nitrate ($CH_3NHNH_2 \cdot HNO_3$) is expected in the MMH case, with its largest yield anticipated in the run with excess NO_2. Indeed, a broad absorption at ~1390 cm^{-1} is evident in Figure 20b, whose contour matches that of the spectrum of the product from the direct reaction of MMH and HNO_3 (see later, Section 3.6.2). The much weaker nitrate absorption at ~825 cm^{-1} and other weak bands seen in the authentic sample are not clearly discernible among the other unknown bands in Figure 20. Due to obvious interferences, it is not possible to obtain a reliable measure of the methylhydrazinium nitrate produced.

Also seen in Figure 20b is the unknown absorption at ~1300 cm^{-1}, which would be somewhat less intense than it appears if it were not superimposed on the broad ~1390 cm^{-1} band of methylhydrazinium nitrate. Based on the observed time behavior, the 1300 cm^{-1} absorption appears to be associated with other bands (marked with the symbol ✝ in Figure 20b) at the approximate positions 792, 886, and 989 cm^{-1}. Moreover, this group of absorptions is associated with a band at ~1730 cm^{-1} (not shown in the plot) which appeared as the strongest absorption (except for those of

HONO) in the product spectrum, despite heavy distortions from the unmatched-ed H_2O and NO_2 lines. N-Methylformamide, which was identified in an early work (Reference 49) as a product of MMH + N_2O_4 reaction in solution, has been ruled out as a product of the present reaction system. Since the formation of other compounds with C=O groups is highly unlikely in this reaction, the most plausible explanation for the 1730 cm^{-1} band is that it arises from an -O-N=O group whose N=O stretching frequency is driven from its normal range of 1610-1685 cm^{-1} (Reference 50) to the higher position observed by influence of an electronegative substituent. The presence of the 792 cm^{-1} absorption supports this interpretation, since organic nitrites are known to possess an absorption band near 800 cm^{-1}. It is possible that other characteristic functional group absorptions in the ~1550-1650 cm^{-1} region, which may provide further clues as to the identity of this unknown, might have been missed in the interpretation due to the severe interferences encountered in this spectral range. That HONO may somehow be involved in the formation of this unknown product is suggested as well by the relatively lower yield of HONO per MMH consumed in this run (F-4) compared with the other runs, despite the highest initial NO_2/MMH ratio employed (Table 8).

A group of absorption bands due to a second unidentified product is also seen in Figure 20b. However, these absorptions are more clearly seen in Figure 21, which shows the product spectra for the run in air where both NO and NO_2 were present (run F-2). The residual spectrum (Figure 21b) resulting from subtraction of most known absorptions show mainly this group of bands, at the approximate positions 1032, 1120, 1213, and 1450 cm^{-1} (marked by the symbol #), together with the absorption bands of CH_3NNH and $CH_3NHNH_2 \cdot HNO_3$ and an indication of a small yield of the first unknown (by its 1300 cm^{-1} band). The 1450 cm^{-1} band of the second unknown overlaps a fundamental of CH_3NNH at ~1460 cm^{-1} (Reference 51), but the latter should be significantly weaker based on the strength of the other associated absorptions. The unknown's 1450 cm^{-1} absorption most likely arises from the N=O stretch of an -N-N=O group (Reference 50), with the 1032 cm^{-1} band being a candidate for the N-N stretching mode. As in the case of the first unknown, no positive identification can be given at this time.
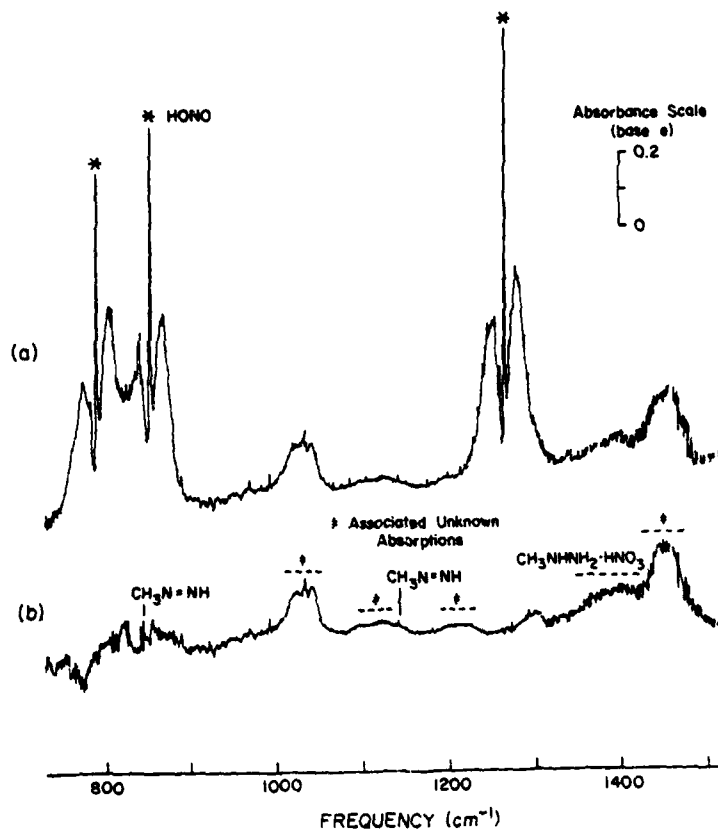
Figure 21. Product Spectra from MMH + NO/NO₂ Reaction
(Run F-2); Res = 1 cm⁻¹, Pathlength = 102.4 m.
(a) At t = 131.8 min, (b) Residual Spectrum
from (a).

The first unknown, with associated functional group absorption at ~ 1730 cm^{-1}, was observed in highest yields in excess NO_2; its yield in this run (F-4) relative to the MMH consumed was ~ 7-12 times higher than those in the other runs and roughly correlated with the initial NO_2/MMH ratio. The second unknown (with a functional group absorption at ~ 1450 cm^{-1}) was formed in all of the runs except F-3 (the run with excess MMH). Per MMH consumed, the yield of the second unknown was ~ 2 times lower in excess NO_2 (run F-4) than the yields in runs where both NO and NO_2 were present, either in N_2 (run F-1) or in air (run F-2).

Methylhydrazinium nitrate was observed in all of the runs. As judged from the product spectra, the highest amounts were formed in the excess NO_2 run (F-4), analogous to the N_2H_4 + NO_2 system, with ~ 3-4 times smaller yields for the other experiments. It appears certain that, at least for run F-4, the inclusion of methylhydrazinium nitrate and the two unknown compounds would dramatically improve both the carbon and nitrogen balance.

The rate of decay of NO_2 in the presence of excess MMH and of MMH in excess NO_2 are reasonably consistent with the overall reaction being first order in each reactant. Plots of ln[MMH] in the excess NO_2 run (F-4) and of ln[NO_2] in excess MMH (runs F-1 and F-3) against time are shown in Figure 22 for the first ~ 35 min of the reaction. The slight curvature observed in the plot for run F-3 can be attributed to decreasing concentrations of the excess MMH during the reaction.

The apparent MMH + NO_2 rate constants derived from the decays shown in Figure 22 (where the rates obtained from the NO_2 decays were corrected using the observed Δ[NO_2]/Δ[MMH] ratios) were not significantly different for the three runs, being $(2.3 \pm 0.3) \times 10^{-3}$ ppm^{-1} min^{-1} in run F-1 (NO_2 decay in excess MMH in N_2), $(2.7 \pm 0.2) \times 10^{-3}$ ppm^{-1} min^{-1} in run F-3 (NO_2 decay in excess MMH in air), and $(3.3 \pm 0.9) \times 10^{-3}$ ppm^{-1} min^{-1} in run F-4 (MMH decay in excess NO_2 in air). This contrasts with the results for the corresponding N_2H_4 + NO_2 experiments, where the rate in excess hydrazine in air was significantly higher than in the other two runs. However, the apparent MMH + NO_2 rate constant derived from the NO_2 decay near the end of the excess MMH run (F-3) and that derived from the MMH decay in the presence of excess NO in air (F-2) are ~ 2-3 times higher than these. The higher rate of NO_2 decay near the end of run F-3 can be attributed to NO_2 consumption by reaction with CH_3NNH (see below). The data indicate an
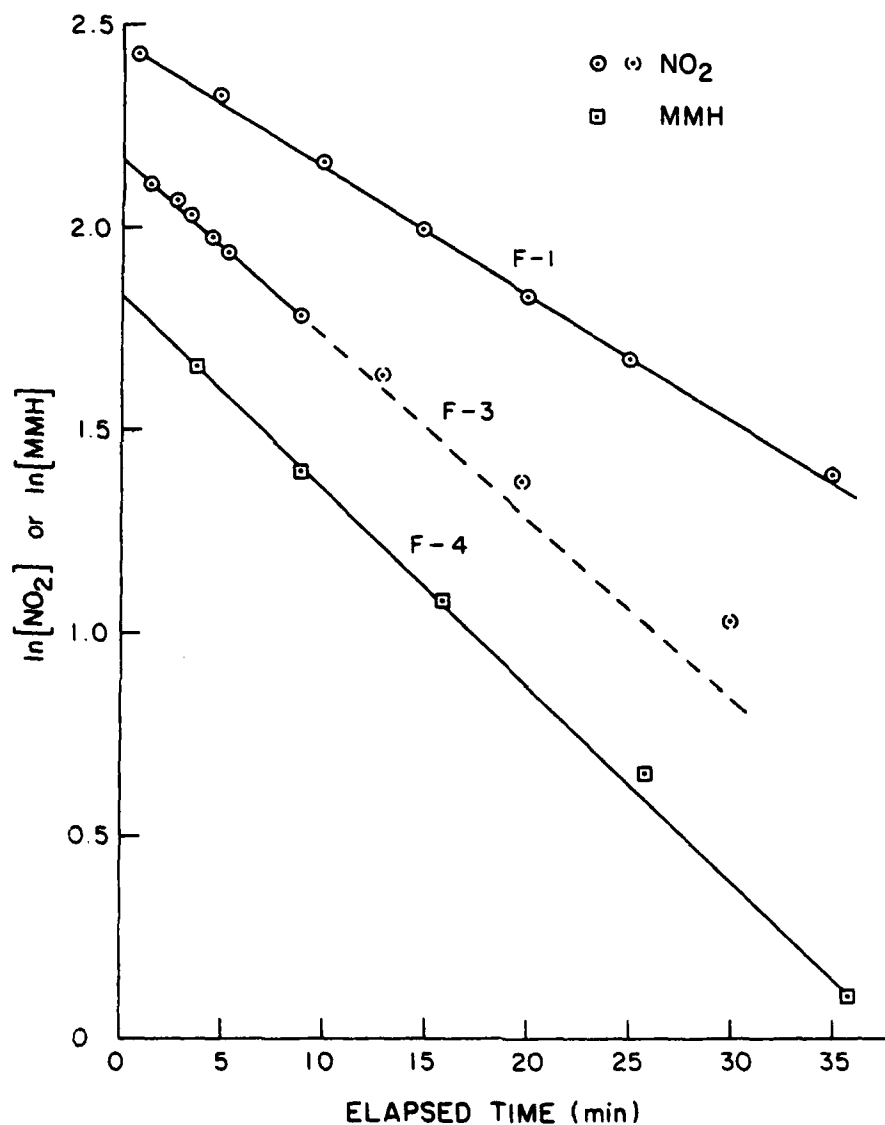
Figure 22. Plots of ln[MMH] or ln[NO$_2$] Against Elapsed Time for Selected MMH + NO$_x$ Experiments. (Concentrations are in ppm, and Data for Runs F-1, F-3, and F-4 are Offset by 0.8, 0.6, and 0.5 Log Units, Respectively.) ▣, ⊖ – Data Used to Obtain Lines Shown; (·) – Data Not Used to Obtain Lines Shown.

94

upper limit rate constant of $\sim 2 \times 10^{-3}$ ppm^{-1} min^{-1} ($\sim 1.4 \times 10^{-18}$ cm^3 molecule^{-1} sec^{-1}) for the initial MMH + NO$_2$ reaction, which is ~ 6 times higher than the upper limit estimated for the elementary rate constant of the N$_2$H$_4$ + NO$_2$ reaction.

The observed suppression of the CH$_3$NNH yield in excess NO$_2$ (run F-4) indicates that it reacted with NO$_2$, since the CH$_3$NNH built up to a maximum and subsequently declined (see Figure 19). The rate of the CH$_3$NNH decay following the consumption of MMH provided a lower limit estimate for the apparent CH$_3$NNH + NO$_2$ rate constant of $\sim 3 \times 10^{-18}$ cm^3 molecule^{-1} sec^{-1}, which is comparable to that found above for the MMH + NO$_2$ reaction.

3.4.3 Chamber Experiment Results for Unsymmetrical Dimethylhydrazine + NO$_x$

The detailed concentration-time data for the reactants and products in the four UDMH + NO$_x$ experiments are given in Appendix G and a summary of the conditions and results are given in Table 9. In the UDMH + NO/NO$_2$ experiment performed in N$_2$, a second NO$_2$ injection was made to react with the remaining UDMH after the initially-injected NO$_2$ was consumed (run G-1); the results are summarized in Table 9 in the two columns for that run. No correction to the amount of UDMH consumed due to dark decay was made since the latter process was negligible in the time scale of these experiments (see Section 3.2.3).

As is the case with the other hydrazines, the results of the UDMH + NO$_x$ run performed in N$_2$ (run G-1) show that UDMH reacted with NO$_2$ but not with NO. The UDMH + NO$_2$ reaction occurred much faster than either the N$_2$H$_4$ + NO$_2$ or MMH + NO$_2$ reaction, with three of the runs going to completion in less than 10 minutes.

The concentration-time plots for the reactants and products observed in the two UDMH + NO$_2$ experiments performed in air in the absence of NO are depicted in Figures 23 and 24; Figure 23 shows the results of the excess UDMH run (G-3) and Figure 24 shows those for the excess NO$_2$ run (G-4). The major products observed in these experiments were HONO and tetramethyltetrazene-2 (TMT). The yields of each, relative to UDMH consumed, were nearly identical for the two runs and independent of the initial UDMH/NO$_2$ ratio: $\sim 200\%$ for HONO and $\sim 45\%$ for TMT (Table 9). The reactant stoichiometry in the absence of NO was also independent of the initial UDMH/NO$_2$ ratio, with identical values of ~ 2 for $\Delta[NO_2]/\Delta[UDMH]$ in

TABLE 9. SUMMARY OF CONDITIONS AND RESULTS
FOR THE UDMH + NO_x EXPERIMENTS.

Run ID[a]		$G-1$[b]	$G-1$[c]	$G-2$	$G-3$	$G-4$
Matrix Gas		N_2	N_2	Air	Air	Air
Time Range (min)[d]		136.4-146.8	170-177.4	1.8-50.8	0.4-9.4	0.4-8.8
Initial UDMH	(ppm)	10.2	8.4	3.3	10.1	4.0
NO	(ppm)	5.5	4.9	15.4	-	-
NO_2	(ppm)	3.9	~6[e]	3.3	3.9	18.6
Δ[UDMH]	(ppm)	1.9	1.9	2.4	1.9	4.0
NO oxidized[f]	(ppm)	~0	~0	2.2	-	-
Δ[NO][g]	(ppm)	0.6	0.5	2.4	-	-0.3
Δ[NO_2][h]	(ppm)	3.9	~6	4.8	3.9	8.2
Δ[NO]/Δ[UDMH]		0.3	0.3	1.0	-	-0.08
Δ[NO_2]/Δ[UDMH]		2.1	Footnote i	2.0	2.1	2.1
Yields/(Δ[NO_x]):						
HONO		0.78	Footnote i	0.57	1.0	1.0
Yields/(Δ[UDMH]):						
HONO		1.8	1.7	1.7	2.1	2.0
TMT		0.38	0.30	0.22	0.46	0.45
$(CH_3)_2NNO$		~0	~0	0.05	~0	~0
N_2O		0.09	0.09	0.17	< 0.02	< 0.01
NH_3		< 0.01	< 0.01	0.01	< 0.01	< 0.01
Unknown (units[j]/ppm)		5	2	9	< 0.4	< 0.2

[a]Refers to table number in Appendix G where detailed data are given.

[b]First NO_2 injection.

[c]Second NO_2 injection.

[d]Times given in corresponding data table in Appendix G used for initial
and final reactant and product concentrations.

[e]Estimated amount injected, exact value uncertain.

[f]Calculated amount of NO oxidized due to the reaction $NO + NO + O_2 \rightarrow 2NO_2 =$
$2k[O_2]\int[NO]^2 dt$, where $k = 1.9 \times 10^{-38}$ cm^6 molecule^{-2} sec^{-1} (Reference 48)
and $[NO]^2$ is integrated over the indicated time range.

[g]Δ[NO] $= \Delta$[NO]$^{obs} -$ (NO oxidized).

[h]Δ[NO_2] $= \Delta$[NO_2]$^{obs} +$ (NO oxidized).

[i]Highly uncertain because of uncertainty in amount of NO_2 injected.

[j]Units $= ((993$ cm^{-1} absorbance)/(IR pathlength)$) \times 10^4$.
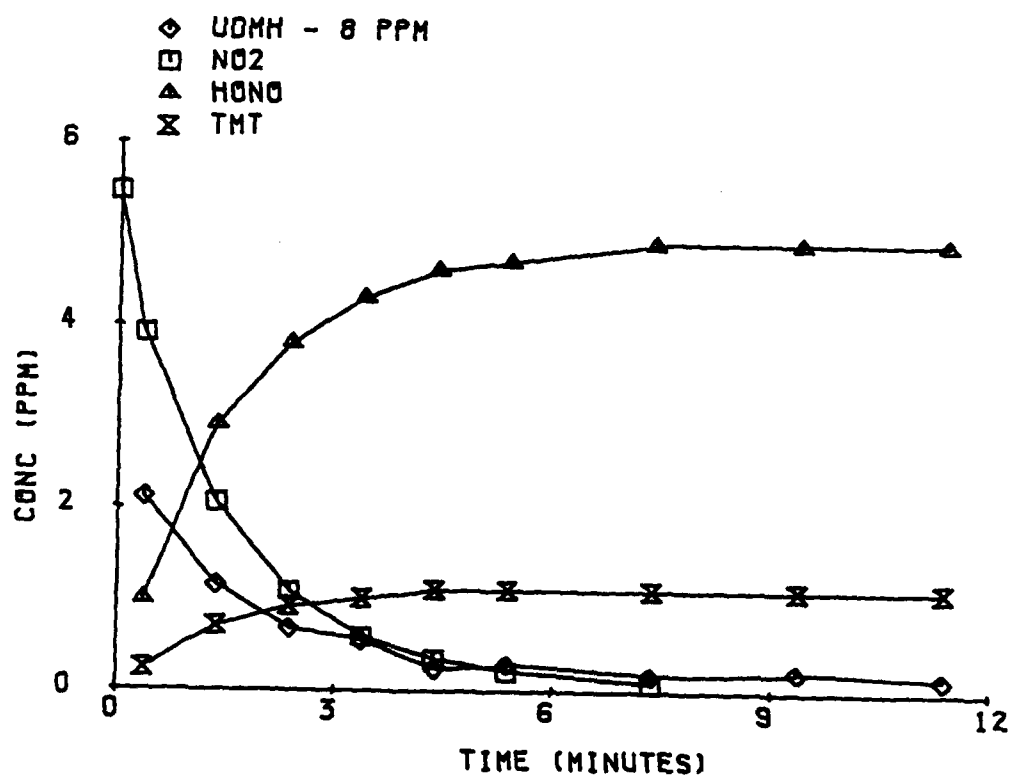
Figure 23. Concentration-Time Plots for Reactants and Selected Products Observed in the UDMH + NO_2 Run G-3 in Excess UDMH.
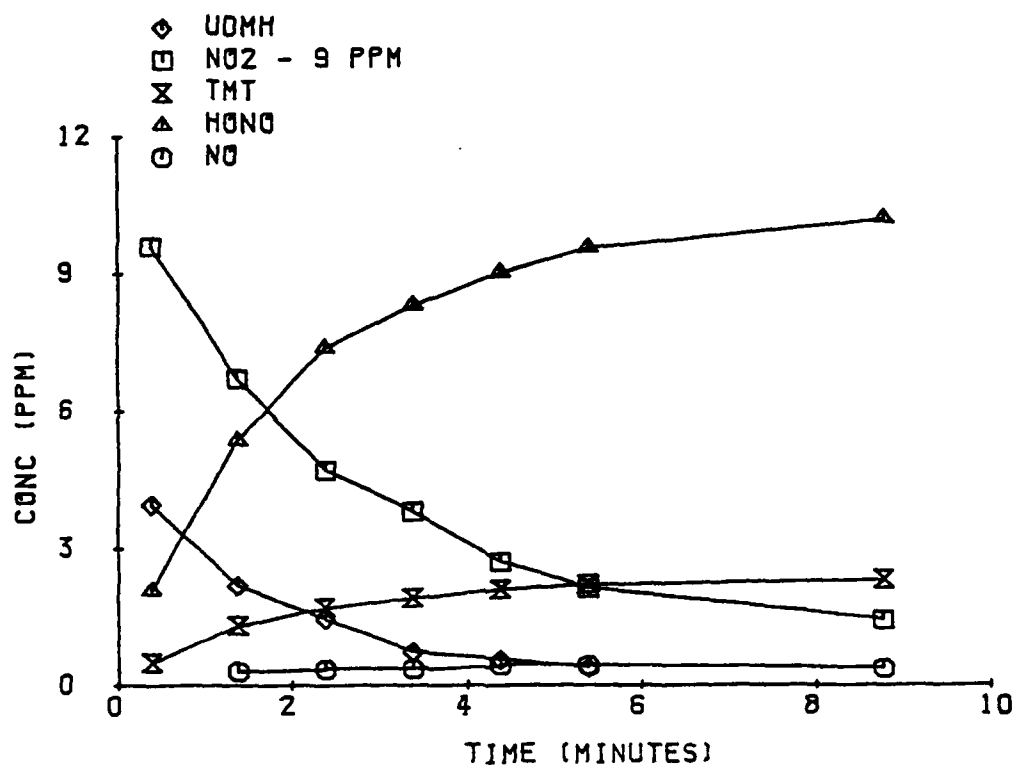
Figure 24. Concentration-Time Plots for Reactants and Selected Products
Observed in the UDMH + NO_2 Run G-4 in Excess NO_2.

both runs. The only other product observed in greater than 2% yield was NO, which formed to a maximum concentration of ~0.4 ppm in the excess NO_2 run. This insensitivity of the product yields and reactant stoichiometry to the hydrazine/NO_2 reactant ratio for UDMH contrasts with the results for the other hydrazines, and suggests a much simpler mechanism in the UDMH + NO_2 system than for the others (see Section 3.4.4).

When NO was present along with NO_2 in the reaction mixture, either in air or in N_2 (runs G-1, G-2), the relative yields of HONO and TMT decreased, significant amounts of NO were consumed, the yields of N_2O increased, and formation of an unidentified product was observed in the infrared spectrum. In addition, $(CH_3)_2NNO$ was detected in the run conducted in air (run G-2). The amount of NO consumed varied from ~30% of the UDMH consumed when the reaction was conducted in the presence of ~5 ppm of NO in N_2 (run G-1) to ~100% (corrected for NO reaction with O_2) of the UDMH consumed in the presence of 10-15 ppm of NO in air (run G-2). The yields of N_2O and the unknown product were also higher in the run conducted with the higher NO levels.

The relative simplicity of the UDMH + NO_2 reaction in the absence of NO is reflected in the carbon and nitrogen balance obtained from the data of runs G-3 and G-4 (Appendix G). For the reaction times listed in Table 9, 99% of both the initial carbon and nitrogen could be accounted for at the end of the run with excess UDMH (run G-3); the calculated values for the excess NO_2 run (run G-4) are 93% for carbon and 99% for nitrogen. For runs in the presence of NO (runs G-1, G-2), the values calculated without taking into account the unknown product are 96% C and 95% N for the first NO_2 injection of the N_2 run (G-1); the corresponding figures for the run in air (G-2) are 68% C and 84% N. If all the missing carbon and nitrogen are attributed to a single compound formed in run G-2, the run where relatively higher yields of the unknown were observed, the above calculation suggests an N/C ratio of ~1.8 for the unidentified species.

Figure 25a illustrates the product spectrum, recorded at the end of the experiment where NO_2 was added to excess UDMH (t = 20.8 min, run G-3), after subtraction of unreacted UDMH. The residual spectrum, Figure 25b, resulting from the subtraction of the other known components, displays the strongest band of tetramethyltetrazene-2 (TMT) at 1009 cm^{-1}, along with its other weaker absorptions at 1141, 1245, 1278, and ~1470
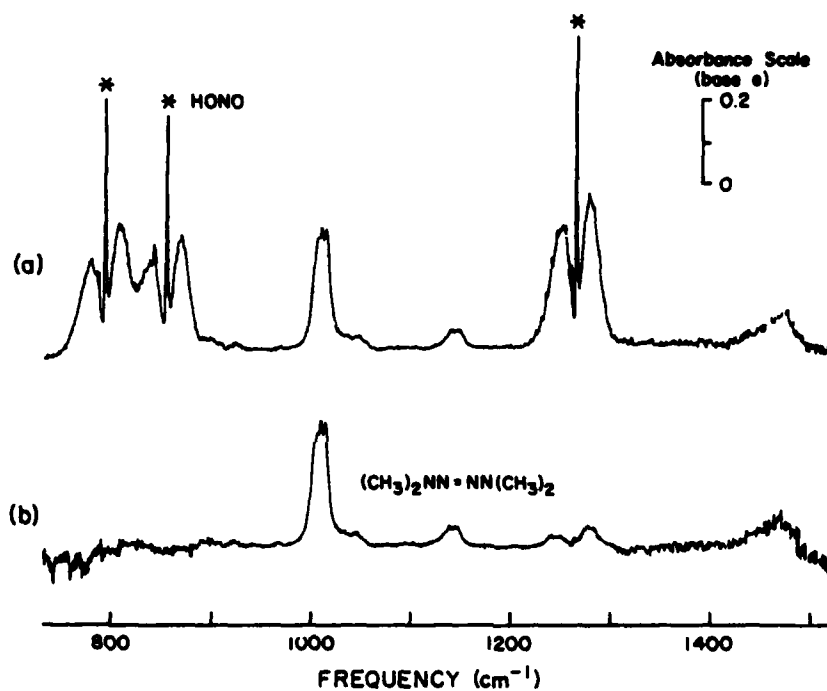
Figure 25. Product Spectra from Excess UDMH + NO_2 Reaction (Run G-3); Res = 1 cm^{-1}, Pathlength = 68.3 m. (a) At t = 20.8 min, (b) Residual Spectrum from (a).
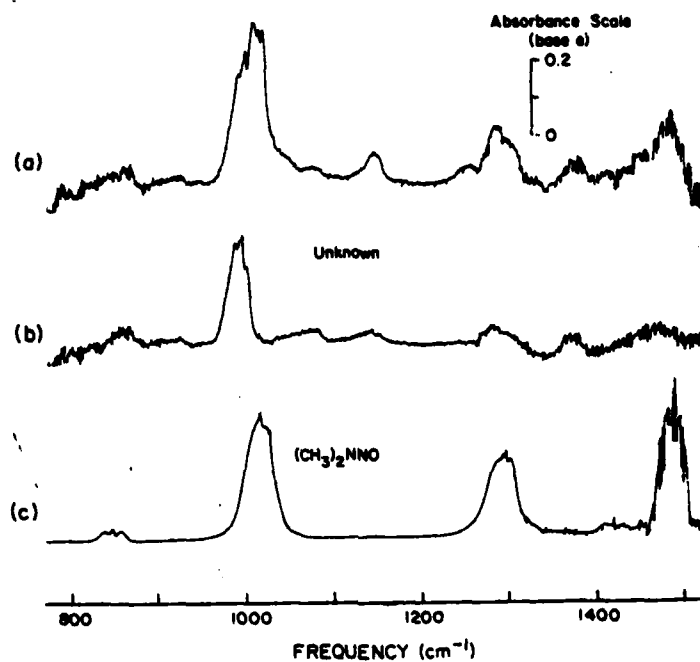
Figure 26. (a) Residual Spectrum from UDMH + NO/NO$_2$ Reaction
(Run G-2, t = 50.8 min.), (b) From (a) after Sub-
traction of (CH$_3$)$_2$NN=NN(CH$_3$)$_2$ and (CH$_3$)$_2$NNO
Absorptions, (c) (CH$_3$)$_2$NNO Reference Spectrum.
Res = 1 cm^{-1}, Pathlength = 102.4 m.

cm^{-1}. TMT was the only carbon-containing product detected in the UDMH + NO_2 runs in the absence of significant amounts of NO. This is consistent with the carbon and nitrogen balance observed for runs G-3 and G-4.

The formation of the unknown product in the UDMH system, when both NO and NO_2 are present, is illustrated by the residual spectrum of Figure 26a for the run conducted in air (t = 50.8 min, Table G-2). The strongest band situated at ~1000 cm^{-1} is actually a composite of the respective strongest absorptions of the unknown compound, TMT, and NDMA. (The presence of NDMA in the product spectra was not immediately obvious and was suspected only upon consideration of the plausible chemical mechanisms involved [see Section 3.4.4.1]). Estimates of the unknown's absorbance and of the concentrations of TMT and NDMA were obtained by iterative subtraction of the absorptions due to the latter two compounds. The resulting spectrum of the unidentified compound obtained by this procedure is presented in Figure 26b. The absorption bands at ~1480 (distorted by unmatched H_2O lines), 1286, 993, and 857 cm^{-1} are very similar in positions to those of the skeletal modes of NDMA (Figure 26c). The ~1480 cm^{-1} absorption is expected of the N=O stretching of the $>$N-N=O group. The spectrum strongly suggests that the unknown product is N-nitroso-N',N'-dimethylhydrazine [$(CH_3)_2$N-NH-NO], which is consistent with the mechanism considered below (Section 3.4.4.1) for the UDMH + NO_x reactions. The nitrogen/carbon ratio of 1.5 for this nitrosohydrazine is also consistent, within experimental uncertainty, with the ratio of ~1.8 derived from the material balance in run G-2. The positive identification of this compound through comparison with an authentic sample was not possible due to the lack of a well-defined preparative procedure in the literature.

Plots of ln[NO_2] for the runs performed in excess UDMH (runs G-1 and G-3) and of ln[UDMH] for the excess NO_2 run (G-4) against time are shown in Figure 27. The decays are reasonably exponential, indicating that the reaction is probably first order in both reactants, as observed for the other hydrazines. The slight curvatures observed are attributable to the consumption of the reactant which was in excess. The apparent rate constants derived from the decays shown in Figure 27 (with a stoichiometry factor of 2 being applied to calculate the apparent rate from the NO_2 decays) were essentially identical for all three runs, being (3.2 ± 0.1) x 10^{-2} ppm^{-1} min^{-1} for run G-1 (NO_2 decay in excess UDMH in N_2), (3.5 ± 0.3)
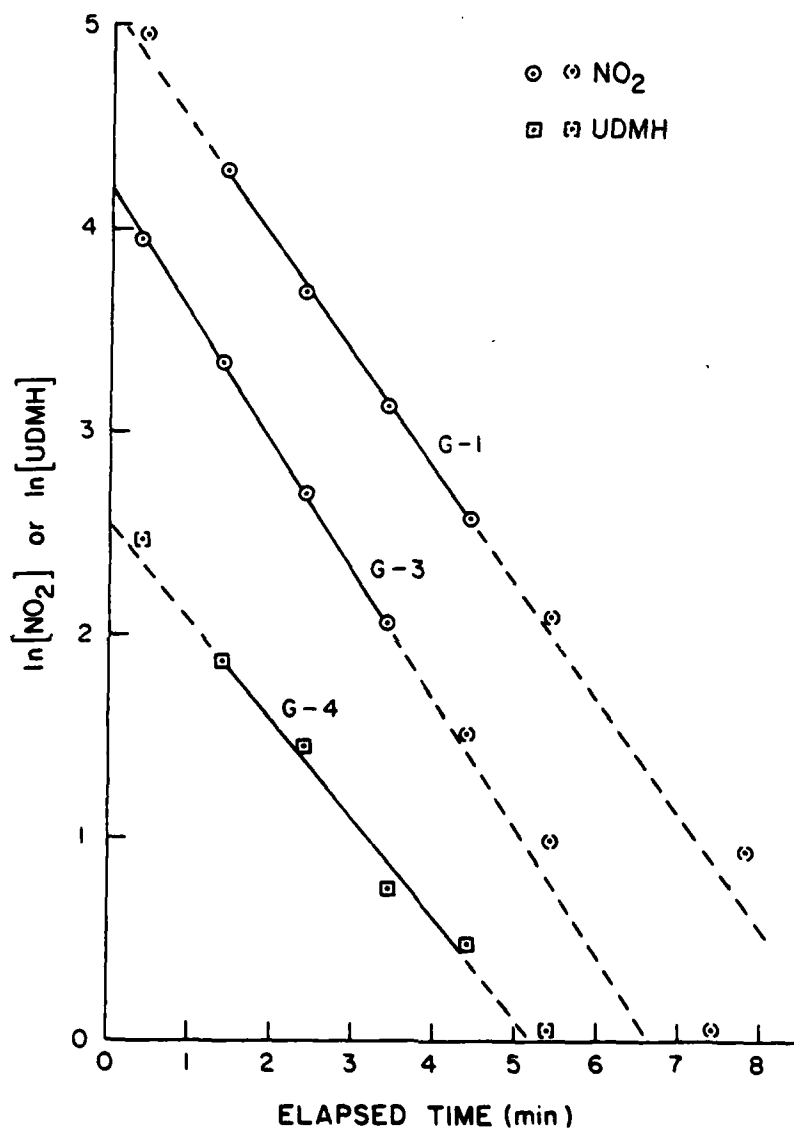
Figure 27. Plots of ln[UDMH] or ln[NO₂] Against Elapsed Time for Selected UDMH + NOₓ Runs. (Concentrations are in ppm, and Data for Runs G-1, G-3 and G-4 are Offset by 3.6, 2.6, and 1.1 Log Units, Respectively.) ▣, θ – Data Used to Obtain Lines Shown; [·], (·) – Data Not Used to Obtain Lines.

x 10^{-2} ppm^{-1} min^{-1} for run G-3 (NO$_2$ decay in excess UDMH in air), and (3.6 ± 0.5) x 10^{-2} ppm^{-1} min^{-1} for run G-4 (UDMH decay in excess NO$_2$ in air). These apparent rate constants thus indicate an upper limit rate constant of ~2 x 10^{-17} cm^3 molecule^{-1} sec^{-1} for the elementary reaction of NO$_2$ with UDMH, ~14 and ~80 times faster than NO$_2$ with MMH, and N$_2$H$_4$, respectively.

3.4.4 Mechanism of the Reactions of Hydrazines with NO$_2$

The results of the exploratory experiments discussed above strongly suggest that hydrazines react at significant rates with NO$_2$ in the gas phase, though the data obtained do not totally eliminate the possibility that the reaction is occurring on the walls. The fact, however, that the magnitude of the rates for the reaction of NO$_2$ with the three hydrazines are in the order UDMH > MMH > N$_2$H$_4$, while the rates of wall decay are N$_2$H$_4$ > MMH >> UDMH, suggests that the rate determining step is not adsorption of the hydrazines on the wall, as might be expected to be the case if the reaction were primarily heterogeneous. Therefore, in the following discussion it will be assumed that the reactions occur entirely in the gas phase, though this must be confirmed by additional experiments in which the surface and the surface/volume ratio is varied.

The observation of large yields of HONO, as well as mechanistic and thermochemical considerations, indicate that the only reasonable initial gas phase reaction between the hydrazines and NO$_2$ is

$$\begin{matrix} R_1 \\ \diagdown \\ \diagup \\ R_2 \end{matrix} N{-}NH_2 + NO_2 \rightarrow HONO + \begin{matrix} R_1 \\ \diagdown \\ \diagup \\ R_2 \end{matrix} N{-}\overset{\bullet}{N}H \qquad (33)$$
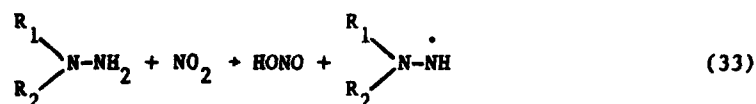
(where R$_1$, R$_2$ = H or CH$_3$). This reaction is mechanistically reasonable, since NO$_2$ is an odd-electron species and thus can be considered to be a free radical which can abstract labile hydrogen atoms if the energetics are favorable; the N$_2$H$_4$ + NO$_2$ reaction is estimated to be ~2 kcal mole^{-1} exothermic (References 41-43). If we assume that H-abstraction from hydrazines by NO$_2$ has an Arrhenius A factor similar to that for H-abstraction from amines and hydrazines by CH$_3$ radicals [e.g., ~2 x 10^{-13} cm^3 molecule^{-1} sec^{-1} (Reference 44)], then the activation energies for the reaction of NO$_2$ with N$_2$H$_4$, MMH, and UDMH would be ~8, 7, and 5 kcal mole^{-1} respectively. These values are not unreasonable for a radical hydrogen

abstraction reaction (Reference 44). The progression of increased apparent rates of reaction (or decreased apparent activation energies) from N_2H_4 to UDMH suggest that, as expected, methyl substitution weakens the N-H bonds, making them more susceptible to abstraction. This is also consistent with the fact that O_3 reacts with MMH and UDMH much faster than it does with N_2H_4.

The subsequent reactions of the hydrazyl radicals, formed in reaction (33) in NO_x-air or NO_x-N_2 systems, will depend on the extent of substitution of the radical. The UDMH + NO_2 system appears to be the simplest of the three studied, since the reactant stoichiometries, product yields, and apparent rate constants depended much less on the reaction conditions than in the case of the other hydrazines. For this reason, the UDMH + NO_2 system will be discussed first.

3.4.4.1 Reaction Mechanism for Unsymmetrical Dimethylhydrazine + NO_x. The reactant stoichiometries and product yields observed in the UDMH + NO_2 runs (in the absence of NO) are entirely consistent with the following mechanism:

(34)

(35)

(36)

(37)
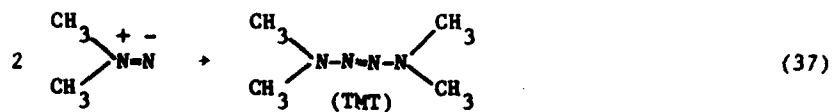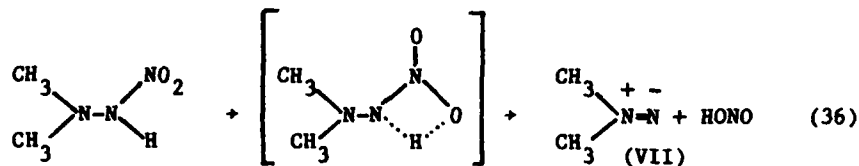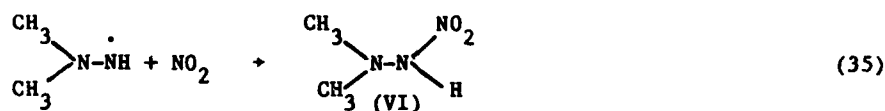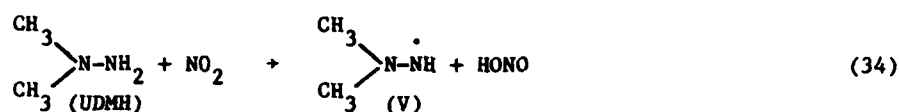
The overall reaction is then

$$\text{UDMH} + 2 \text{ NO}_2 \rightarrow 2 \text{ HONO} + 0.5 \text{ TMT}$$

This mechanism predicts that TMT is the only significant organic product and that $\Delta[\text{NO}_2]/\Delta[\text{UDMH}] = -\Delta[\text{HONO}]/\Delta[\text{UDMH}] = 2.0$ and $-\Delta[\text{TMT}]/\Delta[\text{UDMH}] = 0.5$, consistent with our observations. Since the dimethylhydrazyl radical (V) apparently does not react with O_2 (Section 3.3.6.3) and radical + NO_x reactions are known to be rapid (Reference 48), reaction (35) is a reasonable fate for (V) in the UDMH + NO_2 system. The nitrohydrazine species (VI) is presumably not stable, as indicated by the absence in the product spectra of the normally strong absorptions of the organic-NO_2 group for the runs conducted in the absence of NO. The charge-separated species (VII) in reaction (36) is believed to be involved in a number of reactions of unsymmetrically-disubstituted hydrazines in which tetrazene formation is observed (Reference 30). The dimerization reaction (reaction [37]) is a reasonable fate for (VII), since it forms a stable, non-charge-separated compound, and no molecular rearrangement is involved.

It should be noted, however, that the above mechanism is not the only reasonable mechanism which is consistent with the data. An alternate decomposition pathway for the nitrohydrazine is simply back-decomposition:

$$\text{(38)}$$
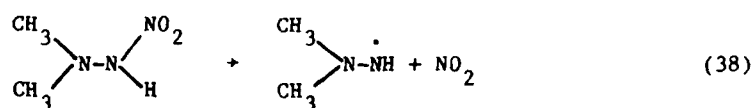
which, if sufficiently rapid at room temperature, would effectively mean that reaction with NO_2 would not be a sink for (V). This back reaction could be important if the N-NO_2 bond were sufficiently weak (bond energy < 20 kcal mole^{-1}). Such is the case for the 0-NO_2 bond in organic peroxy nitrates (ROONO_2) (References 40, 52), which are rapidly formed in photochemical smog systems from RO_2 + NO_2, but do not constitute a significant RO_2 sink because they rapidly back-decompose. It should be noted that for reaction (37) to be important, the N-NO_2 bond in nitrohydrazines must be much weaker than those in nitramines, since the latter are known to be stable compounds (Reference 30). If this were the case, the most probable

sink for the dimethylhydrazyl radicals would be self-reaction:

$$
\begin{array}{c}
\text{CH}_3\text{--N--NH--NH--N--CH}_3 \\
\text{(VIII)} \\
\text{(addition)}
\end{array}
\tag{39}
$$

$$
2 \text{ (CH}_3\text{)}_2\text{N--NH}\cdot
$$

$$
(\text{CH}_3)_2\text{N}\overset{+}{=}\overset{-}{N} + (\text{CH}_3)_2\text{N--NH}_2
\tag{40}
$$

(disproportionation)
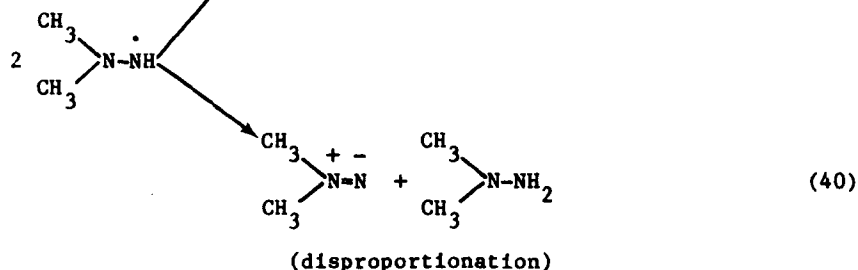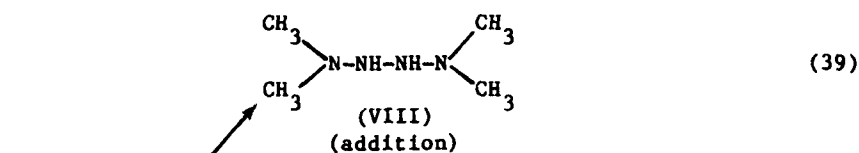
If addition occurs, the tetrazane (VIII) may somehow dehydrogenate to form the observed TMT, but reaction stoichiometries different from those observed would be predicted. Species (VIII), if formed, more likely decomposes to N_2 and dimethylamine (Reference 30), which is not observed. On the other hand, the disproportionation route (reaction [40]), if it dominates over addition, predicts exactly the same overall product yields and stoichiometries as does the mechanism involving reactions (35) and (36), and is also entirely consistent with the data. Thus the results of the UDMH + NO_2 reaction (without NO) can be explained by two different mechanisms.

When NO is included in the reaction mixure, some NO is consumed, the TMT yields are reduced, and formation of N_2O and unidentified product(s) are observed, indicating that NO interacts with the intermediates formed. Since NO, like NO_2, also reacts rapidly with radicals (Reference 48) formation of a nitrosohydrazine is expected to occur.

$$
(\text{CH}_3)_2\text{N--NH}\cdot + \text{NO} \xrightarrow{M} (\text{CH}_3)_2\text{N--N}\begin{array}{c}\text{NO}\\\text{H}\end{array}
\tag{41}
$$

$$
(\text{V}) \qquad\qquad (\text{IX})
$$
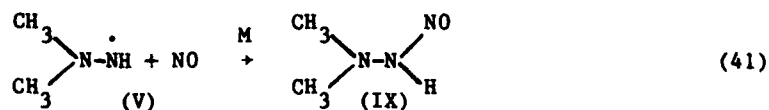
Spectroscopic evidence for the formation of the nitrosohydrazine (IX),

107

accounting for the unassigned infrared absorption bands observed in UDMH + NO_x runs conducted in the presence of NO, is discussed in Section 3.4.3, where it is also indicated that, based on considerations of carbon and nitrogen balances, the yield of this product may be significant. The nitrosohydrazine is expected to be much more stable than the nitrohydrazine, since a decomposition pathway analogous to reaction (36) is not mechanistically reasonable for nitrosohydrazines. However, the $(CH_3)_2NN-N$ bond strength in $(CH_3)_2NNHNO$ is expected to be similar in magnitude to that in $(CH_3)_2NNHNO_2$. Since the nitrosohydrazine is stable, then reaction (38) is expected to be slow. This evidence suggests that the UDMA + NO_2 mechanism in fact proceeds via reactions (34-37).

Although it appears probable that nitrosohydrazine formation occurs when UDMH and NO_2 react in the presence of NO, the observations of non-negligible yields of N_2O and the fact that more NO is consumed than UDMH in run G-2 (Table 9) indicate that this is not the only process occurring. The observation of N_2O can be explained by possible secondary reactions of the nitrosohydrazine, such as:

$$
\begin{array}{l}
\underset{CH_3}{\overset{CH_3}{>}}N-N\underset{H}{\overset{NO}{<}} + NO_2 \rightarrow HONO + \underset{CH_3}{\overset{CH_3}{>}}N-\overset{\bullet}{N}-NO \qquad (42) \\
\qquad (IX)
\end{array}
$$

$$
\underset{CH_3}{\overset{CH_3}{>}}N-\overset{\bullet}{N}NO \rightarrow \underset{CH_3}{\overset{CH_3}{>}}\overset{\bullet}{N} + N_2O \qquad (43)
$$
$$
\qquad (X)
$$
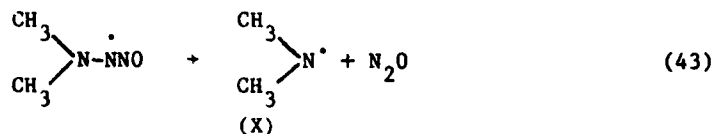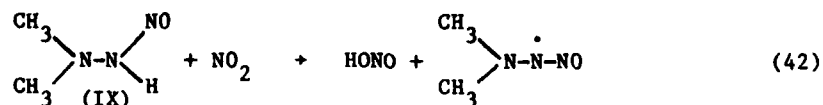
If reactions (42) and (43) occur, formation of N-nitrosodimethylamine and dimethylnitramine should also occur from the reactions of (X) with NO and NO_2, respectively. Indeed, as discussed in Section 3.4.3, there is evidence for formation of small yields of N-nitrosodimethylamine in the run conducted in the presence of NO (run G-2).

The only experimental observation in the UDMH + NO_x system which is difficult to rationalize is the observation that more NO than UDMH is oxidized in run G-2 (Table 9), even after correction for consumption of NO by reaction with O_2. If HO_2 were somehow generated in the mechanism, then additional NO would be consumed due to the reaction,

$$HO_2 + NO \rightarrow OH + NO_2 \tag{44}$$

with more than half of the OH formed reacting with additional NO under the conditions of run G-2:

$$OH + NO \xrightarrow{M} HONO \tag{45}$$

If the N–H bond in the nitrosohydrazine is weaker than ~50 kcal mole^{-1}, HO_2 formation might occur via

$$(46)$$

followed by

$$HNO + O_2 \rightarrow NO + HO_2 \tag{47}$$

or via

$$(48)$$
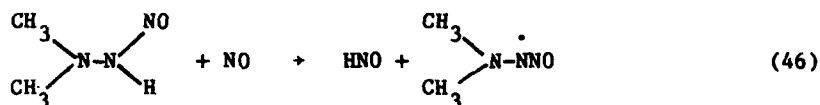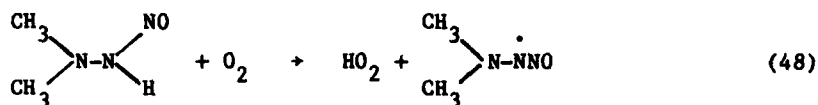
However, the thermochemistry, atmospheric chemistry, and stability of nitrosohydrazine are presently unknown and the above reactions must be considered to be entirely speculative at the present time.

3.4.4.2 <u>Mechanism for Reactions of Hydrazine and Monomethyl-hydrazine with NO$_x$</u>. The reactant stoichiometries and product yields observed in the N_2H_4 + NO_2 and the MMH + NO_2 experiments were much more variable than those observed for UDMH, indicating that the reaction mechanism is probably more complex. As discussed in Section 3.3.4 for the hydrazines + O_3 reactions, N_2H_4 and MMH differ from UDMH in that the hydrazyl radical can react with O_2 via β-hydrogen abstraction to yield diazenes and HO_2,

109

$$\underset{H}{\overset{R}{\diagdown}}\!\!\dot{N}\!-\!NH + O_2 \rightarrow RN=NH + HO_2 \tag{49}$$
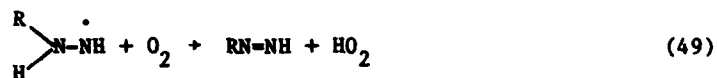
(R = H or CH_3), a route not possible in the UDMH system. If the reaction with O_2 is slow, or if $[O_2]$ is low as in the runs performed in an N_2 atmosphere, diazene formation can also occur from the reaction of NO_2 with the hydrazyl radical, either directly by H-abstraction,

$$\underset{H}{\overset{R}{\diagdown}}\!\!\dot{N}\!-\!NH + NO_2 \rightarrow HONO + R-N=NH \tag{50a}$$
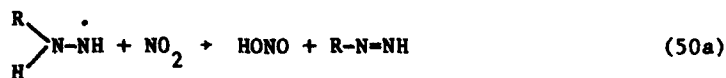
or by addition followed by rearrangement and decomposition:

$$\tag{50b}$$

$$R-N=NH + HONO$$
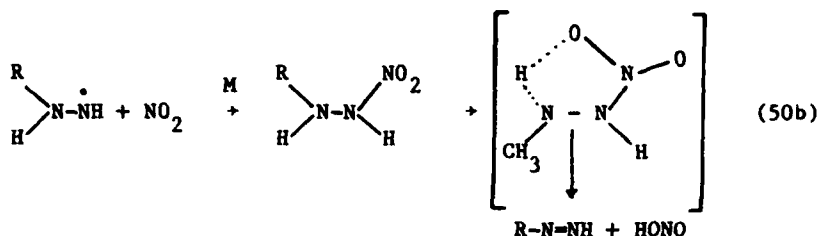
Formation of the appropriate diazenes are indeed observed in the N_2H_4 + NO_x and MMH + NO_x systems, though it is clear that they undergo subsequent reaction with NO_2, which accounts in part for the observed variability of reactant stoichiometries and product yields.

Evidence that diazene and methyldiazene react with NO_2 comes from the fact that their yields were suppressed as the $[NO_2]/[hydrazine]$ ratio increased, as well as from the fact that CH_3NNH went through a maximum and subsequently declined when formed in excess NO_2 (Table F-4 and Figure 19) but exhibited no such behavior when formed in excess MMH (Table F-3 and Figure 18). One would expect the most probable mode of reaction to be hydrogen abstraction, yielding HONO, N_2, and a radical fragment (H or CH_3).

$$RN=NH + NO_2 \rightarrow HONO + RN_2 \tag{51}$$
$$\Big\downarrow O_2$$
$$RO_2 + N_2$$
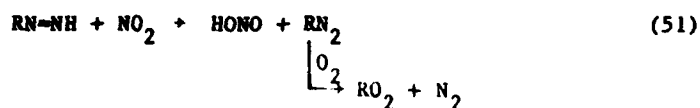
with reaction (51) being estimated (References 41, 53) to be exothermic for N_2H_2. The reaction of NO_2 with N_2H_2 is apparently much faster than its reaction with CH_3NNH, since the N_2H_2 was suppressed to a far greater extent (to below its IR detection limit) than CH_3NNH when the reaction was conducted in excess NO_2.

HO$_2$ radicals are expected to be formed in both systems from the reaction of O_2 with the hydrazyl radicals (reaction [49]) and, in the N_2H_4 system, from the reaction of N_2H_2 with NO_2 (reaction [51]). Evidence for the formation of HO_2 in the MMH system comes from the observation of peroxynitric acid (HO_2NO_2) in the runs not containing NO, where HO_2NO_2 is formed from the rapid, reaction of HO_2 with NO_2.

$$HO_2 + NO_2 \overset{M}{\underset{\leftarrow}{\rightarrow}} HO_2NO_2 \qquad\qquad (52,-52)$$

The thermal decomposition of HO_2NO_2 (reaction [-52]) is sufficiently rapid (Reference 17) that HO_2NO_2 is not a permanent HO_2 sink, and indeed in both runs (F-3 and F-4) where it was observed, HO_2NO_2 went through a maximum and declined to below its IR detection limit before the MMH + NO_2 reaction had gone to completion. Because of this, our failure to observe HO_2NO_2 in the N_2H_4 + NO_2 runs does not rule out its formation in that system. The steady state concentration of such a rapidly decomposing species is approximately proportional to its rate of formation; since HO_2NO_2 would be formed ~6 times slower in the N_2H_4 + NO_2 systems than in the MMH + NO_2 system (since the overall reaction proceeds ~6 times slower), the HO_2NO_2 levels in the N_2H_4 runs would thus be only ~1/6 those in the corresponding MMH + NO_2 runs, which is below our IR detection limit.

Peroxynitric acid was not observed in the MMH + NO_2 runs performed with NO present. This is expected, since HO_2 is rapidly converted to OH by reaction with NO.

$$HO_2 + NO \rightarrow OH + NO_2 \qquad\qquad (44)$$

The OH radicals formed will react with NO (to form HONO), with NO_2 (to form HNO_3),

$$\overset{M}{OH + NO \rightarrow HONO} \tag{45}$$

$$\overset{M}{OH + NO_2 \rightarrow HNO_3} \tag{53}$$

or with the hydrazine, with the relative importance of these depending on the ratio of the reactants. The formation of HNO_3 from reaction (44) followed by (53) would account for the hydrazinium or methylhydrazinum nitrate aerosols in the runs with added NO, but not (see below) its formation in the runs where NO is not present. Reaction (44) also accounts for the observed consumption of NO caused by the reaction of N_2H_4 and MMH with NO_2.

Although as discussed above, many of the observations made in these exploratory $N_2H_4 + NO_x$ and MMH + NO_x runs can be rationalized on the basis of the probable reactions expected to occur, a number of other observations are more difficult to understand. In particular, for both N_2H_4 and MMH, the formation of significant amounts of HNO_3, as evidenced by the formation of relatively large quantities of hydrazinium and methylhydrazinium nitrates, and the lack of formation of H_2O_2 and (for MMH) methylhydroperoxide in the runs not containing NO, are difficult to explain. In the absence of NO, the mechanism discussed above gives no obvious source of the hydroxyl radicals required to form HNO_3 via reaction (53), and no obvious major sink for HO_2 and CH_3O_2 which does not involve H_2O_2 or CH_3OOH formation. (Although HO_2 and CH_3O_2 will react rapidly with NO_2 to form respectively $HOONO_2$ and CH_3OONO_2, the rapid back-decomposition of these species, with CH_3OONO_2 [References 40, 52] decomposing even more rapidly than $HOONO_2$ [discussed above], means that their formation cannot represent a significant NO_x sink, as evidenced by the failure to observe either of these species at the end of the runs.) Thus there appears to be an unknown HNO_3 source and an unknown HO_2 and CH_3O_2 sink in the $N_2H_4 + NO_2$ and MMH + NO_2 runs not containing added NO.

Several possibilities can be considered to account for the unknown sink for HO_2 and source for HNO_3. One possibility is that NO is somehow being generated in this system. This would provide both a sink for HO_2 via reaction (44) and a source for HNO_3 via reaction (53). NO could possibly be formed from the reversible and heterogeneous decomposition of HONO,

$$2 \text{ HONO} \rightleftarrows \text{NO} + \text{NO}_2 + \text{H}_2\text{O} \qquad (54,-54)$$
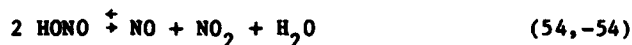
but reaction (54) may be too slow in our chamber to be important. Another possibility is a rapid reaction between NO_2 and H_2O_2,

$$\text{NO}_2 + \text{H}_2\text{O}_2 \rightarrow \text{HNO}_3 + \text{OH} \qquad (55)$$

since a surface-dependent reaction between H_2O_2 and NO_2 is observed when they are mixed at much higher reactant concentrations (Reference 54). It is unclear, however, whether this can be important under the low concentrations and much lower surface/volume conditions employed in our study. A third possibility is that HO_2 and HONO react to form OH and HNO_3,

$$\text{HO}_2 + \text{HONO} \rightarrow \left[\text{HOON} \begin{matrix} \diagup \text{OH} \\ \cdot \\ \diagdown \text{O} \end{matrix} \right] \rightarrow \text{OH} + \text{HNO}_3 \qquad (56)$$
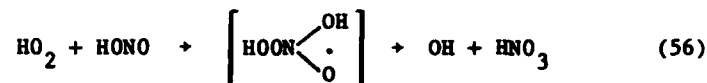
since this reaction is calculated to be ~9 kcal mole^{-1} exothermic (Reference 41). We are aware of no evidence in the literature for or against the occurrence of reaction (56). At the present time, all these possibilities must be considered totally speculative, and additional research in this area is needed.

The organic products formed in the MMH + NO_x system constitute another area of significant uncertainty. As discussed in Section 3.4.2, there are unassigned IR bands corresponding to at least two unknown products being formed in this system (see also Table 8). We are unable, based on chemical and mechanistic considerations, to suggest reasonable identities for these products. In addition, although it is evident that CH_3NNH reacts with NO_2 (see above), we do not observe the expected products from this reaction. Formation of methylperoxy radicals is expected [see reaction (51)]; yet, as mentioned above, methylhydroperoxide is not observed in the runs conducted in the absence of NO. In the presence of NO, formation of HCHO, CH_3ONO and CH_3ONO_2 would be expected via the following reactions:

$$\text{CH}_3\text{O}_2 + \text{NO} \rightarrow \text{CH}_3\text{O}^{\cdot} + \text{NO}_2 \qquad (57)$$

$$\text{CH}_3\text{O}^{\cdot} + \text{O}_2 \rightarrow \text{HO}_2 + \text{HCHO} \qquad (58)$$

113

$$CH_3O^{\cdot} + NO \xrightarrow{M} CH_3ONO \qquad (59)$$

$$CH_3O^{\cdot} + NO_2 \xrightarrow{M} CH_3ONO_2 \qquad (60)$$
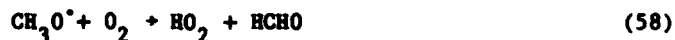
Since these products were not observed, this suggests that methyl radicals are not formed when NO_2 and CH_3NNH react. Clearly the unknown products formed must be identified before the remaining details of the MMH + NO_x reaction mechanism can be determined.

3.5 THE REACTIONS OF HYDRAZINES WITH FORMALDEHYDE

The reactions of N_2H_4 and UDMH with HCHO were carried out to clarify their extent of participation in the other reaction systems studied. For example, it was observed that upon consumption of UDMH in the Aerozine-50 + O_3 reaction both the remaining N_2H_4 and the HCHO formed decayed at a significant rate (see Section 3.3.5). It then became necessary to verify the presence of formaldehyde hydrazone ($H_2NN=CH_2$) by generating a reference spectrum and to obtain an approximate measure of the N_2H_4 + HCHO reaction rate.

3.5.1 Reaction of N_2H_4 with HCHO

One experiment was performed in which ~11 ppm of N_2H_4 was injected into the indoor Teflon® chamber containing ~10 ppm of formaldehyde in air. The detailed concentration-time profiles obtained are shown in Table 10 and selected product spectra are shown in Figure 28. Figure 28a, where the absorptions of unreacted N_2H_4 and HCHO and traces of NH_3 have been subtracted, was recorded at t = 3.8 min. Figure 28c is the residual spectrum at the end of the experiment (t = 48.8 min) where all the featured absorption bands are due to $H_2NN=CH_2$ (Reference 5); the C=N stretching frequency was observed at ~1610 cm^{-1} (not presented in the plot). A closer comparison of Figures 28a and 28c indicates that another species was formed in the early stage of the reaction. Upon proportionate subtraction of the spectrum in Figure 28c from that of Figure 28a, the absorption bands of the unknown at 1012 and 1122 cm^{-1} are clearly observed in Figure 28b. No other significant absorptions were apparent in the entire difference spectrum.

The unknown product is apparently formed as a transient intermediate, since its highest concentration is observed in the first spectrum (Figure
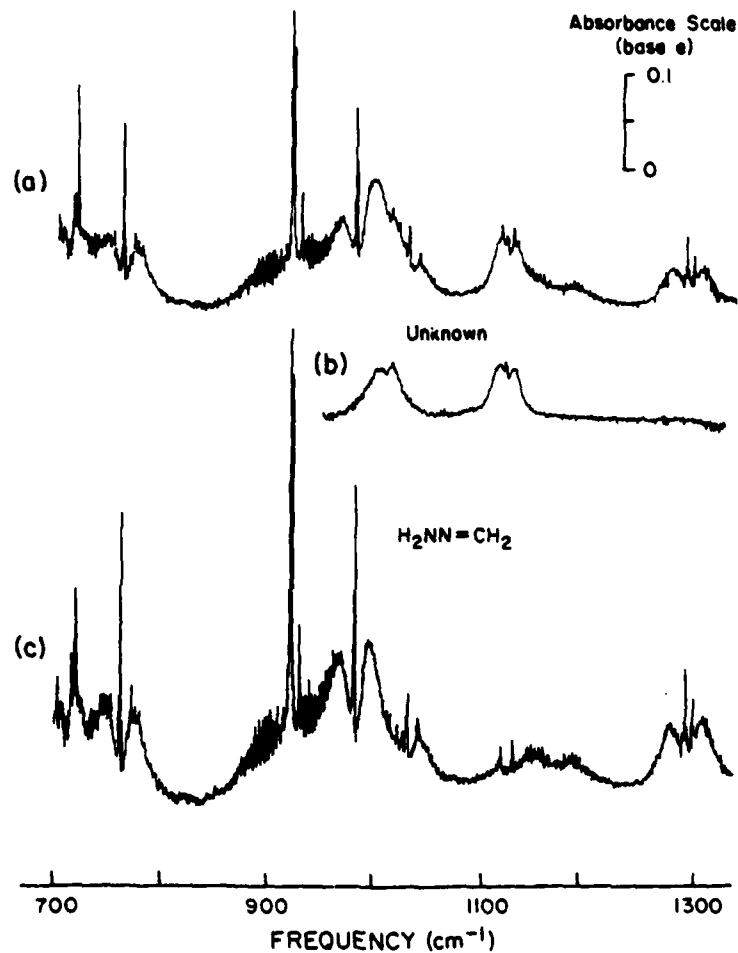
Figure 28. Product Spectra from N_2H_4 + HCHO Reaction (Table 10);
Res = 1 cm^{-1}, Pathlength = 68.3 m. (a) At t = 3.8 min,
(b) From (a) after Subtraction of $H_2NN=CH_2$ Absorptions,
(c) $H_2NN=CH_2$ as the Only Product at t = 48.8 min.

115

TABLE 10. REACTANT AND PRODUCT CONCENTRATIONS VS. TIME IN
N_2H_4 + HCHO REACTION (T = 27°C, RH = 12%;
6400 ℓ CHAMBER; RES = 1 CM^{-1}, PATHLENGTH = 68.3 M).

Elapsed Time (min)	Concentration (ppm)			Absorbance at	
	N_2H_4	HCHO	NH_3	982.1 cm^{-1} $H_2NN=CH_2$	1122.4 cm^{-1} Unknown
-7		10.1			
0	10.9 (calc'd)				
3.78	3.41	3.28	0.15	0.144	0.056
7.78	2.42	2.63	0.16	0.168	0.043
11.78	1.87	2.22	0.17	0.182	0.035
16.78	1.23	1.63	0.17	0.202	0.023
27.78	0.36	0.89	0.18	0.225	0.007
34.78	-	0.52	0.17	0.231	0.004
48.78	-	0.33	0.18	0.237	-

28a) at 3.8 min after the reaction started, and it subsequently declined
to undetectable levels by the end of the run (see Table 10). From a
mechanistic point of view, it is reasonable to expect the intermediate to
have the structure $H_2N-NH-CH_2OH$, since the following appears to be reason-
able reactions accounting for hydrazone formation:

$$H_2N-NH_2 + HCHO \rightarrow [H_2N-\overset{+}{NH_2}CH-\overset{-}{O}] \rightarrow H_2N-NH-CH_2OH \qquad (61)$$
$$(XI) \qquad\qquad (XII)$$

$$H_2N-NH-CH_2OH \rightarrow H_2N-N=CH_2 + H_2O \qquad (62)$$
$$(XII)$$
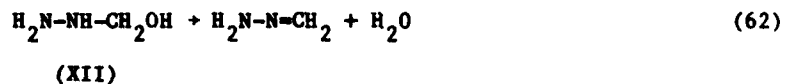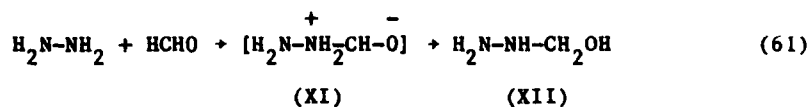
with the re-arrangement of (XI) apparently occuring much faster than the
decomposition of (XII). If this mechanism is correct, then the rate of
decay of the 1122.4 cm^{-1} absorption for t $\geq$ 16.8 min (when formation of
the unknown should be relatively slow) indicates an apparent unimolecular
decay rate constant of ~0.1 min^{-1} (~1.6 x 10^{-3} sec^{-1}) for compound

116

(XII). From spectroscopic considerations, the possibility that the unknown species is indeed compound (XII) cannot be verified or ruled out at the present time.

The N_2H_4 + HCHO reaction is moderately fast, going to completion in 30 min in the experiment performed in this study with ~1:1 reactant stoichiometry. (The observed 1:1 stochiometry allowed a value of ~5.8 cm^{-1} atm^{-1} for the absorption coefficient of the 921.3 cm^{-1} Q branch of $H_2NN=CH_2$ to be estimated, which was employed in deriving concentrations for this species in the Aerozine-50 + O_3 experiment [Section 3.3.5].) Since the stoichiometry is ~1:1, and since the initial concentrations of each reactant were essentially the same, the decay curves should fall on a second order plot (i.e., $1/[HCHO]$ and $1/[N_2H_4]$ being linear when plotted against time) if it is a simple second order reaction, as would be the case (for example) if the mechanism consisted of reactions (61) and (62) above. However, when the concentrations are plotted in this way, the plots are not linear; the initial and final apparent rates of reaction are faster than the rates observed around the middle of the run. Thus, it is probable that the reaction of N_2H_4 with HCHO is not a simple gas phase process such as implied by reactions (61) and (62) above, but is either heterogeneous in nature, or, if it is indeed a gas phase process, proceeds via a more complex reaction mechanism than indicated by reactions (61) and (62).

3.5.2 The Reaction of Unsymmetrical Dimethylhydrazine with Formaldehyde

Two experiments were carried out for the UDMH + HCHO system: the first was with initial concentrations of ~15 ppm UDMH and ~6 ppm HCHO and the second with ~6 ppm UDMH and ~18 ppm HCHO. The detailed concentration-time data for these runs are given in Tables 11 and 12, and FT-IR spectra at selected times during the run with excess HCHO are presented in Figure 29. Figure 29a (t = 2.8 min) essentialy shows only the absorption bands of UDMH and the spread of the well-resolved lines of HCHO starting at ~1000 cm^{-1}. Figure 29b is the spectrum of the reaction mixture at the end of the experiment (t = 150.8 min) and shows the development of a product. Subtraction of the absorptions of unreacted UDMH and HCHO revealed the spectrum (Figure 29c) of formaldehyde dimethylhydrazone $[(CH_3)_2NN=CH_2]$, which was verified by comparison with a published gas-

117

TABLE 11.   REACTANT AND PRODUCT CONCENTRATIONS VS. TIME IN
UDMH + HCHO REACTION; EXCESS UDMH (T = 24°C, RH = 11%;
6400 ℓ CHAMBER; RES = 1 CM^{-1}, PATHLENGTH = 68.3 M).

Elapsed Time (min)	Concentration (ppm)			Absorbance at 1010 cm^{-1} $(CH_3)_2NN=CH_2$
	UDMH	HCHO	NH$_3$	
-7		5.86		
0	14.9 (calc'd)			
9.78	14.5	5.08	0.06	0.032
15.78	14.2	4.88	0.06	0.045
25.78	13.6	4.36	0.06	0.071
35.78	13.2	3.97	0.06	0.094
45.78	12.7	3.39	0.06	0.115
55.78	12.3	3.17	0.06	0.139
66.78	12.0	2.63	0.06	0.157
78.78	11.5	2.13	0.06	0.177

TABLE 12.   REACTANT AND PRODUCT CONCENTRATIONS VS. TIME IN
UDMH + HCHO REACTION; EXCESS HCHO (T = 24°C, RH = 11%;
6400 ℓ CHAMBER; RES = 1 CM^{-1}, PATHLENGTH = 68.3 M).

Elapsed Time (min)	Concentration (ppm)			Absorbance at 1010 cm^{-1} $(CH_3)_2NN=CH_2$
	UDMH	HCHO	NH$_3$	
-5		18.0		
0	5.5 (calc'd)			
2.78	5.41	17.4	0.03	0.007
5.78	5.23	17.2	0.03	0.011
10.78	4.99	17.1	0.04	0.024
15.78	4.81	16.9	0.04	0.031
30.78	4.32	16.2	0.03	0.059
50.78	3.51	16.0	0.04	0.090
70.78	2.84	15.3	0.04	0.123
90.78	2.30	14.8	0.04	0.148
110.78	1.75	14.3	0.04	0.172
131.78	1.31	14.0	0.03	0.191
150.78	0.99	13.6	0.04	0.208
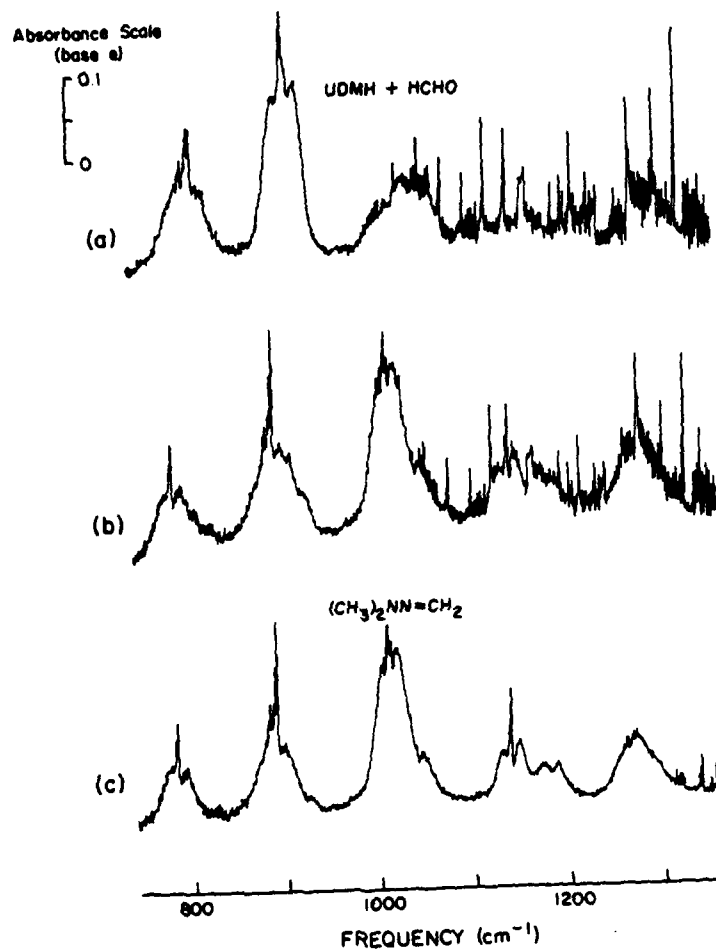
Figure 29. Infrared Spectra from UDMH + Excess HCHO Reaction
(Table 12); Res = 1 cm^{-1}, Pathlength = 68.3 m.
(a) Reaction Mixture at t = 2.8 min, (b) Reaction
Mixture at t = 150.8 min, (c) From (b) Minus
Absorptions of Unreacted UDMH and HCHO.

phase infrared spectrum (Reference 55). It was the only product observed in the UDMH + HCHO experiments. In contrast with the N_2H_4 case, there was no evidence from the infrared spectra that a transient intermediate was formed at any time during the reaction.

The data of Tables 11 and 12 indicate that, as in the case of N_2H_4, the overall reactant stoichiometry was ~1:1 for both runs. However, the data indicate a significantly slower rate for the UDMH + HCHO reaction than for N_2H_4 + HCHO. As with N_2H_4 + HCHO, the kinetics do not appear to be simple, since UDMH decay in excess HCHO, or HCHO decay in excess N_2H_4 were significantly non-exponential; the decay rates in both cases increased with time, despite the fact that the reactant in excess was also being consumed. Thus we conclude that the reactions of HCHO with both N_2H_4 and UDMH are either primarily heterogeneous in nature or proceed via more complex pathways.

3.6 THE REACTIONS OF HYDRAZINE WITH NITRIC ACID

As discussed in Section 3.4, formation of nitric acid salts was observed in the hydrazines + NO_x experiments and verified by comparison with spectra generated from the direct reaction of nitric acid vapor with the vapors of the hydrazines. The procedure followed was to inject incremental amounts of the hydrazine into an excess amount of HNO_3 in order to additionally investigate the possibility of di- or tri-basic salt formation.

3.6.1 Hydrazinium Nitrate

Three separate 2.0 ppm (calculated) aliquots of N_2H_4, were added to ~8 ppm of HNO_3 with spectra recorded between injections. The amount of HNO_3 consumed was not well defined during the first N_2H_4 injection, due to a problem in the introduction of HNO_3 into the chamber (as evidenced by the presence of HNO_3 droplets in the glass injection tube) which resulted in inhomogeneous mixing. After the homogeneity of HNO_3 in the chamber was assured, the second and third increments of N_2H_4 were each found to consume 2.1 ppm of HNO_3, indicating 1:1 stoichiometry. The N_2H_4 + HNO_3 reaction was apparently "instantaneous," since no N_2H_4 absorptions were detected in the infrared spectra recorded immediately after mixing. Light scattering from the reaction mixture was visually evident. Within the experimental uncertainties, the ratios of the strongest absorption

120

band for the three accumulative injections was 1:2:3. These results indicate that the only salt formed was the monobasic salt $NH_2NH_2 \cdot HNO_3$ (or alternatively, $NH_2NH_3^+NO_3^-$), and further suggests that, despite evidence of aerosol formation, the IR spectrum can be used to estimate the "gas-phase" concentration of hydrazinium nitrate, at least for the concentration range indicated here.

The infrared absorption bands of hydrazinium nitrate are presented in Figure 30a for the region $\sim$800-1700 cm^{-1}. Strong interfering H_2O lines above $\sim$1400 cm^{-1} were masked to bring out more clearly the band contours of the nitrate salt. The broad, strongest band seen at $\sim$1300-1450 cm^{-1} is a superposition of the characteristic frequency of NO_3^- at $\sim$1350 cm^{-1} and that of the $-NH_3^+$ group at $\sim$1410 cm^{-1}. This composite peak is analogous to that for the NO_3^- and NH_3^+ modes of $NH_4^+ NO_3^-$ and is also characteristic of the nitrate salts of other hydrazines (see following). Two other characteristic NO_3^- absorptions are seen at 824 and 1044 cm^{-1}, with the other bands at $\sim$978 and $\sim$1100 cm^{-1} agreeing with those of the $NH_2NH_3^+$ group of other hydrazinium salts (e.g., $NH_2NH_2 \cdot HCl$).

3.6.2 Methylhydrazinium Nitrate

With two 3.2 ppm aliquots of MMH injected into $\sim$7 ppm initial HNO_3, 3.0 and 2.8 ppm of HNO_3, respectively, were consumed, indicating that within the experimental uncertainties the stoichiometry was 1:1. As in the case of N_2H_4, the reaction was extremely rapid, being complete within the mixing time, and the band intensities were proportional to the amount of MMH which reacted, despite visual indication of the formation of an aerosol phase.

The infrared spectrum of methylhydrazinium nitrate ($CH_3NHNH_2 \cdot HNO_3$) is presented in Figure 30b. As expected, the NO_3^- and $-NH_3^+$ group absorptions are similar in contours and positions with those found in $NH_2NH_2 \cdot HNO_3$.

3.6.3 N,N-Dimethylhydrazinium Nitrate

The stepwise addition of 2.0 ppm and 7.0 ppm UDMH to $\sim$10 ppm initial HNO_3 "instantaneously" consumed 1.6 ppm and 6.0 ppm of HNO_3, respectively. Within the experimental uncertainty, the results indicate a 1:1 reactant stoichiometry as was observed for the other hydrazines. Likewise, aerosol formation was evident, but the measured band intensities were still proportional to the total amount of UDMH which reacted in each injection.
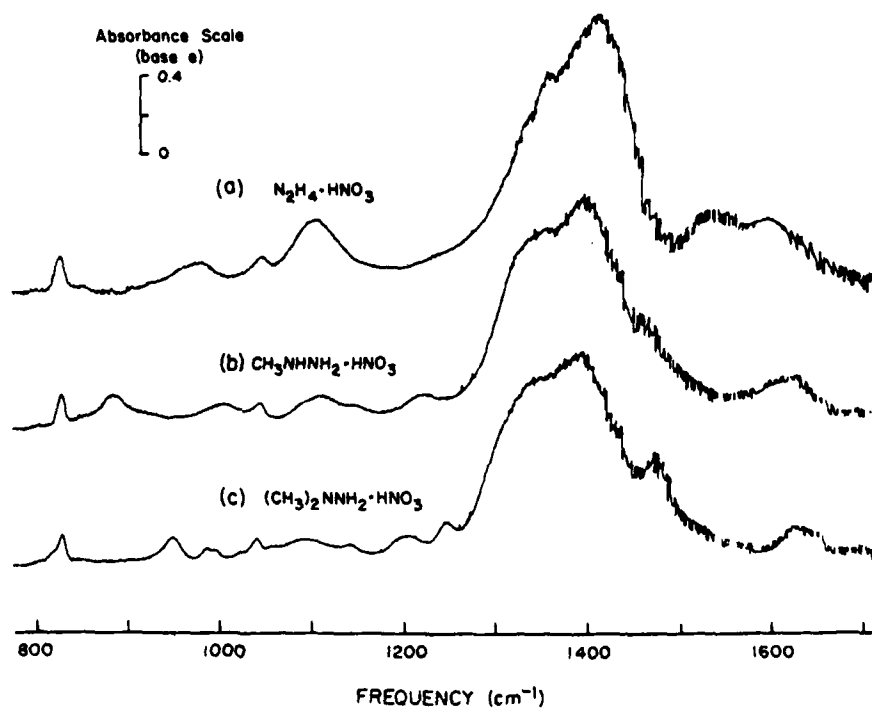
Figure 30.   Product Spectra from the Reactions of Hydrazines with
             Nitric Acid; Res = 1 cm^{-1}, Pathlength = 68.3 m.   Each
             Spectrum Normalized to ~6 ppm of Reacted Hydrazine.

122

Figure 30c shows the infrared spectrum of N,N-dimethylhydrazinium nitrate [$(CH_3)_2NNH_2 \cdot HNO_3$ or $(CH_3)_2NNH_3^+NO_3^-$] and indicates the general simi-larity of the NO_3^- and $-NH_3^+$ group absorptions with those of the monobasic salts of the other hydrazines. A general differentiation among the three salts must come from the generally weaker "fingerprint" absorptions of the substituent groups. For each case, the spectrum of the monobasic salt may not be significantly different from that of the dibasic form (e.g., $NH_2NH_2 \cdot 2HNO_3$) in the spectral region examined. The results of the above experiments confirmed, however, that for all three hdyrazines the forma-tion of di- or tri-basic nitrate salts was not significant when the reac-tants were mixed in the vapor phase.

3.7 RATES OF REACTION OF DIMETHYLNITRAMINE AND N-NITROSODIMETHYLAMINE WITH THE HYDROXYL RADICAL

Rate constants for the reaction of OH radicals with the two major oxidation products of UDMH, namely dimethylnitramine (DMN) and N-nitroso-dimethylamine (NDMA), were determined using relative rate constant tech-niques (Reference 14). With this method, the rate of disappearance of the reactant being studied, relative to that of a reference compound whose OH radical rate constant is accurately known, is measured in a chemical sys-tem where OH radicals are generated under conditions such that reaction with OH is the only significant sink for both the reactant being studied and the reference compound. Under such conditions, regardless of the exact chemical system employed to generate the OH radicals, the kinetic differential equations are as follows:

$$-d\ln[\text{reactant}]/dt = k_1[\text{OH}] \qquad (VII)$$

and

$$-d\ln[\text{reference organic}]/dt = k_2[\text{OH}] \qquad (VIII)$$

from which we can derive:

$$\ln\left\{\frac{[\text{reactant}]_{t_o}}{[\text{reactant}]_t}\right\} = \frac{k_1}{k_2} \ln\left\{\frac{[\text{reference organic}]_{t_o}}{[\text{reference organic}]_t}\right\} \qquad (IX)$$

where $[reactant]_{t_0}$, $[reference\ organic]_{t_0}$ are the concentrations of the reactant and reference organic at time t_0; $[reactant]_t$, $[reference\ organic]_t$ are the corresponding concentrations at time t; and k_1 and k_2 are the rate constants for the reaction of OH radicals with the reactant and the reference organic, respectively. Hence, plots of $\ln([reactant]_{t_0}/[reactant]_t)$ against $\ln([reference\ organic]_{t_0}/[reference\ organic]_t)$ should yield straight lines with a zero intercept and a slope of k_1/k_2. Since k_2 is known for the reference compound, the rate constant k_1 for the reaction of OH radicals with the reactant can be derived.

3.7.1 Dimethylnitramine

The chemical system employed to generate the OH radicals for the purpose of measuring the OH + dimethylnitramine rate constant was based on photolysis, at wavelengths > 290 nm, of ppm concentrations of methylnitrite (CH_3ONO) in air, which has been described in detail previously by Atkinson, et al. (References 14, 56). OH radicals are formed via the following reactions:

$$CH_3ONO + h\nu \rightarrow CH_3O^{\bullet} + NO \qquad (63)$$

$$CH_3O + O_2 \rightarrow HCHO + HO_2 \qquad (58)$$

$$HO_2 + NO \rightarrow OH + NO_2 \qquad (44)$$

or overall:

$$CH_3ONO + h\nu + O_2 \rightarrow HCHO + NO_2 + OH$$
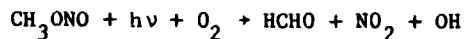
Due to the high photolysis rate of CH_3ONO (References 14, 32, 56, and 57), high concentrations of OH radicals can readily be obtained using this approach. Since dimethylnitramine does not photolyze significantly at the wavelengths (> 290 nm) employed in this system (Reference 58), and since (Section 3.8.1) dimethylnitramine does not react significantly with ozone (formed at low levels from the photolysis of the NO_2 present in this system), its consumption in this system should be due exclusively to reaction with the OH radical.

124

Two irradiations of $CH_3ONO/NO/DMN$/reference organic/air mixtures were carried out, with methanol and dimethyl ether serving as the reference organics. The irradiations were carried out at ~30% of the maximum light intensity, and initial concentrations were : CH_3ONO, 10 ppm; NO, 20 ppm; DMN, 4 ppm; CH_3OH or CH_3OCH_3, 4 ppm. The concentrations of the reactants were monitored by FT-IR spectroscopy for ~1-2 hours.

Figures 31 and 32 show that good straight-line plots based on equation (IX) resulted from these experiments, indicating our assumption that reaction with OH is the major sink for dimethylnitramine and the reference organics employed is probably valid. From least squares analysis of these data, we obtain:

$$k(OH + DMN)/k(OH + CH_3OH) = 5.9 \pm 1.0$$

and

$$k(OH + DMN)/k(OH + CH_3OCH_3) = 1.32 \pm 0.07$$

with the indicated errors being two least squares standard deviations.

Using literature rate constants for the reactions of OH radicals with CH_3OH and CH_3OCH_3 at room temperature of $(1.0 \pm 0.1) \times 10^{-12}$ cm^3 molecule^{-1} sec^{-1} (Reference 59) and $(3.5 \pm 0.35) \times 10^{-12}$ cm^3 molecule^{-1} sec^{-1} (References 59, 60) respectively, then rate constants for the reaction of OH radicals with DMN of $(5.9 \pm 1.2) \times 10^{-12}$ cm^3 molecule^{-1} sec^{-1} and $(4.62 \pm 0.53) \times 10^{-12}$ cm^3 molecule^{-1} sec^{-1} may be derived from the DMN + CH_3OH and DMN + CH_3OCH_3 systems, respectively. (The indicated errors include uncertainties in the OH radical rate constants for CH_3OH and CH_3OCH_3.) A weighted average of these data yields a rate constant of

$$k(OH + DMN) = 4.8 \times 10^{-12} \ cm^3 \ molecule^{-1} \ sec^{-1}$$

with an estimated overall uncertainty of ~15%.

3.7.2 N-Nitrosodimethylamine

Since N-nitrosodimethylamine (NDMA) photolyses rapidly, the generation of OH radicals via CH_3ONO photolysis cannot be used without introducing severe uncertainties. Hence, in this case the thermal decomposition of peroxyacetyl nitrate [$CH_3C(O)OONO_2$ or PAN] in the presence of excess NO in the dark was used to generate OH radicals. In this system,
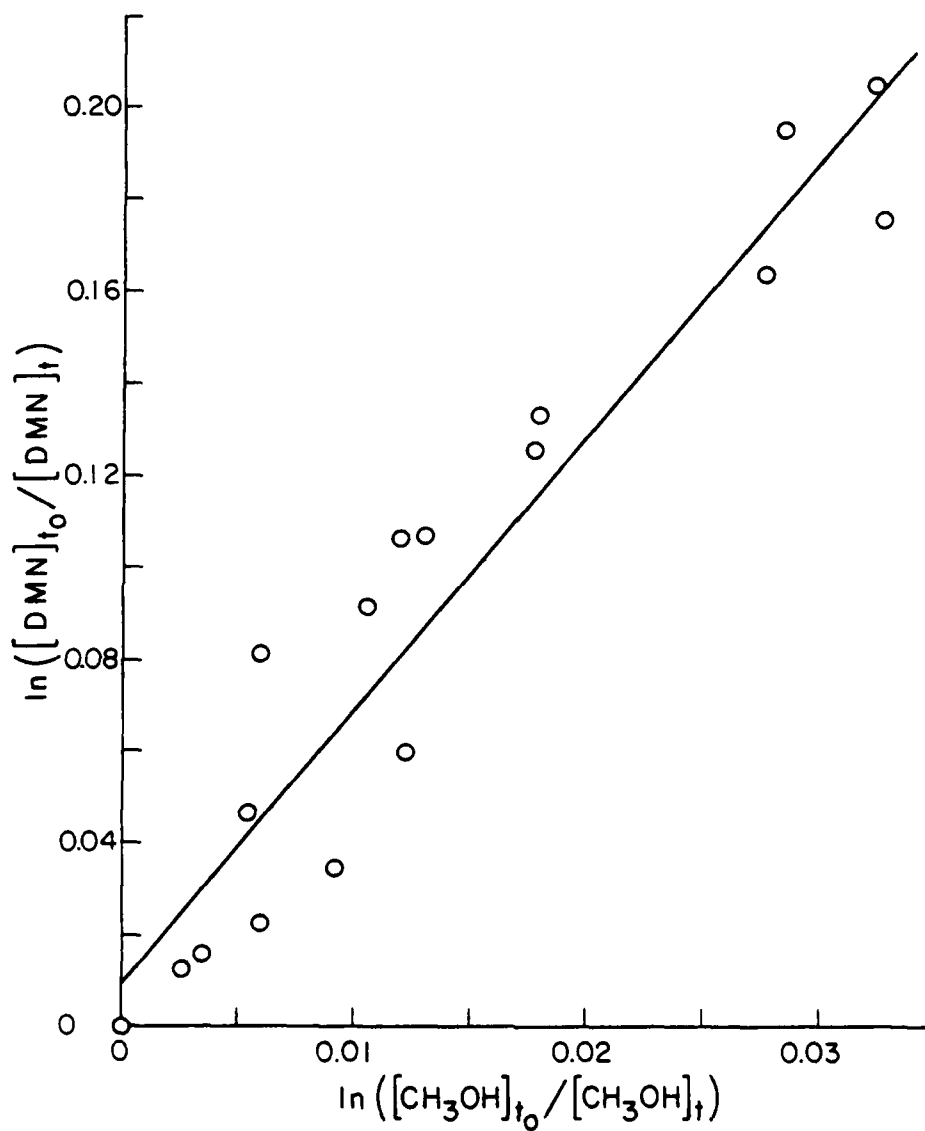
Figure 31. Plots of $\ln([DMN]_{t_0}/[DMN]_t)$ Against $\ln[CH_3OH]_{t_0}/[CH_3OH]_t)$ from the DMN/CH$_3$OH/CH$_3$ONO/NO Irradiation.
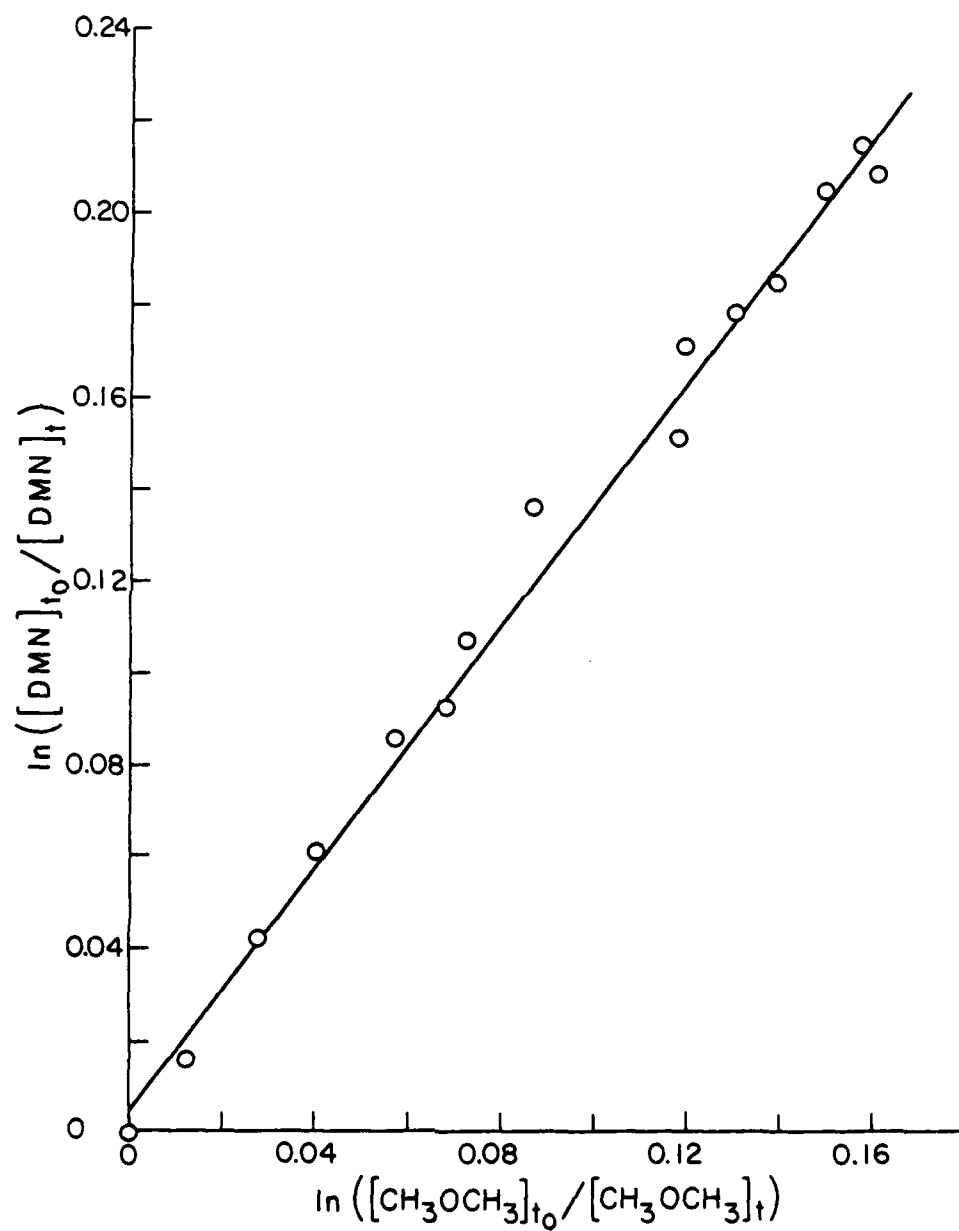
Figure 32. Plots of $\ln([DMN]_{t_0}/[DMN]t)$ Against $\ln([CH_3OCH_3]_{t_0}/[CH_3OCH_3]t)$ from the DMN/CH_3OCH_3/CH_3ONO/NO Irradiation.

127

OH radicals are generated via the following sequence of reactions (References 61-64):

$$CH_3\overset{O}{\overset{\|}{C}}OONO_2 \; \underset{\rightleftarrows}{} \; CH_3\overset{O}{\overset{\|}{C}}OO^\bullet + NO_2 \qquad (64,-64)$$

$$CH_3\overset{O}{\overset{\|}{C}}OO^\bullet + NO \rightarrow CH_3\overset{O}{\overset{\|}{C}}O^\bullet + NO_2 \qquad (65)$$

$$CH_3\overset{O}{\overset{\|}{C}}O^\bullet \overset{fast}{\rightarrow} CH_3 + CO_2 \qquad (66)$$

$$CH_3 + O_2 \overset{M}{\rightarrow} CH_3O_2 \qquad (22)$$

$$CH_3O_2 + NO \rightarrow CH_3O + NO_2 \qquad (57)$$

$$CH_3O + O_2 \rightarrow HCHO + HO_2 \qquad (58)$$

$$HO_2 + NO \rightarrow OH + NO_2 \qquad (44)$$

or overall:

$$PAN + 3 \, NO \overset{2 \, O_2}{\rightarrow} HCHO + 4 \, NO_2 + OH$$
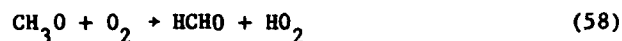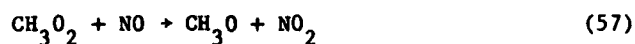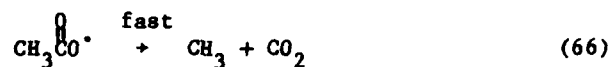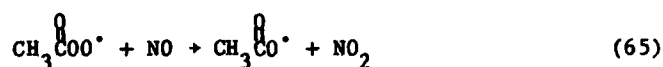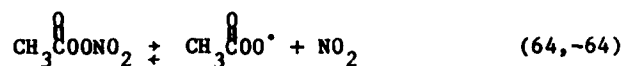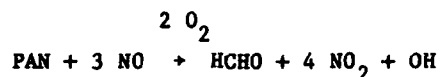
This technique has the advantage that the radicals are formed in the dark, and thus it can be used with highly photoreactive compounds such as NDMA. However, the formation rate of OH radicals in this system is relatively slow, and the OH radical concentrations obtained with this technique are significantly lower than those obtainable from CH_3ONO photolysis since, in the presence of excess NO, the rate-determining step is the thermal decomposition of PAN ($k = 3.7 \times 10^{-4}$ sec^{-1} at 298 K [Reference 40] corresponding to PAN half-life of 31 min at 298 K). A further disadvantage of this technique is the fact that high NO to NO_2 conversion rates occur, along with the loss of OH radicals via the combination reactions

$$OH + NO \overset{M}{\rightarrow} HONO \qquad (45)$$

$$OH + NO_2 \overset{M}{\rightarrow} HNO_3 \qquad (53)$$

While these reactions also occur in the CH_3ONO photolysis system, the

128

rapid photolysis of HONO (Reference 67) regenerates OH radicals in the photolytic system.

$$HONO + h\nu \rightarrow OH + NO \qquad . \qquad (67)$$

Three runs were attempted with different reference organics: methanol, ethene, and propene. Initial concentrations were: PAN, 5 ppm; NO, 25 ppm; NDMA, 5 ppm; reference organic, 5 ppm. The reactions were monitored by FT-IR spectroscopy for ~2.5 to 3 hours. For the runs employing methanol and ethene, the amount of NDMA and reference compound consumed were too small (< 5% consumption for each) to allow meaningful kinetic information to be derived. The run with propene as the reference compound was more successful: ~10-15% of the propene was consumed, and the amount of NDMA reacting, though small (~5%), was sufficient to allow an approximate estimate of its rate constant to be made using equation (IX). Figure 33 shows the plot of equation (IX) from the data of the NDMA/propene/PAN/ NO run. Although the data are highly scattered because of the relatively low OH radical levels and the resulting small amount of NDMA consumed, they indicate that

$$k(OH + NDMA)/k(OH + propene) = 0.083 \pm 0.035$$

with the errors reflecting two standard deviations. Using an OH + propene rate constant of 2.5×10^{-11} cm^3 molecule^{-1} sec^{-1} (Reference 59), we thus derive

$$k(OH + NDMA) = (2 \pm 1) \times 10^{-12} \ cm^3 \ molecule^{-1} \ sec^{-1}$$

3.7.3 Discussion

The reactions of hydroxyl radicals with dimethylnitramine and N-nitrosodimethylamine are expected to occur via an H abstraction from a C-H bond on a methyl radical,

$$(CH_3)_2 N\text{-}NO_x + OH \rightarrow \overset{\overset{\displaystyle CH_3}{|}}{CH_2 N\text{-}NO_x} + H_2O$$
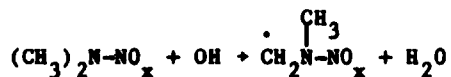
and can thus be compared with analogous abstractions from methyl groups on
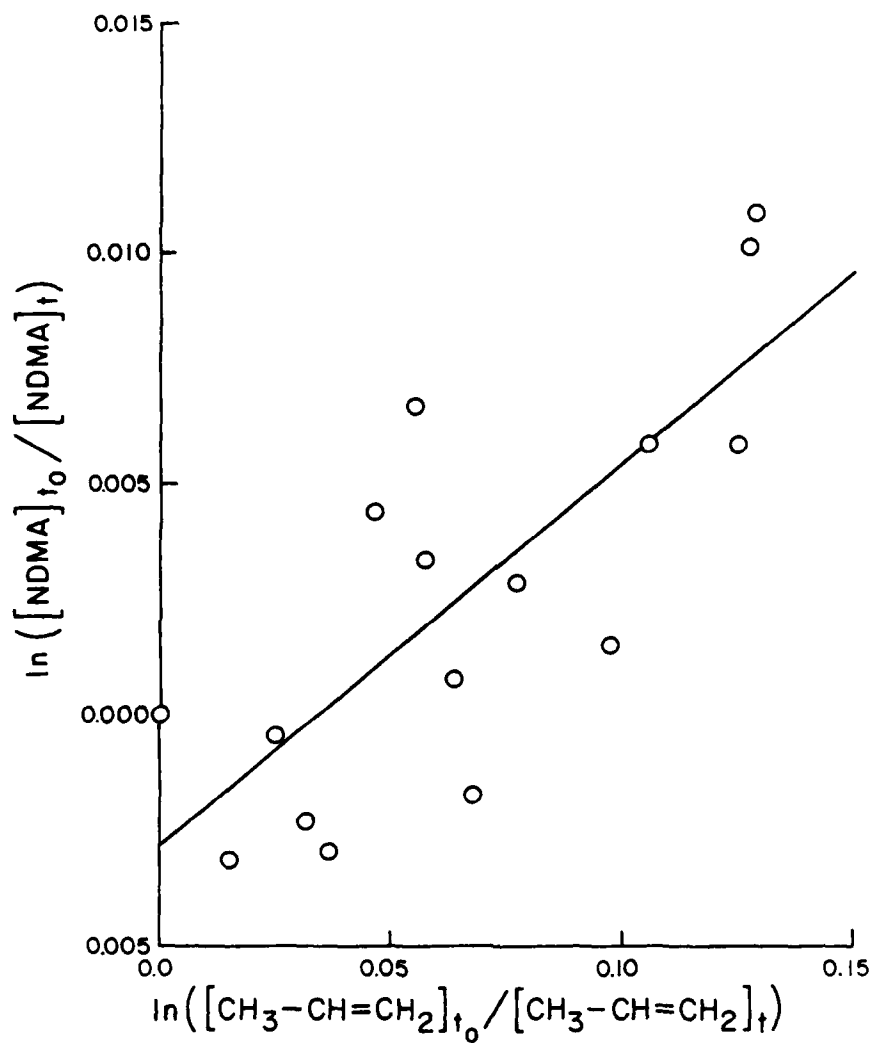
Figure 33. Plots of $\ln([NDMA]_{t_0}/[NDMA]_t)$ Against $\ln([CH_3CH=CH_2]_{t_0}/[CH_3CH=CH_2]_t)$ from the NDMA/$CH_3CH=CH_2$/PAN/NO Experiment.

130

other classes of compounds. The rate constant per C-H bond is (in units of 10^{-12} cm^3 molecule^{-1} sec^{-1}) 0.80 ± 0.12 for DMN and 0.33 ± 0.17 for NDMA, respectively. This can be compared with rate constants (in the same units) of 0.07 for abstraction from primary C-H bonds in the simple alkanes (Reference 59) and with ~7 for abstraction from the C-H bonds in the alkylamines (Reference 66). Thus, while the rate constants for the reactions of OH radicals with DMN and NDMA can be considered to be surprisingly low when they are assumed to be analogous to the simple amines, it is clear that H-atom abstractions by OH radicals from the C-H bonds in these compounds are still much more rapid than those encountered in the simple alkanes.

If one assumes an average OH radical concentration of ~1 x 10^6 molecules cm^{-3} for the lower troposphere (Reference 8), then the calculated atmospheric half lives due to removal by reaction with OH radicals are ~1.7 days for DMN and ~4 days for NDMA. Since NDMA has a photolytic half-life of less than ~10 minutes (see Section 3.8.2), reaction with the OH radical is a relatively minor atmospheric sink for this compound. On the other hand, reaction with OH radicals will probably be the major degradation pathway for DMN.

3.8 OTHER REACTIONS OF DIMETHYLNITRAMINE AND N-NITROSODIMETHYLAMINE

3.8.1 Dark Decay and Reaction with Ozone

The decay of 3.5 ppm of N-nitrosodimethylamine in the 6400 ℓ Teflon® chamber, shielded from ambient light, was monitored by FT-IR spectroscopy. There was no measurable change in concentration detected after 6 hours. Likewise, no change in the NDMA concentration could be measured 3 hours after ~12 ppm of O_3 was subsequently introduced, indicating that the NDMA + O_3 reaction proceeds at a negligible rate, with a rate constant of < 3 x 10^{-20} cm^3 molecule^{-1} sec^{-1}.

The above experiment was repeated for dimethylnitramine (DMN) with similar results: no measurable dark decay was observed in 3 hours and no detectable change in DMN concentration occurred within 3 hours in its mixture with excess O_3, leading to a similar upper limit for the rate constant for reaction of O_3 with DMN.

3.8.2 Photolysis of N-Nitrosodimethylamine in the Presence of Ozone

The relatively rapid photolysis of N-nitrosodimethylamine is probably its primary mode of degradation in the atmosphere in the daytime, and thus its photolysis rate was measured in order to obtain an indication of its atmospheric lifetime. However, photolysis of pure NDMA in air would lead to observed rates of decay which are significantly slower than the rate of the elementary photodecomposition reaction

$$(CH_3)_2N-NO \xrightarrow{h\nu} (CH_3)_2\overset{\bullet}{N} + NO \qquad (69)$$
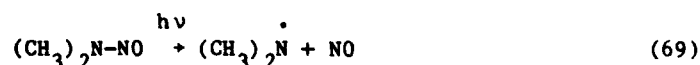
because of the rapid recombination of the fragments to reform NDMA.

$$(CH_3)_2\overset{\bullet}{N} + NO \rightarrow (CH_3)_2N-NO \qquad (70)$$
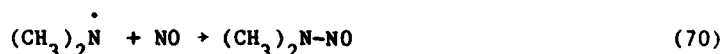
In this study, that problem was circumvented by the inclusion of excess O_3 in the NDMA-air mixture during its photolysis. The O_3 will react rapidly with the NO formed by reaction (71), and thus suppress NO levels sufficiently so that reaction (70) should become unimportant.

$$NO + O_3 \rightarrow NO_2 + O_2 \qquad (71)$$

Thus, an experiment was performed in which 4 ppm of NDMA and 12 ppm of O_3 were photolyzed in air in the indoor Teflon® chamber, using black light irradiation with a light intensity corresponding to a measured NO_2 photolysis rate of ~0.45 min^{-1}. (The light intensity measurement was made several months prior to this experiment, and thus must be considered strictly as an upper limit because of possible degradation of the light intensities of the lamps over this period.)

Figure 34a shows the infrared spectrum (~750-1400 cm^{-1}) of the reaction mixture before irradiation and Figure 34b illustrates the changes which occurred at t = 35.8 min into the irradiation. The products observed were dimethylnitramine (DMN), HCHO, CH_3NO_2, CO, HNO_3, NO_2 and N_2O_5. A reference spectrum of DMN, the major product, is included in Figure 34c for comparison. The spectral analysis for the reactants would be impossible without the iterative subtraction method afforded by our data manipulation software, since absorptions of DMN, NDMA, and O_3 mutually overlap

TABLE 13. REACTANT AND PRODUCT CONCENTRATIONS VS. TIME DURING
IRRADIATION[a] OF $(CH_3)_2NNO$ IN THE PRESENCE OF EXCESS O_3
[T(AVG) = 28°C; 6400 ℓ CHAMBER; RES = 1 CM^{-1}, PATHLENGTH = 68.3 M].

Elapsed Time (min)	Concentration (ppm)								
	$(CH_3)_2NNO$	O_3	$(CH_3)_2NNO_2$	CH_3NO_2[b]	HCHO	CO	HNO_3	N_2O_5	NO_2
-28	4.05	12.0							
-15	3.97	12.0							
0	START OF IRRADIATION								
1.38	3.67	11.8	0.17	0.31	0.69	–	0.05	–	0.10
3.38	2.31	9.32	1.1	0.42	0.79	–	0.10	0.10	0.29
5.38	1.59	8.13	1.6	0.65	0.98	–	0.18	0.12	0.31
7.38	1.18	7.38	1.8	0.81	1.1	–	0.29	0.13	0.31
9.38	0.80	6.89	2.1	0.98	1.2	0.08	0.37	0.12	0.28
11.38	0.59	6.24	2.2	1.1	1.3	0.08	0.43	0.11	0.28
13.38	0.40	6.00	2.3	1.1	1.3	0.10	0.51	0.12	0.26
15.38	0.29	5.69	2.4	1.2	1.3	0.10	0.55	0.11	0.22
25.78	–	5.03	2.5	1.3	1.3	0.19	0.79	0.04	0.12
35.78	–	4.72	2.5	1.3	1.3	0.27	0.94	0.02	0.08

[a]Light intensity corresponds to NO_2 photolysis rate of ~ 0.45 min^{-1}.
[b]An absorption coefficient of 18 cm^{-1} atm^{-1} (Reference 68) for the 1590 cm^{-1} peak of CH_3NO_2 was employed.

in the 1000–1060 cm^{-1} region which include the measurement band for NDMA. The detailed concentration-time data are given in Table 13 and Figure 35 shows a semi-logarithmic plot of the decay of NDMA with irradiation time.

Figure 35 shows that the decay of NDMA was exponential over the duration of the irradiation experiment, with a decay rate of 0.175 ± 0.003 min^{-1}. Based on (a) absorption coefficients given by Lindley (Reference 16), (b) our measured spectral distribution, (c) the NO_2 photolysis rate in the indoor Teflon® chamber, (d) currently accepted NO_2 absorption coefficients and photodecomposition quantum yields (Reference 40), and (e) assuming the photodecomposition quantum yield of NDMA is 1.0 at all wavelengths (Reference 67), we calculate the elementary photodecomposition rate of NDMA to be 0.21 min^{-1}. (The technique for this calculation is the

133
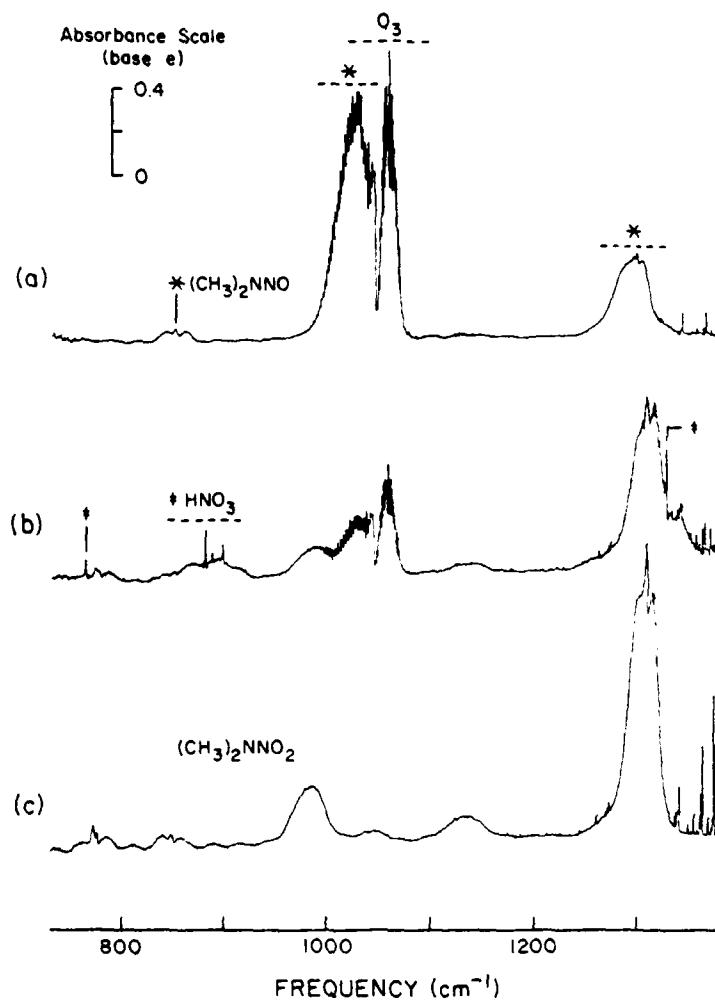
Figure 34. (a) Infrared Spectrum of $(CH_3)_2NNO$ and O_3 Mixture before Irradiation (Table 13), and (b) at t = 35.8 Minutes of Photolysis. (c) $(CH_3)_2NNO_2$ Reference Spectrum. Res = 1 cm^{-1}, Pathlength = 68.3 m.

134
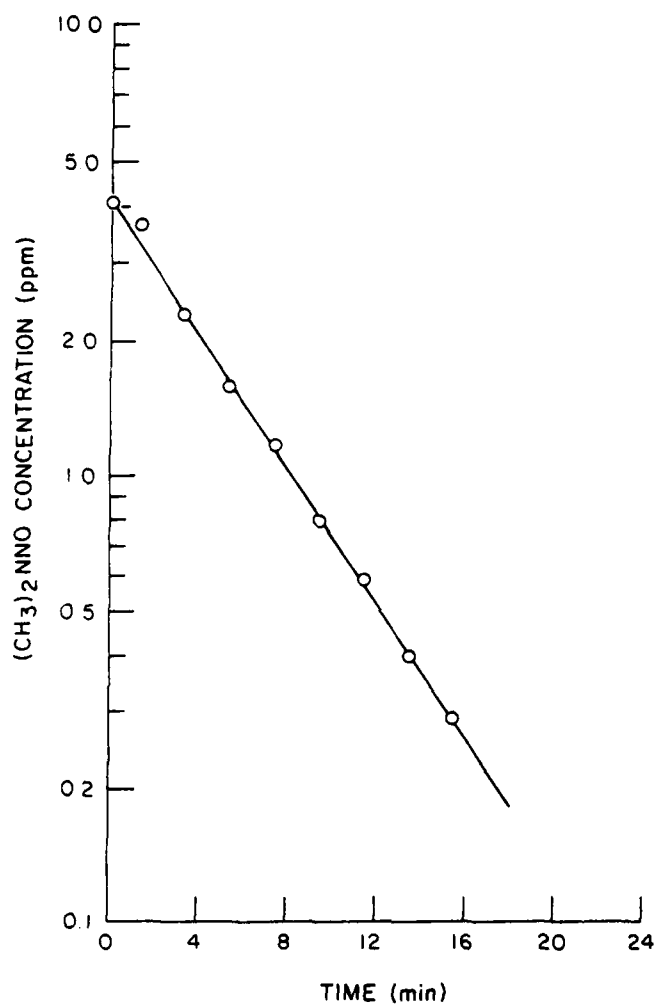
Figure 35. Concentration of $(CH_3)_2NNO$ vs. Irradiation Time
in the Photolysis of $(CH_3)_2NNO$ and O_3 Mixture
(Table 13).

135

same as used by Lindley [Reference 16], and is hence not reproduced here.) Thus our measured photolysis rate is within the experimental errors of that calculated, and hence supports the assumption that the primary quantum yield of NDMA is unity at all wavelengths > 290 nm.

The observed products account for ~90% of the carbon and ~95% of the nitrogen in the initial NDMA, with ~63% of each being contained in the major product, DMN. DMN is expected to be formed from the reaction of the dimethylamino radical with NO_2, the latter resulting from the reaction of NO with O_3:

$$(CH_3)_2N^{\bullet} + NO_2 \xrightarrow{M} (CH_3)_2N\text{-}NO_2 \tag{72a}$$
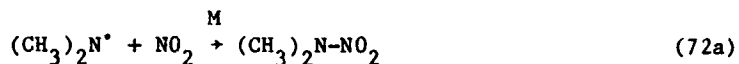
Lindley, et al. (References 16, 68) observed that when dimethylamino radicals are formed in air, monomethylmethyleneamine formation will also occur via the following reactions:

$$(CH_3)_2N^{\bullet} + NO_2 \rightarrow HONO + CH_3\text{-}N\text{=}CH_2 \tag{72b}$$

$$(CH_3)_2N^{\bullet} + O_2 \rightarrow HO_2 + CH_3\text{-}N\text{=}CH_2 \tag{73}$$
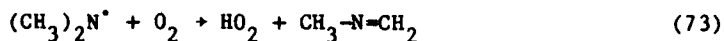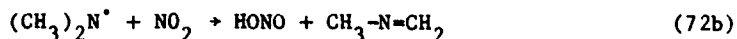
Based on k_{72b}/k_{72a} and k_{73}/k_{72a} rate constant ratios of (0.22 ± 0.04) and $(3.9 \pm 0.3) \times 10^{-7}$, respectively, as given by Lindley, et al. (Reference 68) and using the average NO_2 level observed in our experiment, we predict an ~65% yield of DMN in our experiment, in excellent agreement with the observed yield of 63% yield. Thus, it appears that the dimethylamino radical reacts only via reactions (72) and (73) in our system, and we can conclude that if the dimethylamino radical reacts with O_3, the rate constant must be at least ~100 times slower than that for its reaction with NO_2.

The fact that monomethylmethyleneamine is not observed in our experiment can be attributed to the fact that it probably reacted with O_3. In particular, such a reaction can account for the observed formation of HCHO and CH_3NO_2:

136

$$CH_3-N=CH_2 + O_3 \rightarrow \left[CH_3-\overset{\overset{\displaystyle O-O}{|\quad\,\,|}}{N} - CH_2 \right] \rightarrow CH_3-\overset{\overset{\displaystyle O-O^\bullet}{|}}{\overset{\bullet}{N}} + HCHO \qquad (74)$$

$$\left[CH_3-N\overset{\overset{\displaystyle O}{\diagup}}{\underset{\underset{\displaystyle O}{\diagdown}}{|}} \right] \rightarrow CH_3NO_2$$
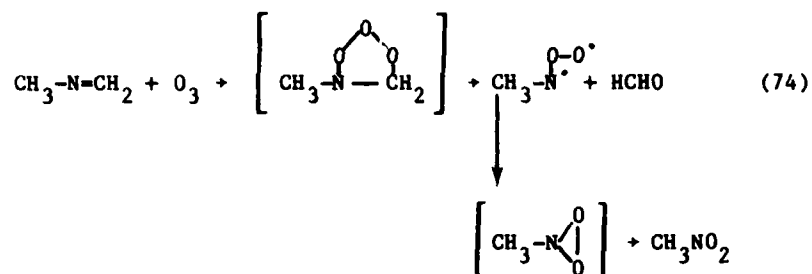
The observed formation of CO can be attributed to alternate fragmentation pathways in the $O_3 + CH_3N=CH_2$ reaction, or to the reaction of OH with HCHO, where OH is expected to be formed from the reaction of NO with the HO_2 formed in reaction (73).

$$HO_2 + NO \rightarrow OH + NO_2 \qquad (44)$$

$$OH + HCHO \rightarrow H_2O + HCO \qquad (75)$$
$$\overset{\displaystyle O_2}{\underset{\displaystyle \quad\rightarrow HO_2 + CO}{|}}$$
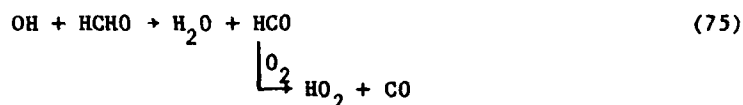
Other than DMN and nitromethane, the major nitrogen-containing product is HNO_3, with smaller amounts of N_2O_5 and NO_2 also being present. (Although NO is not observed, it is expected to be present in trace amounts, since it is continuously formed by the rapid NO_2 photolysis, as well as by the decomposition of NDMA.) The observed N_2O_5 is formed from the reaction of NO_2 with O_3.

$$NO_2 + O_3 \rightarrow NO_3 + O_2 \qquad (76)$$

$$NO_3 + NO_2 \rightleftarrows N_2O_5 \qquad (77,-77)$$

while the HNO_3 can be formed either from heterogeneous N_2O_5 hydrolysis

$$N_2O_5 + H_2O \rightarrow 2\ HNO_3 \qquad (78)$$

or from the reaction of OH with NO_2.

137

$$OH + NO_2 \xrightarrow{M} HNO_3 \qquad\qquad (53)$$

Thus, all of the products and intermediates observed in the present NDMA/O$_3$ photolysis experiment can be accounted for. This supports the validity of the mechanism proposed above for this system.

SECTION IV
CONCLUSIONS AND RECOMMENDATIONS

4.1 SUMMARY OF RESULTS AND CONCLUSIONS

The experiments described in this report have resulted in a greatly increased data base concerning the atmospheric reactions of hydrazines and their major oxidation products. In particular, information has been obtained concerning the reactions of hydrazine, monomethylhydrazine, and unsymmetrical dimethylhydrazine with ozone under a wider variety of conditions than has previously been available. These experiments have also resulted in the characterization of the behavior of a number of products in these chemical systems. We have shown that these hydrazines undergo reactions at significant rates with nitrogen dioxide, nitric acid, and formaldehyde when present at ppm levels in air. A quantitative determination of the major atmospheric sink processes of N-nitrosodimethylamine and dimethylnitramine, both important oxidation products of unsymmetrical dimethylhydrazine, have been obtained. Additionally, data concerning the dark decay behavior of the hydrazines in large Teflon$^{\circledR}$ reaction chambers have been expanded.

The major purpose of the experimental program whose results are described in this report was to elucidate the detailed chemical mechanisms for the major atmospheric reactions of the three hydrazine fuels studied. In this regard, this study has had mixed success. The mechanisms for the reactions of UDMH with NO_2, the reactions of the hydrazines with HNO_3, and of the photolysis of N-nitrosodimethylamine appear to be well established as a result of this investigation. In addition, the rate constants for the reaction of OH radicals with dimethylnitramine and N-nitrosodimethylamine were measured under atmospheric conditions. These data indicate that our previously proposed mechanism (Reference 3) for the reactions of N_2H_4 and MMH with ozone are probably largely correct, although significant uncertainties still remain. On the other hand, our new and more extensive data concerning the reaction of UDMH with ozone, whose mechanism we previously thought to be relatively straightforward (References 3, 10, 39), cannot be explained in terms of any reasonable mechanism we can devise. Likewise, there are major uncertainties in the mechanisms for the reactions of NO_x with N_2H_4 and MMH. In addition, the

139

reactions of N_2H_4 and UDMH with formaldehyde are either very complex or heterogeneous.

In the following sections, the results and conclusions from the specific systems studied are summarized, and several recommendations for future research are given.

4.1.1 Dark Decay of the Hydrazines

When present at ppm levels in air, N_2H_4, MMH, and UDMH all undergo dark decays at measurable rates in the large-volume Teflon® chambers (3800 ℓ and 6400 ℓ) employed, N_2H_4 decayed about three times faster than MMH, while MMH decayed about 10–20 times faster than UDMH. These decay rates approximately doubled when the chamber volume was cut in half and the chamber surface characteristics, as modified by hydrazine "conditioning," had a significant effect on decomposition rate. The measured decay rates increased significantly with humidity, with N_2H_4 and MMH decaying 50%–100% faster at ~50% RH than at ~20% RH, and UDMH decaying ~5 times faster at ~50% RH. Some diazene or methyldiazene was observed in the decomposition of N_2H_4 and MMH, respectively, together with production of NH_3. For UDMH, only trace amounts of NH_3 were observed. Hydroxyl radicals are apparently not involved in the dark decays of these hydrazines. There was no definitive evidence for synergistic effects when UDMH and N_2H_4 were present together in our chamber, though the UDMH decay rate may be enhanced slightly. The mechanism of the dark decays of these hydrazines, which is undoubtedly heterogeneous in nature, remains largely unknown at this time.

4.1.2 Reactions of Hydrazines with Ozone

The initial reaction of N_2H_4 with O_3 has an estimated rate constant of ~3 x 10^{-17} cm^3 molecule^{-1} sec^{-1}. This, however, is considered to be an upper limit because the intermediates involved react at significant rates with both N_2H_4 and O_3. We were not successful in obtaining quantitative information concerning the initial O_3 + MMH and O_3 + UDMH rate constants, as they are too fast (> 10^{-15} cm^3 molecule^{-1} sec^{-1}) to measure by the techniques employed.

The assumption, based on mechanistic grounds, made in our previous report (Reference 3) that hydroxyl radicals are involved in the mechanisms of reaction of N_2H_4, MMH, and UDMH with O_3 has been experimentally verified. Organic tracers which react only with OH radicals, when added to

140

the O_3 + hydrazine reaction mixtures, are observed to decline, with the largest decline resulting when O_3 is in excess. Also, the presence of a large excess of an OH radical trap resulted in significant changes in reactant stoichiometries in the O_3 + N_2H_4 and O_3 + MMH systems, and in changes in product yields for all three hydrazines.

The formation of diazene (N_2H_2) in the O_3 + N_2H_4 system, postulated on mechanistic grounds in our previous report (Reference 3), has been confirmed by direct observation of its infrared spectrum. It has also been confirmed that it reacts rapidly ($k \geq 10^{-15}$ cm^3 molecule^{-1} sec^{-1}) with O_3, as predicted.

The products observed in the MMH + O_3 system (CH_3NNH, CH_2N_2, HCHO, H_2O_2, CH_3OH, CO, HCOOH, NH_3 and N_2O) were the same as reported previously, but more quantitative information concerning their yields (particularly, estimates of the absolute yields of CH_3NNH) are available from this study. We believe that the major products formed in this system have been identified.

Most of the major products formed in the O_3 + UDMH reaction have also been identified. As reported previously, the major product is N-nitrosodimethylamine, but formation of lesser (but non-negligible) yields of CH_3NNH, HCHO and CH_3OOH are also observed in the present study. This is the first reported observation of CH_3NNH and CH_3OOH in the O_3 + UDMH system. The formation of these fragmentation products, which are suppressed by the presence of the radical trap, are accounted for by the OH + UDMH reaction proceeding to an appreciable extent via abstraction from C-H bonds (as opposed to abstraction from the weak N-H bonds).

The dependence of product yields, reactant stoichiometries, and reaction rates in the O_3 + hydrazine systems on initial reactant ratios and on the presence and absence of the radical trap have been determined for the first time. For the N_2H_4 + O_3 and MMH + O_3 systems, where the stoichiometries and product yields depended significantly on the reaction conditions, the results were largely consistent with our previously proposed mechanism (Reference 3), except for the observed formation of diazomethane in the presence of the radical trap (see below). On the other hand, the fact that the addition of the radical trap does not significantly change the ~3:2 O_3:UDMH reactant stoichiometry (which is independent of initial reactant ratios) in the UDMH system, despite evidence for formation of

hydroxyl radicals in that system, is totally inconsistent with our previously assumed mechanism. At present we are unable to devise a UDMH + O_3 mechanism which is consistent with all of the new data.

Although the O_3 + N_2H_4 and O_3 + MMH mechanisms presented previously are for the most part consistent with the new data obtained in this study, the results could be equally well explained by assuming a different initial reaction pathway than previously assumed (i.e., N-oxide formation, followed by rearrangement and decomposition to H_2O and N_2H_2, rather than H atom abstraction forming OH, O_2, and N_2H_3 as previously adopted). Thus the exact mode of the initial O_3 + hydrazine reaction is still unknown.

An exploratory experiment performed by reacting N_2H_4 with O_3 in N_2 rather than in air clearly indicates, as predicted, that O_2 is involved in the reaction mechanism. The rates of reaction and amounts of O_3 consumed were enhanced when O_2 was low, and it is presumed that the reaction of O_3 with hydrazyl radicals (N_2H_3) becomes important under these conditions. Other reactions of N_2H_3 radicals, such as self-reaction or reaction with HO_2, may also be important in that system, but their rate constants, and thus their significance, are presently unknown.

The observed formation of diazomethane from the MMH + O_3 system in larger yields in the presence of the radical trap than in its absence is inconsistent with our previously assumed mechanism that CH_2N_2 is formed from a reaction of OH radicals with CH_3NNH. The new data are more consistent with CH_2N_2 being formed from a reaction of O_3 (probably with CH_3NNH), but its exact mode of formation is still highly uncertain.

One exploratory experiment was performed in which O_3 was reacted with Aerozine-50, an equimolar mixture of N_2H_4 and UDMH. The results were entirely consistent with the results of experiments where these two hydrazines were reacted separately. There was no evidence for synergistic effects in this system, other than the gradual formation of formaldehyde hydrazone from the reaction of the remaining N_2H_4 with formaldehyde, an oxidation product of UDMH (see below).

4.1.3 Reactions of Hydrazines with Oxides of Nitrogen

All three hydrazines studied were observed to react at significant rates in the gas phase with NO_2, with apparent upper limit rate constants of ~2.5 x 10^{-19} cm^3 molecule^{-1} sec^{-1} for NO_2 + N_2H_4, ~3 x 10^{-18} cm^3 molecule^{-1} sec^{-1} for NO_2 + MMH, and ~2 x 10^{-17} cm^3 molecule^{-1} sec^{-1}

142

for NO_2 + UDMH. None of these hydrazines reacted with NO alone at measurable rates, although some NO was consumed when NO_2 and the hydrazines reacted in its presence.

The reaction of NO_2 with N_2H_4 resulted in the formation of high yields of HONO, hydrazinium nitrate, diazene (in excess N_2H_4 only), and traces of N_2O and NH_3; when NO was present, some NO was converted to NO_2. Analogous products were formed when NO_2 and MMH reacted, namely HONO (in high yields), monomethylhydrazinium nitrate, methyldiazene, and methylhydroperoxide (in excess MMH only) as well as traces of methanol, N_2O, and NH_3. In addition, in the MMH + NO_2 system, two unknown products were observed, and peroxynitric acid was formed as a transient intermediate in the absence of NO, indicating the intermediacy of HO_2 radicals. In both cases, the reactant stoichiometry and product yields were highly dependent on reaction conditions. The initial reaction is probably hydrogen atom abstraction from the hydrazine by NO_2 forming HONO and a hydrazyl radical, with the latter subsequently reacting with O_2 to form HO_2 and the corresponding diazene. Diazene and methyldiazene apparently react with NO_2, with the reaction of the former probably being faster. However, the mechanism of these reactions is highly uncertain since we are unable to reconcile all of our results in the NO_2 + N_2H_4 and NO_2 + MMH systems with a reasonable reaction mechanism. Particular uncertainties concern the fates of HO_2 and CH_3O_2 radicals in these systems (if indeed they are formed), and the source of HNO_3 which is a precursor to the observed nitrate salts when they are formed in the absence of NO.

In contrast to the NO_2 + N_2H_4 and the NO_2 + MMH systems, the NO_2 + UDMH system appears to be much simpler. In the absence of NO, the only significant products formed were HONO and tetramethyltetrazene-2 (TMT), with the reactant stoichiometries and product yields indicating the overall reaction to be

$$UDMH + 2 NO_2 \rightarrow 2 HONO + 0.5 TMT$$
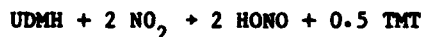
regardless of the initial UDMH/NO_2 ratio. In the presence of NO, the yields of TMT were lower, and an unidentified product, believed to be N-nitroso-N',N'-dimethylhydrazine, as well as N_2O and traces of N-nitrosodimethylamine, were formed. These products are entirely consistent with a

143

relatively straightforward 4-step mechanism (in the absence of NO) involving the initial formation of N,N-dimethylhydrazyl radicals, which react with NO_2 to form N-nitro-N',N'-dimethylhydrazine. The latter nitrohydrazine then undergoes rearrangement and decomposition to form the charge-separated intermediate $(CH_3)_2\overset{+}{N}=\overset{-}{N}$, which subsequently dimerizes to form the observed tetrazene. When NO is present, it could react with the hydrazyl radical to form the nitrosohydrazine, with the latter undergoing a secondary reaction with NO_2 to ultimately give rise to N_2O and N-nitrosodimethylamine.

4.1.4 Reactions of Hydrazines with Formaldehyde

When N_2H_4 or UDMH was mixed with formaldehyde in the gas phase, consumption of the hydrazine and HCHO, with 1:1 stoichiometry, and formation of the corresponding formaldehyde hydrazone $[H_2NN=CH_2$ or $(CH_3)_2NN=CH_2]$ occurred. In the N_2H_4 + HCHO system, a transient intermediate, which may be NH_2NHCH_2OH, was formed; no similar intermediate was evident in the UDMH + HCHO experiments. In both systems, the concentration-time profiles of the reactants were not consistent with the reactions being a simple second order process. The mechanism of these reactions are unknown; they are either primarily heterogeneous or fairly complex.

4.1.5 Reactions of Hydrazines with Nitric and Nitrous Acids

N_2H_4, MMH, and UDMH reacted with HNO_3 in the gas phase to form the corresponding hydrazinium nitrate aerosol at a rate which was too fast to measure by our method (i.e., $> 10^{-15}$ cm^3 molecule^{-1} sec^{-1}). The stoichiometry was 1:1, indicating that only the monobasic salt was formed. On the other hand, no evidence was obtained for a similar gas phase reaction between HONO and these hydrazines, indicating that HONO is probably too weak an acid to react in this manner.

4.1.6 The Atmospheric Reactions of N-Nitrosodimethylamine and Dimethylnitramine

The rate constant for the reaction of hydroxyl radicals with dimethylnitramine was measured to be $(4.8 \pm 0.7) \times 10^{-12}$ cm^3 molecule^{-1} sec^{-1}, and an estimate for the OH + N-nitrosodimethylamine rate constant of $\sim(2 \pm 1) \times 10^{-12}$ cm^3 molecule^{-1} sec^{-1} was obtained. These reactions are significantly slower than expected based on analogous reactions of the simple alkylamines. Reaction with OH radicals is probably the major

simple alkylamines. Reaction with OH radicals is probably the major atmospheric sink for dimethylnitramine, and our result indicates a tropospheric half life of approximately two days for this compound.

The major atmospheric sink for N-nitrosodimethylamine (NDMA) is probably photolysis, since its rate of removal by this process is calculated to be over three orders of magnitude higher than its rate of removal by reaction with OH radicals under tropospheric conditions. The fact that the photodissociation of NDMA occurs with a quantum yield of 1.0 ($\pm \sim$30%) was confirmed in experiments in which NDMA was photolyzed in the presence of O_3. Since O_3 rapidly reacts with NO, it prevented nitrosamine regeneration due to recombination of NO with dimethylamino radicals.

When NDMA was photolyzed in the presence of ozone (a situation which could occur if NDMA was emitted or formed in either clean or polluted atmospheres), dimethylnitramine, HCHO, HNO_3, NO_2, CO, and N_2O_5 and traces of nitromethane (CH_3NO_2) were formed. The formation and relative yields of these products are consistent with the mechanism and relative rate constants for the reaction of dimethylamino radicals with O_2 and NO_x as determined by Lindley, et al. (Reference 68), provided it is assumed that $CH_2=N-CH_3$, formed from the reaction of $(CH_3)_2N$ with O_2, reacts rapidly with O_3 to form formaldehyde and CH_3NO_2. These results also indicate that the reaction of dimethylamino radicals with O_3 must be at least $\sim$100 times slower than its reactions with NO_2.

The rates of reactions of both N-nitrosodimethylamine and dimethylnitramine with O_3 have been shown to be negligible ($< 3 \times 10^{-20}$ cm^3 molecule^{-1} sec^{-1}) under atmospheric conditions. In addition, no appreciable dark decay of these compounds in air could be detected.

4.2 RECOMMENDATIONS FOR FUTURE RESEARCH

A major conclusion which can be drawn from the results of this study is that the three hydrazines investigated and some of their oxidation products are extremely labile, and that they undergo a wide variety of reactions, involving in some cases very complex reaction mechanisms. Although our studies have elucidated some aspects of these mechanisms, the number of remaining uncertainties is considerable, and much more research of a fundamental nature is required before we can obtain a satisfactory understanding of the atmospheric reactions of these amine fuels, as well

as of other labile nitrogen-containing organics. Some suggestions concerning the more significant areas where research is needed are indicated below.

4.2.1 Atmospheric Reactions of Other Hydrazines

Information is required concerning the reactions of hydrazines other than N_2H_4, MMH and UDMH. In particular, studies of tetramethylhydrazine (TTMH), trimethylhydrazine (TMH), and symmetrical dimethylhydrazine (SDMH) would be very useful in elucidating the general hydrazine reaction mechanisms. For example, it would be of interest to determine how reactive tetramethylhydrazine is relative to the other hydrazines. If the initial reaction of O_3 with hydrazines is abstraction from the N-H bonds, then tetramethylhydrazine would not react with O_3, whereas if the reaction proceeds via O-atom transfer, rapid reaction and formation of a stable N-oxide may well occur. In addition, our current mechanism for the initial reactions of NO_2 with hydrazine predicts that tetramethylhydrazine would not react with NO_2, but this needs to be experimentally verified. Similarly, one might expect that formaldehyde would not react with tetramethylhydrazine, but, to our knowledge, this has never been studied.

Trimethylhydrazine would also be an extremely interesting molecule to study. It probably would react rapidly with O_3 and NO_2, and may possibly react with HCHO, but the products formed would depend on the details of the initial reaction, perhaps to a greater extent than those formed from N_2H_4, MMH, and UDMH. For example, if hydrazyl radical formation is involved in the O_3 + hydrazine mechanism, formation of tetramethyltetrazene may occur, but if O-atom transfer occurred, either a stable hydroxylamine or perhaps formaldehyde dimethylhydrazone may be formed. Trimethylhydrazine should also have a relatively straightforward mechanism when reacted with NO_2, as is apparently the case for UDMH.

The reactions of O_3, NO_x, and HCHO with symmetrical dimethylhydrazine should also be studied, though complex mechanisms and a wide variety of products (similar to those from MMH) are expected. Studies of the reactions of these three additional alkylhydrazines would undoubtedly supplement our present understanding of the reactions of the three hydrazines studied in this program, and would be particularly helpful in reducing the number of possible alternative mechanisms.

4.2.2 Effect of O_2 on Gas Phase Reactions of the Hydrazines

The exploratory hydrazine + O_3 experiment conducted in N_2 rather than air turned out to be useful in elucidating the role of O_2 in that mechanism. If a wider variety of such experimental data became available, involving varying O_2 levels, radical traps, initial reactant ratios, etc., it might be possible to develop an unambiguous mechanism for the O_3 + N_2H_4 system. Such experiments should be carried out not only for N_2H_4, but for all five of the above-named alkylhydrazines as well. For UDMH, TMH, and TTMH, one might expect no effect for O_2, but this needs to be experimentally verified.

The effect of reduced O_2 levels on the hydrazine + NO_2 and the hydrazine + formaldehyde systems should also be investigated. One would expect O_2 to have a significant effect on the reactions of NO_2 with N_2H_4, MMH, and SDMH, but not on the NO_2 + UDMH and NO_2 + TMH systems or the reactions of formaldehyde with the hydrazines; however, experimental verification is needed.

4.2.3 Additional Tracer and Radical Trap Experiments

The role of radicals in the NO_2 + hydrazine systems is highly uncertain, and could be elucidated by experiments to determine the effects of radical traps and to measure radical levels by the use of tracers. (Tracer experiments may be more difficult in the hydrazine + NO_2 studies than in the hydrazine + O_3 systems, because OH radical levels are expected to be suppressed in the NO_2 experiment by their rapid reactions with NO_2 and, if present, NO and thus may not be easy to measure.) It would be particularly useful to determine if the radical trap suppresses the formation of the hydrazinium nitrates, as might be expected if HNO_3 is formed from OH + NO_2.

It would also be useful to perform radical trap and tracer experiments to rule out the possible role of radicals in the hydrazine + formaldehyde systems.

4.2.4 Atmospheric Reactions of Diazo Compounds

Diazo compounds, such as diazene, methyldiazene, diazomethane, etc., are observed intermediates in the reaction of the hydrazines with O_3 and NO_x, and most of the uncertainties concerning those systems involve reactions of these intermediates. It is difficult to elucidate unambiguously their reaction mechanisms when they are formed from other species,

147

since their reactions are secondary processes; they should be studied by themselves in the absence of the hydrazines and other hydrazine oxidation products. In particular, the mechanisms and products of the reactions of diazene, methyldiazene and diazomethane with OH radicals, O_3, and NO_2 should be studied for a variety of initial reactant concentrations, at various levels of O_2, and (for the O_3 and NO_2 reactions) in the presence of tracers or radical traps.

4.2.5 Additional Studies of the Reactions of Hydrazines with Formaldehyde and Other Oxygenates

The mechanisms for the reactions of the hydrazines with formaldehyde are highly uncertain, and additional studies are required to elucidate them and to determine whether the hydrazines also react with other oxygenates such as acetaldehyde, glyoxal, acetone, formic acid, etc. Some of the studies mentioned above, i.e., radical trap, tracer, variable O_2 runs, studies with other hydrazines, etc., may be useful in this regard, but probably will not be sufficient. At a minimum, the possibility that these reactions are surface-dependent must be investigated by varying the nature of the reaction vessel and the surface/volume ratio. The effect of varying the relative humidity should also be investigated.

4.2.6 Studies of the Products Formed in the Reactions of Nitramines with Hydroxyl Radicals

The results of our studies indicate that the major atmospheric fate of dimethylnitramine, a relatively long-lived oxidation product of UDMH, is via reaction with the hydroxyl radical. However, due to the complicated chemical system employed in the OH + dimethylnitramine rate constant experiment, it was not possible to obtain reliable identities of the products specific to that reaction. Such products must be known before the ultimate atmospheric impact of releases of UDMH and similar compounds can be assessed.

4.2.7 Rate Constant Measurements

The above recommendations concern primarily mechanistic and product studies. However, to obtain more quantitative information regarding these systems, and to eventually be able to predictively model the atmospheric impacts of releases of these compounds, the rate constants of the individual reactions, particularly those which compete with other

148

processes, must be measured. Whenever possible, the rate constants should be measured as a function of temperature, so the Arrhenius parameters can be determined. In this regard, it would be of interest to know whether the $O_3 + N_2H_4$ reaction has an A-factor which is anomalously low, like that for $O_3 + HO_2$, which may or may not be an analogous process (see Section 3.3.6.7).

A partial list of reactions for which kinetic information needed are:

1) Absolute rate constants of the elementary reactions of hydrazine and all five methylhydrazines with O_3 and NO_2 still need to be determined. Experience with this program has shown that it is difficult to eliminate secondary reactions, and novel techniques should be devised.

2) Rate constants for reactions of hydrazyl radicals, both unsubstituted and methyl-substituted, with O_2, NO, NO_2, HO_2, and with themselves need to be determined. If it is not feasible to do absolute rate constant measurements, relative rate constants may be sufficient for kinetic model development.

3) It would be of interest to determine the rate constant for the reactions of HO_2 with the hydrazines and their various diazo intermediates. If such reactions, which are expected to be exothermic, are important, the O_3 + hydrazine mechanisms would be completely different than those proposed in this and our previous reports.

4) The absolute rate constants for the reactions of OH and O_3 with diazo compounds should be measured in systems less likely to have secondary reactions than those employed in this study.

5) A better determination of the OH + N-nitrosodimethylamine rate constant than that reported in Section 3.7.2 would be of interest for theoretical reasons.

6) Also of theoretical interest would be the rate constants for the gas phase reactions of HNO_3 with the hydrazines (and indeed with other amines). In terms of atmospheric implications, the relative rate constants for the reactions of MMH and UDMH with O_3 and HNO_3 should be determined. Since reactions of these hydrazines with both O_3 and HNO_3 are too fast to measure in our system, it is unclear which will be more important in consuming these hydrazines if they are emitted into a polluted atmosphere containing both species.

149

4.2.8 Health Effects

The hydrazines themselves and some of their oxidation products observed in this study are already known to be highly toxic. The formation of a nitrosamine, a known carcinogen, from UDMH is of particular concern. However, the health effects of some other products are not as well characterized. In particular, more studies of the health effects of nitramines are indicated, since our experiments have shown that these compounds have significantly longer atmospheric lifetimes than the hydrazines themselves or their more toxic, but also more labile, products.

4.2.9 Summary of Recommendations

The preceeding list of suggested research topics, which is by no means exhaustive, clearly represents a major research effort which would take a number of years to complete. Indeed, when compared with this list of research tasks, the efforts described in this and our previous report (Reference 3), although substantial, must be considered relatively modest. However, the results of these proposed studies would have significance far beyond our present concern for the atmospheric impacts of the releases of the hydrazine fuels currently in use. Specifically, the resulting improvement in our understanding of the fundamental gas phase chemistry of these and related labile nitrogen-containing compounds would represent a significant advance in our ability to predict the gas phase reactions of a wide variety of chemical systems. These would include many which have not been previously studied, but which may be of scientific, economic or military importance, as well as those systems, such as the atmospheric reactions of hydrazine fuels, which must be adequately understood if we are to protect the environment and human health.

REFERENCES

1. Aerospace Medical Research Laboratory. *Proceedings of the Fourth Annual Conference on Environmental Toxicology*, NTIS AD-781, Paper Nos. 18 and 25-27. Fairborn, Ohio: Aerospace Medical Research Laboratory, December 1973.

2. International Agency for Research on Cancer. *Evaluation of Carcinogenic Risk of Chemicals to Man*. Lyon, Vol. 4. International Agency for Research on Cancer, 1974.

3. Pitts, J. N., Jr.; Tuazon E. C.; Carter, W. P. L.; Winer, A. M.; Harris, G. W.; Atkinson, R.; and Graham, R. A. *Atmospheric Chemistry of Hydrazines: Gas Phase Kinetics and Mechanistic Studies*. Final Report ESL-TR-80-39. Tyndall AFB, Florida: Air Force Eng. Services Ctr., August 1980.

4. Stone, D. A. *The Autoxidation of Hydrazine Vapor*. Report No. CEEDO-TR-78-17, Tyndall AFB, Florida: Air Force Syst. Command, Civ. Environ. Eng. Dev. Off., January 1978.

5. Stone, D. A. *The Autoxidation of Monomethylhydrazine Vapor*. Report No. ESL-TR-79-10. Tyndall AFB, Florida: Air Force Eng. Services Ctr., April 1979.

6. Stone, D. A. *The Vapor Phase Autoxidation of Unsymmetrical Dimethylhydrazine and 50-Percent Unsymmetrical Dimethylhydrazine-50-Percent Hydrazine Mixtures*. Report No. ESL-TR-80-21. Tyndall AFB, Florida: Air Force Eng. Services Ctr., April 1980.

7. Harris, G. W.; Atkinson, R.; and Pitts, J. N., Jr. "Kinetics of the Reactions of the OH Radical with Hydrazine and Methylhydrazine," *J. Phys. Chem.*, 83, 2557. 1979.

8. Jeong, K. M., and Kaufman, F. "Rates of the Reactions of 1,1,1-Trichloroethane (Methylchloroform) and 1,1,2-Trichloroethane with OH," *Geophys. Res. Lett.*, 6, 757. 1979.

9. Singh, H. B.; Ludwig, F. L.; and Johnson, W. B. "Tropospheric Ozone: Concentrations and Variabilities in Clean Remote Atmospheres," *Atmos. Environ.*, 12, 2185. 1978.

10. Tuazon, E. C.; Carter, W. P. L.; Winer, A. M.; and Pitts, J. N., Jr. "Reactions of Hydrazines with Ozone under Simulated Atmospheric Conditions," *Environ. Sci. Technol.*, 15, 823. 1981.

11. Doyle, G. J.; Bekowies, P. J.; Winer, A. M.; and Pitts, J. N., Jr. "Charcoal-Adsorption Air Purification System for Chamber Studies Investigating Atmospheric Photochemistry," *Environ. Sci. Technol.*, 11, 45. 1977.

12. Emmons, W. D. "Peroxytrifluoroacetic Acid. I. The Oxidation of Nitrosamines to Nitramines," *J. Amer. Chem. Soc.*, 76, 3468. 1954.

13. Stephens, E. R. "The Formation, Reactions, and Properties of Peroxyacyl Nitrates (PANs) in Photochemical Air Pollution," _Adv. Environ. Sci. Technol._, 1, 119. 1969.

14. Atkinson, R.; Aschmann, S. M.; Winer, A. M.; and Pitts, J. N., Jr. "Rate Constants for the Reaction of OH Radicals with a Series of Alkanes and Alkenes at 299 ± 2 K," _Int. J. Chem. Kinet._, 14, 507. 1982.

15. Atkinson, R.; Aschmann, S. M.; Winer, A. M.; and Pitts, J. N., Jr. "Rate Constants for the Gas Phase Reactions of O_3 with a Series of Carbonyls at 296 K," _Int. J. Chem. Kinet._, 13, 1133. 1981.

16. Lindley, C. R. C. _The Kinetics of Dimethylamino Radical Reactions in Simulated Atmospheres: The Formation of Dimethylnitrosamine and Dimethylnitramine._ Ohio State University, 1978.

17. Graham, R. A.; Winer, A. M.; and Pitts, J. N., Jr. "Temperature Dependence of the Unimolecular Decomposition of Pernitric Acid and its Atmospheric Implications," _Chem. Phys. Lett._, 51, 215. 1977.

18. Hanst, P. L.; Wilson, W. E.; Patterson, R. K.; Gay, B. W., Jr.; Chaney, L. W.; and Burton, C. S. _A Spectroscopic Study of California Smog._ EPA Publication No. 650/4-75-0006. Research Triangle Park, North Carolina: EPA, 1975.

19. Urry, W. H.; Olsen, A. L.; Bens, E. M.; Kruse, H. W.; Ikoku, C.; and Gaibel, Z. _Autoxidation of 1,1-Dimethylhydrazine._ NAVWEPS Report 8798 (NOTS-TP-3903), CFSTI AD622785, September 1965.

20. Calvert, J. G.; Chan, W. H.; Niple, E.; Nordstrom, R. J.; Shaw, J. H.; Skinner, W. R.; and Uselman, W. M. _Application of Fourier Transform Spectroscopy to Air Pollution Problems._ Report to EPA Grant No. R803868-1, April 1976.

21. McAfee, J. M.; Stephens, E. R.; Fitz, D. R.; and Pitts, J. N., Jr. "Infrared Absorptivity of the 9.6 μm Ozone Band as a Function of Spectral Resolution and Abundance," _J. Quant. Spectrosc. Radiat. Transfer_, 16, 829. 1976.

22. Pitts, J. N., Jr.; McAfee, J. M.; Long, W. D.; and Winer, A. M. "Long-Path Infrared Spectroscopic Investigation at Ambient Concentrations of the 2% Neutral Buffered Potassium Iodide Method for Determination of Ozone," _Environ. Sci. Tech._, 10, 787. 1976.

23. Bell, R. J. _Introductory Fourier Transform Spectroscopy._ New York: Academic Press, 1972.

24. Niki, H.; Maker, P. D.; Savage, C. M.; and Breitenbach, L. P. "FTIR Spectroscopic Observation of Peroxyalkyl Nitrates Formed via ROO + NO_2 → $ROONO_2$," _Chem. Phys. Lett._, 55, 289. 1978.

25. Bowen, E. J., and Birley, A. W. "The Vapor Phase Reaction Between Hydrazine and Oxygen," _Trans. Faraday Soc._, 47, 580. 1951.

26. Stone, D. A. Private Communication. 1980.

27. Vernot, E. H.; MacEwen, J. D.; Geiger, D. L.; and Haun, C. C. "The Air Oxidation of Monomethylhydrazine," Amer. Ind. Hyg. Ass. J., 28, 343. 1967.

28. Stone, D. A. Autoxidation of Hydrazine, Monomethylhydrazine, and Unsymmetrical Dimethylhydrazine. Proceedings of the 1981 International Conference on Fourier Transform Infrared Spectroscopy. SPIE Vol. 289. 1981.

29. Loper, G. L. Gas Phase Kinetic Study of Air Oxidation of UDMH. Proc. Conf. Environ. Chem. Hydrazine Fuels 1977, CEEDO-TR-78-14. 1978.

30. Smith, P. A. S. Open-Chain Nitrogen Compounds. New York: W. A. Benjamin, Inc., Vol. I 1965 and Vol. II 1966.

31. Bellerlay, J. M. "The Autoxidation of Hydrazine and Alkyl Substituted Hydrazine Vapours." Memorandum 92, Propellants, Explosives and Rocket Motor Establishment. Westcott, Aylesbury, Bucks, December 1979.

32. Atkinson, R.; Aschmann, S. M.; Carter, W. P. L.; Winer, A. M.; and Pitts, J. N., Jr. "Kinetics of the Reactions of OH Radicals with n-Alkanes at 299 ± 2 K," Int. J. Chem. Kinet., in press. 1982.

33. Greiner, N. R. "Hydroxyl Radical Kinetics by Kinetic Spectroscopy. VI. Reactions with Alkanes in the Range 300-500°K," J. Chem. Phys., 53, 1070. 1970.

34. Nibler, J. A., and Bondybey, V. E. "Vibrational Potential Function for Diimide, HNNH," J. Chem. Phys., 60, 1307. 1974.

35. Trombetti, A. "Infrared Spectra of Solid Diimide, N_2H_2, and Deuteriodi-imide, N_2D_2," J. Chem. Soc. A, 1086. 1971.

36. Blau, E. J., and Hochheimer, B. F. "Infrared Spectrum and Structure of Diimide," J. Chem. Phys. 41, 1174. 1964.

37. Neudorfl, P. S.; Back, R. A.; and Douglas, A. E. "The Absorption Spectrum of Trans-Diimide in the Vacuum Ultraviolet Region," Can. J. Chem., 59, 506. 1981.

38. Wiberg, N.; Fischer, G.; and Bachhuber, H. "Darstellung, Struktur und Thermolyse von Diimin," Chem. Ber., 107, 1456. 1974.

39. Carter, W. P. L.; Tuazon, E. C.; Winer, A. M.; and Pitts, J. N., Jr. "Gas Phase Reactions of N,N-Dimethylhydrazine with Ozone and NO_x in Simulated Atmospheres," N-Nitroso Compounds, ACS Symposium Series No. 174. 1981.

40. Atkinson, R., and Lloyd, A. C. Evaluation of Kinetic and Mechanistic Data for Modeling of Photochemical Smog, ERT Document No. P-A040. Westlake Village, California: Environmental Research and Technology Inc., July 1980.

41. Benson, S. W. Thermochemical Kinetics. 2nd Ed. New York: John Wiley and Sons, 1976.

42. Foner, S. N., and Hudson, R. L. "Mass Spectrometric Detection of Triazene and Tetrazene and Studies of the Free Radicals NH_2 and N_2H_3," J. Chem. Phys., 29, 442. 1958.

43. Dibeler, V. H., Franklin, J. L.; and Reese, R. M. "Electron Impact Studies of Hydrazine and the Methyl-Substituted Hydrazines," J. Am. Chem. Soc., 81, 68. 1959.

44. Kondratiev, V. N. Rate Constants of Gas Phase Reactions. NSRDS COM-72-10014. January, 1972.

45. Slagle, I. R.; Dudich, J. F.; and Gutman, D. "Identification of Reactive Routes in the Reactions of Oxygen Atoms with Methylamine, Dimethylamine, Trimethylamine, Ethylamine, Diethylamine, and Triethlamine," J. Phys. Chem., 83, 3065. 1979.

46. Foner, S. N., and Hudson, S. L. "Mass Spectrometric Studies of Atom-Molecule Reactions using High-Intensity Crossed Molecular Beams," J. Chem. Phys., 53, 4377. 1970.

47. Su, F.; Calvert, J. G.; and Shaw, J. H. "Mechanism of the Photooxidation of Gaseous Formaldehyde," J. Phys. Chem., 83, 3185. 1979.

48. Hampson, R. F., Jr. Chemical Kinetics and Photochemical Data Sheets for Atmospheric Reactions. Report No. FAA-EE-80-17. U. S. Dept. of Transportation, April 1980.

49. Saad, M. A.; Detweiler, M. B.; and Sweeney, M. A. "Analysis of Reaction Products of Nitrogen Tetroxide with Hydrazines under Nonignition Conditions," AIAA Journal, 10, 1073. 1972.

50. Rao, C. N. R. Chemical Applications of Infrared Spectroscopy. New York: Academic Press, 1963.

51. Ackerman, M. N.; Burdge, J. J.; and Craig, N. C. "Infrared Spectra and Vibrational Assignments of trans-CH_3N-NH, CH_3N-ND, CD_3N-ND," J. Chem. Phys., 58, 203. 1973.

52. Edney, E. O.; Spence, J. W.; and Hanst, P. L. "Synthesis and Thermal Stability of Peroxy Alkyl Nitrates," J. Air Poll. Contr. Assoc., 29, 741. 1979.

53. Baird, N. C. "Structure and Decomposition of the Free Radical HNN: An ab initio MO Study," J. Chem. Phys. 62, 300. 1975.

54. Campbell, I. M.; McLaughlin, D. F.; and Handy, B. J. "Rate Constants for Reactions of OH Radicals with Alcohol Vapours at 292 K," _Chem. Phys. Lett._, _38_, 362. 1976.

55. Harris, W. C. "Vibrational Spectra and Structure of Nitrogen Containing Molecules - I. Formaldehyde Dimethylhydrazone," _Spectrochim. Acta_, _31A_, 11. 1975.

56. Atkinson, R.; Carter, W. P. L.; Winer, A. M.; and Pitts, J. N., Jr. "An Experimental Protocol for the Determination of OH Radical Rate Constants with Organics using Methyl Nitrite Photolysis as an OH Radical Source," _J. Air Pollut. Control Assoc._, _31_, 1090. 1981.

57. Taylor, W. D.; Allston, T. D.; Moscato, M. J.; Fazekas, G. B.; Kozlowski, R.; and Takacs, G. A. "Atmospheric Photodissociation Lifetimes for Nitromethane, Methyl Nitrite, and Methyl Nitrate," _Int. J. Chem. Kinet._, _12_, 231. 1980.

58. Jones, R. N., and Thorn, G. D. "The Ultraviolet Absorption Spectra of Aliphatic Nitramines, Nitrosamines, and Nitrates," _Can. J. Research_, _27B_, 828. 1949.

59. Atkinson, R.; Darnall, K. R.; Lloyd, A. C.; Winer, A. M.; and Pitts, J. N., Jr. "Kinetics and Mechanisms of the Reaction of the Hydroxyl Radical with Organic Compounds in the Gas Phase," _Adv. Photochem._, _11_, 375. 1979.

60. Perry, R. A.; Atkinson, R.; and Pitts, J. N., Jr. "Rate Contants for the Reaction of OH Radicals with Dimethyl Ether and Vinyl Methyl Ether over the Temperature Range 299-427°K," _J. Chem. Phys._, _67_, 611. 1977.

61. Pate, C. T.; Atkinson, R.; and Pitts, J. N., Jr. "Rate Constants for the Gas Phase Reaction of Peroxyacetyl Nitrate with Selected Atmospheric Constituents," _J. Environ. Sci. Health_, _A11_, 19. 1976.

62. Hendry, D. G., and Kenley, R. A. "Generation of Peroxy Radicals from Peroxy Nitrates (RO_2NO_2). Decomposition of Peroxyacyl Nitrates," _J. Amer. Chem. Soc._ _99_, 3198. 1977.

63. Cox, R. A., and Roffey, M. J. "Thermal Decomposition of Peroxyacetylnitrate in the Presence of Nitric Oxide," _Environ. Sci. Technol._ _11_, 900. 1977.

64. Carter, W. P. L.; Winer, A. M.; and Pitts, J. N., Jr. "The Effect of Peroxyacetyl Nitrate in the Initiation of Photochemical Smog," _Environ. Sci. Technol._, _15_, 831. 1981.

65. Stockwell, W. R., and Calvert, J. G. "The Near Ultraviolet Absorption Spectrum of Gaseous HONO and N_2O_3," _J. Photochem._, _8_, 193. 1978.

66. Atkinson, R.; Perry, R. A.; and Pitts, J. N., Jr. "Rate Constants for the Reactions of the OH Radical with $(CH_3)_2NH$, $(CH_3)_3N$, and $C_2H_5NH_2$ over the Temperature Range 298-426°K," <u>J. Chem. Phys.</u>, <u>68</u>, 1850. 1978.

67. Geiger, G.; Stafas, H.; Brühlman, U.; and Huber, J. R. "Photo-dissociation of Dimethylnitrosamine," <u>Chem. Phys. Lett.</u>, <u>79</u>, 521. 1981.

68. Lindley, C. R. C.; Calvert, J. G.; and Shaw, J. H. "Rate Studies of the Reactions of the $(CH_3)_2N$ Radical with O_2, NO and NO_2," <u>Chem. Phys. Lett.</u>, <u>67</u>, 57. 1979.

APPENDIX A

DETAILED DATA TABULATIONS FOR THE OZONE + HYDRAZINE CHAMBER EXPERIMENTS

The detailed concentration-time data for the ten environmental chamber experiments in which O_3 was reacted with N_2H_4 are given in Tables A-1 through A-10. The results of these experiments are discussed in detail in Section 3.3.2.

TABLE A-1. REACTANT AND PRODUCT CONCENTRATIONS VS. TIME IN $N_2H_4 + O_3$ DARK REACTION: EXCESS INITIAL HYDRAZINE (T = 22°C, RH = 16%; 3800 ℓ CHAMBER; RES = 1 CM^{-1}, PATHLENGTH = 68.3 M).

Elapsed Time (min)	Concentration (ppm)					Absorbance at 1276.7 cm^{-1} (Q)
	N_2H_4	O_3	H_2O_2	NH_3	N_2O	N_2H_2
-16	18.4			0.09		
-6	18.0			0.12		
0	5.0 (calc'd, 1st injection)					
0.38	15.9	2.44	1.1	0.15	–	0.042
1.38	12.5	0.76	2.9	0.20	–	0.060
2.38	11.6	0.30	3.3	0.21	–	0.052
3.38	11.3	0.08	3.5	0.24	–	0.048
4.38	11.1	–	3.5	0.23	–	0.045
5.38	11.1	–	3.6	0.25	–	0.041
7.78	10.8	–	3.3	0.24	–	0.041
11.0	25.3 (calc'd, 2nd injection)					
11.38	2.36	12.7	5.9	0.45	0.23	0.035
12.38	–	12.1	6.8	0.53	0.29	–
13.38	–	11.9	6.7	0.51	0.30	–
14.38	–	11.8	6.6	0.49	0.32	–
15.38	–	11.8	6.5	0.46	0.30	–
16.38	–	11.7	6.5	0.42	0.31	–
18.78	–	11.6	6.3	0.36	0.32	–

TABLE A-2. REACTANT AND PRODUCT CONCENTRATIONS VS. TIME IN N_2H_4 + O_3 DARK REACTION: ORGANIC TRACERS[a] ADDED; EXCESS HYDRAZINE (T = 20°C, RH = 25%; 3800 ℓ CHAMBER; RES = 1 CM^{-1}, PATHLENGTH = 68.3 M).

Elapsed Time (min)	Concentration (ppm)					Absorbance at 1276.7 cm^{-1} (Q) N_2H_2	Tracer Data	
	N_2H_4	O_3	H_2O_2	NH_3	N_2O		GC Sampling Time (min)	$\ln \frac{[HME]}{[octane]}$
-39	13.5			0.06			-24	-0.323
-8	12.3			0.08			-16	-0.322
0		3.5 (calc'd)						
0.38	11.2	2.07	0.51	0.07	—	0.026		
1.38	9.27	1.01	1.8	0.10	—	0.042		
2.38	8.46	0.45	2.2	0.12	—	0.037	2	-0.286
3.38	8.13	0.23	2.5	0.12	—	0.034		
4.38	8.08	0.10	2.7	0.12	—	0.031		
5.38	7.83	—	2.7	0.13	—	0.029		
7.38	7.61	—	2.7	0.13	—	0.027		
9.38	7.63	—	2.7	0.13	—	0.022	10	-0.284
11.38	7.47	—	2.6	0.13	—	0.023		
15.78	7.24	—	2.4	0.15	—	0.026		
							17	-0.287

[a]Approximately 0.2 ppm each of n-octane and hexamethylethane (HME) injected at t = -31 min.

TABLE A-3. REACTANT AND PRODUCT CONCENTRATIONS VS. TIME IN $N_2H_4 + O_3$
DARK REACTION: EQUIMOLAR REACTANTS (T = 22°C, RH = 16%;
3800 ℓ CHAMBER; RES = 1 CM^{-1}, PATHLENGTH = 68.3 M).

Elapsed Time (min)	Concentration (ppm)					Absorbance at 1276.7 cm^{-1} (Q)
	N_2H_4	O_3	H_2O_2	NH_3	N_2O	N_2H_2
-13	9.31			0.20		
-6	9.16			0.21		
0		10.2 (calc'd)				
0.38	5.17	5.75	1.6	0.29	—	0.038
1.38	1.47	2.86	3.8	0.37	—	0.027
2.38	0.69	2.06	4.2	0.37	—	0.014
3.38	0.50	1.65	4.4	0.39	—	0.008
4.38	0.32	1.52	4.4	0.39	—	0.006
5.38	—	1.33	4.5	0.39	—	0.004
7.38	—	1.24	4.5	0.44	—	—
9.38	—	1.12	4.5	0.43	—	—
11.38	—	1.04	4.4	0.43	—	—
13.38	—	1.00	4.4	0.44	—	—
15.78	—	0.99	4.3	0.45	—	—

TABLE A-4. REACTANT AND PRODUCT CONCENTRATIONS VS. TIME IN N_2H_4 + O_3 DARK REACTION: ORGANIC TRACERS[a] ADDED; EQUIMOLAR REACTANTS (T = 20°C, RH = 26%; 3800 ℓ CHAMBER; RES = 1 CM^{-1}, PATHLENGTH = 68.3 M).

Elapsed Time (min)	Concentration (ppm)					Absorbance at 1276.7 cm^{-1} (Q) N_2H_2	Tracer Data	
	N_2H_4	O_3	H_2O_2	NH_3	N_2O		GC Sampling Time (min)	ln $\frac{[HME]}{[octane]}$
-18	9.96			0.02			-20	-0.157
-5	9.79			0.02			-12	-0.160
0		10.2 (calc'd)						
0.38	6.65	5.48	1.5	0.08	—	0.042		
1.38	2.45	2.69	4.2	0.14	—	0.039		
2.38	1.64	1.67	4.7	0.14	—	0.021		
3.38	1.18	1.27	5.1	0.15	—	0.017	3	0.024
4.38	0.98	1.02	5.2	0.15	—	0.012		
5.38	0.44	0.84	5.3	0.14	—	0.009		
7.38	0.59	0.62	5.4	0.16	—	0.007		
9.38	0.46	0.53	5.4	0.16	—	0.007	10	0.087
11.38	0.43	0.39	5.3	0.16	—	0.005		
13.38	0.28	0.38	5.3	0.17	—	0.005		
15.78	0.27	0.30	5.3	0.17	< 0.05	0.003	17	0.116
20.78	0.17	0.18	5.2	0.16	< 0.05	—	24	0.120

[a]Approximately 0.2 ppm each of n-octane and hexamethylethane (HME) injected at t = -25 min.

TABLE A-5. REACTANT AND PRODUCT CONCENTRATIONS VS. TIME IN $N_2H_4 + O_3$ DARK REACTION: EXCESS OZONE (T = 21°C, RH = 19%; 3800 ℓ CHAMBER; RES = 1 CM^{-1}, PATHLENGTH = 68.3 M).

Elapsed Time (min)	Concentration (ppm)					Absorbance at 1276.7 cm^{-1} (Q) N_2H_2
	N_2H_4	O_3	H_2O_2	NH_3	N_2O	
−20		16.7				
−15		16.6				
0	4.3 (calc'd)					
0.38	0.56	13.0	0.91	0.12	−	0.010
1.38	−	10.8	1.7	0.20	0.03	−
2.38	−	10.8	1.7	0.22	< 0.07	−
3.38	−	10.6	1.7	0.22	0.05	−
4.38	−	10.6	1.6	0.20	0.06	−
5.38	−	10.6	1.6	0.20	0.06	−
7.78	·	10.5	1.5	0.18	0.06	−
11.78	−	10.5	1.5	0.16	0.06	−
15.78	−	10.4	1.5	0.14	0.07	−

TABLE A-6. REACTANT AND PRODUCT CONCENTRATIONS VS. TIME IN N_2H_4 + O_3 DARK REACTION: ORGANIC TRACERS[a] ADDED; EXCESS OZONE (T = 20°C, RH = 23%; 3800 ℓ CHAMBER; RES = 1 CM^{-1}, PATHLENGTH = 68.3 M).

Elapsed Time (min)	Concentration (ppm)					Absorbance at 1276.7 cm^{-1} (Q) N_2H_2	Tracer Data	
	N_2H_4	O_3	H_2O_2	NH_3	N_2O		GC Sampling Time (min)	$\ln \dfrac{[HME]}{[octane]}$
-53		16.3					-34	-0.126
-20		15.9					-15	-0.126
0	4.8 (calc'd)						0	
0.38	1.07	12.2	1.1	0.03	0.04	0.019		
1.38	-	9.07	2.1	0.09	0.05	0.005		
2.38	-	9.02	2.0	0.09	0.05	0.003	2	0.034
3.38	-	8.94	2.0	0.10	0.07	<0.003		
4.38	-	8.96	2.0	0.08	0.06	-		
5.38	-	8.98	1.9	0.08	0.05	-		
6.38	-	8.83	1.9	0.06	0.06	-		
7.38	-	8.91	2.0	0.06	0.07	-		
9.38	-	8.87	1.8	0.04	0.06	--	10	0.141
11.38	-	8.83	1.8	0.03	0.06	-		
19.78	-	8.80	1.7	-	0.07	-	18	0.147

[a]Approximately 0.2 ppm each of n-octane and hexamethylethane (HME) injected at t = -40 min.

TABLE A-7. REACTANT AND PRODUCT CONCENTRATIONS VS. TIME IN $N_2H_4 + O_3$ DARK REACTION: WITH N-OCTANE[a] AS RADICAL TRAP; EXCESS INITIAL HYDRAZINE (T = 22°C, RH = 16%; 3800 ℓ CHAMBER; RES = 1 CM^{-1}, PATHLENGTH = 68.3 M).

Elapsed Time (min)	Concentration (ppm)					Absorbance at 1276.7 cm^{-1} (Q) N_2H_2
	N_2H_4	O_3	H_2O_2	NH_3	N_2O	
-13	17.3			0.40		
-7	17.0			0.43		
0		4.4 (calc'd)				
0.38	15.6	2.77	0.24	0.45	–	0.016
1.38	13.9	1.38	0.72	0.43	–	0.025
2.38	13.2	0.56	0.81	0.47	–	0.021
3.38	12.8	0.26	0.95	0.54	–	0.021
4.38	12.6	0.08	1.1	0.50	–	0.017
5.38	12.5	< 0.07	1.1	0.49	–	0.019
6.38	12.5	–	1.1	0.48	–	0.019
7.38	12.3	–	1.0	0.49	–	0.017
8.38	12.3	–	1.0	0.51	–	0.019
9.38	12.0	–	0.90	0.53	–	0.020
10.38	12.0	–	0.93	0.54	–	0.023
13.78	11.9	–	0.82	0.53	–	0.023
20.0		26.1 (calc'd)				
20.38	7.86	17.8	0.58	0.61	–	0.015
21.38	3.67	13.8	0.70	0.63	–	0.005
22.38	2.01	11.1	0.68	0.66	–	–
23.38	1.31	9.73	0.88	0.66	–	–
24.38	0.76	9.15	0.76	0.68	–	–
25.38	0.54	8.63	0.94	0.65	–	–
28.78	–	7.74	0.90	0.65	–	–

[a]Approximately 270 ppm n-octane was introduced into the chamber before injection of reactants.

TABLE A-8. REACTANT AND PRODUCT CONCENTRATIONS VS. TIME IN $N_2H_4 + O_3$ DARK REACTION: WITH N-OCTANE[a] AS RADICAL TRAP; EQUIMOLAR REACTANTS ($T = 23^\circ C$, RH = 15%; 3800 ℓ CHAMBER; RES = 1 CM^{-1}, PATHLENGTH = 68.3 M).

Elapsed Time (min)	Concentration (ppm) 1276.7 cm^{-1} (Q)					Absorbance at
	N_2H_4	O_3	H_2O_2	NH_3	N_2O	N_2H_2
-16	10.3			-		
-6	10.3			-		
0	10.0 (calc'd)					
0.38	8.75	7.01	0.06	0.08	-	0.007
1.38	6.56	5.04	0.27	0.07	-	0.008
2.38	5.54	3.29	0.26	0.07	-	0.003
3.38	4.91	2.21	0.43	0.09	-	< 0.004
4.38	4.62	1.72	0.39	0.09	-	-
5.38	4.26	1.29	0.53	0.10	-	-
7.38	3.85	0.73	0.53	0.08	-	-
9.38	3.62	0.45	0.57	0.10	-	-
11.38	3.35	0.28	0.56	0.10	-	-
13.38	3.25	0.18	0.54	0.10	-	-
15.38	3.18	0.09	0.57	0.12	-	-
18.78	3.08	-	0.56	0.12	-	-
21.78	3.00	-	0.50	0.11	-	-
24.78	3.00	-	0.50	0.13	-	-
27.78	3.11	-	0.54	0.12	-	-
30.78	2.86	-	0.51	0.15	-	-
33.78	2.77	-	0.46	0.14	-	-

[a]Approximately 270 ppm n-octane was introduced into the chamber before injection of reactants.

TABLE A-9. REACTANT AND PRODUCT CONCENTRATIONS VS. TIME IN N_2H_4 + O_3 DARK REACTION: WITH N-OCTANE[a] AS RADICAL TRAP; EXCESS OZONE (T = 23°C, RH = 15%; 3800 ℓ CHAMBER; RES = 1 CM^{-1}, PATHLENGTH = 68.3 M).

Elapsed Time (min)	Concentration (ppm) 1276.7 cm^{-1} (Q)					Absorbance at
	N_2H_4	O_3	H_2O_2	NH_3	N_2O	N_2H_2
-25	16.7					
-19	16.8					
-12	16.6					
0	4.2 (calc'd)					
0.38	2.32	14.8	–	0.03	–	–
1.38	2.24	12.1	–	0.05	–	0.004
2.38	1.33	10.3	–	0.04	–	< 0.003
3.38	0.85	10.0	< 0.14	0.06	–	< 0.003
4.38	0.59	9.49	–	0.06	–	< 0.003
5.38	0.26	9.06	< 0.20	0.05	–	< 0.003
6.38	< 0.27	8.88	< 0.14	0.06	–	–
7.38	–	8.58	–	0.06	–	–
8.38	–	8.49	–	0.07	–	–
9.38	–	8.37	–	0.07	–	–
10.38	–	8.40	< 0.15	0.07	–	–
12.78	–	8.25	< 0.20	0.06	–	–

[a]Approximately 270 ppm n-octane was introduced into the chamber before injection of reactants.

TABLE A-10. REACTANT AND PRODUCT CONCENTRATIONS VS. TIME IN THE DARK
REACTION OF N_2H_4 WITH O_3 IN N_2 ATMOSPHERE[a]; EQUIMOLAR REACTANTS
(T = 21°C, RH < 10%; 3800 ℓ CHAMBER; RES = 1 CM^{-1}, PATHLENGTH = 68.3 M).

| Elapsed Time (min) | Concentration (ppm) | | | | | | Absorbance at 1276.7 cm^{-1} (Q) N_2H_2 |
	N_2H_4	O_3	H_2O_2	N_2O	HONO	NH_3	
-11		11.7					
-7		11.7					
0	11.7 (calc'd)						
0.38	2.82	3.42	1.1	0.13		0.20	0.045
1.38	3.75	0.23	1.6	0.18	0.22	0.36	0.049
2.38	3.48	–	1.5	0.16	0.18	0.39	0.050
3.38	3.09	–	1.4	0.14	0.16	0.40	0.051
4.38	2.91	–	1.2	0.14	0.10	0.41	0.057
5.38	2.82	–	1.2	0.13	0.14	0.42	0.055
7.38	2.95	–	1.1	0.13	0.25	0.42	0.055
9.38	2.75	–	1.0	0.13	0.17	0.43	0.055
11.38	2.78	–	0.92	0.14	0.15	0.43	0.055
13.38	2.58	–	0.78	0.15	0.17	0.44	0.059
15.38	2.49	–	0.80	0.15	0.21	0.44	0.061
17.78	2.41	–	0.68	0.13	0.16	0.46	0.062
24.78	2.34	–	0.54	0.13	0.18	0.46	0.064

[a]Approximately 1300 ppm O_2 was injected as part of the O_3 sample.

APPENDIX B

DETAILED DATA TABULATIONS FOR THE OZONE + MONOMETHYLHYDRAZINE CHAMBER EXPERIMENTS

The detailed concentration-time data for the nine environmental chamber experiments in which ozone was reacted with MMH are given in Tables B-1 through B-9. The results of these experiments are discussed in Section 3.3.3.

TABLE B-1. REACTANT AND PRODUCT CONCENTRATIONS VS. TIME IN MMH + O_3 DARK REACTION: EXCESS INITIAL MMH (T = 22°C, RH = 14%; 3800 ℓ CHAMBER; RES = 1 CM^{-1}, PATHLENGTH = 68.3 M).

| Elapsed Time (min) | Concentration (ppm) | | | | | | | | | | | Absorbance at 845.2 cm^{-1} (Q) |
	MMH	O_3	CO	HCHO	HCOOH	CH_3OH	CH_3OOH	CH_2N_2	H_2O_2	NH_3	N_2O	CH_3NNH
-10	16.3									0.07		
-5	15.8									0.08		
0	4.21 (calc'd, 1st injection)											
0.38	11.8	–	–	–	–	0.07	1.5	0.25	0.77	0.07	–	0.082
1.38	11.0	–	–	–	–	0.10	1.9	0.64	1.0	0.09	–	0.093
2.38	10.9	–	–	–	–	0.13	1.7	0.73	0.95	0.08	–	0.094
3.38	10.8	–	–	–	–	0.12	1.7	0.74	0.88	0.08	–	0.094
4.38	10.9	–	–	–	–	0.13	1.8	0.75	0.91	0.10	–	0.094
5.38	10.8	–	–	–	–	0.12	1.7	0.75	0.97	0.10	–	0.092
7.38	10.7	–	–	–	–	0.12	2.0	0.74	0.88	0.09	–	0.088
10.38	10.7	–	–	–	–	0.12	2.0	0.76	0.84	0.11	–	0.088
12.78	10.7	–	–	–	–	0.12	2.1	0.75	0.86	0.10	–	0.096
17.0		25.8 (calc'd, 2nd injection)										
17.38	0.54	9.84	0.44	2.8	0.18	1.20	8.4	0.48	2.0	0.18	0.06	0.029
18.38	–	10.9	0.59	3.4	0.22	1.35	8.7	0.20	2.0	0.17	0.09	–
19.38	–	10.9	0.72	3.4	0.23	1.39	8.7	0.10	2.0	0.16	0.12	–
20.38	–	10.8	0.75	3.4	0.23	1.39	8.6	0.04	2.0	0.15	0.14	–
21.38	–	10.6	0.74	3.4	0.24	1.39	8.8	–	2.0	0.13	0.14	–
22.38	–	10.6	0.77	3.6	0.24	1.40	8.9	–	2.0	0.10	0.14	–
24.78	–	10.4	0.80	3.6	0.25	1.42	8.8	–	1.9	0.04	0.14	–
28.78	–	10.4	0.83	3.5	0.25	1.40	8.8	–	1.9	–	0.16	–

169

TABLE B-2. REACTANT AND PRODUCT CONCENTRATIONS VS. TIME IN MMH + O_3 DARK REACTION: ORGANIC TRACERS[a] ADDED; EXCESS MMH
(T = 21°C, RH = 28%; 3800 ℓ CHAMBER; RES = 1 CM⁻¹, PATHLENGTH = 68.3 M).

Elapsed Time (min)	Concentration (ppm)[b]										Absorbance at 845.2 cm⁻¹ (Q) CH_3NNH	Tracer Data	
	MMH	O_3	CO	HCHO	HCOOH	CH_3OH	CH_3OOH	CH_2N_2	H_2O_2	NH_3		GC Sampling Time (min)	$\ln\left(\frac{[HME]}{[octane]}\right)$
-35	18.8									0.16		-20	-0.320
-5	17.8[a]									0.17		-13	-0.321
0		5.1 (calc'd)										0	
0.38	13.0	-	-	-	-	0.11	1.4	0.28	0.82	0.16	0.090		
1.38	11.8	-	0.05	-	-	0.17	1.9	0.67	0.98	0.17	0.101		
2.38	11.8	-	0.04	-	-	0.17	1.7	0.77	0.96	0.17	0.101		
3.38	11.8	-	0.06	-	-	0.17	1.7	0.77	0.96	0.15	0.101	3	-0.308
4.38	11.7	-	0.04	-	-	0.16	2.0	0.79	0.94	0.15	0.099		
5.38	11.7	-	0.04	-	-	0.16	2.1	0.78	0.91	0.17	0.100		
7.78	11.7	-	0.04	-	-	0.16	2.2	0.79	0.96	0.17	0.102		
12.78	11.7	-	0.04	-	-	0.16	2.2	0.79	0.92	0.17	0.100	10	-0.306
17.78	11.5	-	0.04	-	< 0.01	0.16	2.5	0.79	0.89	0.18	0.098	17	-0.308

[a] Approximately 0.2 ppm each of n-octane and hexamethylethane (HME) injected at t = -28 min.

[b] N_2O levels below detection limit (0.04 ppm) in this experiment.

TABLE B-3. REACTANT AND PRODUCT CONCENTRATIONS VS. TIME IN MMH + O_3 DARK REACTION: EQUIMOLAR REACTANTS (T = 23°C, RH = 14%; 3800 ℓ CHAMBER; RES = 1 CM^{-1}, PATHLENGTH = 68.3 M).

| Elapsed Time (min) | Concentration (ppm) | | | | | | | | | | | Absorbance at 845.2 cm^{-1} (Q) |
	MMH	O_3	CO	HCHO	HCOOH	CH_3OH	CH_3OOH	CH_2N_2	H_2O_2	NH_3	N_2O	CH_3NNH
-10	8.87									0.13		
-4	8.88									0.14		
0	9.5 (calc'd, 1st injection)											
0.38	1.64	0.54	0.05	0.82	0.03	0.32	3.4	0.49	1.0	0.17	-	0.080
1.38	-	-	0.14	1.2	0.06	0.48	4.6	0.94	1.3	0.17		0.067
2.38	-	-	0.20	1.2	0.06	0.50	4.6	0.98	1.3	0.17		0.060
3.38	-	-	0.21	1.2	0.06	0.52	4.7	0.97	1.3	0.16	< 0.04	0.056
4.38	-	-	0.20	1.2	0.05	0.53	4.9	0.99	1.3	0.17		0.055
5.36	-	-	0.19	1.1	0.06	0.51	4.8	0.99	1.3	0.17		0.053
7.78	-	-	0.21	1.2	0.06	0.53	4.8	1.0	1.3	0.17	< 0.04	0.053
12.0	9.5 (calc'd, 2nd injection)											
12.38	-	-	0.22	1.7	0.07	0.64	5.3	0.34	1.4	0.18	-	0.008
13.38	-	-	0.35	2.0	0.08	0.66	5.5	0.09	1.3	0.16		-
14.38	-	-	0.41	1.9	0.08	0.67	5.2	0.04	1.3	0.16		-
15.38	-	-	0.43	1.9	0.09	0.66	5.3	-	1.2	0.15	< 0.04	-
16.38	-	-	0.42	1.8	0.08	0.66	5.2	-	1.2	0.14		-
17.38	-	-	0.45	1.9	0.08	0.68	5.4	-	1.3	0.11		-
19.78	-	-	0.47	1.9	0.09	0.67	5.4	-	1.2	0.10	< 0.05	-

171

171

TABLE B-4. REACTANT AND PRODUCT CONCENTRATIONS VS. TIME IN MMH + O_3 DARK REACTION: ORGANIC TRACERS[a] ADDED; EQUIMOLAR REACTANTS (T ~ 21°C, RH = 28%; 3800 ℓ CHAMBER; RES = 1 CM^{-1}, PATHLENGTH = 68.3 M).

Elapsed Time (min)	Concentration (ppm)[b]										Absorbance at 845.2 cm^{-1} (Q) CH_3MMH	Tracer Data	
	MMH	O_3	CO	HCHO	HCOOH	CH_3OH	CH_3OOH	CH_2N_2	H_2O_2	NH_3		GC Sampling Time (min)	$\ln\left\{\frac{[HME]}{[octane]}\right\}$
-23	10.1									0.04		-24	0.087
-7	10.0									0.04		-7	0.088
0	10.3 (calc'd)											0	
0.38	2.20	0.60	0.09	0.62	0.03	0.30	3.3	0.49	1.1	0.06	0.089		
1.38	0.26	–	0.14	1.3	0.05	0.52	4.9	1.1	1.5	0.08	0.075		
2.38	–	–	0.17	1.1	0.06	0.55	4.8	1.1	1.5	0.07	0.073	2	0.203
3.38	–	–	0.15	1.4	0.05	0.56	5.0	1.1	1.5	0.07	0.072		
4.38	–	–	0.17	1.3	0.05	0.52	4.8	1.1	1.4	0.08	0.066		
5.38	–	–	0.15	1.2	0.05	0.56	5.0	1.1	1.5	0.07	0.068		
7.78	–	–	0.16	1.1	0.05	0.56	5.1	1.1	1.4	0.08	0.064		
12.78	–	–	0.16	1.1	0.06	0.56	5.0	1.1	1.4	0.08	0.068	9	0.207
17.78	–	–	0.16	1.1	0.05	0.57	5.0	1.1	1.4	0.08	0.065	15	0.207

[a] Approximately 0.2 ppm each of n-octane and hexamethylethane (HME) injected at t = -28 min.

[b] N_2O levels below detection limit (0.04 ppm) in this experiment.

TABLE B-5. REACTANT AND PRODUCT CONCENTRATIONS VS. TIME IN MMH + O_3 DARK REACTION: EXCESS OZONE (T = 23°C, RH = 14%; 3800 ℓ CHAMBER; RES = 1 CM^{-1}; PATHLENGTH = 68.3 M).

Elapsed Time (min)	Concentration (ppm)											Absorbance at 845.2 cm^{-1} (Q)
	MMH	O_3	CO	HCHO	HCOOH	CH_3OH	CH_3OOH	CH_2N_2	H_2O_2	NH_3	N_2O	CH_3NNH
-18		15.3										
-12		15.1										
0	4.0 (calc'd)											
0.38	–	10.5	–	1.1	0.02	0.31	2.3	0.08	0.39	0.04	–	–
1.38	–	9.75	0.19	1.4	0.03	0.38	2.7	–	0.54	0.03	–	–
2.38	–	9.91	0.33	1.3	0.03	0.37	2.6	–	0.56	0.05	–	–
3.38	–	9.89	0.31	1.3	0.03	0.38	2.6	–	0.52	0.01	–	–
4.38	–	9.91	0.31	1.3	0.03	0.38	2.5	–	0.49	–	–	–
5.38	–	9.86	0.32	1.2	0.03	0.36	2.5	–	0.54	–	–	–
7.78	–	9.72	0.33	1.3	0.03	0.36	2.5	–	0.51	–	< 0.04	–

TABLE B-6. REACTANT AND PRODUCT CONCENTRATIONS VS. TIME IN MMH + O_3 DARK REACTION: ORGANIC TRACERS[a] ADDED; EXCESS OZONE (T = 23°C, RH = 20%; 3800 ℓ CHAMBER; RES = 1 CM^{-1}, PATHLENGTH = 68.3 M).

Elapsed Time (min)	Concentration (ppm)[b]										Absorbance at 845.2 cm^{-1} (Q) CH$_3$NNH	Tracer Data	
	MMH	O_3	CO	HCHO	HCOOH	CH$_3$OH	CH$_3$OOH	CH$_2$N$_2$	H$_2$O$_2$	NH$_3$		GC Sampling Time (min)	$\ln\left\{\dfrac{[HME]}{[octane]}\right\}$
-69		16.0											
-50		16.0										-23	0.069
-11		15.4										-14	0.079
0	4.9 (calc'd)											0	
0.38	–	9.83	0.27	1.2	0.03	0.33	2.4	0.16	0.45	0.09	–		
1.38	–	9.15	0.36	1.5	0.06	0.40	2.7	0.10	0.56	0.11	–		
2.38	–	9.13	0.37	1.5	0.04	0.38	2.3	0.06	0.50	0.13	–		
3.38	–	9.03	0.40	1.6	0.04	0.40	2.5	–	0.52	0.13	–		
4.38	–	9.05	0.40	1.5	0.05	0.42	2.5	–	0.52	0.13	–	4	0.444
5.38	–	9.12	0.41	1.5	0.05	0.40	2.4	–	0.54	0.14	–		
7.78	–	9.04	0.43	1.6	0.04	0.38	2.6	–	0.52	0.12	–		
12.78	–	8.91	0.43	1.6	0.05	0.41	2.5	–	0.49	0.11	–	11	0.471
22.78	–	8.75	0.51	1.5	0.05	0.40	2.5	–	0.48	0.07	–	18	0.468

[a]Approximately 0.2 ppm each of n-octane and hexamethylethane (HME) injected at t = -79 min.

[b]N$_2$O levels below detection limit (0.04 ppm) in this experiment.

174

TABLE B-7. REACTANT AND PRODUCT CONCENTRATIONS VS. TIME IN MMH + O_3 DARK REACTION: WITH N-OCTANE[a] AS RADICAL TRAP; EXCESS INITIAL MMH (T = 22°C, RH = 14%; 3800 ℓ CHAMBER; RES = 1 CM^{-1}, PATHLENGTH = 68.3 M).

| Elapsed Time (min) | Concentration (ppm) | | | | | | | | | | | Absorbance at 845.2 cm^{-1} (Q) |
	MMH	O_3	CO	HCHO	HCOOH	CH_3OH	CH_3OOH	CH_2N_2	H_2O_2	NH_3	N_2O	CH_3NNH
-19	18.7									0.10		
-7	18.9									0.11		
										0.13		
0		4.3 (calc'd)										
0.10*	15.9	0.29	–	0.15	–	0.11	0.49	0.08	0.27	0.09	–	0.039
0.35	14.0	0.18	–	0.51	–	0.16	1.2	0.28	0.53	0.15	–	0.080
0.60	13.7	–	–	0.34	–	0.20	1.5	0.43	0.18	< 0.2	–	0.066
0.85	13.5	–	–	0.59	–	0.22	1.2	0.62	0.45	0.13	–	0.085
1.10	12.9	–	–	0.48	–	0.16	1.6	0.63	0.19	0.11	–	0.065
1.35	13.1	–	–	0.59	–	0.20	1.6	0.74	0.47	< 0.17	–	0.072
1.60	13.3	–	–	0.75	–	0.18	1.6	0.79	0.54	0.14	–	0.082
1.85	12.9	–	–	0.53	–	0.18	1.6	0.79	0.30	< 0.17	–	0.073
2.10*	13.3	–	–	0.48	–	0.22	1.6	0.82	0.51	0.11	–	0.072
3.38	13.2	–	–	0.53	–	0.22	1.8	0.87	0.41	0.10	–	0.076
4.38	13.2	–	–	0.34	–	0.22	1.8	0.86	0.40	0.12	–	0.074
5.38	13.2	–	–	0.29	–	0.22	1.8	0.87	0.36	0.10	–	0.073
7.38	13.1	–	–	0.29	–	0.21	1.9	0.87	0.34	0.13	–	0.073
10.38	13.2	–	–	0.17	–	0.22	2.0	0.87	0.37	0.11	–	0.071
12.78	12.8	–	–	–	–	0.22	1.8	0.87	0.39	0.13	–	0.074

(continued)

TABLE B-7. REACTANT AND PRODUCT CONCENTRATIONS VS. TIME IN MMH + O_3 DARK REACTION: WITH N-OCTANE[a] AS RADICAL TRAP; EXCESS INITIAL MMH (T = 22°C, RH = 14%; 3800 ℓ CHAMBER; RES = 1 CM^{-1}, PATHLENGTH = 68.3 M) (CONCLUDED).

Elapsed Time (min)	Concentration (ppm)											Absorbance at 845.2 cm^{-1} (Q)
	MMH	O_3	CO	HCHO	HCOOH	CH_3OH	CH_3OOH	CH_2N_2	H_2O_2	NH_3	N_2O	CH_3NNH
20.0		24.2 (calc'd)										
20.10*	3.67	6.8	–	3.0	0.04	1.3	3.8	2.1	0.61	0.15	–	0.132
20.35	–	7.8	–	5.0	0.12	2.4	5.7	3.2	0.89	0.18	–	0.039
20.60	–	8.1	–	5.8	0.14	2.5	6.2	3.0	0.95	0.12	–	–
20.85	–	7.8	–	6.0	0.15	2.5	6.2	2.6	0.86	0.15	–	–
21.10	–	7.3	–	5.3	0.13	2.5	4.9	2.4	0.85	0.16	–	–
21.35	–	7.6	–	5.8	0.14	2.5	5.8	2.2	0.80	0.14	–	–
21.60	–	7.0	–	5.7	0.13	2.5	5.4	2.0	0.73	0.15	–	–
21.85	–	7.0		6.2	0.14	2.5	6.6	1.8	0.54	0.15	–	–
22.10*	–	6.5	–	5.8	0.14	2.5	6.2	1.7	0.58	0.16	–	–
23.38	–	7.05	0.07	6.5	0.14	2.60	5.8	1.1	0.75	0.13	–	–
24.38	–	6.72	0.05	6.7	0.14	2.63	5.8	0.77	0.69	0.09	–	–
25.38	–	6.47	0.10	6.7	0.15	2.57	6.0	0.57	0.76	0.09	–	–
27.78	–	6.15	0.09	6.7	0.15	2.62	5.7	0.28	0.75	0.09	–	–
33.78	–	6.02	0.09	6.9	0.16	2.64	5.7	0.05	0.79	0.03	–	–

[a] Approximately 270 ppm n-octane was introduced into the chamber before injection of reactants.
[b] Pairs of asterisks bracket the data recorded every 15 sec (6 scans, 1 cm^{-1} resolution).

176

TABLE B-8. REACTANT AND PRODUCT CONCENTRATIONS VS. TIME IN MMH + O$_3$ DARK REACTION: WITH N-OCTANE[a] AS RADICAL TRAP; EQUIMOLAR REACTANTS (T = 24°C, RH = 14%; 3800 ℓ CHAMBER; RES = 1 CM^{-1}, PATHLENGTH = 68.3 M).

Elapsed Time (min)	Concentration (ppm)											Absorbance at 845.2 cm^{-1} (Q)
	MMH	O$_3$	CO	HCHO	HCOOH	CH$_3$OH	CH$_3$OOH	CH$_2$N$_2$	H$_2$O$_2$	NH$_3$	N$_2$O	CH$_3$NNH
-10	9.73									0.07		
-6	9.57									0.07		
0		9.5 (calc'd)										
0.10*	6.5	1.4	–	0.71	–	0.23	0.99	0.10	0.14	0.10	–	0.055
0.35	2.3	0.48	–	1.3	0.03	0.63	2.7	1.3	0.26	0.07	–	0.091
0.60	1.8	0.13	–	1.1	0.03	0.69	2.8	2.0	0.19	0.11	–	0.101
0.85	1.7	–	–	1.4	0.03	0.73	2.3	2.1	0.35	0.06	–	0.094
1.10	1.4	–	–	1.2	0.03	0.73	2.3	2.1	0.34	0.10-	–	0.093
1.35	1.4	–	–	1.7	0.02	0.75	3.1	2.2	0.14	0.10	–	0.085
1.60	1.4	–	–	1.5	0.03	0.74	2.2	2.1	0.39	0.12	–	0.090
1.85	1.2	–	–	1.6	0.03	0.73	2.6	2.2	0.34	0.12	–	0.089
2.10*	1.3	–	–	1.6	0.02	0.71	3.4	2.2	0.33	0.12	–	0.085
3.38	1.19	–	–	1.5	0.03	0.75	2.8	2.2	0.31	0.09	–	0.084
4.38	1.11	–	–	1.3	0.03	0.74	2.5	2.2	0.33	0.09	–	0.084
5.38	1.13	–	–	1.5	0.03	0.77	2.9	2.2	0.33	0.09	–	0.079
7.78	0.94	–	–	1.4	0.03	0.74	2.9	2.2	0.23	0.10	–	0.081

(continued)

TABLE B-8. REACTANT AND PRODUCT CONCENTRATIONS VS. TIME IN MMH + O_3 DARK REACTION: WITH N-OCTANE[a] AS RADICAL TRAP; EQUIMOLAR REACTANTS (T = 24°C, RH = 14%; 3800 ℓ CHAMBER; RES = 1 CM^{-1}, PATHLENGTH = 68.3 M) (CONCLUDED).

| Elapsed Time (min) | Concentration (ppm) | | | | | | | | | | | Absorbance at 845.2 cm^{-1} (Q) CH$_3$NNH |
	MMH	O_3	CO	HCHO	HCOOH	CH$_3$OH	CH$_3$OOH	CH$_2$N$_2$	H$_2$O$_2$	NH$_3$	N$_2$O	
12.0		9.5 (calc'd)										
12.10*	0.43	4.5	–	1.5	0.05	0.85	3.3	2.1	0.45	0.13	–	0.066
12.35	–	6.4	–	2.0	0.05	1.2	4.0	2.0	0.50	0.13	–	0.024
12.60	–	6.6	–	2.9	0.05	1.2	3.7	1.9	0.44	0.08	–	–
12.85	–	6.2	–	2.8	0.04	1.2	3.9	1.8	0.27	0.13	–	–
13.10	–	6.2	–	3.1	0.04	1.3	3.5	1.6	0.57	0.11	–	–
13.35	–	6.0	0.07	3.2	0.04	1.3	3.9	1.5	0.39	0.14	–	–
13.60	–	6.0	0.08	2.9	0.05	1.3	3.3	1.5	0.41	0.09	–	–
13.85	–	5.9	0.03	3.1	0.05	1.3	3.1	1.3	0.46	0.09	–	–
14.10*	–	5.9	0.02	3.2	0.05	1.3	3.7	1.2	0.39	0.09	–	–
15.38	–	5.87	0.07	3.4	0.05	1.31	3.5	0.87	0.26	0.09	–	–
16.38	–	5.85	0.08	3.7	0.05	1.34	3.3	0.65	0.20	0.10	–	–
17.38	–	5.72	0.06	3.8	0.05	1.31	3.5	0.49	0.23	0.09	–	–
19.78	–	5.51	0.08	3.7	0.05	1.31	3.3	0.26	0.31	0.09	–	–
23.78	–	5.27	0.09	3.8	0.05	1.32	3.6	0.10	0.30	0.07	–	–
28.78	–	5.13	0.10	3.9	0.06	1.32	3.6	0.04	0.37	0.06	–	–

[a]Approximately 270 ppm n-octane was introduced into the chamber before injection of reactants.
[b]Pairs of asterisks bracket the data recorded every 15 sec (6 scans, 1 cm^{-1} resolution).

TABLE B-9. REACTANT AND PRODUCT CONCENTRATIONS VS. TIME IN MMH + O_3 DARK REACTION: WITH N-OCTANE[a] AS RADICAL TRAP; EXCESS OZONE (T = 24°C, RH = 14%; 3800 ℓ CHAMBER; RES = 1 CM^{-1}, PATHLENGTH = 68.3 M).

Elapsed Time (min)	Concentration (ppm)											Absorbance at 845.2 cm^{-1} (Q)
	MMH	O_3	CO	HCHO	HCOOH	CH_3OH	CH_3OOH	CH_2N_2	H_2O_2	NH_3	N_2O	CH_3NNH
-15		17.6										
-8		17.5										
0	4.5 (calc'd)											
0.10*	-	13.9	0.08	0.47	-	0.22	1.3	0.18	0.11	0.05	-	-
0.35	-	9.9	0.12	1.9	0.03	0.76	1.5	1.1	0.30	0.03	-	-
0.60	-	9.3	0.05	2.2	0.02	0.88	1.6	0.99	0.25	-	-	-
0.85	-	8.8	0.09	2.6	0.02	0.89	1.1	0.89	0.30	-	-	-
1.10	-	9.0	0.11	2.6	0.03	0.93	1.4	0.80	0.36	-	-	-
1.35	-	8.9	0.09	2.2	0.03	0.86	1.0	0.73	0.28	-	-	-
1.60	-	8.9	0.08	2.4	0.03	0.78	2.1	0.66	0.33	-	-	-
1.85	-	8.9	0.11	2.6	0.02	0.86	1.5	0.61	0.25	< 0.05	-	-
2.10*	-	8.8	0.07	2.3	0.03	0.84	1.5	0.53	0.26	-	-	-
3.38	-	8.91	0.18	2.4	0.03	0.86	1.2	0.32	0.28	-	-	-
4.38	-	8.69	0.22	2.2	0.03	0.85	1.2	0.20	0.29	-	-	-
5.38	-	8.76	0.21	2.4	0.03	0.88	1.2	0.12	0.23	-	-	-
7.78	-	8.68	0.20	2.2	0.03	0.88	1.1	0.04	0.25	< 0.03	-	-

[a]Approximately 270 ppm n-octane was introduced into the chamber before injection of reactants.
[b]Asterisks indicate the span of data recorded every 15 sec (6 scans, 1 cm^{-1} resolution).

179

APPENDIX C

DETAILED DATA TABULATIONS FOR THE OZONE + UNSYMMETRICAL
DIMETHYLHYDRAZINE CHAMBER EXPERIMENTS

The detailed concentration-time data for the seven environmental chamber experiments in which ozone was reacted with UDMH are given in Tables C-1 through C-7. The results of these experiments are discussed in Section 3.3.4.

TABLE C-1. REACTANT AND PRODUCT CONCENTRATIONS VS. TIME IN UDMH + O_3 DARK REACTION: EXCESS INITIAL UDMH (T = 24°C, RH = 11%; 6400 l CHAMBER; RES = 1 CM⁻¹, PATHLENGTH = 102.4 M).

Elapsed Time (min)	Concentration (ppm)[a]												Absorbance at 845.2 cm⁻¹ (Q)
	UDMH	O_3	CO	HCHO	HCOOH	CH_3OH	CH_3OOH	$(CH_3)_2NNO$	H_2O_2	NH_3	HONO	NO_2[b]	CH_3NNH
-23	8.06		-								-		
-5	8.07		-								-		
0		3.5 (calc'd, 1st injection)											
1.38	5.63	-	-	0.35	-	0.02	-	1.4	0.11	-	0.10	-	0.013
2.38	5.64	-	-	0.32	-	0.03	-	1.4	0.09	-	0.09	-	0.017
3.38	5.57	-	-	0.22	-	0.02	-	1.4	0.11	-	0.09	-	0.015
4.38	5.59	-	-	0.23	-	0.03	-	1.4	0.07	-	0.09	-	0.016
5.38	5.63	-	-	0.18	-	0.03	-	1.4	0.11	-	0.09	-	0.017
7.78	5.56	-	-	0.24	-	0.02	-	1.4	0.09	-	0.10	-	0.017
12.78	5.60	-	-	0.55	-	0.03	-	1.4	0.14	-	0.08	-	0.010
17.78	5.65	-	-	0.50	-	0.03	-	1.4	0.12	-	0.09	-	0.007
22.78	5.59	-	-	0.60	-	0.03	-	1.4	0.15	-	0.09	-	0.008
32.78	5.63	-	-	0.78	-	0.02	-	1.4	0.13	-	0.12	-	0.009
36.0		10.6 (calc'd, 2nd injection)											
36.38	0.29	1.23	-	1.3	0.03	0.08	1.5	4.6	0.56	-	0.21	0.18	0.016
37.38	-	1.20	0.06	1.5	0.03	0.11	1.6	4.9	0.59	-	0.23	0.13	-
38.38	-	1.15	0.10	1.6	0.04	0.11	1.5	4.9	0.64	0.03	0.23	0.12	-
39.38	-	1.09	0.09	1.6	0.03	0.10	1.5	4.9	0.67	0.03	0.21	0.13	-
40.38	-	1.11	0.11	1.6	0.04	0.12	1.5	4.9	0.61	0.03	0.23	0.13	-
41.38	-	1.09	0.10	1.6	0.04	0.12	1.5	4.9	0.67	0.03	0.23	0.13	-
43.78	-	1.03	0.09	1.6	0.04	0.12	1.5	4.9	0.63	0.03	0.23	0.11	-
48.78	-	0.98	0.12	1.3	0.04	0.12	1.4	4.9	0.61	0.02	0.21	0.09	-
54.78	-	0.93	0.11	1.3	0.04	0.12	1.3	4.9	0.61	0.03	0.21	-	-

[a] CH_2N_2 formed during 1st O_3 injection with maximum conc. of 0.05 ppm observed at t = 32.78 min; initially decreased after 2nd O_3 injection, rose to 0.05 ppm at t = 40.38 min, and decreased.
[b] NO_2 concentrations given are upper limit estimates.

181

TABLE C-2. REACTANT AND PRODUCT CONCENTRATIONS VS. TIME IN UDMH + O_3 DARK REACTION: ORGANIC TRACERS[a] ADDED; EXCESS UDMH (T = 23°C, RH = 29%; 3800 ℓ CHAMBER; RES = 1 cm^{-1}, PATHLENGTH = 68.3 M).

Elapsed Time (min)[c]	Concentration (ppm)[b]												Absorbance at 845.2 cm^{-1} (Q) CH_3NHN
	UDMH	O_3	CO	HCHO	HCOOH	CH_3OH	CH_3OOH	$(CH_3)_2NNO$	H_2O_2	NH_3	HONO	NO_2	
-36	16.8		-							0.10			
-7	16.4[a]		-							0.11			
0		4.3 (calc'd)											
0.38	13.6	-	0.09	0.36	0.01	0.05	-	1.4	0.08	0.12	0.07	-	0.011
1.38	13.2	-	0.09	0.37	0.01	0.03	-	1.7	0.16	0.13	0.09	-	0.010
2.38	13.2	-	0.08	0.53	0.01	0.03	-	1.7	0.16	0.13	0.08	-	0.011
3.38	13.2	-	0.10	0.39	0.01	0.02	-	1.7	0.20	0.13	0.09	-	0.012
4.38	13.2	-	0.10	0.43	0.01	0.02	-	1.7	0.16	0.13	0.09	-	0.013
5.38	13.1	-	0.08	0.55	-	0.05	-	1.7	0.12	0.13	0.09	-	0.013
7.78	13.2	-	0.10	0.44	0.01	0.04	-	1.7	0.17	0.13	0.08	-	0.011

Tracer Data:

GC Sampling Time (min)[c]	-23	-15	0	2	10	21
ln ([HME]/[octane])	0.683	0.677		0.694	0.694	0.694

[a] Approximately 0.2 ppm each of n-octane and hexamethylethane (HME) injected at t = -27 min.
[b] CH_2N_2 maximum conc. of 0.05 ppm observed at t = 7.78 min.
[c] Elapsed time and GC sampling time are both referred to start of O_3 injection (t = 0).

162

TABLE C-3. REACTANT AND PRODUCT CONCENTRATIONS VS. TIME IN UDMH + O_3 DARK REACTION: EQUIMOLAR INITIAL AMOUNTS OF REACTANTS (T = 23°C, RH = 14%; 3800 ℓ CHAMBER; RES = 1 CM^{-1}, PATHLENGTH = 68.3 M).

Elapsed Time (min)	UDMH	O_3	CO	HCHO	HCOOH	CH_3OH	CH_3OOH	$(CH_3)_2NNO$	H_2O_2	NH_3	HONO	NO_2[b]	Absorbance at 845.2 cm^{-1} (Q) CH_3NHNH
-12	10.1		0.20									-	
-5	10.1		0.20									-	
0		9.9 (calc'd, 1st injection)											
0.38	4.22	-	0.19	0.93	0.03	0.04	0.7	3.6	0.56	0.08	0.18	0.07	0.019
1.38	3.13	-	0.22	1.1	0.03	0.07	0.9	4.1	0.52	0.09	0.28	0.08	0.017
2.38	3.22	-	0.22	0.99	0.02	0.06	0.8	4.2	0.61	0.06	0.28	-	0.016
3.38	3.18	-	0.27	0.98	0.03	0.07	0.7	4.1	0.59	0.04	0.27	-	0.018
4.38	3.09	-	0.27	1.0	0.03	0.07	0.9	4.1	0.51	0.06	0.29	-	0.017
5.38	3.13	-	0.28	1.1	0.03	0.06	0.8	4.1	0.58	0.05	0.28	-	0.018
7.78	3.14	-	0.28	0.97	0.03	0.05	0.7	4.1	0.55	0.06	0.28	-	0.018
12.0		15.9 (calc'd, 2nd injection)											
13.38	-	10.5	0.35	1.7	0.07	0.15	1.7	6.0	0.92	0.05	0.29	0.20	-
14.38	-	10.1	0.41	2.0	0.06	0.17	1.9	6.2	0.86	0.04	0.29	0.19	-
15.38	-	9.99	0.44	1.9	0.07	0.20	2.1	6.1	0.91	0.04	0.28	0.17	-
16.38	-	9.95	0.45	2.1	0.07	0.21	2.2	6.2	0.84	0.03	0.30	0.14	-
17.38	-	9.87	0.42	2.1	0.07	0.22	2.2	6.2	0.82	0.04	0.30	0.14	-
21.78	-	9.82	0.47	2.1	0.07	0.21	2.2	6.1	0.79	0.04	0.28	0.13	-

[a] CH_2N_2 observed during 1st O_3 injection with maximum conc. of 0.06 ppm at t = 7.78 min.
[b] NO_2 concentrations given are upper limit estimates.

183

TABLE C-4. REACTANT AND PRODUCT CONCENTRATIONS VS. TIME IN UDMH + O_3 DARK REACTION: ORGANIC TRACERS[a] ADDED; EQUIMOLAR REACTANTS (T = 23°C, RH = 28%; 3800 ℓ CHAMBER; RES = 1 cm^{-1}, PATHLENGTH = 68.3 M).

| Elapsed Time (min)[c] | Concentration (ppm)[b] | | | | | | | | | | | | Absorbance at 845.2 cm^{-1} (Q) CH_3NNH |
	UDMH	O_3	CO	HCHO	HCOOH	CH_3OH	CH_3OOH	$(CH_3)_2NNO$	H_2O_2	NH_3	HONO	NO_2	
-23	9.77		-								0.11		
-7	9.60		-								0.11		
0		9.9 (calc'd)											
0.38	3.84	< 0.07	0.05	0.94	0.02	0.07	0.67	3.5	0.43	0.16	0.14	-	0.014
1.38	2.68	-	0.05	1.1	0.02	0.08	0.85	4.2	0.48	0.16	0.24	-	0.019
2.38	2.70	-	0.08	1.1	0.02	0.09	0.53	4.2	0.47	0.15	0.25	-	0.021
4.38	2.64	-	0.10	0.96	0.02	0.08	0.42	4.2	0.51	0.15	0.25	-	0.018
5.38	2.72	-	0.08	1.0	0.03	0.08	0.60	4.2	0.46	0.14	0.26	-	0.018
8.38	2.62	-	0.09	1.0	0.03	0.08	0.55	4.2	0.47	0.15	0.27	-	0.021

Tracer Data:

GC Sampling Time (min)[c]	-24	-13	0	2	13
ln ([HME]/[octane])	0.394	0.393		0.471	0.473

[a] Approximately 0.2 ppm each of n-octane and hexamethylethane (HME) injected at t = -32 min.
[b] CH_2N_2 maximum conc. of 0.07 ppm observed at t = 8.38 min.
[c] Elapsed time and GC sampling time are both referred to start of O_3 injection (t = 0).

184

TABLE C-5. REACTANT AND PRODUCT CONCENTRATIONS VS. TIME IN UDMH + O_3 DARK REACTION: ORGANIC TRACERS[a] ADDED; EXCESS OZONE (T = 21°C, RH = 23%; 3800 ℓ CHAMBER; RES = 1 CM^{-1}, PATHLENGTH = 68.3 M).

Elapsed Time (min)[b]	Concentration (ppm)												Absorbance at 845.2 cm^{-1} (Q) CH_3NNH
	UDMH	O_3	CO	HCHO	HCOOH	CH_3OH	CH_3OOH	$(CH_3)_2NNO$	H_2O_2	NH_3	HONO	NO_2	
-77		17.4	-							-			
-14		16.7[a]	-							-			
0	4.5 (calc'd)												
0.38	-	9.40	-	0.79	0.02	0.11	0.86	2.8	0.39	-	0.03	< 0.09	-
2.38	-	8.38	-	1.1	0.02	0.11	0.94	3.0	0.40	-	0.04	-	-
3.38	-	8.39	-	1.0	0.03	0.12	0.80	3.0	0.42	-	0.03	-	-
4.38	-	8.40	-	1.0	0.03	0.13	1.1	3.0	0.41	-	0.04	-	-
5.38	-	8.28	-	1.1	0.03	0.14	1.1	3.0	0.35	-	0.04	-	-
7.78	-	8.16	-	1.0	0.03	0.10	0.85	3.1	0.32	-	0.04	-	-

Tracer Data:

				HCHO	HCOOH	CH_3OH	CH_3OOH	$(CH_3)_2NNO$	H_2O_2
GC Sampling Time (min)[b]				-25	-18	0	2	11	18
ln ([HME]/[octane])				0.300	0.294		0.400	0.420	0.423

[a]Approximately 0.2 ppm each of n-octane and hexamethylethane (HME) injected at t = -50 min.
[b]Elapsed time and GC sampling time are both referred to start of UDMH injection (t = 0).

185

TABLE C-6. REACTANT AND PRODUCT CONCENTRATIONS VS. TIME IN UDMH + O_3 DARK REACTION: WITH N-OCTANE[a] AS RADICAL TRAP; EXCESS INITIAL UDMH (T = 26°C, RH = 11%; 6400 ℓ CHAMBER; RES = 1 CM^{-1}, PATHLENGTH = 102.4 M).

Elapsed Time (min)	UDMH	O_3	CO	HCHO	HCOOH	CH_3OH	CH_3OOH	$(CH_3)_2NNO$	H_2O_2	NH_3	HONO	NO_2[c]	Absorbance at 845.2 cm^{-1} (Q) CH_3NNH
-11	7.98		-							-			
-5	7.96		-							-			
0		3.3 (calc'd, 1st injection)											
0.38	6.16	-	-	-	-	0.02	~	1.3	-	-	0.01	-	-
1.38	5.96	-	-	-	-	0.03	~	1.4	-	-	0.02	-	-
2.38	6.06	-	-	-	-	0.04	~	1.4	-	-	0.02	-	-
3.38	6.06	-	-	-	-	0.04	~	1.4	-	-	0.02	-	-
4.38	6.00	-	-	-	-	0.03	~	1.4	-	-	0.04	-	-
5.38	6.01	-	-	-	-	0.03	~	1.4	-	-	0.02	-	-
7.78	5.91	-	-	-	-	0.03	~	1.4	-	-	0.02	-	-
12.78	6.01	-	-	-	-	0.03	~	1.4	-	-	0.02	-	-
17.78	5.94	-	-	-	-	0.03	~	1.4	-	-	0.04	-	-
22.78	5.95	-	-	-	-	0.02	~	1.4	-	-	0.03	-	-
32.78	6.00	-	-	-	-	0.03	~	1.4	-	-	0.05	-	-
37.0		10.3 (calc'd, 2nd injection)											
37.38	0.70	0.37	-	0.45	0.01	0.12	0.96	5.3	0.21	-	0.08	0.06	0.017
38.38	-	-	0.04	0.60	0.02	0.14	1.0	5.9	0.23	-	0.12	0.05	0.017
39.38	-	-	0.05	0.47	0.02	0.14	0.91	5.8	0.26	-	0.10	0.08	< 0.02
40.38	-	-	0.07	0.47	0.02	0.14	0.92	5.8	0.24	-	0.10	0.05	< 0.02
41.38	-	-	0.08	0.58	0.02	0.12	1.2	5.9	0.27	-	0.09	0.06	< 0.01
42.38	-	-	0.07	0.60	0.02	0.14	0.92	5.9	0.26	-	0.10	0.06	-
45.78	-	-	0.10	0.36	0.02	0.14	0.81	5.9	0.24	-	0.08	0.06	-
50.78	-	-	0.08	0.39	0.02	0.13	0.79	5.9	0.27	-	0.08	0.07	-
55.78	-	-	0.07	0.60	0.02	0.14	0.96	5.9	0.25	-	0.09	0.07	-

[a] Approximately 230 ppm n-octane introduced into chamber before injection of reactants.
[b] CH_2N_2 formed during 2nd O_3 injection with maximum conc. of 0.08 ppm observed at t = 55.78 min.
[c] NO_2 concentrations given are upper limit estimates.

186

TABLE C-7. REACTANT AND PRODUCT CONCENTRATIONS VS. TIME IN UDMH + O_3 DARK REACTION: WITH N-OCTANE[a] AS RADICAL TRAP; EQUIMOLAR INITIAL AMOUNTS OF REACTANTS (T = 23°C, RH = 13%; 3800 l CHAMBER; RES = 1 CM^{-1}, PATHLENGTH = 68.3 M).

Elapsed Time (min)[b]	Concentration (ppm)[c]												Absorbance at 845.2 cm^{-1} (Q) CH$_3$NNH
	UDMH	O_3	CO	HCHO	HCOOH	CH_3OH	CH_3OOH	$(CH_3)_2NNO$	H_2O_2	NH_3	HONO	NO_2	
-11	10.8		-							-			
-5	10.9		-							-			
0		10.3 (calc'd, 1st injection)											
0.10*	7.8	0.35	-	x	x	0.08	x	2.3	x	-	-	x	x
0.35	4.7	-	-	x	x	0.11	x	4.5	x	-	0.06	x	x
0.60	4.3	-	-	x	x	0.12	x	4.8	x	-	0.13	x	x
0.85	4.0	-	-	x	x	0.13	x	4.8	x	-	0.10	x	x
1.10	4.4	-	-	x	x	0.15	x	4.9	x	-	0.09	x	x
1.35	4.3	-	-	x	x	0.12	x	4.9	x	-	0.15	x	x
1.60	4.4	-	-	x	x	0.08	x	4.8	x	-	0.11	x	x
1.85	4.2	-	-	x	x	0.15	x	4.8	x	-	0.11	x	x
2.10*	4.2	-	-	x	x	0.11	x	4.8	x	-	0.11	x	x
3.38	4.20	-	-	0.62	0.01	0.13	-	4.8	0.19	-	0.10	-	0.011
4.38	4.22	-	-	0.66	0.01	0.14	-	4.8	0.15	-	0.11	-	0.008
5.38	4.16	-	-	0.60	0.01	0.12	-	4.8	0.19	-	0.10	-	0.014
7.78	4.22	-	-	0.70	0.01	0.12	-	4.8	0.22	-	0.10	-	0.011

187

TABLE C-7. REACTANT AND PRODUCT CONCENTRATIONS VS. TIME IN UDMH + O_3 DARK REACTION: WITH n-OCTANE[a] AS RADICAL TRAP; EQUIMOLAR INITIAL AMOUNTS OF REACTANTS (T = 23°C, RH = 13%; 3800 ℓ CHAMBER; RES = 1 CM^{-1}, PATHLENGTH = 68.3 M) (CONCLUDED).

Elapsed Time (min)[b]	Concentration (ppm)[c]												Absorbance at 845.2 cm^{-1} (Q)
	UDMH	O_3	CO	HCHO	HCOOH	CH_3OH	CH_3OOH	$(CH_3)_2NNO$	H_2O_2	NH_3	HONO	NO_2	CH_3NNH
13.0	16.3 (calc'd, 2nd injection)												
13.10*	0.44	5.9	–	1.3	0.02	0.23	x	7.8	0.30	–	0.07	x	–
13.35	–	9.5	–	1.5	0.03	0.30	x	8.2	0.39	–	0.13	x	–
13.60	–	9.9	–	1.3	0.02	0.37	x	8.0	0.38	–	0.10	x	–
13.85	–	9.6	–	< 2.1	0.01	0.22	x	8.1	0.22	–	< 0.18	x	–
14.10	–	9.9	–	1.2	0.03	0.32	x	8.1	0.38	–	0.08	x	–
14.35	–	9.6	–	< 1.8	0.03	0.21	x	8.1	0.31	–	0.10	x	–
14.60	–	9.9	–	1.6	0.03	0.19	x	8.1	0.38	–	0.11	x	–
14.85	–	9.6	–	1.5	0.03	0.24	x	8.1	0.30	–	0.08	x	–
15.10*	–	9.8	–	1.4	0.02	0.25	x	8.2	0.40	–	0.07	x	–
16.38	–	9.77	–	1.5	0.03	0.27	0.90	8.1	0.36	–	0.07	–	–
17.38	–	9.74	–	1.2	0.03	0.29	0.87	8.1	0.34	–	0.10	–	–
18.38	–	9.57	–	1.4	0.03	0.27	0.96	8.1	0.43	–	0.09	–	–
20.78	–	9.63	–	1.4	0.03	0.27	0.81	8.1	0.36	–	0.07	–	–

[a]Approximately 270 ppm n-octane was introduced into the chamber before injection of reactants.
[b]Pairs of asterisks bracket the data recorded every 15 sec (6 scans, 1 cm^{-1} resolution).
[c]Entries marked with "x" correspond to concentrations which could not be measured reliably due to the higher noise level of the spectra with fewer averaged scans. Dashes represent concentrations which are below normal detection limits (see Table 1 of text).

188

APPENDIX D

DETAILED DATA TABULATIONS FOR THE OZONE + AEROZINE-50
CHAMBER EXPERIMENT

The detailed concentration-time data for the environmental chamber experiment in which ozone was reacted with Aerozine-50 are given in Table D-1. The results of these experiments are discussed in Section 3.3.5.

TABLE D-1. REACTANT AND PRODUCT CONCENTRATIONS VS. TIME IN THE DARK REACTION OF AEROZINE-50 WITH O_3 (T = 23°C, RH = 15%; 3800 ℓ CHAMBER; RES = 1 CM^{-1}, PATHLENGTH = 68.3 M).

Elapsed Time (min)	Concentration (ppm)[a]														Absorbance at 1276.7 cm^{-1} (q)
	N_2H_4	UDMH	O_3	CO	HCHO	HCOOH	CH_3OH	CH_3OOH	$(CH_3)_2NNO$	H_2O_2	HONO	H_2O	NO_2	NH_3	H_2N_2
~10	7.65	8.00												0.08	
-5	7.52	8.02												0.10	
0			16.8 (calc'd)												
0.38	4.34	0.89	0.87	0.14	1.1	0.02	0.08	–	4.8	2.0	0.14	0.06	–	0.18	0.059
1.38	3.14	–	0.48	0.22	1.1	0.04	0.10		5.4	2.6	0.17	0.08	–	0.21	0.045
2.38	2.57	–	0.25	0.23	0.86	0.04	0.11		5.4	2.8	0.19	0.07	–	0.26	0.037
3.38	2.29	–	0.20	0.25	0.86	0.05	0.11	< 0.74	5.3	2.8	0.16	0.05	0.07	0.26	0.037
4.38	2.27	–	0.19	0.27	0.67	0.05	0.10		5.4	2.9	0.22	0.06	0.07	0.25	0.030
5.38	2.36	–	0.11	0.26	0.82	0.05	0.12		5.3	2.9	0.17	0.06	0.08	0.24	0.027
7.78	2.06	–	–	0.26	0.79	0.05	0.11		5.3	3.1	0.19	0.06	0.11	0.28	0.027
14.78	1.66	–	–	0.26	0.58	0.06	0.13	< 0.74	5.4	2.8	0.21	0.07	0.12	0.29	0.026
18.0			17.4 (calc'd)												
18.38	0.48	–	12.8	0.29	0.79	0.08	0.09	< 1.8	5.1	2.8	0.24	0.06	0.10	0.36	0.015
19.38	–	–	13.3	0.36	1.2	0.09	0.11		4.8	2.8	0.29	0.10	0.14	0.42	–
20.38	–	–	13.1	0.40	1.3	0.09	0.12		4.7	2.7	0.29	0.11	0.15	0.41	–
21.38	–	–	12.8	0.46	1.4	0.10	0.11	< 1.8	4.7	2.7	0.29	0.10	0.13	0.35	–
22.38	–	–	12.7	0.46	1.2	0.10	0.16		4.6	2.7	0.29	0.11	0.12	0.29	–
23.38	–	–	12.6	0.53	1.4	0.10	0.09		4.7	2.7	0.29	0.11	0.09	0.25	–
25.78	–	–	12.3	0.55	1.4	0.11	0.12	< 1.8	4.6	2.6	0.29	0.11	0.06	0.17	–

[a]An estimated 0.8 ppm of formaldehyde hydrazone ($H_2NN=CH_2$) was formed at t = ~15 min and disappeared shortly after the second O_3 injection.

APPENDIX E

DETAILED DATA TABULATIONS FOR THE NO_x + HYDRAZINE CHAMBER EXPERIMENTS

The detailed concentration-time data for the four environmental chamber experiments in which NO_x was reacted with N_2H_4 are given in Tables E-1 through E-4. The results of these experiments are discussed in Section 3.4.1.

191

TABLE E-1. REACTANT AND PRODUCT CONCENTRATIONS VS. TIME IN THE DARK REACTION OF N_2H_4 WITH NO AND NO_2 IN N_2 ATMOSPHERE; EXCESS N_2H_4 (T = 20°C, RH < 10%; 3800 ℓ CHAMBER; RES = 1 CM^{-1}, PATHLENGTH = 68.3 M).

Time Elapsed (min)	Concentration (ppm)[a]						Absorbance at 1276.7 cm^{-1} (Q)
	N_2H_4	NO	NO_2	HONO	N_2O	NH_3	N_2H_2
-12		6.1	–				
0	10.5 (calc'd)						
0.78	8.75	5.9	–	–	–	0.19	–
12.78	9.15	5.9	–	–	–	0.30	–
23.78	9.02	5.9	–	–	–	0.31	–
37.78	8.73	5.8	–	–	–	0.36	–
47.78	8.59	6.0	–	–	–	0.32	–
62.78	8.55	5.9	–	–	–	0.36	–
77.78	8.35	6.0	–	–	–	0.39	–
82.0			~5.9 (calc'd)				
82.78	7.96	5.5	5.3	0.06	0.11	0.41	–
88.78	8.07	5.9	5.3	0.20	0.13	0.40	–
102.78	7.84	5.9	4.8	0.40	0.17	0.46	–
117.78	7.47	5.8	4.2	0.64	0.20	0.54	–
133.78	7.13	5.8	3.8	0.85	0.22	0.58	–
147.78	6.47	5.6	3.5	1.0	0.21	0.59	–
162.78	6.34	5.6	3.2	1.2	0.23	0.62	–
177.78	6.06	5.6	2.9	1.3	0.24	0.64	< 0.005

[a]See text for a discussion of the hydrazinium salt(s) formed.

TABLE E-2. REACTANT AND PRODUCT CONCENTRATIONS VS. TIME IN THE DARK
REACTION OF N_2H_4 WITH NO AND NO_2 IN AIR; INITIAL EXCESS NO (T = 24°C,
RH = 11%; 6400 ℓ CHAMBER; RES = 1 CM^{-1}, PATHLENGTH = 102.4 M).

Time Elapsed (min)	Concentration (ppm)[a]						Absorbance at 1276.7 cm^{-1} (Q) N_2H_2
	N_2H_4	NO	NO_2	HONO	N_2O	NH_3	
−37	4.28					0.19	
−23	4.02					0.25	
−7	4.11					0.25	
0			~21 (calc'd)				
2.78	3.54	19.0	2.4	0.21	0.16	0.30	–
8.78	3.53	18.4	2.6	0.22	0.16	0.30	–
13.78	3.46	18.1	3.1	0.23	0.15	0.32	–
23.78	3.42	17.0	3.8	0.23	0.18	0.32	–
32.78	3.32	16.3	4.4	0.28	0.18	0.35	–
47.78	3.14	15.3	5.1	0.41	0.22	0.39	–
62.78	2.90	14.4	5.9	0.53	0.24	0.43	–
77.78	2.58	13.5	6.6	0.64	0.26	0.48	–
92.78	2.50	12.8	7.1	0.86	0.32	0.52	–
107.78	2.19	12.1	7.7	1.1	0.33	0.56	–
122.78	2.01	11.4	8.0	1.3	0.35	0.60	–
137.78	1.82	10.9	8.2	1.4	0.39	0.63	–
152.78	1.64	10.2	8.7	1.6	0.42	0.66	–
182.78	1.33	9.4	9.1	1.9	0.44	0.72	–

[a]See text for a discussion of the hydrazinium salt(s) formed.

TABLE R-3. REACTANT AND PRODUCT CONCENTRATIONS VS. TIME IN THE DARK REACTION OF N_2H_4 WITH NO_2 IN AIR; EXCESS N_2H_4 (T = 22°C, RH = 13%; 3800 l CHAMBER; RES = 1 CM^{-1}, PATHLENGTH = 68.3 M).

Time Elapsed (min)	Concentration (ppm)[a]						Absorbance at 1276.7 cm^{-1} (Q)
	N_2H_4	NO	NO_2	HONO	N_2O	NH_3	N_2H_2
-10	8.81					0.08	
-5	8.66					0.08	
0			~5.6 (calc'd)				
0.78	8.20	–	4.3	0.06	–	0.10	–
5.78	8.09	–	4.4	0.19	–	0.13	–
15.78	7.53	–	3.9	0.42	0.04	0.17	0.006
30.78	6.99	–	3.4	0.68	0.06	0.21	0.008
45.78	6.60	–	3.0	0.91	0.09	0.24	0.010
60.78	6.13	~	2.6	1.1	0.09	0.27	0.012
75.78	5.97	~	2.2	1.3	0.11	0.30	0.012
90.78	5.56	~	2.0	1.5	0.10	0.31	0.015
105.78	5.09	–	1.7	1.6	0.10	0.33	0.016
120.78	4.70	–	1.5	1.7	0.10	0.35	0.017

[a]See text for a discussion of the hydrazinium salt(s) formed.

TABLE E-4. REACTANT AND PRODUCT CONCENTRATIONS VS. TIME IN THE DARK REACTION OF N_2H_4 WITH NO_2 IN AIR; EXCESS NO_2 (T = 25°C, RH = 11%; 6400 ℓ CHAMBER; RES = 1 CM^{-1}, PATHLENGTH = 102.4 M).

Time Elapsed (min)	Concentration (ppm)[a]						Absorbance at 1276.7 cm^{-1} (Q)
	N_2H_4	NO	NO_2	HONO	N_2O	NH_3	N_2H_2
-18	4.86					0.05	
-8	4.85					0.04	
-4	4.77					0.05	
0				~21 (calc'd)			
9.78	4.29	-	20.0	0.18	0.23	0.09	-
18.78	4.11	-	19.7	0.39	0.31	0.19	-
23.78	3.99	-	19.5	0.48	0.36	0.23	-
37.78	3.60	-	18.9	0.78	0.47	0.37	-
52.78	3.22	-	18.4	1.1	0.55	0.46	-
67.78	2.95	-	18.1	1.4	0.63	0.55	-
97.78	2.48	-	17.4	1.8	0.68	0.62	-
112.78	2.20	-	16.9	2.3	0.71	0.69	-
127.78	1.92	-	16.1	2.5	0.76	0.75	-
142.78	1.73	-	16.2	2.8	0.80	0.78	-
158.78	1.45	-	15.7	3.2	0.81	0.83	-
172.78	1.32	-	15.3	3.5	0.84	0.86	-
187.78	0.84	-	15.1	4.1	0.88	0.91	-

[a]See text for a discussion of the hydrazinium salt(s) formed.

APPENDIX F

DETAILED DATA TABULATIONS FOR THE NO_x + MONOMETHYLHYDRAZINE CHAMBER EXPERIMENTS

The detailed concentration-time data for the four environmental chamber experiments in which NO_x was reacted with MMH are given in Tables F-1 through F-4. The results of these experiments are discussed in Section 3.4.2.

TABLE F-1. REACTANT AND PRODUCT CONCENTRATIONS VS. TIME IN THE DARK REACTION OF MMH WITH NO AND NO_2 IN N_2 ATMOSPHERE; EXCESS MMH (T = 22°C, RH < 10%; 3800 ℓ CHAMBER; RES = 1 CM^{-1}, PATHLENGTH = 68.3 M).

Time Elapsed (min)	Concentration (ppm)[a]									Absorbance at 845.2 cm^{-1} (Q)
	MMH	NO	NO_2	HONO	$HOONO_2$	N_2O	NH_3	CH_3OH	CH_3OOH	CH_3NNH
-12		6.0	-							
-5		6.0	-							
0	10.5 (calc'd)									
5.38	10.3	6.0	-	-	-	-	0.14	-	-	-
20.78	9.95	6.0	-	-	-	-	0.22	-	-	-
50.78	9.69	5.9	-	-	-	-	0.27	-	-	-
95.78	9.56	5.9	-	-	-	-	0.24	-	-	-
101.0			~6.0 (calc'd)							
101.78	9.07	5.7	5.1	0.19	-	-	0.28	-	-	-
105.78	8.73	5.7	4.6	0.78	-	0.09	0.29	-	-	0.017
110.78	8.29	5.6	3.9	1.3	-	0.09	0.29	-	-	0.024
115.78	8.03	5.6	3.3	1.8	-	0.11	0.30	-	-	0.035
120.78	7.70	5.3	2.8	2.2	-	0.12	0.30	0.04	-	0.035
125.78	7.40	5.1	2.4	2.5	-	0.11	0.29	0.06	-	0.041
135.78	7.01	4.9	1.8	3.0	-	0.11	0.30	0.07	-	0.047
145.78	6.67	4.8	1.4	3.4	-	0.14	0.30	0.08	-	0.054
155.78	6.48	4.5	1.1	3.7	-	0.12	0.29	0.09	-	0.055
170.78	6.27	4.3	0.77	4.0	-	0.14	0.30	0.11	-	0.064
185.78	6.05	4.2	0.58	4.3	-	0.12	0.30	0.12	-	0.068

[a]See text for a discussion of $CH_3NHNH_2 \cdot HNO_3$ and unknown products formed.

TABLE F-2. REACTANT AND PRODUCT CONCENTRATIONS VS. TIME IN THE DARK REACTION OF MMH WITH NO AND NO_2 IN AIR; INITIAL EXCESS NO (T = 23°C, RH = 11%; 6400 ℓ CHAMBER; RES = 1 CM^{-1}, PATHLENGTH = 102.4 M).[2]

Time Elapsed (min)	845.2 cm⁻¹ (Q) MMH	NO	NO_2	HONO	$HOONO_2$	N_2O	NH_3	CH_3OH	CH_3OOH	Absorbance at CH_3NNH
					Concentration (ppm)[a]					
−35	4.41						−			
−19	4.40						−			
−4	4.38						−			
0			~21 (calc'd)							
1.78	4.17	19.4	1.7	0.24	−	0.16	0.03	−	−	−
11.78	3.69	17.9	2.1	0.68	−	0.22	0.04	−	−	0.015
21.78	3.39	16.7	2.6	1.1	−	0.23	0.03	−	−	0.027
34.78	2.85	15.2	2.9	1.8	−	0.27	0.05	−	−	0.040
41.78	2.59	14.5	3.1	2.1	−	0.28	0.05	−	−	0.049
56.78	2.11	13.2	3.4	2.9	−	0.28	0.05	0.02	−	0.059
71.78	1.61	12.0	3.8	3.5	−	0.31	0.07	0.04	−	0.061
86.78	1.20	10.7	4.0	4.1	−	0.34	0.08	0.04	−	0.063
101.78	0.89	9.7	4.4	4.6	−	0.35	0.08	0.06	−	0.055
116.78	0.61	8.7	4.6	5.1	−	0.36	0.09	0.07	−	0.060
131.78	0.36	8.0	4.9	5.5	−	0.35	0.10	0.08	−	0.065

[a]See text for a discussion of $CH_3NHNH_2 \cdot HNO_3$ and unknown products formed.

TABLE F-3. REACTANT AND PRODUCT CONCENTRATIONS VS. TIME IN THE DARK REACTION OF MMH WITH NO_2 IN AIR; EXCESS MMH (T = 22°C, RH = 13%; 3800 ℓ CHAMBER; RES = 1 CM^{-1}, PATHLENGTH = 68.3 M).

Time Elapsed (min)	Concentration (ppm)[a]									Absorbance at 845.2 cm^{-1} (Q)
	MMH	NO	NO_2	HONO	$HOONO_2$	N_2O	NH_3	CH_3OH	CH_3OOH	CH_3NNH
-11	10.0						0.11			
-6	9.87						0.13			
0			~5.5 (calc'd)							
0.38	9.58	–	4.4	0.08	–	–	0.16	–	–	–
1.38	9.41	–	5.0	0.21	–	–	0.15	–	–	0.007
2.38	9.36	–	4.8	0.33	–	–	0.16	–	–	0.007
3.38	9.32	–	4.6	0.44	0.04	–	0.14	–	–	0.007
4.38	9.17	–	4.4	0.55	0.05	–	0.15	–	–	0.015
5.38	9.16	–	4.2	0.67	0.07	–	0.16	–	–	0.012
8.78	8.62	–	3.6	1.0	0.10	–	0.17	–	–	0.024
12.78	8.45	–	3.1	1.3	0.08	–	0.18	–	–	0.028
19.78	8.12	–	2.4	1.7	0.09	–	0.21	–	–	0.038
29.78	7.53	–	1.7	2.3	0.06	–	0.22	–	0.54	0.048
39.78	7.28	–	1.3	2.6	0.05	–	0.23	–	0.52	0.049
49.78	6.94	–	1.0	2.9	0.03	–	0.24	–	0.91	0.051
64.78	6.50	–	0.75	3.1	–	–	0.27	0.04	1.1	0.048
79.78	6.06	–	0.53	3.3	–	–	0.26	0.08	1.3	0.050
94.78	5.70	–	0.40	3.5	–	–	0.28	0.09	1.5	0.046

[a]See text for a discussion of $CH_3NHNH_2 \cdot HNO_3$ and unknown products formed.

TABLE F-4. REACTANT AND PRODUCT CONCENTRATIONS VS. TIME IN THE DARK REACTION OF MMH WITH NO_2 IN AIR; EXCESS NO_2 (T = 25°C, RH = 12%; 6400 ℓ CHAMBER; RES = 1 CM^{-1}, PATHLENGTH = 102.4 M).

Time Elapsed (min)	Concentration (ppm)[a]									Absorbance at 845.2 cm^{-1} (Q)
	MMH	NO	NO_2	HONO	$HOONO_2$	N_2O	NH_3	CH_3OH	CH_3OOH	CH_3NNH
-30	4.55						-			
-20	4.49						-			
-10	4.50						-			
0				~21 (calc'd)						
3.78	3.19	-	18.8	1.2	0.07	0.19	-	0.03	-	0.031
8.78	2.47	-	17.0	2.1	0.11	0.18	-	0.02	-	0.055
15.78	1.78	-	14.6	3.1	0.13	0.19	-	0.06	-	0.059
25.78	1.17	-	13.1	4.2	0.06	0.20	0.03	0.05	-	0.060
35.78	0.68	-	11.5	4.9	-	0.21	0.04	0.07	-	0.050
45.78	0.43	-	10.3	5.4	-	0.22	0.05	0.07	-	0.048
55.78	-	-	9.6	5.8	-	0.23	0.05	0.10	-	0.038
65.78	-	-	9.2	6.0	-	0.23	0.05	0.11	-	0.025

[a]See text for a discussion of $CH_3NHNH_2 \cdot HNO_3$ and unknown products formed.

200

APPENDIX G

DETAILED DATA TABULATIONS FOR THE NO$_x$ + UNSYMMETRICAL DIMETHYL-HYDRAZINE CHAMBER EXPERIMENTS

The detailed concentration-time data for the four environmental chamber experiments in which NO$_x$ was reacted with UDMH are given in Tables G-1 through G-4. The results of these experiments are discussed in Section 3.4.3.

TABLE G-1. REACTANT AND PRODUCT CONCENTRATIONS VS. TIME IN THE DARK
REACTION OF UDMH WITH NO AND NO_2 IN N_2 ATMOSPHERE; EXCESS UDMH
(T = 24°C, RH < 10%; 3800 ℓ CHAMBER; RES = 1 CM^{-1}, PATHLENGTH = 68.3 M).

Elapsed Time (min)	Concentration (ppm)							Absorbance at 993 cm^{-1}
	UDMH	NO	NO_2	HONO	N_2O	NH_3	TMT[a,b]	Unknown[b]
-7		5.6	–					
0	11.3 (calc'd)							
2.78	11.1	5.7	–	–	–	0.06	–	
13.78	11.1	5.7	–	–	–	0.06	–	
44.78	11.0	5.7	–	–	–	0.09	–	
89.78	10.9	5.7	–	–	–	0.07	–	
131.78	10.8	5.6	–	–	–	0.07	–	
136.0			~6.3 (calc'd)					
136.38	10.2	5.5	3.9	1.1	0.06	0.09	0.20	–
137.38	9.32	5.2	2.0	2.7	0.09	0.09	0.58	0.02
138.38	9.10	5.3	1.1	3.5	0.09	0.05	0.76	0.03
139.38	8.84	5.3	0.63	3.9	0.13	0.05	0.84	0.04
140.38	8.67	5.2	0.36	4.2	0.15	0.03	0.88	0.05
141.38	8.59	5.2	0.22	4.4	0.17	0.04	0.90	0.05
143.78	8.49	5.0	0.07	4.5	0.21	0.05	0.92	0.06
146.78	8.34	4.9	–	4.6	0.23	0.03	0.93	0.06
149.78	8.38	4.9	–	4.6	0.24	0.05	0.93	0.07
152.78	8.43	4.9	–	4.6	0.25	0.05	0.93	0.07
159.78	8.40	4.9	–	4.7	0.25	0.05	0.93	0.07
170.0			~6.3 (calc'd)					
172.38	7.02	4.6	1.1	6.9	0.33	0.05	1.4	0.08
177.38	6.52	4.4	0.15	7.9	0.42	0.04	1.5	0.10
189.78	6.38	4.2	–	8.0	0.47	0.05	1.5	0.11

[a]TMT = tetramethyltetrazene-2
[b]Estimated from the overlapping absorption bands of TMT and the unknown compound.

TABLE G-2. REACTANT AND PRODUCT CONCENTRATIONS VS. TIME IN THE DARK REACTION
OF UDMH WITH NO AND NO_2 IN AIR; INITIAL EXCESS NO
(T = 23°C, RH = 12%; 6400 ℓ CHAMBER; RES = 1 CM^{-1}, PATHLENGTH = 102.4 M).

Elapsed Time (min)	Concentration (ppm)								Absorbance at 993 cm^{-1}
	UDMH	NO	NO_2	HONO	N_2O	NH_3	TMT[a,b]	$(CH_3)_2NNO$[b]	Unknown[b]
-19	4.96					0.06			
-4	4.93					0.07			
0		~21 (calc'd)							
1.78	3.28	15.4	3.3	2.8	0.27	0.09	0.40	0.19	0.06
5.78	2.59	14.6	1.8	4.2	0.36	0.10			
10.78	2.16	13.9	1.2	5.0	0.44	0.10	0.69	0.20	0.15
15.78	1.77	13.3	0.88	5.5	0.48	0.10			
21.78	1.58	12.9	0.80	5.8	0.56	0.11	0.77	0.28	0.20
25.78	1.38	12.7	0.76	6.0	0.59	0.11			
35.78	1.18	12.1	0.71	6.4	0.63	0.10	0.79	0.30	0.25
40.78	1.09	11.6	0.69	6.7	0.66	0.10			
45.78	1.02	11.3	0.69	6.7	0.67	0.11			
50.78	0.89	10.8	0.72	6.9	0.67	0.11	0.82	0.32	0.28

[a]TMT = tetramethyltetrazene-2
[b]Estimated from the overlapping absorption bands of TMT, $(CH_3)_2NNO$, and the unknown compound (see text).

203

TABLE G-3. REACTANT AND PRODUCT CONCENTRATIONS VS. TIME IN THE
DARK REACTION OF UDMH WITH NO_2 IN AIR; EXCESS UDMH
(T = 24°C, RH = 13%; 3800 ℓ CHAMBER; RES = 1 CM^{-1}, PATHLENGTH = 68.3 M).

Elapsed Time (min)	Concentration (ppm)						
	UDMH	NO	NO_2	HONO	N_2O	NH_3	TMT[a]
-12	11.0					-	
-7	10.9					-	
0			~5.5				
0.38	10.1	-	3.9	0.98	-	-	0.23
1.38	9.14	-	2.1	2.9	-	-	0.70
2.38	8.67	-	1.1	3.8	-	-	0.92
3.38	8.54	-	0.58	4.3	-	-	1.0
4.38	8.23	-	0.34	4.6	-	-	1.1
5.38	8.28	-	0.20	4.7	-	-	1.1
7.38	8.17	-	0.08	4.9	-	-	1.1
9.38	8.21	-	-	4.9	-	-	1.1
11.38	8.14	-	-	4.9	-	-	1.1
13.38	8.09	-	-	4.9	-	-	1.1
15.78	8.16	-	-	4.9	-	-	1.1
20.78	8.22	-	-	4.9	-	-	1.1

[a]TMT = tetramethyltetrazene-2

204

TABLE G-4. REACTANT AND PRODUCT CONCENTRATIONS VS. TIME IN THE
DARK REACTION OF UDMH WITH NO_2 IN AIR; EXCESS NO_2
($T = 22^{\circ}C$, RH = 13%; 3800 ℓ CHAMBER; RES = 1 CM^{-1}, PATHLENGTH = 102.4 M).

Elapsed Time (min)	Concentration (ppm)						
	UDMH	NO	NO_2	HONO	N_2O	NH_3	TMT[a]
-12	5.53					0.02	
-6	5.49					0.03	
0			~23 (calc'd)				
0.38	3.95	–	18.6	2.1	0.05	0.04	0.49
1.38	2.18	0.30	15.7	5.4	0.05	0.03	1.3
2.38	1.43	0.34	13.7	7.4	0.05	0.04	1.7
3.38	0.71	0.34	12.8	8.3	0.05	0.03	1.9
4.38	0.54	0.42	11.7	9.0	0.06	0.04	2.1
5.38	0.35	0.41	11.1	9.6	0.06	0.03	2.2
8.78	–	0.33	10.4	10.2	0.06	0.03	2.3
15.78	–	0.20	9.9	10.7	0.04	–	2.3

[a]TMT = tetramethyltetrazene-2